DEVELOPMENT OF AN ION CHROMATOGRAPHIC SYSTEM SUITABLE FOR MONITORING THE GOLD CYANIDATION PROCESS

By

Peter Andrew Fagan

A thesis submitted in fulfillment of the requirements for the degree of
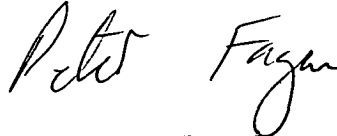
DOCTOR OF PHILOSOPHY

UNIVERSITY OF TASMANIA

School of Chemistry
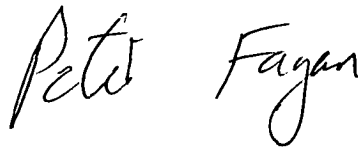
Submitted 5 June 1998

DECLARATION

To the best of my knowledge, this thesis contains no copy or
paraphrase of material previously published or written by another
person, except where due reference is made in the text of the
thesis.

Peter Fagan

5 June 1998

This thesis may be available for loan and copying in

accordance with the Copyright Act 1968.

Peter Fagan

5 June 1998

ii

Acknowledgements

Dedication

I would like to dedicate this thesis to my wife, Lynn Anne Fagan and my parents, Elizabeth Fagan (now deceased) and John Bathurst Fagan.

LIST OF PUBLICATIONS FROM THESIS

<u>Papers in refereed journals</u>

1. P.A. Fagan and P.R. Haddad, "Determination of free cyanide in gold cyanidation process liquors by ion-interaction chromatography with post-column derivatisation", *Journal of Chromatography*, 550 (1991) 559-571.
   (Chapter 3)

2. P.A. Fagan and P.R. Haddad, "Reversed-phase ion interaction chromatography of Cu(I)-cyanide complexes", *Journal of Chromatography*, 770 (1997) 165-174.
   (Chapter 4)

3. P.A. Fagan, B. Paull, P.R. Haddad, R. Dunne and H. Kamar, "Ion chromatographic analysis of cyanate in gold processing samples containing large concentrations of copper(I) and other metallo-cyanide complexes", *Journal of Chromatography*, 770 (1997) 175-183.
   (Chapter 7)

4. P.A. Fagan, P.R. Haddad, R. Dunne and I. Mitchell, "Monitoring the cyanidation of gold-copper ores with ion chromatography: Determination of the CN:Cu(I) mole ratio", *Journal of Chromatography*, 804 (1998) 249-263.
   (Chapters 5 and 6)

<u>Papers in conference proccedings</u>

1. P.A. Fagan, P.R. Haddad, R. Dunne and I. Mitchell, "Advances in ion chromatography for monitoring the gold cyanidation process", *Proceedings Randol '96 Gold Forum*, Squaw Creek, California, U.S.A., April 1996, 321.

LIST OF CONFERENCE PRESENTATIONS FROM THESIS

1. P.A. Fagan and P.R. Haddad, "Monitoring of free cyanide in mine process liquors using a coupled ion chromatographic system", *International Symposium on Ion Chromatography*, San Diego,U.S.A. Sep, 1990.

2. P.A. Fagan and P.R. Haddad, "A field trial of the use of ion chromatography for monitoring of cyanide and cyanide species in the carbon-in-pulp process for gold extraction and recovery", *11th Australian Symposium on Analytical Chemistry*, Hobart, July, 1991.

3. P.A. Fagan, G. Moran and P.R. Haddad, "Studies on the identification of Cu(I)-cyano complexes eluted from a HPLC column", *International Symposium on Ion Chromatography*, Baltimore,U.S.A., Sep, 1993.

4. P.A. Fagan, P.R. Haddad, W.W. Buchberger and P.E. Jackson "Studies on the ion-interaction chromatography of Cu(I)-cyano complexes", *International Symposium on Ion Chromatography*, Turin, Italy, Sep, 1994.

5. P.A. Fagan, P.R. Haddad, R. Dunne and I. Mitchell, "Advances in ion chromatography for monitoring the gold cyanidation process", *Randol '96 Gold Forum*, Squaw Creek, California, U.S.A., April 1996.

LIST OF ABBREVIATIONS

CIP   Carbon-in-Pulp

CIL   Carbon-in-Leach

RIP   Resin-in-Pulp

DL   Dump leach

LP   Leach pad

CPS   Controlled potential sulfidisation

EW   Electrowinning

AARL   Anglo-American Research Laboratories

DO   Dissolved oxygen

AAS   Atomic absorption spectroscopy

ICP-AES   Inductively coupled plasma – atomic emission spectroscopy

FIA   Flow injection analysis

ISE   Ion selective electrode

Rt   Retention time

Min   minute

Hr   Hour

HPLC   High performance liquid chromatography

RP   Reversed-phase

IC   Ion Chromatography

IE   Ion exclusion

AX   Anion-exchange

SAX   Strong anion-exchange

SPE   Solid phase extraction

RPIIC   Reversed-phase ion-interaction chromatography

IIR   Ion interaction reagent

TBA   Tetrabutylammonium

TBAOH   Tetrabutylammonium hydroxide

TPA   Tetrapropylammonium

TPAOH   Tetrapropylammonium hydroxide

MeCN	Acetonitrile
MeOH	Methanol
THF	Tetrahydrofuran
CSA	Camphor sulphonic acid
PCR	Post-column reaction
ID	Internal diameter
NCS	N-chlorosuccinimide
BA	Barbituric acid
INA	Isonicotinic acid
PZ	3-methyl-1-phenyl-2-pyrazolin-5-one
PMD	Polymethine dye
OPA	o-phthalaldehyde
NDA	2,3-naphthalenedialdehyde
ε_{app}	Apparent molar absorptivity
PDA	Photo-diode array
UV	Ultraviolet
Vis	Visible
IR	Infra-red
FTIR	FourierTransform Infra-red
NMR	Nuclear magnetic resonance
R	CN:Cu mole ratio
PAR	CN:Cu(I) peak area ratio
ppm	parts per million (typically mg/L)
RSD	Relative standard deviation
AU	Absorbance units

TABLE OF CONTENTS

CHAPTER ONE
Introduction and literature review

CHAPTER THREE

Initial development of methods for the chromatographic determination of cyanide in gold cyanidation samples

CHAPTER FOUR

Improvements to the PCR detection system and understanding the reversed-phase ion-interaction chromatography of the Cu(I)-cyanide complexes

CHAPTER SIX
Determination of the CN:Cu(I) mole ratio with ion chromatography

CHAPTER SEVEN

Ion chromatographic analysis of cyanate in gold processing samples containing Cu(I) and other metal-cyanide complexes

CHAPTER EIGHT
Conclusions

CHAPTER ONE

Introduction and literature review

1.1 Overview

This thesis reports the development of new ion chromatographic (IC) methodology suitable for monitoring the gold cyanidation process. This project continues a series of related investigations involving the development of IC techniques, based mainly on reversed-phase ion interaction chromatography (RPIIC), for the speciation of metallo-cyanide complexes formed during the cyanidation of auriferous ores [1-4]. The focus of this earlier work was concerned with the development of suitable methodology for the analysis of the products of the cyanidation process, such as those found in tailings dams and environmental samples.

In contrast to the previous investigations, this project has focused on the determination of the various cyano species found during the extraction stage of the gold cyanidation process. These cyano species include uncomplexed ('free') cyanide, metallo-cyanide complexes, thiocyanate and cyanate. It should be noted that the terms 'free' and uncomplexed cyanide are not strictly interchangeable, especially in the presence of labile metallo-cyanide complexes. The change in emphasis from environmental monitoring to process control was originally suggested by Metana Minerals, as a means to improve the efficiency of their cyanide-leaching operations. It should be emphasised that cyanide (usually added as sodium or calcium cyanide) is the most expensive reagent used during the extraction of gold from ore.

Cyanide analyses in the gold mining industry can be divided into two broad categories. These are the determination of cyanide during the gold extraction process and the determination of cyanides in environmental samples as a result of discharges from the extraction process. Cyanide is present in solution as HCN and/or CN^- (depending on the pH) and as metallo-cyanide complexes of widely varying thermodynamic stabilities. Decomposition of the less stable metallo-

cyanide complexes, because of changes in the pH or due to UV irradiation, results in the release of CN⁻ and HCN. Thus, it is common practice in environmental analysis for HCN, CN⁻ and potentially ionisable metallo-cyanide complexes to be determined as a group, with the total cyanide being determined in a separate analysis. However, in the cyanidation process it is essential that an accurate determination of the cyanide available for leaching gold ("free cyanide") be made in order to maximise production efficiency. This thesis is focused on the latter determination, which has important economic and indirect environmental benefits to the gold mining industry.

Relatively simple on-line cyanide analysers have been reported to reduce cyanide consumption by 20-40% [5-7]. These on-line cyanide analysers will be discussed further in Section 1.8. It should be recognised that, in addition to providing significant cost savings to the gold mining industry, on-line cyanide analysers will have a considerable effect in reducing environmental impact by decreasing the cyanide concentration in the effluent from the gold extraction process. The reduced cyanide concentration in the effluent will provide further cost benefits in that it is considerably more expensive to destroy cyanide than to add it to the leaching process.

The original developments in this project were aimed at determining the free cyanide concentration in addition to the metallo-cyanide complexes, with the intention of developing a process control cyanide analyser. This work is discussed in Chapter three. Some unexpected and severe problems were encountered during the first field evaluation of the chromatographic system at the Rothsay Gold Mine in Western Australia. Due to these and other problems (such as management changes at Metana Minerals, closure of the Rothsay Gold Mine and falling gold prices), the project with Metana Minerals was terminated.

The two major problems experienced with the chromatographic system at the Rothsay Gold Mine concerned the chromatography of the Cu(I)-cyanide complexes and instability in the detection system. Consequently, the next stage of the project was aimed at understanding and overcoming these problems. The work is discussed in Chapter four.

Following the improvements to the chromatographic system, and the provision of an Australian Research Council Collaborative grant, a new project was commenced in collaboration with Newcrest Mining Ltd., a major Australian Gold producer. The HPLC instrument and author were relocated to Newcrest's Telfer Gold Mine for approximately 12 months. Considerable method development, combined with a series of evaluations, was conducted during this period at Telfer. The major problem confronted and overcome was to develop methods suitable for monitoring the cyanidation of cupriferous and pyritic ores. The major achievements were the development of methods suitable for rapid and routine determination of the CN:Cu mole ratio and cyanate in cyanide leachates containing high concentrations of $Cu(I)$ cyanide complexes. The standard analytical techniques used to determine these species are both time consuming and problematic. Consequently, these new chromatographic methods are ideally suited for monitoring the cyanidation of cupriferous gold ores. In addition, these analytical methods may also be suitable for monitoring several new technologies designed to both recover copper and recycle cyanide present in the $Cu(I)$-cyanide complexes [8]. These developments are reported in Chapters six and seven.

To assist readers with a limited knowledge of mineral processing and the gold mining industry, the first part of this chapter presents some background information concerning gold, its associated geology and some of the metallurgy involved in the extraction of gold from ores. This part of the thesis is by necessity very brief and greatly over-simplifies the numerous and complex issues associated with these topics.

Following the first part of this chapter, the reader is then presented with some of the problems faced by metallurgists during the cyanidation process and the associated analytical problems, together with some current solutions. This leads to a discussion of the problems experienced when treating gold-copper ores, followed by a brief review of the aqueous chemistry of the $Cu(I)$-cyanide complexes relevant to the gold cyanidation process.

The latter sections of this chapter deal with the analysis of cyanide. This is commenced in section 1.5 with a general review of the methods available for cyanide analysis. This is followed by a review of the analytical methods based on König reaction. Variations of this reaction are the basis of the most widely used spectrophotometric methods available for cyanide and are extensively used in this thesis for the post-column derivatisation of cyanide. The use of ion chromatography for the analysis of cyanide and the metallo-cyanide complexes is then reviewed in section 1.7. The application of automated analytical instruments for controlling the cyanide concentration in the leaching process is then reviewed. This leads to a discussion on the use of ion chromatography for controlling the cyanidation process and for overcoming some of the important analytical problems associated with the determination of cyano species occurring in the cyanidation process.

Before proceeding with the first part of this chapter, it should be recognised that the recovery of gold from an orebody involves a complex series of closely interlinked operations. These operations include the arrangement of considerable financial investment, exploration, surveying, mining, mineral processing and finally, extraction and refining of gold obtained from the ore. External factors beyond the control of the mine owners such as the current ('spot') gold price, exchange rate of the local currency, interest rates and investor confidence can significantly and rapidly alter the viability of a gold mine. For example, the announcement in 1997 by several Central Banks to sell part of their gold reserves, combined with the economic collapse of several South East Asian countries, has significantly decreased the spot gold price to the point that many gold mines around the world may no longer be viable.

1.2 Gold : Some background information

Gold is called the noblest of metals because of its inertness. This term was given by alchemists due to the resistance of the noble metals (gold and silver) to attack by air, even when heated [9]. This unique chemistry has been attributed by theoretical chemists to the relativistic contraction of the 6s orbital well known for the

Lanthanide series of elements. These relativistic effects reach a distinct maximum for gold and are reflected in various bonding parameters such as the ionisation potential and electron affinity of gold [10]. These theoretical studies have been able to rationalise the unique chemical properties of gold, such as the lowest redox potential of any metal and a preference for forming gold-gold bonds [10, 11].

The principal oxidation states for gold are +1 and +3. These states are unknown as aquo-ions in solution. However, gold complexes such as $[Au(CN)_2]^-$ and $[AuCl_4]^-$ can exist in aqueous solution [11]. While gold can be found in a limited number of naturally occurring compounds, most gold is found in its elemental state, either as native gold or as an alloy such as electrum [12]. This is a reflection of the unique chemistry of gold mentioned previously. It has been argued that during the formation of hydrothermal gold deposits, various gold complexes (such as chloro and hydroxy complexes) were formed and transported through the Earth's crust under extreme conditions. Elemental gold was subsequently deposited in various rock formations when the severity of the geochemical conditions had decreased [11, 13].

Gold is associated with many different types of geological formations. There are two general types of auriferous deposits - lode (or vein) and placer deposits. It should be noted that gold deposits may be of any form and may occur in any rock. Thus prospecting for gold can be based as much on providence as on understanding the geology and geochemistry of gold deposits [11].

The majority of the gold recovered prior to the 20th Century was found in Placer gold deposits. Even up to 1982, paleoplacer deposits accounted for 60% of the World gold production [12]. Placer deposits have been formed by weathering processes resulting in the liberation of free gold particles. These are found in either sedimentary deposits (Paleoplacer) or alluvial and eluvial deposits resulting mainly from the last ice age (Recent placer) [11, 12]. The best known example of Paleoplacer deposits occurs in South Africa in the Witwatersrand, from where over 35,000 tonnes of gold has been recovered [12]. It should be noted that some authors

dispute the genesis of the Witwatersrand deposits [11]. Most of the gold found during the Gold rushes of the mid- to late- 1800's was from recent Placer deposits .

Prior to the formation of Placer deposits, gold was deposited in both sedimentary and volcanic regions via several different geological processes, such as hydrothermal and volcanic incursions [11, 12]. It should be noted that there is still some contention concerning the mechanisms by which gold is deposited [11]. While it is beyond the scope of this thesis to discuss these geological processes, the interested reader is directed to two excellent reviews concerning gold geology by Boyle [11] and Paterson [12] and an introductory textbook by Evans [13].

While gold occurs in association with most of the rock-forming minerals, economic deposits are commonly associated with quartz and sulfide minerals (pyrites) [11, 14]. Gold can occur in host minerals in one of three ways [14]:

(a)   Distributed in fractures or at the border between grains of the same mineral.

(b)   Distributed along the border between the grains of two different minerals.

(c)   Totally enclosed in the host mineral.

Pyrite [FeS_2] and arsenopyrite [FeAsS] are the two most common host minerals for gold [14], while over 20% of gold deposits are reported to contain chalcopyrite [$CuFeS_2$] [15]. The gold particles in many chalcopyrite ores are often discrete, while gold is commonly either partially or totally enclosed in pyrite and arsenopyrite ores [14, 15].

There is often considerable variation in the mineralogy within an orebody. This is especially noticeable with the depth profile of an orebody. One of the reasons for this is due to various weathering processes resulting from the percolation of surface waters down through the outcrops of sulfide minerals in the orebody [13]. This is particularly true for pyrite, which breaks down (with the assistance of ubiquitous bacteria such as *thiobacillus ferroxidans*) to form sulfuric acid and insoluble iron hydroxides. Copper, zinc and silver sulfides are dissolved by this dilute sulfuric acid solution and are thus leached from the surface layers of the ore body. As the water

containing these soluble metals percolates down through the orebody, the soluble metals can precipitate out either as secondary minerals such as malachite [$CuCO_3.Cu(OH)_2$] and azurite [$2CuCO_3.Cu(OH)_2$] or further down at the water table as secondary sulfides such as chalcocite [Cu_2S] and covellite [CuS] [13]. Even with these weathering processes, it should be noted that the primary and major (~50%) copper mineral present in the earth's crust is chalcopyrite [9].

The top layers in a weathered sulfide deposit are referred to as the oxidation zone, while the lower layers enriched with secondary sulfides are known as the supergene zone. Between these two zones lies a transitional zone [13]. Due to the common association of pyritic minerals with gold deposits, many gold deposits contain an oxidised zone in which the gold has been largely liberated and is thus relatively easy to recover.

The above discussion concerning the variations in mineralogy is important since the mineralogy will govern the type of metallurgical processes used to recover gold from the ore. For example, coarse grained native gold, as found in placer or vein deposits can be recovered with purely physical methods of mineral processing such as crushing and coarse grinding of an ore (collectively termed comminution) followed by gravity separation of the coarse gold [16]. This is by far the cheapest method of recovering coarse gold [17]. After collection of the coarse gold, the ore is subjected to further grinding prior to hydrometallurgical processing. The predominant hydrometallurgical technique for recovering gold from ores is based on the cyanidation process. This will be discussed in detail in the following section. However, it is important to recognise that many ores contain minerals and extraneous rocky material (gangue) which cannot be economically treated directly with cyanide. This is becoming increasingly important as the easily processed gold deposits are becoming exhausted.

In terms of processing, gold ores can be classified as "free milling", "complex", "refractory" and "pseudo-refractory" [18, 19]. These terms are based upon the liberation of gold from ores using conventional cyanidation practices. It should be noted that there is a diversity of opinion and definitions concerning non-free-milling

ores. Free-milling ores are regarded as giving gold recoveries greater than 90% with a conventional cyanide leach. The weathered ores in the oxidised zones are generally free-milling, although the gold can be coated with an iron oxide which can significantly reduce the gold dissolution rate [19]. La Brooy *et al.* [19] use the term "complex ores" to describe ores which give acceptable gold recovery with increased cyanide consumption. Some authors use the term "pseudo-refractory" to describe ores which require low additional costs and common modifications to gold cyanidation plants [18]. Refractory ores do not give economic gold recoveries, even with increased cyanide additions. It is generally regarded that recoveries below 80% indicate a refractory ore [18].

Many refractory ores contain either pyrite and/or copper minerals. Some of the options for treatment of refractory ores include roasting, pressure-oxidation, bio-oxidation, flotation, controlled-potential sulfidisation (CPS) pre-treatment followed by flotation and alternative leaching reagents [19]. Roasting is used for the oxidation of sulfide and telluride minerals in which the gold grains are enclosed. While roasting is still used, its use is decreasing in favour of alternative oxidation processes such as pressure oxidation and bio-oxidation that are more cost-efficient and less environmentally damaging. Flotation is usually used to prepare a concentrate prior to the oxidation of sulfide, stibnite and telluride minerals [20].

Flotation enables the separation of minerals and is used extensively in mineral processing to prepare concentrates that are subsequently treated by various methods [16]. Flotation of gold ores can be used to remove the unwanted minerals allowing cyanidation of the gold concentrate such as in the separation of gold-rich pyrite from arsenopyrite [18, 20, 21]. Alternatively, a metal (commonly copper) concentrate containing most of the gold can be prepared and subsequently smelted to recover the gold and other metals [18].

CPS pre-treatment is used for the treatment of oxidised and transition copper ores prior to flotation as conventional flotation methods are not suitable for this type of ore [18, 20, 22, 23]. In this process, NaHS is added with the E_h controlled at approximately 450 mV [20]. CPS flotation can be used for the preparation of :

a gold-rich/copper-poor concentrate suitable for cyanidation.

a gold-copper concentrate for smelting.

a copper-poor flotation tails containing gold that can be treated by cyanidation.

Alternative leaching reagents such as hypochlorous acid, thiourea, thiosulfate, hydrochloric acid and ammonia/cyanide have all been used in the treatment of refractory ores [19, 24]. However, the use of these alternative reagents is still very limited compared to cyanide.

1.3 The extraction of gold from ores with cyanide

1.3.1 Cyanidation process

Prior to commencing this section, the interested reader is directed to several excellent reviews for further information concerning the extraction of gold from ores [17, 19, 24-27] and an outstanding monograph [28].

The original patents for the extraction of gold from ores with cyanide and subsequent recovery with zinc dust were granted in 1887 and 1888 [29]. While the gold dissolution reaction was originally described by Elsner in 1849, it was not until 1954 that the electrochemical aspects of this reaction were described in detail [30]. While extensive research has been conducted since then, there is still some controversy over the complete mechanism [24]. The currently accepted mechanism can be described as shown in Eqns.1.1-1.4 [24, 26, 31]. However, it should be noted that these reactions are considered a simplistic view of a very complex system [32].

Anodic Reactions

$$Au \rightarrow Au^+ + e^- \qquad \text{(Eqn. 1.1a)}$$

$$Au^- + CN^- \rightarrow [AuCN]_{ads} \qquad \text{(Eqn. 1.1b)}$$

$$[AuCN]_{ads} + CN^- \rightleftharpoons [Au(CN)_2]^- \qquad \text{(Eqn. 1.1c)}$$

OR

$$Au^- + OH^- \rightarrow [AuOH]_{ads} \qquad \text{(Eqn. 1.2a)}$$

$$[AuOH]_{ads} + 2\,OH^- \rightleftharpoons [Au(OH)_3] + 2e^- \qquad \text{(Eqn. 1.2b)}$$

Cathodic reactions

$$O_2 + 2\,H_2O + 2e^- \rightarrow 2\,OH^- + H_2O_2 \qquad \text{(Eqn. 1.3a)}$$

$$2\,OH^- + H_2O_2 + 2e^- \rightarrow 4\,OH^- \qquad \text{(Eqn. 1.3b)}$$

Overall reaction

$$2\,Au + 4CN^- + 1/2\,O_2 + H_2O \rightarrow 2\,[Au(CN)_2]^- + 2\,OH^- \qquad \text{(Eqn. 1.4)}$$
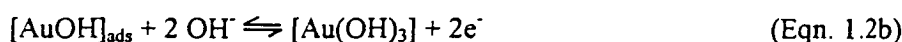
Eqn. 1.1-1.4 demonstrates that the gold cyanidation process can be considered an example of chemically induced metal corrosion. A schematic of the electrochemical mechanism of gold dissolution is shown in Fig. 1.1. In the leaching process, Au(0) is oxidised to Au(I) by oxygen. Oxygen is adsorbed and cathodically reduced on the gold surface to OH^- or H_2O_2, while Au(I) is stabilised in solution by complexation with CN^- to form $[Au(CN)_2]^-$ [24, 33, 34]. Without the presence of cyanide, the oxidation of gold generally results in the formation of oxide films (Eqn. 1.2) on the gold surface. Cyanide allows gold to be dissolved at a low solution E_h over a wide range of pH values [24]. The oxidation potential for gold in alkaline (pH 10) cyanide solution is -0.4 V, thus only requiring the mild oxidising conditions provided by air or oxygen [34]. The only gold-cyanide complex formed during the leaching process is $[Au(CN)_2]^-$ [35].
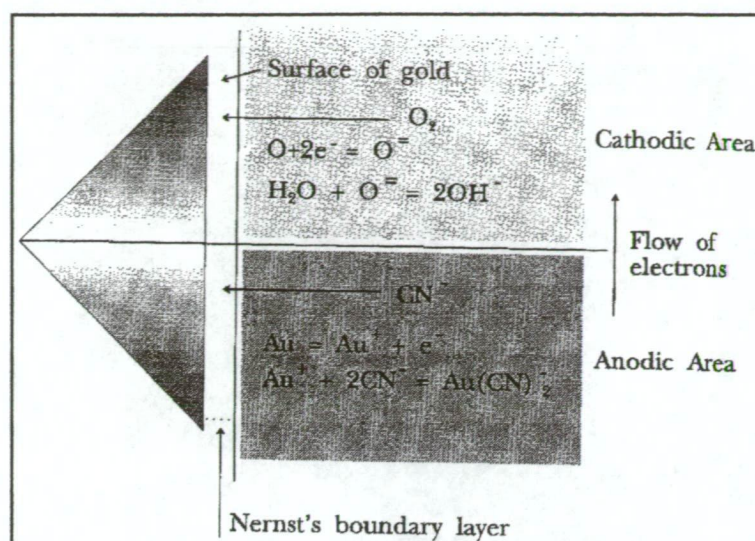
Fig. 1.1 : Schematic showing electrochemical mechanism of gold dissolution in cyanide solution. Source : Fig. 1 from [34].

Alkaline conditions are required for the cyanidation process because of the high pKa value for HCN (9.2 at 20°C in pure water [36]). The operating pH of cyanidation plants can vary from 9 to 11, depending on ore mineralogy and leach water [19]. Lime is generally used to control the leach pH. An important exception is found in the Western Australian gold fields near Kalgoorlie. The leach water is very saline and contains high concentrations of magnesium salts, which buffer the leach at approximately pH 9.3 [37]. Since higher pH values result in precipitation of $Mg(OH)_2$, economic and engineering considerations force these plants to operate with a leach pH in the range 9.0-9.2 [37]. Fortuitously, the pKa of cyanide is decreased to 8.8 in the presence of 40g/L NaCl due to activity effects [38].

The rate of gold dissolution depends on several factors. The most important factors are cyanide and dissolved oxygen concentrations, pH of the leachate, the ratio of total surface area of gold particles to cyanide concentration and redox potential (E_h) [31, 34]. Other factors include the rate of agitation in the leachate, the leach temperature and the presence of interfering components from the ore or leach water used in the leachate [34, 37].

Because the gold dissolution rate in aerated aqueous cyanide solution is reasonably slow, it is important to finely grind the ore to enable dissolution of most of the gold in 20-30 hours [17]. This time period is the usual residence time in a typical leaching circuit. With optimum cyanide concentration ($\sim$ 500 ppm NaCN), clean gold particles dissolve at a rate of 3.25 mg/cm^2/hr. These values indicate that a 325-mesh gold particle will dissolve in 13 hours, while a 100-mesh particle will take approximately 44 hours to dissolve [39]. This is another reason for the removal of coarse gold (> 100-mesh) by gravity concentration methods prior to cyanidation.

The rate-limiting step of the cyanidation process is controlled by either the diffusion rate of cyanide or oxygen through the Nernst boundary layer to the gold surface [24, 32, 34, 40]. At low cyanide concentrations (< 250 ppm CN), the rate is controlled by the diffusion of cyanide. The diffusion rate for oxygen to the gold surface controls the gold dissolution rate when the cyanide/oxygen molar ratio exceeds 10. It has been inferred from electrochemical studies that the adsorption of high concentrations of cyanide on the gold surface can passivate the surface, thus reducing the cathodic reaction [41].

The ore is generally ground in the presence of water to form a slurry (called a pulp) containing 30-50% solids. It should be noted that because comminution costs are high, there is an optimum between ground particle size and percentage of gold recovered. The leach pulp is passed through a series of leaching stages (usually tanks) which are agitated and aerated. The comminution and leaching circuits are collectively termed the "mill".

Since low grade ores cannot be economically treated in this manner, heap leaching has gained increasing importance over the past 20 years. In heap leaching, ore is mined (by open-cut mining) and transported to a specially prepared pad where it is crushed and placed on the pad. The ore heap may subsequently be agglomerated with a cement type material. When the ore heap reaches a certain height on the pad (typically 10 m), a spray system is mounted on top of the pad. This allows a dilute cyanide solution to continually trickle through the ore heap to the bottom of the pad. The pregnant cyanide solution is collected from the bottom of the pad and passed

through columns containing activated carbon to remove the $[Au(CN)_2]^-$. The barren effluent from the carbon columns is dosed with more cyanide before being reused. An even simpler variation of heap leaching is dump (or "run-of-mine") leaching. In this case, ore is transported to a specially prepared pad where it is "dumped" without any crushing. While the best overall gold recoveries from heap and dump leaching operations are approximately 80 % and 65% respectively, the processing costs are up to 10 times less than for a conventional milling operation [19, 42]. It should be noted that these recoveries may take up to 12 months, whereas in a milling circuit, the gold is recovered in a few days. These considerations are important as there are considerable costs (such as mining, reagents and labour costs) to be met while waiting for gold to be recovered from the heap or dump leach operation. It should also be noted that while heap and dump leaching have revolutionised the treatment of low grade ores, not all low grade ores are amenable to this type of treatment [43].

Conventional cyanidation plants use compressed air for the source of dissolved oxygen (DO) in the pulp. Consequently, the gold dissolution rate in these plants is restricted to the DO concentration available from air. This approach is used because it is easier to maintain and monitor a high cyanide concentration rather than a high DO concentration [44]. Both theoretical and practical studies have shown that increasing the oxygen concentration in the leachate allows for an increase in the gold dissolution rate and reduction in cyanide concentrations [45-48]. These studies have led to the relatively recent development and commercial use of various methods for increasing the oxygen level in solution by the use of compressed air, pure oxygen, hydrogen peroxide or calcium peroxide [48]. However, the use of oxidants has to be evaluated carefully for each mine due to the numerous side-reactions that can occur with different ores and leach water [34, 49]. For example, the presence of copper minerals may prevent the use of hydrogen peroxide due to the catalytic degradation of hydrogen peroxide and cyanide by Cu^{2+} [50, 51], while highly saline water (a common occurrence in the largest gold belt in Australia) can reduce the effect of oxidants [37]. An additional concern is the possibility of increasing the passivation layer on the gold surface, thus preventing effective cyanidation [24]. It has been shown that, in certain cases, the presence (either naturally occurring or added during

the leaching process) of certain heavy metal cations such as Pb^{2+} or Hg^{2+} can disrupt the passivation layer on the gold surface and thereby increase the rate of cyanidation [26, 44, 46, 52, 53].

1.3.2 Recovery of $[Au(CN)_2]^-$ from leachate

Various methods have been employed to recover the $[Au(CN)_2]^-$ complex from the leachate. The two predominant recovery methods are the Merril-Crowe process and the Carbon-In-Pulp/Carbon-In-Leach process (CIP/CIL) which use zinc or activated carbon, respectively [Labrooy, 1994 #1009]. Ion-exchange resins have been developed for Resin-In-Pulp processes (RIP). While RIP has only had very limited use in Western countries, it has been used to recover approximately 50% of the gold produced in countries belonging to the former Soviet Union [54].

The first method employed to recover gold from the cyanide leachate used zinc (either dust or shavings) [29]. The chemistry behind this recovery process is a series of electrochemical reactions involving the dissolution of zinc and precipitation of gold as shown in Eqns. 1.5-1.7 [55]. It is necessary to perform this operation in de-oxygenated solutions to prevent excessive consumption of zinc, as shown in Eqn. 1.5 and to prevent re-dissolution of precipitated gold [33]. It is also necessary to use a clear solution, so that the precipitated gold can be easily collected. This was achieved in the Merrill-Crowe process by filtering the leach pulp under vacuum to obtain a clear, de-aerated solution into which zinc dust was fed [29, 55]. Prior to this filtering step, the leachate is usually passed through a series of clarifiers such as counter-current decanters (CCD) or hydrocyclones to remove most of the suspended solids in the leach pulp.

$$2\ Zn + 8\ CN^- + O_2 + 2\ H_2O \rightleftharpoons 2\ [Zn(CN)_4]^{2-} + 4\ OH^- \qquad \text{Eqn. 1.5}$$

$$2\ [Au(CN)_2]^- + Zn \rightleftharpoons 2Au + [Zn(CN)_4]^{2-} \qquad \text{Eqn. 1.6}$$

$$Zn + H_2O + 2\ [Au(CN)_2]^- \rightleftharpoons 2\ Au + HZnO_2^- + 3H^+ + 4\ CN^- \qquad \text{Eqn. 1.7}$$
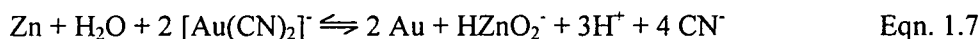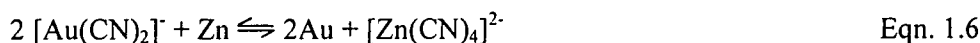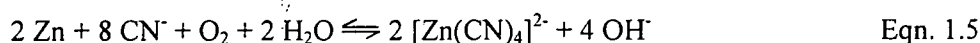
The development of the CIP process using activated carbon to recover the $[Au(CN)_2]^-$ complex has replaced zinc cementation processes (such as the Merrill-

Crowe) as the major recovery method [56]. However, zinc cementation is still used in older gold mining regions and is still preferred for some high grade gold ores, ores containing high silver:gold ratios and small gold mines [56].

The development of activated carbon for gold recovery is an interesting combination of advances in science and engineering, economic effects, changes in government regulation and professional dogma. The recovery of gold with activated carbon was patented as early as 1894 [57]. However, its use was not economically viable at this time as the only method of recovering gold from carbon was by burning the carbon. The original development of the CIP process is attributed to Chapman at the University of Arizona in the 1930's. One of the methods developed by Chapman for recovering the gold from the activated carbon was by stripping the carbon with a hot cyanide solution, which removed the need for burning or smelting the carbon [57]. The Chapman system was further modified by Zadra [at the US Bureau of Mines (USBM)] in the early 1950's. Zadra developed alternative stripping solutions and more importantly, electrowinning cells to recover the gold from eluted from the carbon and the use of a kiln to regenerate the activated carbon. These developments allowed the carbon to be recycled, thus making its use economically feasible. However, while a few smaller operations did employ activated carbon, it was not until 1973 that the first large scale CIP plant was constructed and commissioned at the Homestake Gold Mine in South Dakota, USA [29, 58]. There were several reasons for the construction of the CIP plant:

- The existing plant required replacement.

- Several improvements to the Zadra process had been developed by the USBM for use at the Cripple Creek and Cretchell Gold mines [58].

- Considerable amounts of mercury had been used at Homestake in an amalgamation process to recover 60% of the gold from the grinding circuit. New environmental regulations introduced in 1970 required the discharge of mercury from the Homestake Gold mine to be stopped. These new regulations required a drastic change in procedures [59].

The price of gold was de-regulated in 1971 after being controlled for over twenty years under the Bretton-Woods agreement [60]. This agreement held the gold price constant at $US 35 per ounce for this period. After this agreement was abandoned by the US government due to fiscal problems, the price of gold rose quickly in the early 1970's, rising to a record $850 per ounce in January 1980 [61]. This increase in gold price no doubt contributed to the success of the Homestake CIP plant.

Following the success of the CIP process at the Homestake mine, there have been numerous CIP plants installed around the world, with many following the design used at Homestake [58, 62]. Mintek (formerly The South African Council for Mineral Technology) and the Anglo-American Research Laboratories (AARL) in South Africa contributed greatly to the understanding and improvements in the CIP process in the late 1970's [56, 57].

The effect of the increased gold price mentioned above also contributed to these developments. Additional factors favouring the CIP process are :

-   The ability to easily accommodate ores with a high clay content (commonly found in Western Australian ores) which were difficult to filter in the Merrill-Crowe process [63].

-   The CIP process is preferential for the treatment of lower grade ores as it achieves lower solution gold concentrations in the tails [63].

-   It has also been asserted that the capital and operating costs of CIP and CIL plants are 60-90% those of Merrill-Crowe installations [64]. This is primarily due to the removal of equipment and labour costs required to produce a clear filtrate for the Merrill-Crowe process.

The above factors greatly contributed to the rapid increase in global gold production during the 1970's and 1980's, with the most significant increases occurring in Australia [28, 63]. Muir [33] has compared the advantages and disadvantages of using zinc or activated carbon to recover $[Au(CN)_2]^-$ from the leachate. This comparison is shown in Table 1.1.

1.3.2.1 Some background information on the carbon adsorption process

There have been extensive investigations concerning the adsorption of the Au(I) cyanide complex onto activated carbon. It is now accepted that $[Au(CN)_2]^-$ is adsorbed without chemical change on the activated carbon [65]. Adams and Fleming [66] have proposed that, under normal plant conditions of high ionic strength, adsorption occurs via the formation of an ion-pair with cations such as Na^+ and Ca^{2+}, although this mechanism is disputed by other authors [65]. It has also been suggested that at low ionic strength, an ion-exchange mechanism may account for the adsorption process [67]. Unfortunately, current experimental techniques (such as XPS and FTIR) are unable to distinguish between the ion-pair and ion exchange mechanisms [67].

The activated carbon used in the CIP/CIL process must be abrasion resistant so that it can be mixed in the leach pulp and subsequently removed by screening without loss of fine carbon particles loaded with gold. The carbon must be sufficiently coarse to allow effective separation from the pulp and must be sufficiently porous so to allow as large a surface area as possible for adsorption. It has been shown that the most important parameter for activation of the carbon is the activation temperature and the micropore volume is the structural parameter of greatest significance [68].

The carbon of choice for many plants is made from coconut shells because of its hardness and resistance to abrasion [58]. The other two most common sources for carbon are peat and coal [69], while various fruit kernels have also been used for producing activated carbon [70]. Recent work indicates that activated carbon prepared from *Eucalyptus globulus* may be superior to that obtained from coconut shells [71]. Otherb recent work has demonstrated that synthetic carbons (prepared by the reduction of methane) are superior to their vegetable counterparts [68].

Recovery system	Advantages	Disadvantages
Zinc	- Efficient - Simple - Cheap	- Sensitive to pH and [CN⁻] - Sensitive to impurities (S^{2-}, As, Sb, Cu^{2+}) - Sensitive to O_2 - Non-selective - Labour intensive
Carbon	- Efficient - Simple - Cheap if carbon recycled - Clean product - Particularly suited to low grade ores and CIP/CIL - Insensitive to O_2 - Relatively insensitive to impurities	- Partially selective - Subject to Cu and Ca contamination - Can be difficult to completely strip Au

Table 1.1: Comparison of advantages and disadvantages zinc (Merril-Crowe) and carbon (CIP/CIL) methods of recovering gold from solution. Adapted from [33].

1.2.3.2 Operation of a typical CIP/CIL plant

In the CIP process, the leaching and adsorption stages are kept separate. That is, there are leaching tanks (where all the leaching from the ore occurs), followed by a series of adsorption tanks, where the activated carbon is added. Most of the $[Au(CN)_2]^-$ complex in the leach pulp is then adsorbed onto the activated carbon. Between the leaching and adsorption stages, there are hydrocyclones that separate large ore particles from the slurry, which are then sent back to the leaching tanks. Typically there are up to 3 leaching tanks and up to 6 adsorption tanks. The carbon is moved through the adsorption tanks in a counter current movement so that the adsorption kinetics are most favourable in the adsorption tanks with the lowest gold

concentration [33]. Generally, the gold concentration in the leach pulp discharged to the tails dam is less than 20 ppb.

The CIL process is similar to the CIP process. The major difference is that carbon is added into the leaching tanks to allow concurrent leaching and adsorption, which enhances leaching from the ore and preventing preg-robbing. Preg-robbing is a term used to describe an ore which adsorbs the $[Au(CN)_2]^-$ complex. Many minerals (including several pyritic minerals), carbonaceous material and organic compounds and silica have been shown to be preg-robbing [72-76]. Consequently, many plants operate with a combined CIP/CIL process to avoid gold losses. This compromise will be closer to CIP for high grade/slow leaching ores and closer to CIL for low grade/fast leaching/preg-robbing ores [19].

The loaded carbon is removed from the first adsorption tank and subsequently the gold is stripped from the carbon. Various stripping procedures have been used since the inception of CIP plants. Most stripping procedures are based on either the Zadra method and its refinements or alternative methods developed by the AARL. The Zadra method uses hot caustic NaCN solutions. Part of the AARL process uses deionized water, which is not suitable in arid regions with highly saline underground waters, a common occurrence for Australian gold mines. High pressure and organic solvents have been used to enhance stripping rates [57]. An alternative stripping procedure, the Micron process, was developed in Western Australia. This process uses a methanol reflux to strip the carbon in 6-8 hours and is not affected by salinity or organically fouled carbon [26]. However, due to scaling problems and the flammability of methanol, the Micron process has not been widely adopted in the gold industry [77].

1.3.3 Problems with the gold cyanidation process

There are three fundamental reasons why ores may not be amenable to conventional cyanidation [19]. In highly refractive ores, the gold can be totally or partially enclosed in the host mineral preventing leach reagents from contacting the gold [14]. In complex ores, reactive minerals may consume leach reagents decreasing the

cyanide and/or oxygen concentrations below that required to leach gold. Finally, preg-robbing or precipitation may remove the $[Au(CN)_2]^-$ complex from the leach liquor.

There are numerous minerals associated with gold deposits that consume both oxygen and cyanide during the cyanidation process. For example, oxidation of pyrrhotite (FeS) and chalcocite (Cu_2S) in alkaline cyanide solution can be represented, as shown in Eqns. 1.8 and 1.9 [44, 78]

$$2\ FeS + O_2 + 12\ CN^- + H_2O \rightarrow 2\ [Fe(CN)_6]^{4-} + 2\ S^0 + 4\ OH^- \qquad \text{(Eqn. 1.8)}$$

$$2\ Cu_2S + O_2 + 14\ CN^- + H_2O \rightarrow 2\ [Cu(CN)_3]^{2-} + 4\ OH^- + 2\ SCN^- \qquad \text{(Eqn. 1.9)}$$
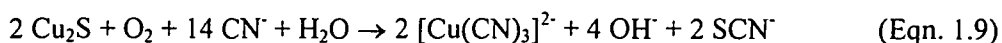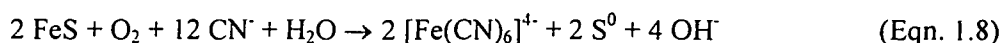
Since gold is a very rare element with an average natural abundance of 4 ppb [9], it is quite common for these undesirable minerals to be in much greater abundance than gold. Because these minerals consume cyanide, they are termed "cyanicides". Cyanicides are those substances found in ores, concentrates and tailings that cause a loss of cyanide from the leach solution and thus result in excessive cyanide consumption. Cyanicides include natural acids (carbonic and humic); cyanide soluble salts such as sulfates and arsenates; ferrous salts and oxidation compounds of copper, zinc, arsenic, and antinomy; and certain sulfur compounds that react to form thiocyanate [17].

It is considered that, on a global basis, the two most important cyanicides are sulfide minerals (pyrites) and copper minerals [28]. It should also be noted that both sulfide and copper minerals often occur together for the reasons outlined in Section 1.2. For example, it is estimated that approximately 50% of global copper deposits occur as chalcopyrite ($CuFeS_2$) [9]. The reaction of pyrites and cyanide under aerobic conditions has been investigated by Luthy [79, 80]. A summary of the reaction pathways is shown in Fig. 1.2. The ultimate sulfur-containing products of these reactions are sulfate and thiocyanate. The effects of copper minerals on the cyanidation process are discussed in the next section. In addition to the products shown in Eqns. 1.8 and 1.9, other metallo-cyanide complexes and cyanate can be formed during the cyanidation process.

Cyanate is formed by the oxidation of cyanide. While aqueous solutions of cyanide are thermodynamically unstable, the rate of oxidation is slow at high pH values, if no catalysts are present [31]. Activated carbon has been shown to be a catalyst for the oxidation of cyanide to cyanate [81-83]. The oxidation becomes especially noticeable during the stripping of gold from activated carbon with hot caustic cyanide. The high temperature is used to facilitate rapid stripping. The oxidation on activated carbon is enhanced in the presence of Cu^{2+} or $[Cu(CN)_2]^-$ [81]. This is because cupric ions are reduced and complexed in the presence of excess cyanide, while cyanide is oxidised to cyanogen, which subsequently undergoes hydrolysis to form cyanate, as shown in Eqn. 1.10 [84, 85]. The $[Cu(CN)_3]^{2-}$ complex is shown in Eqn. 1.10, as this is the major Cu(I) complex found in typical cyanide leachates [35]. The rate of cyanogen hydrolysis is considerably slower than the oxidation rate and is dependent on the solution pH [84, 85]. In addition, the $[Cu(CN)_2]^-$ complex adsorbed on the activated carbon is readily oxidised by air to malachite, as shown in Eqn. 1.11, thus providing a continual source of Cu(II) [81]. This synergistic catalytic oxidation of cyanide in the presence of both activated carbon and Cu(II) has been proposed as a means for the destruction of cyanide wastes in tails dams [86].

$$Cu^{2+} + 5\ CN^- \rightarrow [Cu(CN)_3]^{2-} + (CN)_2 \qquad \text{(Eqn. 1.10a)}$$

$$(CN)_2 + 2OH^- \rightarrow CN^- + CNO^- + H_2O \qquad \text{(Eqn. 1.10b)}$$

$$2\ Cu^{2+} + 7\ CN^- + 2OH^- \rightarrow 2\ [Cu(CN)_3]^{2-} + CNO^- + H_2O \qquad \text{(Eqn. 1.10c)}$$

$$2\ [Cu(CN)_2]^- + 5\ O_2 + 9\ H_2O \rightarrow Cu(OH)_2CuCO_3 + 3\ CO_3^{2-} + 4\ NH_4^+ \qquad \text{(Eqn. 1.11)}$$
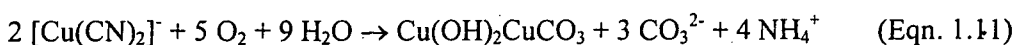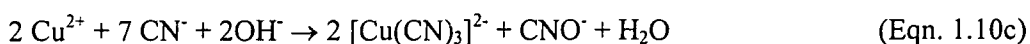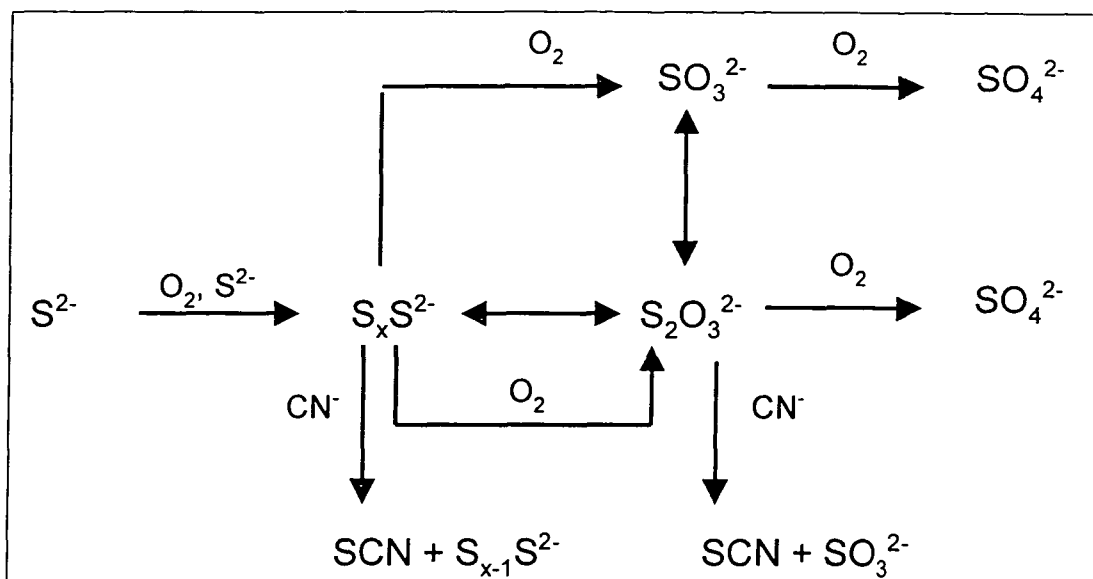
Fig. 1.2: Schematic for the reactions of sulfides (from pyrites) and cyanide in aerated solution. S_xS^{2-} represents polysulfides. The ultimate products of these reactions are sulfate and thiocyanate. This reaction scheme was adapted from [79].

1.3.4 Effects of copper minerals

The effects of copper minerals on the gold cyanidation process are well known to gold metallurgists and have been reviewed by several authors [15, 22, 39, 87-89]. A discussion of the aqueous chemistry of the Cu(I)-cyanide complexes relevant to the gold cyanidation process is presented in section 1.4. To simplify terminology, the CN:Cu mole ratio will commonly be referred to as R throughout this thesis.

1.3.4.1 High cyanide consumption due to dissolution of copper minerals

Gold-copper ores with reactive copper minerals will be dissolved in an alkaline cyanide solution until either all the cyanide or cyanide-soluble copper minerals have been consumed. The rate of copper dissolution decreases as cyanide is consumed. If an excess of mineral is used, the alkaline cyanide solution will dissolve copper minerals until the R value of the solution is between 2.5 and 3.5 [39]. Several authors have reported that the cyanide consumption is directly proportional to the copper content of an ore. Two papers cited by Nguyen [89] found that cyanide consumption increased from 2 to 7 kg NaCN/tonne of ore (kg/t) as the copper

content rose from 0.1% to 0.5%. The gold recovery decreased from 90% to 70% over this range of copper contents. Kittel and Harbort [23] report that for each 0.01% increase in cyanide-soluble copper content above 0.06%, the cyanide consumption was increased by 0.3 kg/t. The difference in the rate of cyanide consumption between these reports is due to differences in copper mineralogy.

The cyano products of the dissolution reactions of copper minerals are the Cu(I)-cyanide complexes and cyanate as shown in Eqn. 1.10. While three Cu(I)-cyanide complexes exist, the major Cu(I)-cyanide complex present in typical gold cyanidation leachates is $[Cu(CN)_3]^{2-}$ [35]. Additional cyano species such as thiocyanate and other metallo-cyanide complexes may also be formed from other elements present in the copper minerals.

It was mentioned above that the degree of cyanide solubility varies with copper mineralogy. This was investigated in 1931 by Leaver and Woolf [90], with the results shown in Table 1.2. Because of these differences, it is important to discriminate between the acid-soluble copper content and cyanide-soluble copper content in an ore [89, 91]. It should be noted that the cyanide solubility of chalcopyrite is the lowest for all the copper minerals. This is fortunate, as this is the major copper mineral [9]. However, it should be noted that a recent paper has reported the cyanide solubility of chalcopyrite to be approximately 35% of the total copper [52], which is much higher than the value of 5.6% reported by Leaver and Woolf [90]. An additional point to note is that many of the surface and near surface gold deposits are being exhausted [19]. Consequently, in the case of gold-copper deposits, the copper minerals at lower depths in existing deposits are more likely to occur as secondary copper minerals, as discussed in Section 1.2. Most of these copper minerals are much more reactive than chalcopyrite and are almost completely cyanide soluble, as shown in Table 1.2.

A more recent study has noted the difference in copper and gold solubility with four different minerals, as shown in Table 1.3. These results are interesting as they demonstrate the severe effect of the more reactive copper minerals on the dissolution of gold. The copper concentration in solution decreased after 24 hours for the most

reactive mineral, cuprite. This was due to precipitation of CuCN and other copper compounds from solution. This precipitation occurred due to the low R value in this leach slurry.

Mineral		Total Cu dissolved (%)	
		at 23°C	at 45°C
Azurite	$2\,CuCO_3 \cdot Cu(OH)_2$	94.5	100.0
Malachite	$CuCO_3 \cdot Cu(OH)_2$	90.2	100.0
Cuprite	Cu_2O	85.5	100.0
Chrysocolla	$CuSiO_3$	11.8	15.7
Chalcocite	Cu_2S	90.2	100.0
Chalcopyrite	$CuFeS_2$	5.6	8.2
Bornite	$FeS \cdot 2Cu_2S \cdot CuS$	70.0	100.0
Enargite	$3\,CuS \cdot As_2S_5$	65.8	75.1
Tetrahedrite	$4\,Cu_2S \cdot Sb_2S_3$	21.9	43.7
Metallic copper	Cu	90.0	100.0

Table 1.2: Solubility of copper minerals in 20 mM NaCN solutions with a 24 hour leaching period. Reproduced from [39], which was citing work reported in 1931 by Leaver and Woolf [90].

Copper mineral	After 4 hours		After 24 hours	
	Cu (mg/L)	Au (%)	Cu (mg/L)	Au (%)
$CuFeS_2$	237	40	425	100
CuO	657	30	757	70
Cu_2S	812	10	815	27
Cu_2O	1022	10	862	25

Table 1.3: Solubility of copper and gold from different copper minerals leached with 1.6 g/L NaCN. Initial concentration of copper in leach slurry from each mineral was 15 g/L. Source : Table 2 from [92].

Early studies by Hedley and Kentro [93], which are cited by many authors, have shown that the gold leaching rate in the presence of Cu(I)-cyanide complexes is dependent on the R value and not on the cyanide concentration determined by the standard silver nitrate titration. This is demonstrated in Fig. 1.3. It is important to note that a relatively low concentration of NaCN (2.2 mM) achieves the maximum rate of gold dissolution when no copper is present. However, when copper is present, it is essential that the ratio of total cyanide concentration (determined by acid distillation) to the total copper concentration is known so that efficient gold leaching can be attained. Hedley and Kentro [93] observed that the gold dissolution rate decreased rapidly when R was less than 3, and increased almost linearly when R was increased from 3 to 4, at which point the gold dissolution rate was equivalent to that of free cyanide. The gold leaching rate increased slowly when R was greater than 4. In a review, Muir *et al.* [22] stated that the gold leaching rate with an R value of 4 was approximately half that with free cyanide. This comment would appear to be in conflict with the above studies by Hedley and Kentro [93].

Recent work has supported the earlier studies by Hedley and Kentro [93]. This is demonstrated in Fig. 1.4, which shows the effect of cyanide soluble copper on gold dissolution for 1, 4 and 24 hour leaching periods. For the above reasons, metallurgists will try to avoid treating gold-copper ores directly with cyanide due to the high cyanide consumption. However, if direct cyanidation of cyanide soluble copper ores is required, then it is important to maintain an optimal R value. An R value of 4 is commonly recommended, especially when treating the ore in a leaching circuit. It has been stated that each mole of cyanide-soluble copper requires 5 moles of cyanide to enable efficient gold dissolution [39, 94]. This ratio of 5:1 is presumably due to the presence of many cyanide-soluble Cu(II) minerals which consume cyanide via the redox reaction shown in Eqn. 1.10.
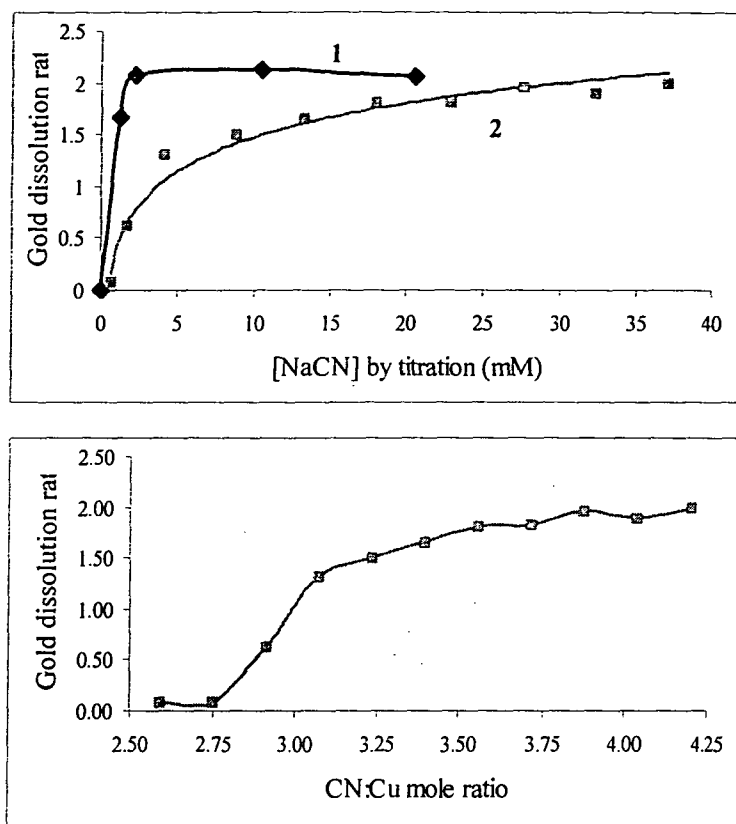
Fig. 1.3: Effect of cyanide-soluble copper on gold dissolution rate. **(a)** (Top): Comparison of [NaCN] (determined by $AgNO_3$ titration) required when : **(1)** No Cu present during leaching. **(2)** Total [Cu] in solution = 31.8 mM. **(b)** (Bottom): Effect of $[CN_{TOTAL}]:[Cu_{TOTAL}]$ (R) on gold dissolution rate shown in **(2)**. The gold dissolution rate units are: $mg/cm^2/hr$. Source: [93]
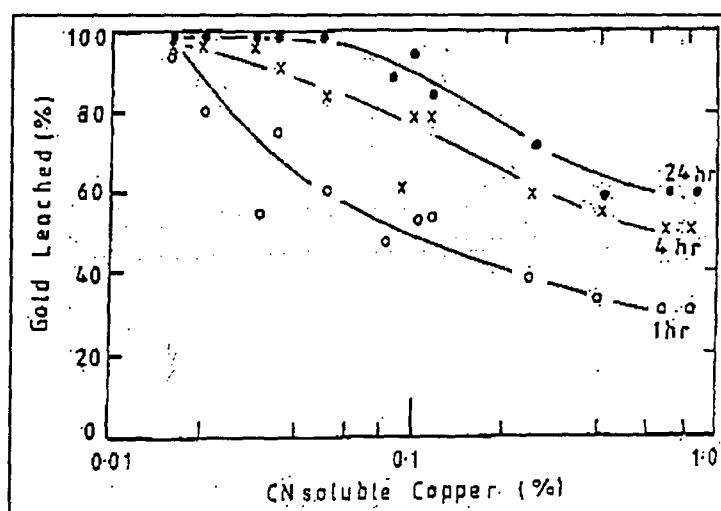
Fig. 1.4: Effect of cyanide soluble copper on gold dissolution. Leaching periods of 1, 4 and 24 hours are shown. Source : Fig. 2 from [89].

It should be noted that various reports exist in the literature in which gold leaching was still occurring, albeit very slowly, when R values were well below 3, and as low as 2.2 [88, 89, 93, 95]. Consequently, heap and dump leaching operations can use an R value lower than 4 due to the much longer contact times between the leachate and ore.

It is also worth noting that various observations have found that the rate of dissolution for both gold and copper decreases with the R value, although the leaching kinetics are much more rapid for cyanide-soluble copper minerals compared to gold at the same R value [96]. These changes in the gold and copper dissolution rates can be directly attributed to changes in the speciation of the Cu(I)-cyanide complexes. These changes in speciation will be discussed in the following section.

There have been various reports concerning the leaching of gold with Cu(I)-cyanide complexes. Based on earlier experiments [22, 97], La Brooy [22, 97] has inferred that CN^- and $[Cu(CN)_4]^{3-}$ have similar relative gold leaching rates, while the leaching rate is much less with $[Cu(CN)_3]^{2-}$. This is consistent with the earlier observations since the $[Cu(CN)_4]^{3-}$ would only be a minor species in typical cyanidation leachates.

Parsons et al. [88] analysed the same experimental data used by La Brooy [22, 97] and found that the gold leaching rate in the presence of free cyanide is approximately 25 times greater than with Cu(I)-cyanide complexes and no measurable "free" cyanide. However, measuring "free" cyanide in the presence of Cu(I)-cyanide complexes is problematic, as shown in Fig. 1.4, due to the lability of the cyanide ligands [98, 99]. This issue will be discussed later.

The almost linear increase in the gold leaching rate observed as the R value was increased from 3 to 4 was further investigated by Zheng et al. [41]. Based on a comparison of experimental results and calculated equilibrium concentrations of the three Cu(I)-cyanide complexes, it was concluded that the increase in concentration of uncomplexed (free) cyanide could not alone account for the increase in gold leaching rate. Based on this conclusion, it was proposed that some of the Cu(I)-cyanide complexes must be involved in the increase in gold leaching rate. While these

observations and arguments are useful, it must be recognised that there is still some debate concerning the values of the stability constants of the Cu(I)-cyanide complexes, as will be shown in the following section. Consequently, the above argument may be flawed if the stability constants used for these calculations are incorrect.

Based on thermodynamic calculations, Vukcevic [92] has recently proposed the following equations (Eqns. 1.12-1.15) for the formation of $[Au(CN)_2]^-$ from each of the three Cu(I)-cyanide complexes. For comparison, the free energy calculated for the formation of $[Au(CN)_2]^-$ from CN^- (Eqn. 1.2) was -46.86 kcal/mol. The kinetics of these reactions were not discussed. However, as mentioned above, the observations of previous workers would indicate that the kinetics involving the $[Cu(CN)_2]^-$ complex (Eqn. 1.15) would be very slow, if at all possible.

$$Au + 2\ [Cu(CN)_4]^{3-} + 1/4\ O_2 + 1/2\ H_2O \rightarrow [Au(CN)_2]^- + 2\ [Cu(CN)_3]^{2-} + OH^-$$

$$\Delta G = -42.68\ \text{kcal/mol} \qquad \text{(Eqn. 1.13)}$$

$$Au + 4\ [Cu(CN)_3]^{2-} + 1/2\ O_2 + H_2O \rightarrow [Au(CN)_2]^- + 4\ [Cu(CN)_2]^- + 2\ OH^-$$

$$\Delta G = -69.32\ \text{kcal/mol} \qquad \text{(Eqn. 1.14)}$$

$$Au + [Cu(CN)_2]^- + 1/4\ O_2 + 1/2\ H_2O \rightarrow [Au(CN)_2]^- + Cu^+ + OH^-$$

$$\Delta G = -48.89\ \text{kcal/mol} \qquad \text{(Eqn. 1.15)}$$
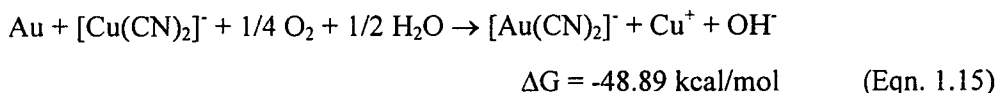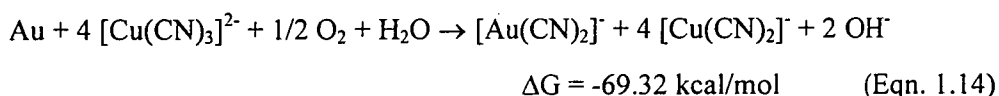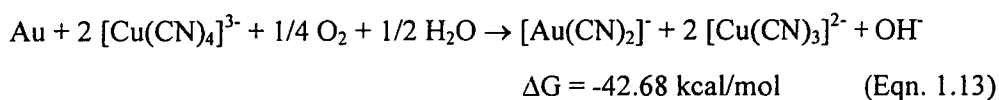
1.3.4.2 Effect of Cu(I)-cyanide complexes on activated carbon

The Cu(I) cyanide complexes formed during cyanidation can foul the activated carbon in the CIP/CIL circuit. This fouling is a function of R since only the $[Cu(CN)_2]^-$ complex is strongly adsorbed on activated carbon, while the multi-charged $[Cu(CN)_3]^{2-}$ and $[Cu(CN)_4]^{3-}$ complexes are repelled by the negatively charged carbon surface [100, 101]. If sufficient $[Cu(CN)_2]^-$ is adsorbed on the carbon, then gold loadings will be reduced, which can potentially lead to gold losses as shown in Fig. 1.5 [89]. In addition, it is difficult to remove the adsorbed $[Cu(CN)_2]^-$ from the carbon. For this reason, it is important for the CIP/CIL plant operator to maintain a high cyanide concentration when treating cyanide soluble copper minerals, even in the latter stages of the CIP/CIL circuit.
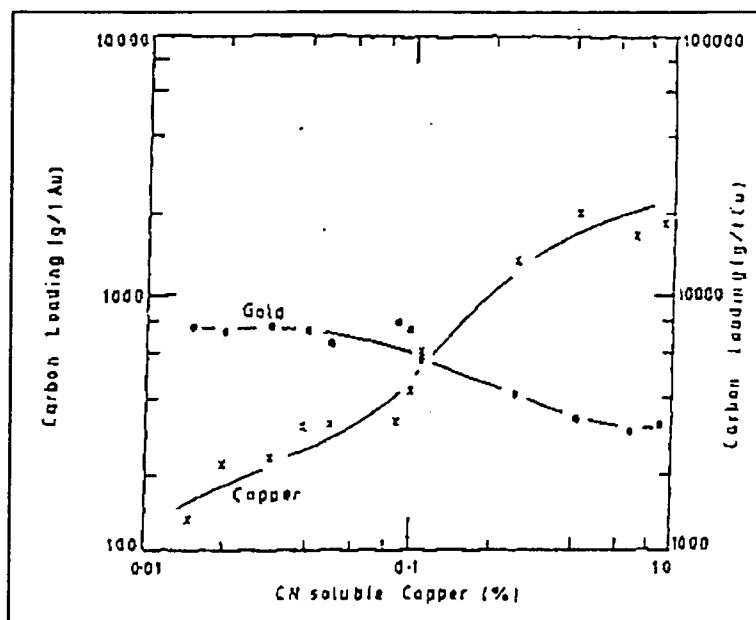
Fig. 1.5: Effect of cyanide soluble copper on carbon loadings. Note the different scales for gold and copper loadings. Source: Fig. 3 [89].

1.3.4.3 Analysis of cyanide in the presence of Cu(I)-cyanide complexes

It has already been shown that it is difficult to determine the concentration of free cyanide in the presence of Cu(I)-cyanide complexes with the titrimetric method used for monitoring the cyanidation process. The titrimetric method is based on an argentometric titration as shown in Eqn. 1.16 [39, 98, 102]. This titration was initially developed by Liebig in 1851 [103], with the endpoint being indicated by the development of turbidity due to the formation of insoluble AgCN after all the excess cyanide had been consumed to form the soluble $[Ag(CN)_2]^-$ complex, as shown in Eqn. 1.16b. Déniges [104] modified the Liebig method in 1893 by the introduction of a potassium iodide indicator and the use of an ammonical buffer. The endpoint is detected in the Déniges method by the development of turbidity due to the formation of a AgI precipitate, as shown in Eqn. 1.16c. Variations of this method are still in common use on many gold mines. The Ag^+ sensitive indictor, 5-(4'-dimethylaminobenzyliden)-rhodanin, is now the most commonly recommended indicator for the argentometric titration of cyanide [39, 105, 106].

$$Ag^+ + CN^- \rightleftharpoons AgCN_{(s)} \qquad\qquad \text{(Eqn. 1.16a)}$$

$$AgCN_{(s)} + CN^- \rightleftharpoons [Ag(CN)_2]^- \qquad \text{(Eqn. 1.16b)}$$

$$Ag^+ + I^- \rightleftharpoons AgI_{(s)} \qquad\qquad \text{(Eqn. 1.16c)}$$

There can be difficulties in observing the end-point with a visual indicator when the samples are either coloured or contain high levels of suspended solids [107]. In addition, high concentrations of anions such as sulfate or phosphate, which form silver compounds of low solubility, can also cause interferences in the silver nitrate titration [102]. The problems due to sample colouration can be avoided by monitoring the titration potentiometrically. Potentiometric titration can also reduce the errors between different operators [108].

The metallo-cyanide complexes of zinc and copper both interfere in the titrimetric determination of free cyanide. However, while the Cu(I) complexes have a significant effect on the gold dissolution rate, the zinc complexes are considered to have the same leaching ability as free cyanide [98]. It should be noted that a potential problem could arise in a carbon adsorption circuit in the presence of large concentrations of zinc cyanide complexes as these complexes can competitively occupy adsorption sites on the carbon [109].

The titrimetric interference from the Cu(I)-cyanide complexes was reported as early as 1901 [110]. There have been several studies on the potentiometric titration of the Cu(I)-cyanide complexes [85, 98, 111, 112], with the studies by Willis [98] and Lee [112] focused on the gold cyanidation process. The variation in potential observed during the separate potentiometric titrations of a KCN solution and a Cu(I)-cyanide solution with an R value close to 3 is shown in Fig. 1.6 [98]. An inflection is found at approximately the composition of $[Cu(CN)_3]^{2-}$. The inflection is not very steep and shows the $[Cu(CN)_3]^{2-}$ complex is not very stable. Brigando [111] observed that the titration of a solution prepared from $K[Cu(CN)_4]$ had an additional inflection point and that a temperature range between 0°C and ambient had no effect on the potentiometric titration curves. From these and other studies, it was found that the positive interference results from the partial dissociation of the $[Cu(CN)_3]^{2-}$ complex

during the titration as shown in Eqn. 1.17, resulting in an indefinite endpoint and an over-estimation of the free cyanide concentration [98].

$$[Cu(CN)_3]^{2-} \rightleftharpoons [Cu(CN)_2]^- + CN^- \qquad \text{(Eqn. 1.17)}$$
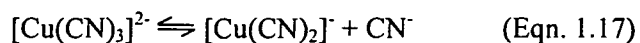
Because of the over-estimation, the apparent free cyanide determined by titration should be sufficient to leach gold at a moderate rate, which is not the case as shown in Fig. 1.3 [93]. Willis also noted [98] : "...even if a titration shows the presence of a particular complex at the end-point, it does not necessarily imply that this complex was present in the original solution." Willis also observed that titrating a solution containing substantially only $[Cu(CN)_3]^{2-}$ before and after the addition of a known amount of alkali cyanide (NaCN or KCN) resulted in the titration increasing by less than that expected for the solution with added alkali cyanide.

To overcome this analytical problem, it is necessary to determine both the cyanide and copper concentrations in solution. The copper analysis can be rapidly performed with atomic absorption spectrometry (AAS). The standard method for determining the cyanide concentration in the presence of metallo-cyanide complexes requires treatment with acid and subsequent distillation of the liberated HCN, which is then collected in a NaOH solution. Suction is applied after the NaOH trap to enable air sparging of the distillation flask. The gas flow rate is critical since an insufficient flow rate will not purge all the HCN, while an excessive flow rate will result in the loss of some HCN from the NaOH trap [105, 113]. The configuration of a typical apparatus is shown in Fig. 1.7.

While the acid distillation procedure is used widely, especially for environmental purposes, it is a laborious and time-consuming method, which requires careful attention in order to obtain complete recovery of the liberated cyanide. Consequently, such a technique is not used regularly for monitoring the cyanidation process when treating cyanide-soluble copper minerals.
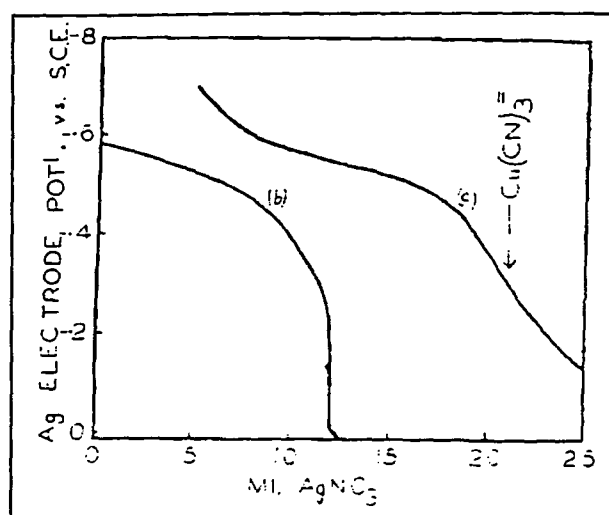
Fig. 1.6: Potentiometric titrations of (**b**) KCN and (**c**) 14.3 mM Cu(I)-cyanide (R=3.11) solutions with 20 mM AgNO$_3$. Source : Fig. 4 from [98]. Note the titration curve for (c) is offset by 5 mL for clarity.
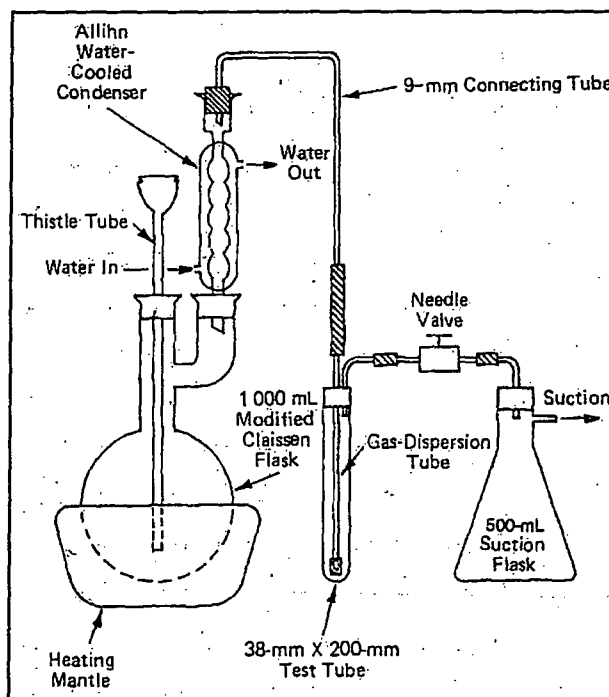
Fig. 1.7: Cyanide distillation apparatus. Source : Fig. 412.1 from [105]

The most commonly used method on operational gold mines for estimating the R value during the cyanidation of gold-copper ores is to use the silver nitrate titration described above, combined with a periodic copper analysis. This requires the use of

"fudge" factors, which have previously been determined in controlled laboratory tests. Unfortunately, the copper results are often only available after several hours. This can result in significantly reduced R values in the leachate when treating ore of a variable composition. Because of these reasons, gold mines tend to use excessive cyanide to compensate for ore variations.

1.3.4.4 Other problems associated with copper minerals

Increased lime consumption may be required to increase the pH [89, 114]. This increased pH will increase the dissociation of HCN, thus indirectly increasing R, which is important for reasons discussed earlier.

The large concentrations of Cu(I)-cyanide complexes in the effluent passed to the tailings dams can pose a significant environmental hazard, depending on the location of the gold mine.

1.3.4.5 Some processing options for dealing with copper minerals

It is generally considered that ores containing from 0.1 to 1.0 % copper or higher are uneconomical to treat by conventional cyanidation due to the large consumption of cyanide [87].

When gold-copper ores are treated in a conventional cyanidation plant, the metallurgists aim to operate the leaching circuit with an R value close to 4 for the reasons discussed above. However, the R value is difficult to monitor for reasons that were also discussed above. In addition, the cyanide soluble copper concentration in the ore passing through the mill is often fluctuating. This can result in gold losses when the cyanide soluble copper levels rise and the R value subsequently decreases. To overcome this, operators often use excess cyanide to prevent gold losses, which can result in expensive reagent costs. The cost of environmental remediation (if required by government regulations) will also increase with excessive cyanide consumption. Additional leaching tanks and/or decreased ore processing rates can help to alleviate these problems by increasing the residence time

---

in the leaching circuit (and thus allow a lower R value) [15]. However, both these engineering solutions incur financial penalties.

Several alternative methods for treating gold-copper ores are in use or have been proposed. It should be recognised that the ore mineralogy and gold grade will influence the economic viability of a particular process. Chamberlain [8] has recently reviewed the process options available and set the following limits concerning gold grade: If the gold grade is less than 2 grams/tonne (g/t), then heap leaching is generally the only viable option. If the gold grade is 2 - 4 g/t, then it may be possible to treat the ore with a conventional mill or flotation or gravity separation. If the gold grade is greater than 4 g/t and the ore is refractory, then various oxidative processes such as roasting may be viable. It should be noted that these limits were set when the gold price was about $US380 ± $US 20 per troy ounce. Since then, the spot gold price has decreased by about $US100 ± $US 20 per troy ounce, thus reducing the economic viability of lower grade deposits.

When treating gold-copper ores with cyanide, recovery of copper and/or cyanide can make it possible to treat ores containing higher copper grades. Numerous methods have been proposed for these operations. However, it is only in relatively recent times that these processes have been considered seriously. A major incentive for these changes is due to the increasingly common treatment of gold-copper ores. An additional motive is the requirement to decrease the amount of cyanide released to the environment. The cost of treating cyanide wastes can thus be offset if the cyanide can be re-used in the gold extraction process.

One obvious approach is to directly treat the waste in an AVR (acidification-volatilisation-regeneration) process. In this process, the effluent from the processing plant is treated with sulfuric acid to generate HCN, which is volatised from solution (by agitation and air-sparging) and subsequently trapped in an alkaline (usually lime) solution. The alkaline cyanide solution can then be re-used in the cyanidation process. The Cyanisorb process is an example of a commercially available AVR that is currently in operation at Coeur Gold New Zealand [8, 115]. A related process developed by Metallgesellschaft Natural Resources (MNR) also regenerates cyanide

[17, 115a]. The MNR process is reported to be particularly suitable for the treatment of leachates containing Cu(I)-cyanide complexes. Sodium sulfide is added during the MNR process to form a copper sulfide precipitate, which can be subsequently recovered by flotation [116] or solvent extraction [115a].

AVR processes are not designed to recover copper and are required to treat all the effluent from the leaching process. Copper recovery and reduced treatment volumes can be attained by selectively removing the Cu(I)-cyanide complexes from the leachate. A pregnant solution enriched in the Cu(I)-cyanide complexes can be subsequently treated to recover the cyanide and copper. A review of some earlier patents for recovery of cyanide and copper is available [117].

Four recent processes that have been developed to recover the Cu(I)-cyanide complexes from the leachate use activated carbon [118], chelating resins [119, 120], ion-exchange resins [8, 120] or solvent extraction [8, 78].

The Sceresini process uses activated carbon to adsorb Cu(I)-cyanide complexes in the early stages of the leaching process [118]. A low cyanide concentration is maintained in the early stages of the leaching process to allow a low CN:Cu mole ratio and minimal gold leaching. These conditions allow the removal of the cyanide soluble copper from the ore as the $[Cu(CN)_2]^-$ complex. The $[Cu(CN)_2]^-$ complex is subsequently stripped from the activated carbon and treated with sulfuric acid to recover the copper and cyanide. The final copper product is a cupric sulfate solution.

Vitrokele developed the V912 resin for the removal of gold and other metallo-cyanide complexes from the leachate. Processes have been developed which use this resin to recover the Cu(I)-cyanide complexes. The loaded resin is stripped and the pregnant stripping solution is subsequently treated with sulfuric acid to generate CuCN and cyanide [119, 120].

Henkel have developed new ion exchange resins and two solvent extraction reagents (LIX 79 and XI 7950) which are suitable for the selective removal of metallo-cyanide complexes [8, 121]. These Henkel extractants are based on the guanidine functionality.

Dreisinger *et al.* have developed novel process options for the extraction of Cu(I)-cyanide complexes from the leachate with the Henkel solvent extraction reagent XI 7950 [78]. The pregnant solution obtained by solvent extraction is then passed to an electrowinning (EW) cell for recovery of copper at the cathode and liberation of cyanide. In order to prevent oxidation of cyanide to cyanate at the anode, it is necessary to separate the anode with a Na^+-permeable membrane or to have other species in the EW cell which are more easily oxidised than cyanide. To obtain efficient EW and to avoid unwanted side-reactions, Dreisinger *et al.* [78] found that it was important for the CN:Cu mole ratio to be maintained between 3.0 and 3.5. Preliminary pilot plant studies have found a CN:Cu mole ratio of 3.2 to be suitable. High total copper concentration (~ 1.1 M) and low current densities are also necessary to achieve optimum EW. Similar observations have recently been reported in a separate study by Bek and Shuraeva [122]. It is also noteworthy that cyanide can be recovered from thiocyanate by anodic oxidation in the process developed Dreisinger and co-workers. The anodic oxidation of thiocyanate is given by Eqn.1.18. It is believed that the oxidation proceeds via the intermediate formation of thiocyanogen, $(SCN)_2$ [123].

$$SCN^- + 4\ H_2O \rightarrow SO_4^{2-} + HCN_{(aq.)} + 7\ H^+ + 6e^- \qquad \text{(Eqn.1.18)}$$
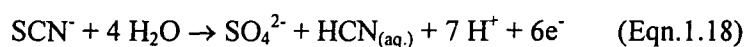
The Newmont/DuPont AuGMENT process uses an ion-exchange resin to extract the Cu(I)-cyanide complexes [8, 123a]. The copper and cyanide are recovered in a coupled solvent extraction/EW process. A membrane EW cell is also used in the AuGMENT process to prevent oxidation of cyanide to cyanate at the anode.

A major part of this thesis (Chapters six and seven) is devoted to the development of ion chromatographic methods suitable for the routine determination of the cyano species generated in the Dreisinger or Newmont/DuPont AuGMENT processes. Unfortunately, due to the reduced gold price and potential problems involved with the use of a membrane electrode, these processes are not considered viable at the current time [116].

1.4 Aqueous chemistry of the Cu(I)-cyanide complexes

This brief review is meant to provide some background information on the aqueous chemistry of the Cu(I)-cyanide complexes. Further details can be obtained from the following two reviews. Shantz and Reich [87] have prepared an excellent review of copper-cyanide chemistry with respect to metallurgy. The most comprehensive review of the transition metallo-cyanide complexes is supplied in the monograph by Sharpe [124].

The aqueous chemistry of the Cu(I)-cyanide complexes has been extensively investigated. These investigations have used ultra-violet (UV) [125-129], vibrational {Infra-Red (IR) [130, 131] and Raman [132-135]} and NMR [136-138] spectroscopic techniques, electrochemical methods [139-142] and calorimetric methods [143, 144]. It has been established from IR and Raman investigations that three monomeric Cu(I)-cyanide complexes exist in aqueous cyanide solution, namely $[Cu(CN)_2]^-$, $[Cu(CN)_3]^{2-}$ and $[Cu(CN)_4]^{3-}$ [130, 133, 135]. The $[Cu(CN)_2]^-$, $[Cu(CN)_3]^{2-}$ and $[Cu(CN)_4]^{3-}$ are respectively linear, trigonal-planar and tetrahedral ions in aqueous solution [124, 135]. Radiochemical and C-13 NMR studies have shown that the CN⁻ ligands in the Cu(I)-cyanide complexes are very labile [99, 138]. These findings support the titrimetric results described previously in section 1.3.4.3.

1.4.1 Vibrational spectroscopy of the Cu(I)-cyanide complexes

The most characteristic information concerning the three Cu(I)-cyanide complexes and indeed most of the metallo-cyanide complexes, can be gained from vibrational spectroscopy [124]. The observed IR frequencies (in wavenumbers) and IR molar absorptivities for the Cu(I)-cyanide complexes for the characteristic asymmetric C-N stretching vibration (v_6) are shown in Table 1.4 [124]. The characteristic Raman bands are also shown in Table 1.4 for comparison. The change in IR spectra of the $[Cu(CN)_3]^{2-}$ and $[Cu(CN)_4]^{3-}$ complexes as the R value is increased from 2.8 to 6.0 is shown in Fig. 1.8. The Raman spectra of the Cu(I)-cyanide complexes as the R value is increased from 2.3 to 6.1 are shown in Fig. 1.9. It is interesting to note that the CN⁻ and $[Cu(CN)_4]^{3-}$ bands in both IR and Raman spectra are almost co-

incidental. However, while the IR molar absorptivity of CN⁻ is very small compared to the Cu(I)-cyanide complexes, the Raman intensities of CN⁻ and the Cu(I)-cyanide complexes are similar. Since the gold dissolution rates due to CN⁻ and $[Cu(CN)_4]^{3-}$ are similar, it is has been suggested that Raman spectroscopy is suitable for monitoring the gold cyanidation process [145]. This will be discussed further in Section 1.8.

Species	IR (cm⁻¹)	IR absorptivity (l.mol⁻¹.cm⁻¹)	Raman (cm⁻¹)
$[Cu(CN)_2]^-$	2125	165	2137 (P)
$[Cu(CN)_3]^{2-}$	2094	1090	2094, 2108 (P)
$[Cu(CN)_4]^{3-}$	2076	1657	2078, 2094 (P)
CN⁻	2078	Not known	2077

Table 1.4: Vibrational spectral characteristics of the Cu(I)-cyanide complexes. The IR data for the Cu(I) cyanide complexes is taken from [130]. The IR frequency for CN⁻ is from [146]. The Raman data is from [135]. Note two peaks were observed in the Raman spectra for the $[Cu(CN)_3]^{2-}$ and $[Cu(CN)_4]^{3-}$ complexes. The Raman bands marked with (P) are polarised bands.
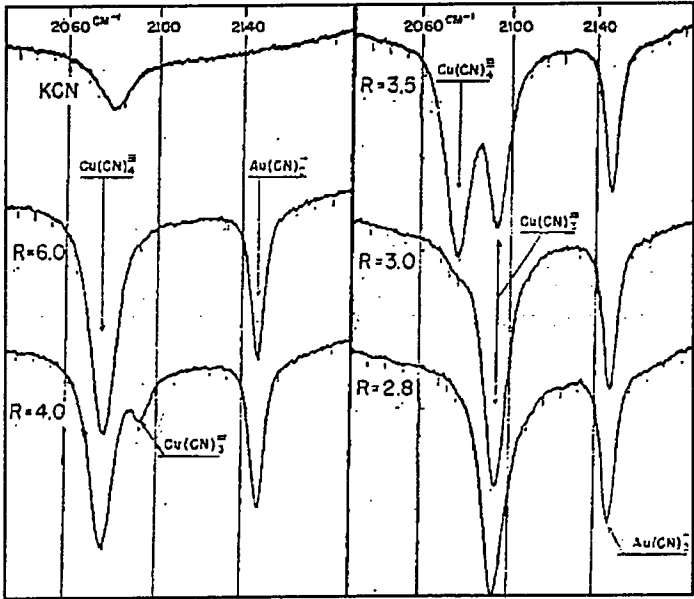
Fig. 1.8: IR spectra of aqueous $[Cu(CN)_3]^{2-}$ and $[Cu(CN)_4]^{3-}$.
Total [Cu] = 0.1 M. [KCN] = 1.0 M. Source : Fig. 1 of [130].
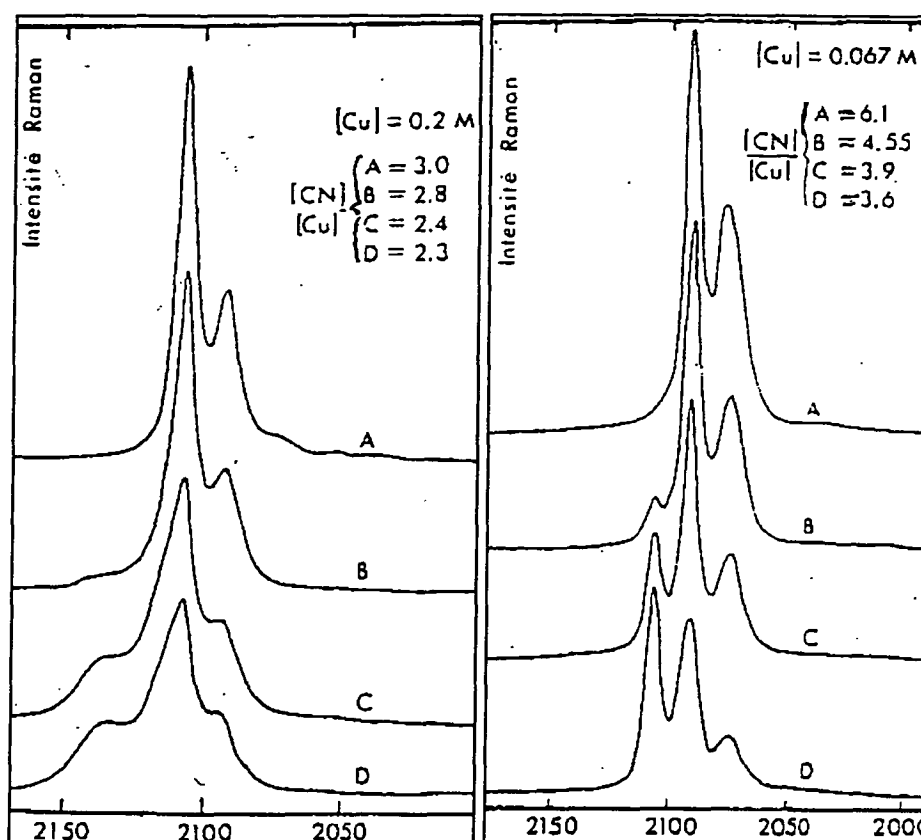
Fig. 1.9: Raman spectra of aqueous Cu(I)-cyanide complexes. (Frequency units: cm^{-1})
CN:Cu mole ratio is varied from 2.3 to 6.1. Source : Fig. 1 of [135].

1.4.2 Ultraviolet spectroscopy of the Cu(I)-cyanide complexes

The Cu(I)-cyanide complexes display intense UV absorption which has been attributed to charge transfer from the filled metal d orbitals to the empty ligand-based $2\pi_u$ orbital [147]. The intense UV absorption displayed by many other metallo-cyanide complexes may be due to charge transfer bands or d↔d transitions [124, 148].

The UV spectra of the Cu(I)-cyanide complexes are quite distinctive with two maxima occurring at approximately 210 and 235 nm and three isosbestic points observed at 205-210nm, 234-236 nm and 243-246 nm, as shown in Fig. 1.10 [127-129, 149]. The isosbestic point of most interest, due to its longer wavelength and large molar absorptivity, occurs at 235 nm.

The λ_{max} occurs close to 210 nm. It should be noted that two early papers in 1957 and 1959 reported the λ_{max} at the second most intense maximum (239 nm) [111, 126]. This was possibly due to the limitation of the spectrometers used by these workers. However, this error was not reported by Simpson [125] in 1958, who observed the λ_{max} at 210 nm, and the second most intense peak at 235 nm. Pohlandt [150] employed the second λ_{max} for the selective detection of the Cu(I)-cyanide complexes after the chromatographic separation of the metallo-cyanide complexes. The UV spectra do not provide as much definitive information as the vibrational spectra concerning the nature of the individual complexes. Several authors have reported on the UV spectra of the Cu(I)-cyanide complexes [111, 125, 127-129, 151, 152]. All these authors have observed a gradual change of the spectrum as the CN:Cu mole ratio is altered, as shown in Fig. 1.10.

A list of the spectral characteristics observed when $K[Cu(CN)_2]$ is dissolved in water or acetonitrile is shown in Table 1.5. It is worth noting that the spectral characteristics in the two solvents are quite similar. This is important, since the photo-diode array studies on the eluted Cu(I)-cyanide peak reported in Chapter 4 of this thesis employ aqueous eluents containing 20-25% acetonitrile.

The apparent molar absorptivity at various wavelengths has been reported by several authors, as shown in Table 1.6 [125-129, 151, 153, 154]. Some of these authors have calculated the individual spectra of the three Cu(I)-cyanide complexes. The calculated molar absorptivities of the three complexes are also shown in Table 1.6. The calculated spectra of the $[Cu(CN)_3]^{2-}$ and $[Cu(CN)_4]^{3-}$ complexes are shown in Fig. 1.10(b). It should be noted that the calculated spectra of individual complexes are similar. This limits the ability of UV spectroscopy to be able to discriminate accurately between the individual complexes.

Fig. 1.10 (Following page): UV spectra of aqueous Cu(I)-cyanide complexes. (a) (Top): R varied from 2.2 (Spec. #3) to 2.8 (Spec. #9). Source : Fig. 1 of [128]. (b) (Bottom): R varied from 4 (Spec. #1) to 144 (Spec. #12). The spectra labelled $[Cu(CN)_3]^{2-}$ and $[Cu(CN)_4]^{3-}$ are the calculated spectra of these individual complexes. Source : Fig. 8 of [127].

A list of the spectral characteristics observed when K[Cu(CN)$_2$] is dissolved in water or acetonitrile is shown in Table 1.5. It is worth noting that the spectral characteristics in the two solvents are quite similar. This is important, since the photo-diode array studies on the eluted Cu(I)-cyanide peak reported in Chapter 4 of this thesis employ aqueous eluents containing 20-25% acetonitrile.

The apparent molar absorptivity at various wavelengths has been reported by several authors, as shown in Table 1.6 [125-129, 151, 153, 154]. Some of these authors have calculated the individual spectra of the three Cu(I)-cyanide complexes. The calculated molar absorptivities of the three complexes are also shown in Table 1.6. The calculated spectra of the [Cu(CN)$_3$]$^{2-}$ and [Cu(CN)$_4$]$^{3-}$ complexes are shown in Fig. 1.10(b). It should be noted that the calculated spectra of individual complexes are similar. This limits the ability of UV spectroscopy to be able to discriminate accurately between the individual complexes.

Water		Acetonitrile	
λ (nm)	ε_{app}	λ (nm)	ε_{app}
209.2	21,000	212.8	23,000
222.2	11,000	224.7 (*)	8500
233.1	11,500	234.5	11,300
242.7 (*)	5,800	241.0 (*)	8,900
-	-	246.9 (*)	3900
265.3 (*)	1,400	263.2 (*)	330
-	-	285.7 (*)	56

Table 1.5: UV spectral characteristics of K[Cu(CN)$_2$] dissolved in either pure water or pure acetonitrile. Apparent molar absorptivities (ε_{app}) are expressed in l.mol^{-1}.cm^{-1}.
(*) Indicates a shoulder band. Source : [147].

λ (nm)	ε_{app}	ε_2	ε_3	ε_4	Reference
225	-	9200 (max)	-	-	[125]
234	-	10,600 (max)	-	-	[125]
235	-	-	-	11,000 (max)	[125]
238	-	7500	11,600 (max)	10,000	[125]
239	9,400 - 11,800 *	-	-	-	[126]
202	-	-	20,900 (max)	13,300	[127]
218	-	-	8,600	17,400 (max)	[127]
234	-	-	10,000	12,400	[127]
238	-	-	11,800 (max)	9,600	[127]
205	-	16,800	21,300 (max)	-	[128]
210	-	20,400 (max)	16,600	-	[128]
235	-	11,000 (max)	9,400	-	[128]
238	-	8500	11,400 (max)		[128]
204	20,700 (max)	-	-	-	[153]
221	5,400 (max)	-	-	-	[153]
238	10,700 (max)	-	-	-	[153]
235	11,300	-	-	-	[149]

Table 1.6: Molar absorptivities ($l.mol^{-1}.cm^{-1}$) of the Cu(I)-cyanide complexes at various wavelengths. The apparent molar absorptivity (ε_{app}) is from experimental measurements. The molar absorptivities (ε_2, ε_3 and ε_4) of the di-, tri- and tetra-cyano complexes, respectively, were calculated.

Notes:

(*) : These ε_{app} values were obtained as the concentration of $K_3[Cu(CN)_4]$ was increased from 3.0 - 35.7 μM.

(max) : The molar absorptivity shown is at a wavelength maxima.

The spectral features of the Cu(I)-cyanide complexes are potentially useful for the identification of these complexes with a photo-diode array (PDA) detector after the chromatographic separation of the metallo-cyanide complexes, as will shown in Chapter four of this thesis. Spectral deconvolution of chromatographic peaks is a powerful tool for determining peak purity and for enabling identification of co-eluting components [155]. A recent paper has combined PDA detection with the

RPIIC separation of the metallo-cyanide complexes to enable spectroscopic examination of all the eluted peaks, thereby providing secondary confirmation of peak identity [156]. This procedure was important for this laboratory as it employed eluent recycling in order to reduce analytical costs. Eluent recycling resulted in losses of acetonitrile from the eluent and subsequent variations in the retention times of the analytes [156a].

1.4.3 NMR spectroscopy of the Cu(I)-cyanide complexes

The NMR studies have used both Cu-63 and C-13 NMR [136, 138] and have provided some evidence of the bonding and structure of the Cu(I)-cyanide complexes. This information is determined from the effect on line broadening and change in the chemical shift. These studies have shown that NMR is the least suitable spectroscopic technique for characterisation of the Cu(I)-cyanide complexes in aqueous solution.

1.4.4 Equilibria and stability constants of the Cu(I)-cyanide complexes

The relative concentrations of the three Cu(I)-cyanide complexes are governed by the following equilibria (Eqns.1.19a-g) and the corresponding equilibrium constants (Eqns. 1.20a-g). The most important factor controlling these equilibria is the CN:Cu mole ratio in solution. The solution pH will also become an important factor at low pH values.

$$Cu^+ + CN^- \rightleftharpoons CuCN \qquad \text{(Eqn.1.19a)}$$

$$CuCN + CN^- \rightleftharpoons [Cu(CN)_2]^- \qquad \text{(Eqn.1.19b)}$$

$$[Cu(CN)_2]^- + CN^- \rightleftharpoons [Cu(CN)_3]^{2-} \qquad \text{(Eqn.1.19c)}$$

$$[Cu(CN)_3]^{2-} + CN^- \rightleftharpoons [Cu(CN)_4]^{3-} \qquad \text{(Eqn.1.19d)}$$

$$Cu^+ + 2CN^- \rightleftharpoons [Cu(CN)_2]^- \qquad \text{(Eqn.1.19e)}$$

$$Cu^+ + 3CN^- \rightleftharpoons [Cu(CN)_3]^{2-} \qquad \text{(Eqn.1.19f)}$$

$$Cu^+ + 4CN^- \rightleftharpoons [Cu(CN)_4]^{3-} \qquad \text{(Eqn.1.19g)}$$
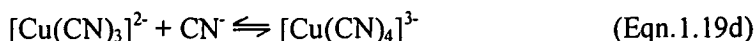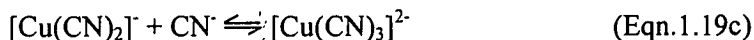
$$k_1 = [CuCN] / [Cu^+][CN^-] \qquad\qquad \text{(Eqn. 1.20a)}$$

$$k_2 = [Cu(CN)_2^-] / [CuCN][CN^-] \qquad\qquad \text{(Eqn. 1.20b)}$$

$$k_3 = [Cu(CN)_3^{2-}] / [Cu(CN)_2^-][CN^-] \qquad\qquad \text{(Eqn. 1.20c)}$$

$$k_4 = [Cu(CN)_4^{3-}] / [Cu(CN)_3^{2-}][CN^-] \qquad\qquad \text{(Eqn. 1.20d)}$$

$$\beta_2 = \frac{[Cu(CN)_2^-]}{[Cu^+][CN^-]^2} \qquad\qquad \text{(Eqn. 1.20e)}$$

$$\beta_3 = \frac{[Cu(CN)_3^{2-}]}{[Cu^+][CN^-]^3} \qquad\qquad \text{(Eqn. 1.20f)}$$

$$\beta_4 = \frac{[Cu(CN)_4^{3-}]}{[Cu^+][CN^-]^4} \qquad\qquad \text{(Eqn. 1.20g)}$$

Early potentiometric measurements were used to calculate the solubility product $[Cu^+]x[CN^-]$, which was found to be 3.2×10^{-20} [139]. The inverse of this solubility product ($10^{19.5}$) has been used as the formation constant for CuCN [157]. The conditional formation constant of CuCN has recently been estimated in 1 M NaCl to be $10^{16.3}$ [142]. Note that the authors were unsure as to the accuracy of this estimate. It should be noted that the formation constant of CuCN was based on a stability constant of 10^{24} for the $[Cu(CN)_2]^-$ complex in both these investigations. Other workers have reported significantly lower values for this stability constant.

Kurnia et $al.$ [158] states "The stability constants of the Cu(I)-cyanide complexes have not been well characterised in aqueous solution. There are several reasons for this, including the difficulty of detecting the $CuCN^0$(aq) species on account of the instability of Cu(I) at low CN^- concentrations, the sparing solubility of CuCN(s), the very high stability of the $[Cu(CN)_3]^{2-}$(aq) species and its similarity in strength to $[Cu(CN)_4]^{3-}$(aq)." The instability of Cu(I) arises from the rapid oxidation of the Cu^+(aq) ion to the Cu^{2+}(aq) ion without the influence of stabilising ligands such as

halides (eg. Cl⁻) , pseudo-halides (eg. CN⁻) or miscible non-aqueous solvents (eg. acetonitrile) [9].

For the above reasons, most of the published data only concern the stability constants of the three Cu(I)-cyanide complexes. The first stability constant reported was $10^{27.3}$ for the $[Cu(CN)_4]^{3-}$ complex [159]. This was determined in 1904 using potentiometric experiments. These results were later re-calculated, considering activity coefficients and using a better value for the potential of the Cu/Cu+ couple. The re-calculated value obtained was log β_4 = 28.9 [130].

Since 1904, numerous investigations have reported significant variations in the values of the stability constants obtained for the three complexes. These investigations have used spectroscopy (UV or IR), potentiometric or calorimetric measurements. The results of these investigations have been summarised in several compilations of stability constants of the metallo-cyanide complexes [36, 160-165]. Some of the values reported are shown in Table 1.7. The overall stability constants β_2, β_3 and β_4 recommended by the latest IUPAC critical review are $10^{21.7}$, $10^{27.0}$ and $10^{28.5}$ for the $[Cu(CN)_2]^-$, $[Cu(CN)_3]^{2-}$ and $[Cu(CN)_4]^{3-}$ complexes, respectively [164].

The values displayed in Table 1.7 show that the greatest variations exist for the $[Cu(CN)_2]^-$ complex. This is generally considered to be due mainly to the precipitation of CuCN at low CN:Cu mole ratios, which is to be expected given the large formation constant of CuCN. Ritchie [166] has suggested that this instability may be a reflection of the low solubility of the $[Cu(CN)_2]^-$ complex. It has been noted that aqueous solutions of the potassium salts of Cu(I)-cyanide complexes are unstable when the R value is below 2.8 [130]. The sodium salts are both more stable and more soluble than the potassium salts at lower R values [130, 167]. Recent thermodynamic calculations and experimental work have proposed the three routes for the precipitation of copper from solutions containing sufficiently high concentrations of the $[Cu(CN)_2]^-$ complex, as shown in Eqns. 1.21-1.23 [92].

Log formation / stability constant				Method	Year	Ref.
CuCN	$[Cu(CN)_2]^-$	$[Cu(CN)_3]^{2-}$	$[Cu(CN)_4]^{3-}$			
19.5 (*¹)	23.8	-	-	Pot.	1950	[139]
-	-	4.59	1.70	IR spec.	1956	[130]
-	21.7	4.6	2.3	Pot.	1957	[140]
-	-	4.10	-	UV spec.	1958	[125]
-	-	4.59	1.72	UV spec.	1959	[126]
-	-	5.0 (k_3)	2.64 (k_4)	Cal.	1965	[143]
-	-	5.3	1.5	Cal., Tit.	1967	[144]
-	16.26	5.20	2.62	UV spec.	69-74	[127-129]
-	21.7 (β_2)	5.1 (k_3)	1.1 (k_4)	Pot.	1972	[141]
-	23.84	4.54	1.84	Pot.	1973	[168]
16.3	23.97 (β_2)	5.43 (k_3)	2.38 (k_4)	Pot.	1993	[142]
- (*²)	14.43 (β_2)	5.32 (k_3)	1.85 (k_4)	Pot. Tit	1996	[158]

Table 1.7: Formation and stability constants of Cu(I)-cyanide complexes. Unless stated, the overall stability constant β_2 is used for the $[Cu(CN)_2]^-$ complex, while the stepwise stability constants k_3 and k_4 are used for the $[Cu(CN)_3]^{2-}$ and $[Cu(CN)_4]^{3-}$ complexes. Most of the stability constants shown have been corrected so that standard conditions of zero ionic strength and 25°C are shown. Those stability constants that have not been corrected are designated as conditional stability constants : β_2', k_3' and k_4'.

Methods : Pot. = Potentiometric; Tit. = Titration; cal. = Calorimetry;

IR spec. = IR spectroscopy; UV spec. = UV spectroscopy.

(*¹) This was determined as a solubility product. See text for discussion.

(*²) 10% acetonitrile was present in the solutions shown in this row.

$$[Cu(CN)_2]^- + 1/4\ O_2 + OH^- \rightarrow CuO + 2CN^- + 1/2\ H_2O \qquad \Delta G = -22.12\ kcal/mol$$
$$\text{(Eqn. 1.21)}$$

$$2\ [Cu(CN)_2]^- + 2\ OH^- \rightarrow Cu_2O + 4CN^- + H_2O \qquad \Delta G = -18.29\ kcal/mol$$
$$\text{(Eqn. 1.22)}$$

$$[Cu(CN)_2]^- + 1/2\ O_2 \rightarrow CuCN + OCN^- \qquad \Delta G = -80.52\ kcal/mol$$
$$\text{(Eqn. 1.23)}$$
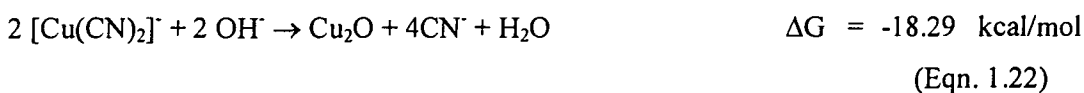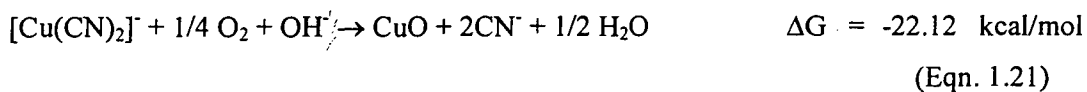
The $[Cu(CN)_3]^{2-}$ complex is particularly stable in aqueous solution, and is the predominant complex in solution over a wide range of R values typically found in gold cyanidation leachates. This stability is due to the unusually high stepwise formation constant (k_3) of this species (See table 1.7). It has been calculated that the $[Cu(CN)_3]^{2-}$ complex displays higher thermodynamic stability in aqueous solution than the other two Cu(I)-cyanide complexes, as shown in Eqn. 1.24 [169].

$$[Cu(CN)_2]^- + [Cu(CN)_4]^{3-} \Leftrightarrow 2 [Cu(CN)_3]^{2-} \qquad Log\ K = 3.82 \qquad (Eqn.\ 1.24)$$
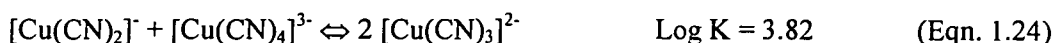
The $[Cu(CN)_4]^{3-}$ complex is of minor importance since it does not become a major species until very high R values and the fourth CN ligand is only very weakly bonded to the Cu(I) complex. This is demonstrated by the similar behaviour of the fourth CN ligand and uncomplexed cyanide ("free" cyanide) with respect to gold cyanidation. Thus for practical (i.e. leaching) purposes, cyanide in excess of an R value of 4 can be considered to be uncomplexed, even though calculations based on the stability constants show that the average number of CN ligands is less than 4 when the R value is 4.0.

It is worth noting the effect of acetonitrile on the stability constants of the Cu(I)-cyanide complexes, especially for the β_2 value [158]. The effect of acetonitrile on the Cu(I)-cyanide stability constants is important in this thesis (see Chapter four) since aqueous eluents containing 20-25% acetonitrile are used, which assist in the stabilisation of the eluted Cu(I)-cyanide complexes. The effect of 10% acetonitrile on the stability constants is shown in last row of Table 1.7. There were no significant differences when the acetonitrile concentrations were increased to 20% and 30% [158]. It should be stated that acetonitrile is a well known ligand for Cu(I). Early work established the formation constant for the $[Cu(CH_3CN)_2]^+$ complex in aqueous acetonitrile to be $10^{4.35}$ [170]. Parker and co-workers [171] have used this chemistry to develop a hydrometallurgical process, which employs acetonitrile in the extraction and refining of copper. Unfortunately, the minerals processing industry has avoided use of acetonitrile due to its volatility, flammability and the potential carcinogenicity of materials present in industrial grade acetonitrile [77].

Ionic strength has a significant effect on the stability constants. This is especially important for the $[Cu(CN)_4]^{3-}$ complex due to the advantageous effect this complex has on the gold leaching rate compared to the $[Cu(CN)_3]^{2-}$ complex [97]. Shantz and Reich calculated the concentrations of the three Cu(I)-complexes, CN^- and HCN with total copper concentrations of 1, 10 and 100 mM and R values varying from 2.5 to 10 for each copper concentration. These calculations showed that the $[Cu(CN)_4]^{3-}$ complex is predominant at higher R values and higher total copper concentrations, while the $[Cu(CN)_3]^{2-}$ complex is dominant throughout most of the range [87]. Recent experimental results obtained in 1 M NaCl have found the overall conditional formation constants $\beta_2{}'$, $\beta_3{}'$ and $\beta_4{}'$ under these conditions to be $10^{23.97}$, $10^{29.40}$ and $10^{31.78}$ for the $[Cu(CN)_2]^-$, $[Cu(CN)_3]^{2-}$ and $[Cu(CN)_4]^{3-}$ complexes respectively. It is noteworthy that the stepwise conditional formation constant $k_4{}'$ ($10^{2.38}$), is significantly higher than the corresponding stepwise formation recommended by IUPAC ($10^{1.5}$) [164]. The value of $k_4{}'$ obtained with IR spectroscopy using 100 mM total copper concentration was found to be $10^{2.2}$ [130]. The large total copper concentration was required for the IR spectroscopic measurements as the IR molar absorptivities of the Cu(I)-cyanide complexes are not large and this work was reported in 1956, prior to the advent of FTIR and sensitive IR detectors. A recent study employing FTIR has been able to achieve much lower detection limits for the metallo-cyanide complexes [146].

The previous discussion concerning the effect of total copper concentration on the stability constant of the $[Cu(CN)_4]^{3-}$ complex has interesting ramifications for recent innovations in the recovery of Cu(I)-cyanide complexes from gold cyanidation leachates. Dreisinger [78] has noted that higher total copper concentrations (up to 1.1 M) are preferable in the electrowinning of copper from solutions containing Cu(I)-cyanide complexes, as described in section 1.3.4.5. At these higher total copper concentrations, the above discussion indicates that the abundance of the $[Cu(CN)_4]^{3-}$ complex is increased for a given R value. The increased abundance of the $[Cu(CN)_4]^{3-}$ complex should allow an increase in the gold leaching rate for the reasons discussed in section 1.3.4.4.

In contrast to the effect of high total copper concentration, very low total copper concentrations may significantly reduce the value of β_2. Early work by Spitzer [172] noted that the stability constant for the $[Cu(CN)_2]^-$ complex decreased from approximately $10^{23.3}$ to 10^{16} when the total copper concentration was reduced from 100 mM to 0.25 mM. Later authors subsequently discounted the stability constant obtained in the diluted solution as due to erroneous measurements [130]. However, more recent work using UV spectroscopy reported Log $\beta_2 = 16.26$ [129]. The total copper concentration was also very low (50 μM) in these measurements due to the high molar UV absorptivity of the Cu(I)-cyanide complexes. In the latest IUPAC review, Beck [164] has discounted these low values for β_2 in favour of values derived from potentiometric measurements.

1.5 Analysis of cyanide

The following sections review the analytical methods available for the analysis of cyanide. This section briefly reviews the major techniques used for the analysis of cyanide. It should be noted that due to the toxicity of cyanide, most analytical methods are focused on the determination of trace concentrations of cyanide. Section 1.6 reviews the analytical methods based on the König reaction. Section 1.7 reviews the ion chromatographic methods that have been developed to determine cyanide and the metallo-cyanide complexes. Finally, section 1.8 reviews the analytical methods and instruments that have been developed for monitoring the gold cyanidation process.

The determination of cyanide may be performed using one of six main techniques, namely titrimetry, spectrophotometry, atomic absorption spectrophotometry (AAS), spectrofluorometry, potentiometry, and amperometry. These methods have been thoroughly reviewed by several authors [106, 113, 173-177]. Titrimetry has already been discussed in previous sections. The other five methods are briefly discussed below.

Flow injection analysis (FIA) and related flow analytical systems have enabled many of these techniques to be used on an automated basis. In addition, the use of membrane diffusion cells has allowed the separation of cyanide from other components, thereby greatly improving the detection selectivity [178-182]. This is achieved by acidifying the flow stream containing the cyanide sample and allowing diffusion of HCN across a gaseous permeable membrane into an alkaline receiving flow stream.

1.5.1 Spectrophotometric methods

Numerous spectrophotometric methods have been reported in the literature. These can be subdivided into three main categories, namely those based on the König reaction, those involving metal complexes and a group of miscellaneous methods [106]. The König reaction, which will be discussed in section 1.6, is the single most commonly used method for cyanide analysis.

Spectrophotometric methods can be classified as direct methods or indirect methods. In the former, cyanide causes an increase in absorbance, such as in the formation of the $[Ni(CN)_4]^{2-}$ complex which is monitored at 267 nm [183-186]. The indirect methods use a decrease in absorbance of a metallo-complex (eg Cu(II)-EDTA or Hg(II)-EDTA) due to the formation of a metallo-cyanide complex [187].

1.5.2 Methods using atomic absorption spectrophotometry

These methods utilise the rapid formation of some metallo-cyanide complexes from either a solid metal surface or a highly insoluble metal sulfide. The solubilised metal (as the metallo-cyanide complex) is detected by AAS. Nickel [185], silver [188, 189] and copper [190] have been used.

1.5.3 Spectrofluorometric methods

Several fluorometric methods have been developed, using nicotinamide [191], p-benzoquinone [192], pyridoxal [193], o-phthalaldehyde (OPA) and 2,3-napthalenedialdehyde (NDA) [194]. The dye produced in the König reaction with either pyridine or isonicotinic acid and barbituric acid has also been observed to produce an intense fluorescence [195, 196].

1.5.1 Potentiometric methods

The most common potentiometric methods employ cyanide-sensing ion-selective electrodes (ISE's). Cyanide ISE's have been used extensively and are now an accepted standard method [105]. Two excellent reviews are presented by Lakshminarayanaiah [197] and Midgley [198]. Two types of ISE suitable for cyanide analysis are available commercially. The first of these electrodes employs a AgI solid-state membrane. The electrode response is determined by the release of I^-, as shown in Eqn. 1.25. The second type is a silver-sensing electrode, which invariably contains Ag_2S in the solid state membrane. The electrochemical mechanism attributed to the creation of the electrode response for this type of electrode is due to the dissolution of silver from the surface of the Ag_2S membrane, as shown in Eqn. 1.26 [199]. The response time and reproducibility of the second type of electrode at low cyanide concentrations can be improved by the use of dilute $[Ag(CN)_2]^-$ solutions. More recently, cyanide ISE's based on silver chalcogencide [200] or cobalt phthalocyanine conjugate-polymer [201] membranes have been developed.

$$2CN^- + AgI \rightleftharpoons [Ag(CN)_2]^- + I^- \qquad \text{Eqn. 1.25}$$

$$2CN^- + Ag \rightleftharpoons [Ag(CN)_2]^- + e^- \qquad \text{Eqn. 1.26}$$
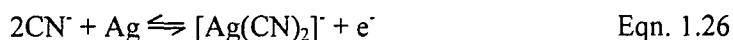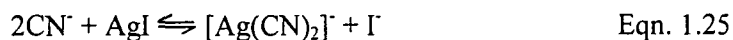
The response of all cyanide ISE's is pH dependent due to the high pKa value for HCN. Sulfide causes severe interference effects for all the cyanide ISE's and

---

permanently damages the commercially available ISE's. High cyanide concentrations will gradually destroy cyanide ISE's, and particularly those containing AgI in the membrane [202].

It should be noted that a limited number of alternative potentiometric methods have been developed that employ either a Cu or Ag wire as a cyanide sensing electrode [203-205]

1.5.2 Amperometric methods

Modern amperometric detection of cyanide has evolved from voltammetric techniques and is based on the oxidation of a Ag working electrode housed in a suitable flow-cell [206]. The electrode reaction is shown in Eqn 1.27.

$$Ag + 2CN^- \rightleftharpoons [Ag(CN)_2]^- + e^- \qquad \text{(Eqn. 1.27)}$$
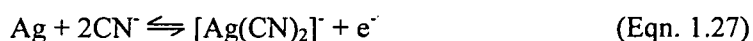
The flow-cell contains the Ag electrode, an auxiliary electrode (commonly glassy carbon) to carry current, and a reference electrode (Ag / AgCl) which monitors the potential of the working electrode in a zero current mode [207]. The use of the Ag working electrode was originally developed by Pihlar *et al.*[206] in 1979 for use in FIA. Since then, it has been used for the detection of trace quantities of cyanide in FIA, so that amperometry has become one of the most sensitive and interference free techniques for cyanide analysis. The lack of interferences is due chiefly to the chemical selectivity of the Ag electrode. At the low working potential (0.0 to +0.2 V) required for this oxidation, other electrochemically active species such as SCN⁻ and CNO⁻ do not interfere. The major interference is from S^{2-}, which causes the formation of a Ag_2S layer that can be removed only by dismantling the flow cell and polishing the Ag electrode [206]. This changes the characteristics of the electrode surface and necessitates re-calibration of the detector. The major drawback with amperometric detection is that stability and reproducibility are not good, due principally to changes in the electrode surface with use [208].

It should be noted that while the Ag electrode is still the preferred working electrode, some authors have reported advantages in using either Au or Cu electrodes [209, 210].

1.6 Determination of cyanide with the König reaction

1.6.1 Mechanism of the König reaction

The König reaction was originally developed in 1904 during the search for new dye-stuffs [211]. Intense dyes were produced when pyridine was treated with brominated cyanide and then allowed to react with a number of compounds. Unfortunately, the dyes faded rapidly. It was not until 1944 that this reaction scheme was first used for the analysis of cyanide [212]. Since then, the König reaction has become the most commonly employed spectrophotometric technique for cyanide analysis due to its high sensitivity and few interferences. Over the years, many variations on the König reaction have been proposed and investigated. It is generally accepted that all these variations of the König reaction can be divided into three general reactions, which are summarised below.

(i)   Halogenation (either chlorination or bromination) of cyanide to give cyanogen halide, CNX.

(ii)   Pyridine (or a derivative) undergoes electrophilic attack by CNX at the hetero-N atom, resulting in ring cleavage and subsequent formation of a conjugated di-aldehyde intermediate [213].

(iii)   Reaction of this aldehyde with initially one, and later two, molecules of a compound that will couple with the aldehydic groups to produce a conjugated, resonance stabilised polymethine dye (PMD) [214, 215]. Suitable coupling reagents contain either an aromatic amine functionality or a reactive methylene group.

The above reactions are illustrated for the isonicotinic acid (III)/barbituric acid (VI) (INA)/BA) variant of the König reaction in Fig. 1.11. The chlorination reagent shown in this reaction scheme is N-chlorosuccinimide (NCS) (I).

(a) N-chlorosuccinimide (I) chlorinates CN⁻ to produce CNCl.
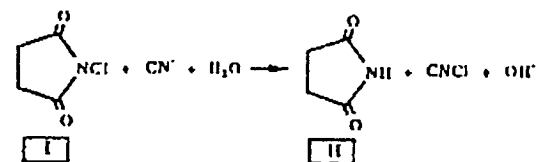
(b) CNCl then reacts with isonicotinic acid (III) to form the intermediate (IV) which hydrolyses to the dialdehyde (V).
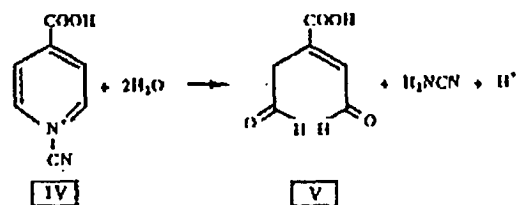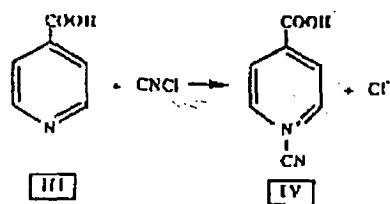
(c) Barbituric acid (VI) condenses with (V) to produce a transient dye (VII) (λ_{max} = 525 nm), which condenses with another molecule of barbituric acid to give a second polymethine dye (VIII) (λ_{max} = 600 nm).

Fig. 1.11: Reaction scheme for the König reaction. (Details on next page)
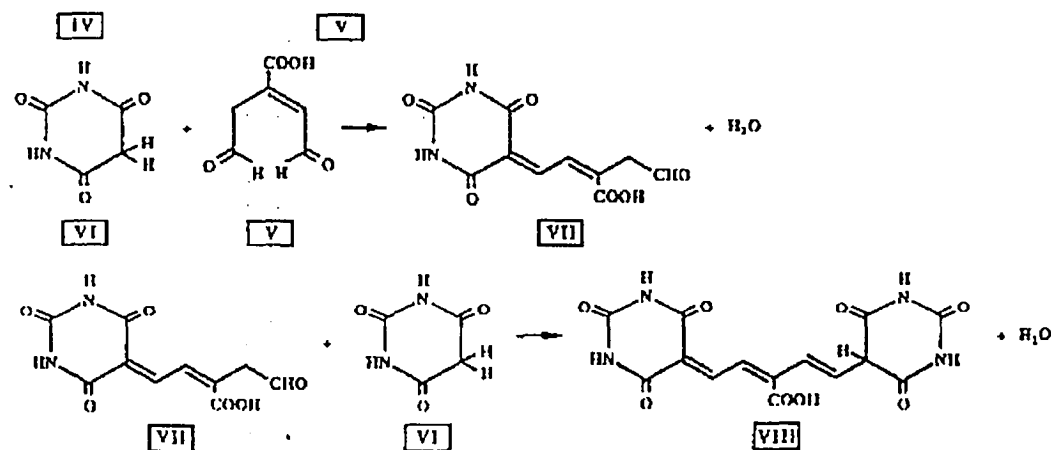
Fig. 1.11: Reaction scheme for the post-column derivatisation. See text for discussion.

(I) N-chlorosuccinimide; (II) succinimide; (III) isonicotininc acid; (IV) reaction intermediate;

(V) pent-2-enedial-3-carboxylic acid; (VI) barbituric acid; (VII) first PMD (λ_{max} = 525 nm);

(VIII) second PMD (λ_{max} = 600 nm).

The first and intermediate PMD (VII) is formed rapidly, while formation of the second and final PMD (VIII) occurs at a considerably slower rate. The λ_{max} and intensity of the final PMD are greater than the intermediate PMD due to the increased conjugation.

Several authors have utilised the rapid formation of the intermediate PMD in the development of spectrophotometric methods suitable for the determination of cyanide by FIA [178, 181, 216] and HPLC-PCR [217, 218]. Recently, Kuban [181] reported that the formation of the intermediate PMD is favoured by a 100-fold excess of pyridine (or a pyridine-derivative) over the coupling reagent.

Chlorination is preferred in a closed post-column reaction system since bromination requires the addition of a reducing reagent to destroy excess bromine, which would otherwise prevent the formation of the dye [219]. The most widely used reducing agent is arsenite. Chloramine-T, sodium hypochlorite and N-chlorosuccinimide have all been used for the chlorination reaction.

Pyridine and two of its derivatives, 4-methyl-pyridine (4-picoline) [220] and pyridine-4-carboxylic acid (isonicotinic acid) [178, 182, 196, 218, 221-225] have been used to form the dialdehyde. Many coupling reagents have been investigated [173]. Several, such as benzidene [212, 219], have been discontinued due to their toxicity. The most commonly used coupling reagents at present are barbituric acid (BA) and 3-methyl-1-phenyl-2-pyrazolin-5-one (pyrazolone, PZ).

1.6.2 Controlling factors in the König reaction

One of the most commonly used variants of the König reaction (pyridine/BA) has been studied extensively in order to determine the factors that regulate the colour forming reactions. The rate of formation of the PMD increased with temperature up to 60°C with no loss in sensitivity, although above 40°C the calibration graphs

became convex [180]. The rate and maximum absorption of the PMD are both dependent on the BA concentration. At higher BA concentrations the rate is considerably faster, but the maximum absorption is greatly decreased [226, 227]. The absorption is also very dependent on the final pH, with maximum absorption occurring at pH = 5.8 [228, 229]. The concentration and quantity of chlorination reagent added have also been shown to have a considerable effect on the sensitivity of the method due to the rapid oxidation of CNCl to cyanate [228-230].

1.6.3 Interferences in the König reaction

The major interferences in the König reaction are from thiocyanate and sulfide. Thiocyanate causes a significant positive error due to the formation of CNCl or CNBr [227], whereas sulfide causes a significant negative error [221]. Other reducing agents such as nitrite and sulfite also interfere by consuming the chlorination reagent. Oxidising agents such as Br_2 interfere by destroying the PMD [227].

1.7 Ion chromatographic analysis of cyanide and metallo-cyanide complexes

Numerous HPLC methods have been developed to enable analysis of cyanide and the metallo-cyanide complexes. Almost all these methods can be classified as belonging to the field of ion chromatography (IC). Otu *et al.* [231] has recently reviewed the analysis of cyanide and the metallo-cyanide complexes by ion chromatography. An excellent monograph on IC is available [232].

Four different separation modes have been reported for the analysis of cyanide. These are, in order of importance, anion exchange (AX), ion exclusion (IE), reversed-phase ion interaction chromatography (RPIIC) and reversed-phase (RP). In contrast, separation of the metallo-cyanide complexes is dominated by RPIIC, with only two reports of separation by AX. This is due to the very strong binding of the metallo-cyanide complexes to AX resins, which is the basis of the RIP process. It is worth noting at this point that several alternative terms are used to describe RPIIC

[232]. Some of these are: Mobile phase ion chromatography (MPIC), Paired-ion chromatography (PIC) and dynamic ion-exchange chromatography.

Numerous detection systems have been developed for use with IC. The combinations of separation conditions and detection systems that have been reported for the analysis of cyanide are summarised in Tables 1.8-1.10, while those for the metallo-cyanide complexes are shown in Tables 1.11 and 1.12.

1.7.1 Electrochemical methods for detection of cyanide

Conductivity and amperometric detection systems are the most common detection systems used in conjunction with the anion-exchange separation of cyanide. Amperometry is the most widely used technique for the detection of low concentrations of cyanide in IC. This has followed the work originally developed by Pihlar [290] for FIA, as described in section 1.5.

Two distinct types of conductivity detection are used in IC. The first type "suppressed" conductivity detection, is based on the pioneering work of Small *et al.* [291]. In this approach, a highly conducting buffer, such as carbonate or borate, is used as the eluent. Conductivity detection is achieved after neutralisation of the eluent in a suppressor. The original suppressors were high capacity cation-exchange columns in the H^+ form, which required periodic regeneration. Modern suppressors employ a combined electrolysis and dialysis unit, thereby allowing continuous operation. However, because the effluent from a suppressor is neutral or slightly acidic, sensitive conductivity detection of anions (esp. cyanide) with pK_a values $\square$ 7 is not possible [292]. Recent work by Dasgupta and co-workers [292-294] has been aimed at overcoming this problem by use of post-suppression devices.

Detection system	Separation mode	Column	Eluent	Reference
Electrochemical				
Conductivity				
- suppressed	AX	Dionex HPIC AS-4	14.7 mM DAE, 10 mM H_3BO_3, 1.0 mM Na_2CO_3, pH 11.0	[233]
- non-suppressed	AX	Wescan anion R	10 mM H_3BO_3, 0.33 mM KH-phthalate, pH 11.9 (10% ACN)	[234]
	AX	Hamilton PRP-X100	10 mM phenol, phenolate buffer, pH 10.1	[235]
	AX	Wescan anion	0.1 mM sodium benzoate, 4.0 mM NaOH	[236]
	AX	TSK-gel IC-Anion–PW	1.0 mM KOH	[237]
	AX	Hamilton PRP-X100	4.0 mM hydroxybenzoate, pH 8.9	[238]
	AX	TSKgel IC-Anion-PW	20mM DME, 1.43mM formic acid, 0.03mM $Na_2B_4O_7$, 20nM TETHAA, pH 10.5	[239]
Resistivity	AX	Dionex anion separator	2.5 mM NaOH	[240]
Amperometry				
Au, Pt, dropping Hg electrodes	AX	Dionex anion separator	5.0 mM NaOH	[241]
Ag electrode	AX	Dionex Fast Run Anion	14.7 mM DAE, 10 mM $Na_2B_4O_7$, 1.0 mM Na_2CO_3, pH 11.0	[242, 243]
Ag electrode	AX	Waters IC Pak A	5 mM KOH	[244]
Ag electrode	AX	Dionex IonPac AS-7	15 mM sodium oxalate, 150 mM NaOH	[245]
Ag electrode	AX	Vydac 302 IC (silica AX)	5 mM KH-phthalate, pH 4.3	[246]
Ag electrode	RPIIC	C18 silica coated with CTAC	100 mM NaCl, 5 mM phosphate buffer	[247]

Table 1.8: Detection systems and separation conditions used for the HPLC analysis of cyanide. Continued on next page. Abbreviations on next page

Detection system	Separation mode	Column	Eluent	Ref.
Potentiometry				
- Cu electrode	AX	Vydac 302 IC (silica AX)	40 mM tartrate, pH 3.2	[204]
- ISE	AX	Wescan 269001 (silica AX)	1.5 mM acetate buffer, pH 6.4	[248]
	AX	Dionex HPIC AS-4	14.7 mM DAE, 10 mM $Na_2B_4O_7$, 1.0 mM Na_2CO_3, pH 11.0	[249]
	AX	Dionex HPIC AS-1	10 mM NaOH	[249]
- Coulometric	AX	Aminex A-25	200 Mm $NaNO_3$	[250]
	IE	Hitachi 2613 cation-exchange	Deionised water	[251]
Indirect UV				
265 nm	AX	Aminex anion exchanger	0.5 mM KH-phthalate	[252]
265 nm	AX	Synchropak AX300	2.5 mM KH-phthalate, 0.4 mM citrate, pH 6.8	[253]
280 nm	AX	Vydac 300 IC	4.0 mM benzoic acid, pH 9.25	[254]
312 nm	AX	Hamilton PRP X-100	0.45 mM 2,4-dihydroxybenzoic acid, pH 10.1	[255]
Radiochemical (^{11}C labeled cyanide)	RP	LiChrosorb RP-18	10 mM octylamine, H_3PO_4, pH 4.7	[256]

Table 1.8: Detection systems and separation conditions used for the HPLC determination of cyanide. Continued from previous page.

Abbreviations: CTAC: cetyltrimethylammonium chloride; DAE: 1,2-diaminoethane; DME: 2-dimethylaminoethanol;

TETHAA: triethylenetetramine-NNN'N''N'''N'''-hexa-acetic acid hexasodium salt; KH-phthalate: Potassium hydrogen phthalate.

Post-column derivatisation	Sep. mode	Column	Eluent	Detection	Reference
König reaction					
- Py/BA	AX	TSK Gel LS-222	200 mM NaClO$_4$, 100 mM acetate buffer, pH 5.0	Vis (580 nm)	[257]
- Py/BA	AX	TSK Gel LS-222	200 mM NaClO$_4$, 100 mM acetate buffer, pH 5.0	Fluorescence	[258]
- INA/PZ	IE	PCS5-052/SCS5-252	1 mM H$_2$SO$_4$	Vis (638 nm)	[217, 218, 259]
Reaction with OPA or NDA and glycine	IE	Shim pack SCR 102H	10mM HClO$_4$	Fluorescence	[260]
Reaction with OPA and NH$_4^+$	IE	Shim pack SCR 102H	10mM ammonium citrate at pH 3.3	Fluorescence	[261]

Table 1.9: Post-column derivatisation reactions used for the detection of cyanide.

Derivatisation reaction	Separation and detection of reaction derivative	Reference
Oxidation to cyanate with hypochlorite or chloramine-T	Anion exchange separation and suppressed conductivity detection of cyanate.	[262, 263] [264]
Hydrolysis of cyanide to formate	Anion exchange separation and suppressed conductivity detection of formate.	[265]
Reaction of CN$^-$ with I$_2$(s). Iodide liberated.	Anion exchange separation and non-suppressed conductivity detection of iodide.	[266]
Reaction of CN$^-$ with polysulfide. SCN$^-$ formed.	Anion exchange separation and non-suppressed conductivity detection of thiocyanate	[267]
Reaction with Ni^{2+} to form [Ni(CN)$_4$]$^{2-}$	RPIIC separation and UV detection of [Ni(CN)$_4$]$^{2-}$	[186, 268]
Reaction with Ag$_{(s)}$ to form [Ag(CN)$_2$]$^-$	RPIIC separation and UV detection of [Ag(CN)$_2$]$^-$	[269]
Reaction with NDA and primary amine	Reversed phase separation and fluorescence detection of isoindole derivative	[270, 271]
Reaction of cyanide with [Fe(1,10-phen)$_3$]$^{2+}$	RPIIC separation and UV detection of [Fe(1,10-phen)$_2$(CN)$_2$]^0	[272]
Reaction of cyanide with quinoline and benzyl chloride	Reversed phase separation and UV detection of 1-benzoyl-1,2-dihydroquinaldonitrile	[273]

Table 1.10: Pre-column derivatisation reactions used for the separation and detection of cyanide as the reaction product. Abbreviations: Py/BA : Pyridine/Barbituric acid; INA/PZ: Isonicotinic acid/Pyrazolone; OPA : O-phthaladehyde; NDA: 2,3-Napthalenedialedhyde

Column	Organic modifier	[Modifier] (%)	[TBA$^+$] (mM)	IIR Counter anions	[Counter anions] (mM)	Detection	Major use	Year	Ref.
Dionex MPIC-NS1	Acetonitrile	40	2.0	Carbonate	0.2	Suppressed Cond.	Electroplating	1982	[274, 275]
Dionex MPIC-NS1	Acetonitrile	40	2.0	Carbonate	1.0	Suppressed Cond.	Electroplating	1983	[276]
Dionex MPIC-NS1	Acetonitrile	30	2.0 (TPA$^+$)	Carbonate	2.0	Suppressed Cond.	Electroplating	1985	[277]
Partsil 5-μm ODS	Methanol	45	170 NMeBu$_3^+$	Br$^-$, Perchlorate	Not specified	Abs (254 nm)	Ligand exchange	1984	[277a]
Partsil 5-μm ODS	Methanol	45	181 (NEt$_4^+$)	Cl$^-$, Perchlorate	50, 100	Abs (254 nm)	Ligand exchange	1984	[277b]
Dionex MPIC-NS1	Acetonitrile	26	2.0	CO$_3^{2-}$, HCO$_3^-$	2.3, 2.8	Suppressed Cond.	Au-CNProc.	1985	[150]
Waters Nova-Pak C-18	Acetonitrile	23	5.0	Low UV PIC A	5.0	Abs (214 nm)	Au-CNProc.	1986	[1]
Not specified	Acetonitrile	40	2.0	Carbonate	0.2	Suppressed Cond.	Electroplating	1987	[278]
Waters Nova-Pak C-18	Methanol	30	2.5	Low UV PIC A	2.5	Abs (210 nm)	Au-CNProc.	1987	[279]
Waters Nova-Pak C-18	Acetonitrile		5.0	Low UV PIC A	5.0	Abs (214 nm)	Au-CNProc.-Env.	1988	[2, 3, 280]
SUPELCOSIL LC-18	Acetonitrile	29	2.0	Phosphate	2.25	Abs (217 nm)	Au-CNProc.	1988	[269]
Dionex MPIC-NS1	Acetonitrile	23	2.0	CO$_3^{2-}$, HCO$_3^-$	0.5, 0.5	Abs (240 nm)	Au-CNProc.	1988	[281] (*)
Dionex MPIC-NS1	Methanol	28.5	2.0	Cyanide	40	Supp. Cond.	Synthesis	1989	[282]
Silasorb C-18	Acetonitrile	30	1.0	Butyrate	1.0	Non-Supp. Cond.	Au-CNProc.	1991	[283, 284]

Table 1.11: Summary of RPIIC separations of the metallo-cyanide complexes (Continued next page).

(*) : Used for the analysis of oxidised S species, thiocyanate and Cu(I)-cyanide complex.

Column	Organic modifier	[Modifier] (%)	[TBA$^+$] (mM)	IIR Counter anions	[Counter anions] (mM)	Detection	Major use	Year	Ref.
Waters Nova-Pak C-18	Mixtures of MeCN, MeOH and THF	Various	5.0	Low UV Pic A TBA Cl TBA Br	5.0	Abs (214 nm)	Au-CNProc-Env.	1991	[4]
Dionex MPIC-NS1	Acetonitrile	35	2.0	Perchlorate	1-10	Abs (215 nm)	Au-CNProc.	1993	[285]
DuPont-Zorbax C-18 Waters Nova-Pak C-18	Acetonitrile	35	4.0	Phosphate	1.25	Abs (215 nm)	Au-CNProc.	1994	[286]
Waters Nova-Pak C-18	Acetonitrile	25	60	Phosphate Perchlorate	150 2.34	Abs (214 nm)	Au-CNProc-Env.	1997	[287]
Waters Nova-Pak C-18	Acetonitrile	22	5.0	Low UV Pic A	5.0	PDA	Au-CNProc-Env.	1997	[156]

Table 1.11: Summary of RPIIC separations of the metallo-cyanide complexe (Continued from previous page). Abbreviations.: TPA$^+$: Tetrapropyl ammonium cation ; Au-CNProc. : Gold cyanidation process leachates; Au-CNProc-Env. : Environmental analysis of tails dams.

Column	Eluent	Detection	Comments	Intended use	Year	Ref.
Dionex IonPac AS5	20 mM NaCN, 20 mM NaOH	UV (215 nm)	Gradient (over 18 min): 30-135 mM NaClO$_4$	Au-CN Proc.	1991	[288]
Dionex HPIC-AG4	50 mM NaClO$_4$, 15 mM NaCN, 20 mM NaOH	UV (215 nm)	Isocratic	Au-CN Proc.	1992	[289]

Table 1.12: Summary of anion exchange separations of the metallo-cyanide complexes.

"Non-suppressed" conductivity detection was developed in an effort to overcome some of the problems associated with the use of a suppressor. Initially, very low capacity resins were developed which enabled the elution of anions with eluents of very low ionic strength and hence low background conductance [295]. This permitted the use of direct conductivity detection without the need for a suppressor. However, these resins were of low efficiency, which restricted their separating ability. Later work resulted in the commercial production of low capacity resins with high efficiency, which are suitable for a wide range of eluents [296, 297].

Due to the prevalence of conductivity detection in IC, the terms "suppressed IC" and "non-suppressed IC" have become commonplace. However, it should be realised that these terms are only relevant when applied to IC with conductivity detection.

A few papers have reported the use of resistance (the inverse of conductance), potentiometric and coulometric methods for the detection of cyanide in IC.

1.7.2 Indirect UV detection of cyanide

Indirect UV detection is most suitable for the detection of anions with low molar absorptivity at the detection wavelength. Indirect UV detection occurs due to the replacement of an eluent anion with a large molar absorptivity with an analyte anion with a small molar absorptivity. This results in a negative detection peak. This detection mode is suitable for cyanide, as it is almost transparent over the entire UV region. Since the cyanide anion is only weakly retained during an anion-exchange separation, a weak eluent is preferred. Benzoic acid (and its derivatives) are ideal eluents because they are weak eluents and contain a strong UV chromophore [232].

1.7.3 Detection of cyanide based on pre-column derivatisation

Several selective detection strategies have been developed in order to overcome the conductivity detection problems associated with cyanide, as shown in Tables 1.8-1.10. One approach is to use amperometric detection under conditions that are specific for cyanide, as discussed above. An alternative approach is to chemically alter the cyanide either before (pre-column) or after (post-column) the separation. Pre-column derivatisation allows preparation of species with enhanced separation

and/or detection properties. Improved separation properties have been achieved by converting cyanide to either a strong acid anion (iodide [266], thiocyanate [267]) or a weak acid anion with a low pK_a value (formate [265], cyanate [262, 263]), as shown in Table 1.10. Improved separation and detection has been achieved by converting cyanide to either the $[Ni(CN)_4]^{2-}$ [186, 268] or $[Ag(CN)_2]^-$ [269] complexes. Improved detection has been achieved by converting cyanide to an organic species with intense UV absorption [273] or fluorescence [270, 271].

1.7.4 Detection of cyanide by post-column derivatisation

An alternative to pre-column derivatisation is to derivatise the analyte (cyanide) after the separation. This is known as post-column reaction (PCR) derivatisation and allows potential interferences in the derivatisation reaction to be chromatographically removed prior to the reaction. An example of this is the IC analysis of cyanide and thiocyanate with PCR detection using variants of the König reaction [217, 257, 258]. Both these analytes are derivatised by the König PCR. However, these analytes are also readily separated by either AX or IE chromatography.

Two main factors need to be considered when selecting a derivatisation reaction [298]. These are firstly, the derivatisation reaction should be rapid in order to ensure minimal dispersion. While the reaction need not go to completion, the extent of reaction should be reproducible. Secondly, the reaction should be specific for the solute(s) required and not give detectable products with the eluent or other species.

Two types of reactor have been developed for post column derivatisations, namely tube reactors and bed reactors. The most common type is the tube reactor. It has been shown that tube reactors have improved radial mixing and less band broadening if they are coiled [299]. The mixing can be further improved by using a 'knitted' reaction coil [300, 301].

Only a small number of papers have been published which use PCR detection for cyanide, as shown in Table 1.9. The reactions used include variations of the König reaction [217, 257], reaction of glycine with either OPA or NDA [260], and a related reaction involving ammonia and citrate [261]. The rapid formation of $[Ni(CN)_4]^{2-}$ from Ni^{2+} in an ammonia buffer may also form the basis of a suitable PCR for cyanide.

1.6.4 Separation of the metallo-cyanide complexes

It was mentioned previously that most of the reported separations of the metallo-cyanide complexes employed RPIIC. In this separation mode, a reversed-phase column is modified by the addition of an ionic hydrophobic reagent (known as an ion-interaction reagent, IIR) in order to increase the retention of oppositely charged ionic solutes. The IIR becomes adsorbed onto the stationary phase, producing a "dynamic ion-exchanger", for which the ion-exchange capacity is governed by the quantity of IIR which is adsorbed. This quantity is controlled chiefly by the nature of IIR and the concentration of organic modifier in the eluent.

The initial RPIIC methods developed for metallo-cyanide complexes employed acetonitrile, tetrabutylammonium hydroxide (TBAOH) and a carbonate buffer. It is interesting to note that prior to the advent of IC, many metallo-cyanide complexes were known to form stable ion pairs with quaternary ammonium reagents [302]. This allowed the development of TLC methods for the separation of the quaternary ammonium ion pairs of the Fe-cyanide complexes and thiocyanate.

The initial RPIIC separations were performed on polymeric resin columns with suppressed conductivity detection. Since the tetrabutylammonium cation (TBA^+) is unaffected by the suppressor, it is necessary to compromise between detection sensitivity and separation efficiency, as both these parameters are affected by the TBA^+ concentration. The TBA^+ concentration was generally restricted to 1-2 mM when used with conductivity detection.

Later work by Padarauskas *et al.* [283, 284] overcame some of the problems associated with the conductivity detection of the metallo-cyanide complexes. This was achieved by use of non-suppressed conductivity detection, which required a counter anion (butyrate) with a low limiting equivalent conductance. The separation was performed on a silica-C18 column with an eluent containing acetonitrile (28%) and TBAbutyrate (1.0 mM). The addition of 1 mM KCN to the eluent, combined with a high eluent pH (9.5), allowed the Cd(II), Zn(II) and Hg(II) cyanide complexes to be separated and detected. However, this high eluent pH was deleterious to the silica-based column and was not recommended for routine analyses.

It has been found that alternative IIR's, such as tetrapropylammonium hydroxide (TPAOH), are not as suitable as TBAOH for the separation of the metallo-cyanide complexes [150]. However, one paper reported that TPAOH was useful in resolving the $[Au(CN)_2]^-$ peak from those of polyphosphonates (dequest agents) which were present in some gold electroplating solutions [277]. It should also be noted that Burnett et al [277a, 277b] have reported the use of several different tertiary and quaternary ammonium salts for the separation of various mixed ligand cyanocobalt(III) cyanide complexes of the general formula $[Co(CN)_5X]^n$, such as $[Co(CN)_5Cl]^{3-}$ and $[Co(CN)_5(OH)_2]^{2-}$.

The initial developments for the analysis of the metallo-cyanide complexes were driven by the analytical requirements of the electroplating industry (especially gold electroplating). RPIIC allowed separation and quantification of the two gold cyanide complexes $[Au(CN)_2]^-$ and $[Au(CN)_4]^{3-}$, as well as the cyanide complexes of other important metals, such as Co and Fe [274, 303]. It has already been mentioned that only the $[Au(CN)_2]^-$ complex can be prepared by dissolution of gold in alkaline cyanide solution. However, the $[Au(CN)_4]^{3-}$ complex can be electrochemically generated during the electroplating process, resulting in reduced electroplating performance.

Prior to the following discussion on the use of IC for monitoring the gold cyanidation process, it should be noted that several other uses for the RPIIC separation of the metallo cyanide complexes have been developed. These include examination of ligand exchange reactions in several mixed ligand cyanocobalt(III) complexes [277a, 277b], formation of various intermediate cobalt-cyanide complexes in the synthesis of the $[Co(CN)_6]^{3-}$ complex [282], and trace analysis of transition metals [303a].

Pohlandt [150, 242, 243] pioneered the use of IC for the analysis of cyano species in the gold cyanidation process. This followed a critical review of 84 alternative methods available for the analysis of cyanide [113]. Pohlandt [150] expanded the RPIIC separation of the metallo-cyanide complexes to allow at least five complexes to be separated. Both suppressed conductivity and UV absorbance detection (240 nm) were used. It was noted that this detection wavelength afforded selective detection of the Cu(I)-cyanide complex compared to the closely eluting Ni and Co-cyanide complexes. The Cu(I)-cyanide complex was not detected with suppressed

conductivity detection due to decomposition of this complex in the suppressor column. It was noted that the Ag-cyanide complex was not detected with either UV (240 nm) or suppressed conductivity detectors. It was assumed that this was because the Ag-cyanide complex was not eluted in this separation. However later work indicated that the Ag-cyanide complex was eluted, but not detected [269]. It was also noted that the Fe(II) and Fe(III) cyanide complexes were co-eluted. This was interesting since earlier reports indicated that the two Fe-cyanide complexes were well resolved under similar separation conditions [274]. Pohlandt [150] also observed that the IIR counter anions in the eluent had a significant effect on the elution order of the Fe-cyanide complexes.

Hilton and Haddad [1] published a paper shortly afterwards that used quite different separation and detection conditions. This was the first reported use of a silica reversed-phase column for the separation of the metallo-cyanide complexes with a RPIIC eluent. In addition, this was also the first reported use of a low UV detection wavelength (214 nm) for the metallo-cyanide complexes. The improved separation conditions enabled up to eight metallo-cyanide complexes to be completely resolved in less than 35 minutes, while the detection conditions enabled a significant improvement in the detection sensitivity. Unlike earlier workers, Haddad and coworkers [2, 4, 304] used a commercially prepared IIR, Low UV PIC A, at a concentration of 5 mM. Some confusion in the literature has resulted from the incorrect identification of the quaternary ammonium cation in Low UV PIC A. It was originally reported that the quaternary ammonium group in Low UV PIC A was tetramethyl ammonium (TMA) [3]. It was subsequently correctly reported that TBA was the quaternary ammonium group in Low UV PIC A [4].

Sensitive detection of the $[Au(CN)_2]^-$ complex was achieved with the Hilton and Haddad [1] method in gold cyanidation leachate samples. This work was continued by Haddad and co-workers [2, 4, 304]. The use of on-line pre-concentration techniques allowed very low concentrations of Au(I) and other metallo-cyanide complexes to be determined in tailings dams and environmental samples.

Similar separation and detection conditions were used by Grigorova et al. [279] to allow analysis of gold cyanidation process leachates and tailings dam liquors. Methanol was used as the organic modifier to reduce the analytical costs. The

concentration of the Low UV PIC A reagent was reduced to 2.5 mM. It was reported that there was significant tailing of the Cu(I) peak with these separation conditions. While Haddad and co-workers used a fixed wavelength detection system, which restricted the detection wavelength, Grigorova *et al.* [279] employed a variable wavelength detector. This allowed the sensitivity at different detection wavelengths to be assessed. It was reported that the most sensitive detection wavelengths were 200 nm for the Ag, Ni, Co and Fe(III)-cyanide complexes, 205 nm for the Au(I) complex, 210 nm for the Cu(I) complex and 220 nm for the Fe(II) complex. A detection wavelength of 210 nm was selected as a compromise.

Following the significant improvements developed by Haddad and co-workers [1, 2, 304], Pohlandt [269] developed a method that used a silica C-18 reversed-phase column and a UV detection wavelength of 215 nm. Pohlandt [269] reported that the detection sensitivity for the Cu(I)cyanide complex decreased with wavelengths below 240 nm. This is surprising and contradictory to other reports [4, 279] and contradictory to the spectral observations described in section 1.4.2.

Pohlandt [269] reported that an eluent containing acetonitrile (29%), TBAOH (2 mM) and a neutral phosphate buffer (2.25 mM) afforded separation of up to eight metallo-cyanide complexes in less than 20 minutes. These conditions allowed resolution of several complexes that were previously co-eluted on a polymeric reversed-phase column. This method was developed for the analysis of gold cyanidation process leachates. It was reported that the uncomplexed and weakly complexed cyanide in a sample could be determined by reaction with a plug of silver wool to form the $[Ag(CN)_2]^-$ complex. Analyses before and after treatment with the silver wool were required when the $[Ag(CN)_2]^-$ complex was present in the original sample.

It was mentioned at the beginning of this section that the metallo-cyanide complexes have been separated on columns with fixed anion-exchange sites (Table 1.12). Separation on AX columns has been achieved by using eluents containing high concentrations of perchlorate and cyanide [288, 289]. Rocklin [288] has reported the only gradient separation of the metallo-cyanide complexes with a gradient of 30-135 mM $NaClO_4$ in 18 min. Otu [289] had to overcome severe chromatographic problems in order to be able to determine the $[Au(CN)_2]^-$ complex in gold

cyanidation leachate samples containing significant concentrations of the Cu(I)-cyanide complexes. High concentrations of ammonia were also required in the eluent to resolve the problem with the Cu(I)-cyanide complexes.

1.8 Process control instruments

This final section examines the analytical methods and instruments that have been used or designed for controlling the cyanide concentration in the gold cyanidation process. It was mentioned in section 1.3 that there are three essential chemical parameters required for efficient leaching of gold from ores. These are leach pH, dissolved oxygen (DO) concentration, and "free" cyanide concentration. The redox potential (E_h) can also be important when leaching reactive sulfide ores [305]. Prior to the use of instruments for the automated control of various parameters of the cyanidation process, considerable variability was observed when the parameters were controlled manually. Fig. 1.12 illustrates the difference between manual and automated cyanide analysis. The automated cyanide analysis was performed on the CYCAD instrument [306].

With respect to the requirements of a process control instrument, Gow *et al.* [307] stated : "The instrument must be compatible with the process characteristics, it must provide an accurate and reliable indication of the variable being measured, and it must give trouble-free performance".

1.8.1 Analytical methods and instruments

There have been several instruments developed for automated cyanide analysis of the gold cyanidation process. These are summarised in Table 1.13. The majority of commercially available cyanide analysers for monitoring the gold cyanidation process are based on the argentometric titration of cyanide with potentiometric detection of the end-point.
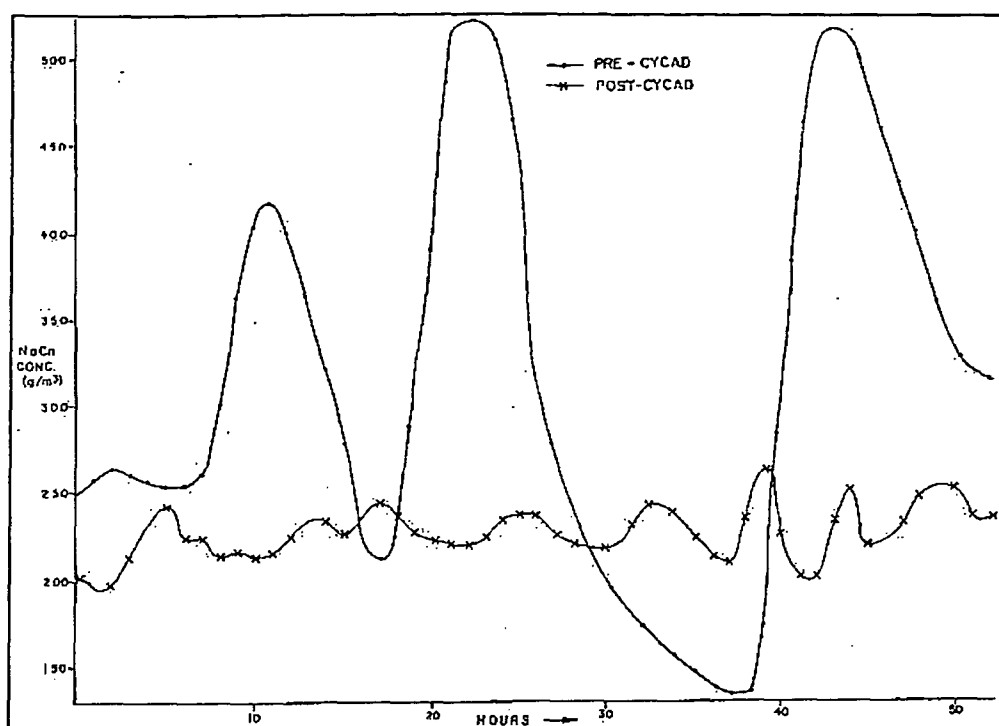
Fig. 1.12: Comparison of process cyanide levels when the cyanide analysis is performed by manual and automated methods. Automated analysis performed with the CYCAD instrument. Source: Fig. 3 of [306].

The earliest automated cyanide analyser would appear to have been developed in 1964 for the Canadian Mines Branch by Ingles [307, 308]. This instrument consisted of a continuous potentiometric titrator. The first commercially available instrument incorporating potentiometric titration was called CYCAD [306]. This instrument was developed by the Anglo-American Research Laboratories (AARL). CYCAD employed gold indicator and "Thalamid" reference electrodes. The gold electrode was reported to have greater long-term stability and reproducibility when compared to that of a silver indicator electrode.

Prior to the CYCAD instrument, there were various reports that mentioned automated cyanide analysers suitable for gold cyanidation liquors. The Kegold electrodes, developed by Mintek in 1974 consisted of a silver button, which measured the potential in contact with cyanide solutions [329]. This potential is the mixed potential due to the corrosion of silver by oxygen in solutions containing cyanide. The measurement is affected by both the cyanide and oxygen concentrations. The dependence on both variables makes it difficult to control only the cyanide concentration with the Kegold electrode. It has been reported that there

are difficulties in using this approach due to the necessity for cleaning and re-calibrating the Kegold electrode at frequent intervals [322], due primarily to the formation of oxide films on the surface of the silver. However, it should be noted that the Hedges Gold Mine has reported successful use of a T.D.I. Kegold automated cyanide monitor [315].

While the Kegold electrode may not be ideal for monitoring the cyanide concentration, it is able to indicate the leaching capability of the leachate since both cyanide and oxygen are required for gold dissolution (Eqn. 1.1-1.4). A more recent invention, the LeachMETER ® cyanidation rate meter is reported to be able to monitor the leaching ability of the leachate [316]. The principles involved in the operation of this device are not available publicly. However, it would appear reasonable to assume that at least part of this device involves monitoring the potential of a gold electrode when placed in a leachate.

In contrast to the above analysers, the Alkay on-line analyser is capable of monitoring the cyanide concentration, dissolved oxygen concentration, pH, lime concentration and gold concentration in separate modules [312]. The Alkay analyser uses potentiometric titration for monitoring the cyanide concentration.

A method of cyanide analysis based on the decrease in absorbance of a Cu(II) solution in the presence of cyanide was reported to be used at several South African Gold mines. This analysis was developed into a commercial cyanide analyser called CYANOSTAT by Polymetron (a Swiss instrument manufacturer and subsidiary of Zellweger) [5, 325]. The chemistry behind the operation of this analyser is relatively simple. The sample is mixed with a Cu^{2+} solution (either sulfate or citrate) to form the colourless Cu(I)-cyanide complexes. EDTA is then added to form an intense blue complex with the remaining Cu(II). The sample and reagents are pumped using a robust peristaltic pump.

Analytical method	Comments	Commercial name	Manufacturer	Year	Ref.
Potentiometric titration					
	Ag indicator electrode	-	-	1966	[307]
	Indicator electrode not specified	-	-	1969	[309]
	Ag indicator electrode			1982	[310]
	Au indicator electrode	CYCAD	AARL	1986	[306]
	Indicator electrode not specified	-	Degussa	1988	[108]
	Au indicator electrode	CYCAD II	AARL	1993	[311]
	Indicator electrode not specified	ALKAY	Tek-Logic	1991	[312]
	Ag indicator electrode	CYANCOR	Corrigan Instrumentation	1991	[7]
	Ag indicator electrode	OTA-3000	Chemtronics	1997	[313]

Table 1.13: Analytical instruments developed for controlling the free cyanide in the gold cyanidation process. (Continued on next page)

Analytical method	Comments	Commercial name	Manufacturer	Year	Ref.
Potentiometric					
Ag electrode	Leaching performance	Kegold	MINTEK / T.D.I.	1974	[314, 315]
Au electrode	Leaching performance	LeachMETER	Mennetech	1991	[316]
CN^- ISE		-	BP Research	1984-1989	[317]
CN^- ISE		-	MINTEK	1984-1989	[314, 318, 319]
CN^- ISE		CYMON	MINTEK	1992,1966	[320, 321]
Voltammetric/Amperometric					
Cu electrode-Amperometric		-	-	1992, 1994	[210, 322]
Cu electrode-Voltammetric		-	-	1987	[323]
Cu electrode-Voltammetric		-	-	1994	[324]

Table 1.13: Analytical instruments developed for controlling the free cyanide in the gold cyanidation process. (Continued on next page)

Analytical method	Comments	Commercial name	Manufacturer	Year	Ref.
Spectrophotometric					
Cu sulfate/EDTA		CYANOSTAT	Polymetron	1987	[5]
Cu citrate/EDTA				1988	[325]
UV abs. of Cu(I)-cyanide complexes	Simplistic deconvolution of spectra to estimate Cu(I) complexes and cyanide.	-	-	1973	[151]
Ion Chromatography					
Anion exchange	Analysis of cyanide	MINTEK	-	1984	[280, 326]
RPIIC	Analysis of metallo-cyanide complexes	AARL	-	1987	[279]
RPIIC	Analysis of metallo-cyanide complexes and cyanide.	MINTEK		1985, 1988	[269] [327]
Miscellaneous					
Membrane	Diffusion of HCN from leachate across membrane	-	-	1991	[328]
Raman	Insensitive. Discrimination of Cu(I)-cyanide complexes possible.	-	-	1995	[145]

Table 1.13: Analytical instruments developed for controlling the free cyanide in the gold cyanidation process.

Various monitoring systems based on the electrochemical detection of cyanide are in use. One of the advantages claimed by the authors of electrochemical systems is the reduction of reagent consumption. The most prevalent electrochemical method employs cyanide ion selective electrodes (ISE's). Unfortunately, there are several problems associated with the use of cyanide ISE's for process control applications [325]. Leach pH and temperature fluctuations will affect the electrode response. Sulfide, which is present in many leachates, will cause changes in electrode potential and eventually destroy the electrode, as discussed earlier. It has been reported that the presence of sulfide resulted in significant overdosing on at least one occasion when using a cyanide ISE [108]. The solid state membrane in commercially available cyanide ISE's is constructed of Ag_2S – AgI, which is gradually dissolved by the high cyanide concentration in the leachate. The high cost and short life of commercially available cyanide ISE's prompted MINTEK to develop its own cyanide ISE's [318, 320]. The detector cell consists of a cyanide selective AgI - Ag_2S electrode and a miniaturised Ag - $AgCl$ reference electrode. The ISE was used in conjunction with a sequential injection manifold.

Crundwell and Jensen [210, 322] have proposed an amperometric instrument with a Cu working electrode. It is reported that sulfide, thiocyanate, and thiosulfate can be tolerated by this device. Initial results indicated that regular calibration would be required on at least every second day. Similar devices have been reported to be in operation in Siberia [324].

1.8.2 Sample filtration

All the commercially available process cyanide analysers require a clear filtrate. It is now accepted that on-line sample filtration is one of the major problems facing operation of an automated cyanide analyser designed for a mill due to the slurry of very small ore particles.

To overcome this filtration problem, some authors have proposed analytical methods that do not require sample filtration. A novel solution uses a hydrophobic PFTE membrane to allow diffusion of HCN from alkaline leach slurries into a NaOH carrier solution [328]. A sensitive spectrophotometric method (the pyridine/barbituric acid variant of the Konig reaction) was used to detect the low

concentration of cyanide in the NaOH carrier solution. The disadvantage of this method was its susceptibility to changes in the ionic strength of the leachate.

An alternative method, which eliminates the need for sampling and filtration systems, uses FT-Raman spectroscopy with fiber optic probes [145, 330]. While this has not as yet been used on an operational gold mine, the technology would appear to be suitable, especially when speciation of the Cu(I)-cyanide complexes is required. The two major disadvantages involved in using Raman spectroscopy are the poor sensitivity and the high cost of Raman instruments. In addition, replacement lasers for Raman instruments can be very expensive and may not be readily available. These considerations make the use of Raman spectroscopy impractical at the current time for controlling the gold cyanidation process.

Direct monitoring of the leachate with cyanide ion selective electrodes has been tried without notable success [306].

1.9 Aims of the project

The primary aim of this project was to develop IC methodology suitable for controlling the gold cyanidation process. This was to be achieved by coupling a suitable cyanide detection system to the existing RPIIC separation system, thereby providing simultaneous determination of "free" cyanide and the metallo-cyanide complexes. This was to then tested under field conditions to assess its potential usefulness to the gold mining industry.

1.10 References

1   D. F. Hilton and P. R. Haddad, *J. Chromatogr.*, 361 (1986) 141.

2   P. R. Haddad and N. E. Rochester, *Anal. Chem.*, 60 (1988) 536.

3   P. R. Haddad and N. E. Rochester, *J. Chromatogr.*, 439 (1988) 23.

4   P. R. Haddad and C. Kalambaheti, *Anal. Chim. Acta*, 250 (1991) 21.

5   R. J. M. Wyllie, *Engineering and Mining Journal*, 188 (1987) 32.

6   R. Bull, *Engineering and Mining Journal*, 190 (1989) 67.

7   C. Dufresne, G. Deschenes, D. Cimon and J. Corrigan, *Minerals Engineering*, 7 (1994) 1427.

8   P. D. Chamberlain, "Randol Gold Forum '96"; Squaw Creek, Olympic Valley, California, USA, 1996; Randol International Ltd., Golden, Colorado, USA; 303.

9   N. N. Greenwood and A. Earnshaw In Chemistry of the elements; Pergamon Press: Sydney, Australia, 1984, pp 1365.

10   H. Schmidbaur, *Interdisciplinary Science Reviews*, 17 (1992) 213.

11   R. W. Boyle, *Gold : History and genesis of deposits*; Van Nostrand Reinhold Co.: New York, 1987.

12   C. J. Paterson, *Mineral Processing and extractive metallurgy review*, 6 (1990) 67.

13   A. M. Evans, *Ore geology and industrial minerals : An introduction*, 3rd ed.; Blackwell Scientific Publications, Melbourne, Victoria, Australia, 1993.

14   C. Gasparrini, *C.I.M. Bulletin*, 76 (1983) 144.

15   D. M. Muir, S. R. La Brooy and C. Cao, "World Gold '89 - Gold Forum on Technology and Practices, Proceedings 1st AusIMM-SME joint Conference"; 5-8 November 1989, Reno, Nevada, USA, Society for Mining, Metallurgy and Exploration, Inc., Littleton, Colorado.; 363.

16   B. A. Wills, *Mineral Processing Technology: An introduction to the practical aspects of ore treament and mineral recovery*, 4th ed.; Pergamon Press: Oxford, 1988.

17   R. B. Bhappu, *Mineral Processing and extractive metallurgy review*, 6 (1990) 67.

18   J. R. Flatt, G. Dunlop, H. W. Fander, K. Wong and B. K. O'Neill, "World Gold '91 - Gold Forum on Technology and Practices , Proceedings 2nd AusIMM-SME Joint Conference"; 21-26 April 1991, Cairns, Australia, 1991; The Australasian Institute of Mining and Metallurgy (AusIMM); 79.

19   S. R. La Brooy, H. G. Linge and G. S. Walker, *Minerals Engineering*, 7 (1994) 1213.

20   R. Dunne, "Randol Gold Forum 1991"; Cairns, Australia, 16-19 April 1991, 1991; Randol International Ltd.; 239.

21   C. T. O'Connor and R. C. Dunne, *Minerals Engineering*, 7 (1994) 839.

22   D. Muir, S. La Brooy and K. Fenton, "World Gold '91"; Cairns 21-25 April 1991, 1991; The Australasian Institute of Mining and Metallurgy (AusIMM); 145.

23   S. Kittel and G. J. Harbort, "International conference on Extractive metallurgy of gold and base metals"; Kalgoorlie, W.A., 1992; The Australasian Institute of Mining and Metallurgy; 211.

24   T. Tran, *Interdisciplinary Science Reviews*, 17 (1992) 356.

25   K. E. Haque, *Mineral Processing and Extractive Metallurgy Review*, 2 (1987) 235.

26   D. Muir, *Bull. Proc. Australas. Inst. Min. Metall.*, 292 (1987) 87.

27   A. R. Udupa, S. K. Kawatra and M. S. Prasad, *Mineral Processing and Extractive Metallurgy Review*, 7 (1990) 115.

28   J. Marsden and I. House, *The chemistry of gold extraction*; Ellis Horwood: New York, 1992.

29   R. S. Shoemaker, "Precious Metals : Mining, Extraction and Processing"; Los Angeles, California, 1984; The Metallurgical Society of AIME; 3.

30   V. Kudryk and H. H. Kellogg, *Journal of Metals*, (1954) 541.

31   X. Wang and K. S. E. Forssberg, *Mineral Processing and extractive metallurgy review*, 6 (1990) 81.

32   M. E. Wadsworth, "H.H.Kellog International Symposium, Quantitative description of metal extraction processes"; Harriman, New York, USA, September 4-6, 1991; The Minerals, Metals and Materials Society; 197.

33   D. Muir, "Carbon in Pulp seminar"; Perth, 1982; Aus. I.M.M.; 7.

34   K. E. Haque, *CIM Bulletin*, 85 (1992) 31.

35   K. Osseo-Asare, T. Xue and V. S. T. Ciminelli, "Precious Metals : Mining, Extraction and Processing"; Los Angeles, California, 1984; The Metallurgical Society of AIME; 173.

36   R. M. Smith and A. E. Martell In Critical Stability Constants.

Volume 4: Inorganic Ligands; Plenum Press: London, 1976; Vol. 4, pp 26.

37   S. R. La Brooy and D. M. Muir, "The AusIMM Proceedings"; 1994; AusIMM; 81.

38   P. Verhoeven, G. Hefter and P. M. May, *Minerals & Metallurgical processing*, (1990) 185.

39   N. Hedley and H. Tabachnick, *Chemistry of cyanidation*; American Cyanamid Company: Wayne, N.J., 1968.

40   F. Habashi ; Montana College of Mineral Science and Technology: Butte, Montana, 1967, pp 42.

41   J. Zheng, I. M. Ritchie, S. R. Labrooy and P. Singh, *Hydrometallurgy*, 39 (1995) 277.

42   A. Lawry, P. Gelfi, I. Mitchell, R. Pyper and R. Dunne, "Recent Trends in Heap Leaching"; Bendigo, Vic., 1994; The Australasian Institute of Mining and Metallurgy; 89.

43   R. E. Browner, J. H. Kyle and V. N. Misra, "World Gold '91 - Gold Forum on Technology and Practices , Proceedings 2nd AusIMM-SME Joint Conference"; 21-26 April 1991, Cairns, Australia; The Australasian Institute of Mining and Metallurgy (AusIMM); 219.

44   P. D. Kondos, W. F. Griffith and J. O. Jara, *Canadian Metallurgical Quarterly*, 35 (1996) 39.

45   D. M. Menne, "Randol Gold Forum 1991"; Cairns, Australia, 16-19 April 1991; Randol International Ltd.; 355.

46   D. M. Menne, *Gold cyanidation - Vol.1 : Chemistry and Kinetics*; electroMAGNETIC Books, 1991.

47   T. Revy, S. Watson and W. Hoecker, "Randol Gold Forum 1991"; Cairns, Australia, 16-19 April 1991, 1991; Randol International Ltd.; 317.

48   S. R. La Brooy and T. Komosa, "International conference on extractive metallurgy of gold and base metals"; Kalgoorlie, W.A., 1992; The Australasian Institute of Mining and Metallurgy, Parkville, Vic.; 147.

49   J. Jara and A. Bustos, *Hydrometallurgy*, 30 (1992) 211 .

50   A. Nugent, K. Brackenbury and J. Skinner, "World Gold '91 - Gold Forum on Technology and Practices , Proceedings 2nd AusIMM-SME Joint Conference"; 21-26 April 1991, Cairns, Australia, 1991; The Australasian Institute of Mining and Metallurgy, 173.

51   J. K. Beattie and G. A. Polyblank, *Australian Journal of Chemistry*, 48 (1995) 861.

52   G. Deschenes and P. J. H. Prudhomme, *Source International Journal of Mineral Processing*, 50 (1997) 127.

53   L. Lorenzen and J. S. J. Vandeventer, *Hydrometallurgy*, 30 (1992) 177.

54   L. Bolinski and J. Shirley, "Randol Gold Forum '96"; April 21-24, 1996, Squaw Creek, CA, USA, 1996; Randol International Ltd.; 419.

55   G. Chi, M. C. Fuerstenau and J. O. Marsden, *International Journal of Mineral Processing*, 49 (1997) 171.

56   J. O. Marsden and M. C. Fuerstenau, "XVIII International Mineral Processing Congress"; Sydney, Australia, 23-28 May 1993, 1993; AusIMM; 1175.

57   S. H. Dayton, *Engineering and Mining Journal*, 188 (1987) 25.

58   P. A. Laxen, G. S. M. Becker and R. Rubin, *Journal of the South African Institute of Mining & Metallurgy*, 94 (1994) 189.

59   C. Gill ; John Wiley and Sons, 1980, pp 190.

60   P. J. N. Sinclair, *Interdisciplinary Science Reviews*, 17 (1992) 229.

61   R. Murphy, *Interdisciplinary Science Reviews*, 17 (1992) 234.

62   R. Wan and J. Miller, *Mineral Processing and extractive metallurgy review*, 6 (1990) 143 .

63   S. R. La Brooy, " First International Conference on Hydrometallurgy"; Beijing, People's Republic of China, 1988; International Academic Publishers (Distributed by Pergamon Press outside PRC); 466.

64   K. Thomas, *CIM Bulletin*, (1991) 33 .

65   W. G. Jones, C. Klauber and H. G. Linge, "World Gold '89, Proc. 1st AusIMM-SME joint Conference"; Reno, Nevada, 1989; Society for Mining, Metallurgy and Exploration, Inc., Littleton, Colorado; 278.

66   M. Adams and C. Fleming, *Metallurgical Transactions B*, 20B (1989) 315.

67   M. Adams, *Hydrometallurgy*, 31 (1992) 111.

68   M. D. Adams, "XVIII International Mineral Processing Congress"; Sydney, Australia, 23-28 May 1993, 1993; AusIMM; 1175.

69   H. von Michaelis, *Engineering and Mining Journal*, 188 (1987) 50.

70   X. Chang-Chun and X. Ji-Yuan, *Mineral processing and extractive metallurgy review*, 6 (1990) 217.

71   R. Arriagada and R. Garcia, *Hydrometallurgy*, 46 (1997) 171.

72   M. D. Adams, S. J. Swaney, J. Friedl and F. E. Wagner, "Hidden Wealth"; Johannesburg, South Africa, 1996; South African Institute of Mining and Metallurgy; 163.

73   K. Osseo-Asare, P. M. Afenya and G. M. K. Abotsi, "Precious Metals : Mining, Extraction and Processing"; Los Angeles, California, 1984; The Metallurgical Society of AIME; 125.

74   G. Beer, "6th AusIMM Extractive Metallurgy Conference"; Brisbane, 3-6 July 1994; Australasian Institute of Mining and Metallurgy (AusIMM); 203.

75   F. W. Petersen and J. S. J. Vandeventer, *International Journal of Mineral Processing*, 50 (1997) 211.

76   G. M. Ritcey, *Can. Metall. Q.*, 25 (1986) 31.

77   D. R. Dunne, C. Metallurgist and N. M. Ltd., Personal Communication, 1998.

78   D. B. Dreisinger, B. Wassink, F. P. de Kocks and P. West-Sells, "Randol Gold Forum '96"; Squaw Creek, Olympic Valley, California, USA, 1996; Randol International Ltd., Golden, Colorado, USA; 315.

79   R. G. Luthy, S. G. Bruce, R. W. Walters and D. V. Nakles, *Journal Water Pollution Control Federation*, 51 (1979) 2267.

80   R. G. Luthy and S. G. Bruce, *Environmental Science and Technology*, 13 (1979) 1481.

81   D. M. Muir, M. Aziz and W. Hoeker, " First International Conference on Hydrometallurgy"; Beijing, People's Republic of China, 1988; International Academic Publishers (Distributed by Pergamon Press outside PRC); 461.

82   M. D. Adams, *J. S. Afr. Inst. Min. Metall.*, 90 (1990) 37.

83   M. D. Adams, *J. S. Afr. Inst. Min. Metall.*, 90 (1990) 67.

84   F. R. Duke and W. G. Courtney, *J. Phys. Chem.*, 56 (1952) 19.

85   R. Parkash and J. Zyka, *Microchemical J.*, 17 (1972) 309 .

86   M. D. Adams, *Minerals Engineering*, 7 (1994) 1165.

87   R. Shantz and J. Reich, *Hydrometallurgy*, 3 (1978) 99.

88   G. J. Parsons, L. A. Newcombe and D. W. Derham, "XVIII International Mineral Processing Congress"; Sydney, Australia, 23-28 May 1993, AusIMM; 1205.

89   H. Nguyen, K. B. Quast and R. Newell, "6th AusIMM Extractive Metallurgy Conference"; Brisbane, 3-6 July 1994; (AusIMM); 197.

90   E. S. Leaver and J. A. Woolf ; U.S. Bureau of Mines: Washington, D.C., 1931.

91   M. M. Latt, T. D. Rice and J. D. Sinniah, *Analyst*, 122 (1997) 1265.

92   S. Vukcevic, *Minerals Engineering*, 9 (1996) 1033.

93   N. Hedley and D. M. Kentro, *Trans. Can. Inst. Min. Metall.*, 48 (1945) 237.

94   H. von Michaelis, "13th Annual Mining and Metallurgy Industries Symposium and Exhibit"; 15-17 May 1985, Salt Lake City, Utah, USA; Instrument Society of America; 1.

95   A. J. Nugent, "Randol Gold Forum 1991"; Cairns, Australia, 16-19 April 1991; Randol International Ltd.; 341.

96   S. Vukcevic, *Minerals Engineering*, 10 (1997) 309.

97   S. R. La Brooy, "Randol Gold Forum Vancouver '92"; March 25-27, 1992, Vanvouver, B.C., Canada, 1992; Randol International Ltd.; 173.

98   G. M. Willis and J. T. Woodcock, *Proc. Australasian Institute of Mining and Metallurgy*, 158-159 (1950) 465.

99   A. G. MacDiarmid and F. H. Norris, *J. Am. Chem. Soc.*, 76 (1954) 4222.

100   N. Tsuchida, M. Ruane and D. Muir, "MINTEK 50 : Proceedings of the Int. Conf. on Mineral Science and Technology"; 1984; ; 647.

101   A. S. Ibrado and D. W. Fuerstenau, *Minerals and Metallurgical Processing*, 6 (1989) 23.

102   C. Ayers In Comprehensive Analytical Chemistry; Wilson, C. L., Wilson, D. W., Eds.; Elsevier: London, 1960; Vol. 1B, pp 222.

103   J. von Liebig, *J. Chem. Soc.*, 4 (1852) 219.

104   G. Deniges, *Ann. Chim. Phys.*, 6 (1895) 381.

105   A. P. H. Association and A. W. W. Association, *Standard methods for the examaination of water and wastewater*, 16th ed.; American Public Health Association (APHA): Washington, DC, 1985.

106   W. J. Williams, *Handbook of Anion Determination*; Butterworths: London, 1979, pp. 70-87.

107   R. S. Schulz and W. P. Staunton, "Perth International Gold Conference (1988 Randol Gold Forum)"; 28 October - 1 November 1988, Perth, Western Australia; Randol International Ltd.; 94.

108   A. Griffiths, "Perth International Gold Conference (1988 Randol Gold Forum)"; 28 October - 1 November 1988, Perth, Western Australia; Randol International Ltd.; 194.

109   A. Gupta, E. F. Johnson and R. H. Schlossel, *Industrial and Engineering Chemistry Research*, 26 (1987) 588.

110   W. H. Virgoe, *Trans. Inst. Min. Metall.*, 10 (1901) 103.

111   J. Brigando, *Bull. Soc. chim.*, 2 (1957) 503.

112   A. F. Lee ; Anglo American Reserach Laboratories: Johannesburg, 1976.

113   C. Pohlandt, E. A. Jones and A. F. Lee, *Journal of the South African Institute of Mining amd Metallurgy*, 83 (1983) 11.

114   E. Stamboliadis, J. McHardy and T. Salman, *Canadian Mining and Metallurgical Bulletin {CMM Bull.}*, 69 (1976) 128.

115   EMJ_Staff, *Engineering and Mining Journal*, 196 (1995) 44.

115a   M. R. Davis, K. C. Sole, J. M. W. Mackenzie and M. J. Virnig, *"Alta Hydrometallurgical Forum"*; Brisbane, 1998

116   D. B. Dreisinger, Personal communication, 1998.

117   EMJ_Staff, *Engineering and Mining Journal*, 168 (1967) 123.

118   B. Sceresini and P. Richardson, "Randol Gold Forum 1991"; Cairns, Australia, 16-19 April 1991; Randol International Ltd.; 265.

119   L. Whittle, "Randol Gold Forum Vancouver '92"; March 25-27, 1992, Vanvouver, B.C., Canada; Randol International Ltd.; 379.

120   D. M. Satalic, P. A. Spencer and M. R. Paterson, "The AusIMM Annual Conference"; 24-28 March 1996, Perth, W.A.; AusIMM; 167.

121   G. A. Kordosky, M. H. Kotze, J. M. W. Mackenzie and M. J. Virnig, "XVIII International Mineral Processing Congress"; Sydney, Australia, 23-28 May 1993; AusIMM; 1195.

122   R. Y. Bek and L. I. Shuraeva, *Russian Journal of Electrochemistry*, 33 (1997) 114.

123   J.-P. Randin In Encyclopedia of electrochemistry of the elements, Vol. VII; Bard, A. J., Ed.; Marcel Dekker: New York, 1976; Vol. 7, pp 206.

123a   C. A. Fleming, W. G. Grot and J. A. Thorpe In U.S. US 5,667,557; E.I. Du Pont De Nemours and Co., USA: U.S., 1997, pp 7 (CA 127:281158k)

124   A. G. Sharpe, *The chemistry of cyano complexes of the transition metals*; Academic Press: London, 1976.

125   E. A. Simpson and G. M. Waind, *J. Chem. Soc.*, 1958 (1958) 1746 .

126   J. H. Baxendale and D. T. Westcott, *J. Chem. Soc.*, 1959 (1959) 2347.

127   C. Kappenstein and R. Hugel, *Rev. Chim. Miner.*, 6 (1969) 1107.

128   J. C. Pierrard, C. Kappenstein and R. Hugel, *Rev. Chim. Miner.*, 8 (1971) 11.

129   C. Kappenstein and R. Hugel, *J. Inorg. Nucl. Chem.*, 36 (1974) 1821.

130   R. A. Penneman and L. H. Jones, *J. Chem. Physics*, 24 (1956) 293.

131   J. S. Coleman, R. George, L. Allaman and L. H. Jones, *J. Phys. Chem.*, 72 (1968) 2605 .

132   G. W. Chantry and R. Plane, *J. Phys. Chem.*, 33 (1960) 736.

133   D. Cooper and R. Plane, *Inorganic Chemistry*, 5 (1966) 16.

134   M. Reisfeld and L. Jones, *J. Molecular Spectroscopy*, 18 (1965) 1965.

135   C. Kappenstein, R. Hugel, A. J. P. Alix and J. L. Beaudoin, *J. Chim. Phys. Phys.-Chim. Biol.*, 75 (1978) 427.

136   T. Yamamoto, H. Haraguchi and S. Fujiwara, *J. Physical Chemistry*, 74 (1970) 4369 .

137   M. Hirota, Y. Koike, H. Ishizuka, A. Yamasaki and S. Fujiwara, *Chemistry Letters*, (1973) 853 .

138   C. Kappenstein, J. Bouquant and R. Hugel, *Inorg. Chem. 18(9): 2615 (1979)*, 19 (1979) 2615.

139   M. G. Vladimirov and I. A. Kakovskii, *Zhur. Priklad. Khim. (Russian J. Applied Chemistry)*, 23 (1950) 580.

140   H. P. Rothbaum, *J. Electrochem. Soc.*, 104 (1957) 682.

141   R. Hancock, N. Finkelstein and A. Evers, *J. Inorg. nucl. Chem.*, 34 (1972) 3747 .

142   G. Hefter, P. M. May and P. Sipos, *J. Chem. Soc., Chem. Commun.*, (1993) 1704.

143   A. Brenner, *J. Electrochemical Society*, 112 (1965) 611.

144   R. Izatt, H. Johnston, G. Watt and J. Christensen, *Inorg. chem*, 6 (1967) 132.

145   W. van Bronswijk and G. S. Walker, "1995 Randol Gold Forum"; Perth, Australia; 83

146   A. D. Stuart and R. Van den Heuvel, *Int. J. Environ. Anal. Chem.*, 49 (1992) 171.

147   W. Mason, *J. American Chemical Society 1973, 95(11): 3574*, 95 (1973) 3574.

148   A. B. P. Lever, *Inorganic electronic spectroscopy, pp. 258-261*, Second ed.; Elsevier, 1984.

149   A. Glasner, S. Sarig, D. Weiss and M. Zidon, *Talanta*, 19 (1972) 51.

150   Pohlandt C., *S. Afr. J. Chem.*, 38 (1985) 110.

151   H. L. Noblitt ; Dept. of mines, energy and resources, Mines branch: Ottawa, 1973; Report R 268

152   C. Kappenstein Ph.D. Thesis, Reims, 1977.

153   M. Erny and R. Lucas, *Compte Rende Acad. Sc. Paris*, 272B (1971) 603.

154   M. Erny and C. Moncuit, *J. inorg. nucl. Chem.*, 39 (1977) 37.

155   R. W. Frei and K. Zech In Journal of Chromatography Library; Elsevier: Amsterdam, 1988; Vol. 39A, pp. 301-302

156   S. B. Black and R. S. Schulz, "27th International Symposium on Environmental Analytical Chemistry"; June 1997, Georgia, USA.

156a   S. B. Black, Personal Communication with respect to above Ref., June 1998.

157   J. A. Sweileh, *Analytica Chimica Acta*, 336 (1996) 131.

158   K. Kurnia, D. E. Giles, P. M. May, P. Singh and G. T. Hefter, *Talanta*, 43 (1996) 2045.

159   F. Kunschert, *Z. anorg. Chem.*, 41 (1904) 359.

160   J. Bjerrum, G. Scharzenbach and G. S. Sillen In Stability Constants of metal-ion complexes, Part II : Inorganic Ligands, Special Publication No. 7; The Chemical Society: London, 1958, pp 33.

161   G. S. Sillen, *Stability Constants of metal-ion complexes*; The Chemical Society: London, 1964.

162   L. G. Sillen In Stability Constants of metal-ion complexes. Part 1: Inorganic Ligands. Special Publication No. 25. Supplement No. 1 to Special Publication No. 17; The Chemical Society, London: London, 1971, pp 53.

163   E. Hogfeldt In Stability Constants of Metal-Ion Complexes. Part A : Inorganic Ligands; Pergamon Press: Sydney, 1982, pp 79.

164   M. T. Beck, *IUPAC : Pure and Applied Chemistry*, 59 (1987) 1704.

165   R. M. Smith and A. E. Martell In Critical stability constants, Volume 6: Second supplement; Plenum Press: London, 1989; Vol. 6, pp 435.

166   Professor Ian Ritchie (CRC Hydrometallurgy, Western Australia), Personal Communication, 1995.

167   C. Kappenstein and R. Hugel, *Inorganic Chemistry*, 16 (1977) 250.

168   R. Y. Bek, B. D. Zhukov, L. I. Borodikhina and N. P. Poddubny, *Izvest sibirsk Otdel Akad Nauk SSSR, Ser Khim (Proceedings of the Siberian Department of the Academy of Sciences of the USSR. Series on Chemical Sciences)*, 4 (1973) 52.

169   C. Kappenstein and R. Hugel, *Inorganic Chemistry*, 17 (1978) 1945.

170   P. Hemmerich and C. Sigwart, *Experientia*, 19 (1963) 488.

171   A. J. Parker, *Search*, 4 (1973) 426.

172   F. Spitzer, *Z. Elecktrochem*, 11 (1905) 345.

173   L. S. Bark and H. G. Higson, *Analayst*, 88 (1963) 751.

---

174   F. D. Snell In Photometric and Fluorometric Methods of Analysis (Non Metals); Wiley Interscience, New York, 1981, pp 652.

175   H. B. Singh and N. Wasi, *Intern. J. Environ. Anal. Chem.*, 26 (1986) 115.

176   J. F. Van Staden, *Water SA*, 13 (1987) 197 .

177   N. K. Kutseva and A. N. Kashin, *Zavod.-Lab.*, 61 (1995) 1.

178   Z. Zhu and Z. Fang, *Anal. Chim. Acta*, 198 (1987) 25.

179   E. Figuerola, A. Florido, M. Aguilar and J. De Pablo, *Fresenius' Z. Anal. Chem.*, 331 (1988) 620.

180   A. Tanaka, K. Mashiba and T. Deguchi, *Anal. Chim. Acta*, 214 (1988) 259.

181   V. Kuban, *Anal. Chim. Acta*, 259 (1992) 45.

182   V. Kuban and P. K. Dasgupta, *Anal. Chem.*, 64 (1992) 1106.

183   M. W. Scoggins, *Anal. chem.*, 44 (1972) 1294.

184   A. T. Haj Hussein, *Anal. Lett.*, 21 (1988) 1285.

185   P. C. Do Nascimento and G. Schwedt, *Anal. Chim. Acta*, 283 (1993) 755.

186   J. A. Cox, H. L. Novak and R. M. Montgomery, *J Chromatogr, A*, 739 (1996) 229.

187   A. T. Haj Hussein, *Microchem. J.*, 39 (1989) 99.

188   E. Jungreis and F. Ain, *Anal. Chim. Acta*, 88 (1977) 191.

189   J. J. Rosentreter and R. K. Skogerboe, *Anal. Chem.*, 63 (1991) 682.

190   A. T. Haj Hussein, G. D. Christian and J. Ruzicka, *Anal. Chem.*, 58 (1986) 38.

191   J. Hanker, S., R. M. Gamson and H. Klapper, *Anal. Chem.*, 29 (1957) 879.

192   G. G. Guilbault and D. N. Kramer, *Anal. Chem.*, 37 (1965) 1395.

193   P. Linares, M. D. Luque de Castro and M. Valcarcel, *Anal. Chim. Acta*, 161 (1984) 257.

194   E. Miralles, D. Prat and M. Granados, *The Analyst*, 122 (1997) 553.

195   T. Toida, S. Tanabe and T. Imanari, *Chem. Pharm. Bull.*, 29 (1981) 3763.

196   A. Tanaka, K. Deguchi and T. Deguchi, *Anal. Chim. Acta*, 261 (1992) 281.

197   N. Lakshminarayanaiah, *Membrane electrodes*; Academic Press: London, 1976.

198   D. Midgley, *Ion-Selective Electrode Rev.*, 3 (1981) 43.

199   V. M. Jovanovic and M. S. Jovanovic, *Anal. Chim. Acta*, 233 (1990) 329.

200   M. Neshkova, *Anal Chim Acta*, 273 (1993) 255.

201   T. Nakamura, C. Hayashi and T. Ogawara, *Bull Chem Soc Jpn. Jun*, 69 (1996) 1555.

202   V. M. Jovanovic, M. Sak-Bosnar and M. S. Jovanovic, *Anal. Chim. Acta*, 196 (1987) 221.

203   P. W. Alexander, P. R. Haddad and M. Trojanowicz, *Anal. Chem.*, 56 (1984) 2417.

204   P. R. Haddad, P. W. Alexander and M. Trojanowicz, *J. Chromatogr.*, 321 (1985) 363.

205   W. Frenzel, C. Y. Liu and J. Oleksy Frenzel, *Anal. Chim. Acta*, 233 (1990) 77.

206   B. Pihlar, P. Kosta and B. Hristovski, *Talanta*, 26 (1979) 805 .

207   P. T. Kissinger and W. R. Heineman, *Laboratory Techniques in Electroanalytical Chemistry*; Marcel Dekker: N.Y., 1984.

208   A. Trojanek In Electrochemical Detectors; Ryan, T. H., Ed.; Plenum Press: N.Y., 1984.

209   D. Pletcher and E. M. Valdes, *Anal. Chim. Acta*, 248 (1991) 173.

210   F. K. Crundwell, *Hydrometallurgy*, 27 (1991) 19.

211   W. Konig, *J. Prakt. Chem.*, 70 (1905) 19.

212   W. N. Aldridge, *Analyst*, 69 (1944) 262.

213   D. M. Smith In Heterocyclic compounds; Sammes, P. G., Ed.; Pergamon Press: Oxford, 1979; Vol. 4, pp 3.

214   J. L. Lambert, J. Ramasamy and J. V. Paukstelis, *Anal. Chem.*, 47 (1975) 916.

215   R. B. Roy, *Int. Lab. (Aust. Ed.)*, (1988) 47.

216   H. C. Ma and J. F. Liu, *Anal. Chim. Acta*, 261 (1992) 247.

217   Y. Inoue, Y. Suzuki and M. Ando, *Bunseki Kagaku*, 42 (1993) 617.

218   Y. Inoue, Y. Suzuki and T. Okubo, *Anal. Sci.*, 11 (1995) 861.

219   J. L. Royer, J. E. Twichell and S. M. Muir, *Anal. Lett.*, 6 (1973) 619.

220   S. Nagashima, *Anal. Chim. Acta*, 91 (1977) 303.

221   S. Nagashima, *Anal. Chim. Acta*, 99 (1978) 197.

222   S. Nagashima, *Intern. J. Environ. Anal. Chem.*, 10 (1981) 99.

223   S. Yasuda, K. Tanihara, K. Tanai and H. Kakiyama, *Bunseki Kagaku*, 31 (1982) 545.

224   J. C. L. Meeussen, M. G. Keizer and W. D. Lukassen, *Analyst*, 117 (1992) 1009.

225   S. A. J. A. Essers, M. Bosveld, R. M. Van der Grift and A. G. J. Voragen, *J. Sci. Food Agric.*, 63 (1993) 287.

226   G. V. L. N. Murty and T. S. Viswanathan, *Anal. Chim. Acta*, 25 (1961) 293.

227   A. Sharma and Thibert, *Microchimica Acta*, 1 (1985) 357.

228   E. Asmus and H. Garschagen, *Fres. Z. anal. Chem.*, 138 (1953) 414.

229   C.-C. Chien, F.-C. Chang and S.-C. Wu, *Mikrochimica Acta*, 2 (1980) 9.

230   S. Nagashima, *Water Res.*, 7 (1983) 833.

231   E. O. Otu, J. J. Byerley and C. W. Robinson, *International Journal of Environmental Analytical Chemistry*, 63 (1996) 81.

232   P. R. Haddad and P. E. Jackson, *Ion Chromatography. Principles and Applications*; Elsevier Science Publishers B.V.: Amsterdam, 1990.

233   R. D. Rocklin and E. L. Johnson, *Anal Chem*, 55 (1983) 4.

234   J. Behnert and P. Behrend, *Labor Praxis*, 8 (1984) 1204.

235   D. P. Lee, *J. Chromatogr. Sci.*, 22 (1984) 327.

236   T. Jupille, *Int. Lab.*, 18 (1985) 82.

237   T. Okada and T. Kuwamoto, *Anal. Chem.*, 57 (1985) 829.

238   E. Borgarello, N. Serpone, S. Torcini, C. Minero and E. Pelizzetti, *Anal. Chim. Acta*, 31 (1986) 317.

239   K. Fujimura, N. Watanabe and T. Sawada, *Bunseki Kagaku*, 43 (1994) 655.

240   R. K. Pinschmidt In Ion chromatographic analysis of environmental pollutants, Vol II; Sawicki, E., Mulik, J. D., Eds.; Ann Arbour Sci. Publ.: Ann Arbour, MI, USA, 1979, pp 41.

241   A. M. Bond, I. D. Heritage, G. G. Wallace and M. J. McCormick, *Anal. Chem.*, 54 (1982) 582.

242   C. Pohlandt, *S. Afr. J. Chem.*, 37 (1984) 133.

243 C. Pohlandt, "Proceedings of MINTEK 50 : International conference on mineral science and technology"; 26-28 March, Sandton, South Africa, 1984; The South African Council for Mineral Technology; 981.

244 P. Jandik, D. Cox and D. Wong, *Int. Lab.*, (1986) 66.

245 Y. Liu, R. D. Rocklin, R. J. Joyce and M. J. Doyle, *Anal. Chem.*, 62 (1990) 766.

246 H. C. Mehra and W. T. Frankenberger, *Microchem. J.*, 41 (1990) 93.

247 K. Ito, Y. Ariyoshi and H. Sunahara, *J. Chromatogr.*, 598 (1992) 237.

248 K. Suzuki, H. Aruga, H. Ishiwada, T. Oshima, H. Inoue and T. Shirai, *Bunseki Kagaku*, 32 (1983) 585.

249 W. Wang, Y. Chen and M. Wu, *Analyst*, 109 (1984) 281.

250 J. E. Girard, *Anal. Chem.*, (1979) 836.

251 K. Tanaka, T. Ishizuka and H. Sunahara, *J. Chromatogr.*, 174 (1979) 153.

252 O. Heisz, *GIT Fachz. Lab.*, 27 (1983) 596.

253 G. Domazetis, *Chromatographia*, 18 (1984) 383.

254 K. Harrison, W. C. j. Beckham, T. Yates and C. D. Carr, *Int. Lab., Apr*, 16 (1986) 90.

255 R. Golombek and G. Schwedt, *J. Chromatogr.*, 367 (1986) 69.

256 T. E. Boothe, A. M. Emran, R. D. Finn, P. J. Kothari and M. M. Vora, *J. Chromatogr.*, 333 (1985) 269.

257 T. Imanari, S. Tanabe and T. Toida, *Chem. Pharm. Bull.*, 30 (1982) 3800.

258 T. Toida, T. Togawa, S. Tanabe and T. Imanari, *J. Chromatog.*, 308 (1984) 133.

259 K. Hiroki, Y. Inoue, T. Sakai and Y. Date : Japan, 1993.

260 K. Gamoh and S. Imamichi, *Anal. Chim. Acta,*, 251 (1991) 255.

261 K. Sumiyoshi, T. Yagi and H. Nakamura, *J. Chromatogr. A*, 690 (1995) 77.

262 M. Nonomura, *Anal. Chem.*, 59 (1987) 2073.

263 M. Nonomura and T. Hobo, *J. Chromatogr.*, 465 (1989) 395.

264 P. Silinger, *Plating and Surface Finishing*, 72 (1985) 82.

265 T. W. Dolzine, G. G. Esposito and D. S. Rinehart, *Anal. Chem.*, 54 (1982) 470.

266 D. L. DuVal, J. S. Fritz and D. T. Gjerde, *Anal. Chem.*, 54 (1982) 830.

267   H. Satake, H. Segawa and S. Ikeda, *Nippon Kagaku Kaishi*, 9 (1988) 1587.

268   K. Kurnia and D. E. Giles, "11th Australian Analytical Chemistry Symposium"; Hobart, 1991; Poster.

269   C. Pohlandt-Watson and M. J. Hemmings, *S. Afr. J. Chem.*, 41 (1988) 136.

270   K. Gamoh and H. Sawamoto, *Anal. Sci.*, 4 (1988) 665.

271   A. Sano, N. Takimoto and S. Takitani, *J. Chromatogr.*, 582 (1992) 131.

272   A. Dong MSc Thesis, UNSW, 1994.

273   L. Madungwe, M. F. Zaranyika and R. C. Gurira, *Anal. Chim. Acta*, 251 (1991) 109.

274   J. Riviello, A. Fitchett and E. Johnson, "43rd Proc. Int. Water Conf."; 1982; Eng Soc. West PA; 458.

275   Dionex Corp. (1983) Application Note 40R: "The determination of Au (I) and Au (III) in gold cyanide plating bath"

276   K. K. Haak and G. O. Franklin, "Annu. Tech. Conf. Proc. - Am. Electroplat. Soc."; 1983.

277   R. E. Smith and C. H. Smith, *LC*, 3 (1985) 578.

277a   Burnett, M.G. and Abou-El-Wafa, M.H.M., *Dalton Trans.*, (1984) 2341.

277b   Burnett, M.G. and McCullagh, J.F., *Inorg. Chem. Acta*, 169 (1990) 31.

278   M. Nonomura, *Met. Finish.*, 85 (1987) 15.

279   B. Grigorova, S. A. Wright and M. Josephson, *J. Chromatogr.*, 410 (1987) 419.

280   P. R. Haddad, "Perth International Gold Conference (1988 Randol Gold Forum)"; 28 October - 1 November 1988, Perth, Western Australia; Randol International Ltd.; 27.

281   C. Pohlandt-Watson, M. J. Hemmings, D. E. Barnes and G. W. Pansi ; Mintek, 1988.

282   J. C. Thompsen and A. B. Carel, *Analyst*, 114 (1989) 1197.

283   A. Padarauskas, I. Stul' gene, R. Kazlauskas and O. Petrukhin, *Zh. Anal. Khim.*, 46 (1991) 1169.

284   A. V. Padarauskas, R. M. Kazauskas and O. M. Petrukhin, *Zavod. Lab.*, 57 (1991) 16.

285   E. O. Otu, C. W. Robinson and J. J. Byerley, *Analyst*, 118 (1993) 1277.

286   L. Giroux and D. J. Barkley, *Can. J. Chem.*, 72 (1994) 269 .

287   Q. Huang, B. Paull and P. R. Haddad, *J. Chromatog.*, 770 (1997) 3.

288   R. D. Rocklin, *J. Chromatogr.*, 546 (1991) 175.

289   E. O. Otu, C. W. Robinson and J. J. Byerley, *Analyst*, 117 (1992) 1145.

290   B. Pihlar and L. Kosta, *Anal. Chim. Acta*, 114 (1980) 275.

291   H. Small, T. S. Stevens and W. C. Bauman, *Anal. Chem.*, 47 (1975) 1801.

292   I. Berglund and P. K. Dasgupta, *Anal. Chem.*, 63 (1991) 2175.

293   H. Shintani and P. K. Dasgupta, *Anal. chem.*, 59 (1987) 1963.

294   A. Sjogren and P. K. Dasgupta, *Anal. Chem.*, 67 (1995) 2110.

295   D. T. Gjerde, J. S. Fritz and G. Schmuckler, *J. Chromatogr.*, 186 (1979) 509.

296   R. W. Siergiej and N. D. Danielson, *J. Chromatogr. Sci.*, 21 (1983) 362.

297   R. E. Barron and J. S. Fritz, *Reactive Polymers*, 1 (1983) 215.

298   R. W. Frei In Chemical Derivatization in Analytical Chemistry; Frei, R. W., Lawrence, J. F., Eds.; Plenum Press: London, 1981; Vol. 1.

299   S. G. Weber In Detectors for Liquid Chromatography; Yeung, E. S., Ed.; John Wiley and Sons Inc.: Toronto, Canada, 1986; Vol. 1.

300   H. Engelhardt and U. D. Neue, *Chromatographia*, 15 (1982) 403.

301   J. R. Poulsen, K. S. Birks, M. S. Gandelman and J. W. Birks, *Chromatographia*, 22 (1986) 231.

302   H. M. N. H. Irving and A. D. Damodaran, *Anal. Chim. Acta*, 53 (1971) 267.

303   K. Haak, *Plat. Surf. Finish.*, 70 (1983) 34.

303a   Chambaz, D. and Haerdi, W., *J. Chromatogr.*, 482 (1989) 335

304   N. E. Rochester and P. R. Haddad, "Proc. 9th. Aust. Symp. Anal. Chem."; Sydney, NSW, 1987; RACI; 329.

305   M. Stoychevski and L. R. Williams, *Trans. Instn. Min. Metall. (Sect. C : Mineral Process. Extr. Metall.)*, 102 (1993) C93.

306   P. J. Brandt, P. Dempsey, J. H. Van Dalen and S. Ashkenazi,   "Gold 100 : Proceedings of the International Conference on Gold"; 1986; ; 555.

---

307   W. A. Gow, H. H. McCreedy and F. J. Kelly, *C.I.M.*, 59 (1966) 872.

308   J. C. Ingles ; Canadian Department of Mines and Technical Surveys: Ottawa, Canada, 1964. Report R127.

309   J. C. Ingles ; MINES BRANCH, DEPT OF ENERGY, MINES AND RESOURCES: Ottawa, Canada, 1969, Report 212.

310   G. F. Atkinson, J. J. Byerley and B. J. Mitchell, *Analyst*, 107 (1982) 398.

311   AARL, *Journal of the South African Institute of Mining and Metallurgy*, 93 (1993) 1.

312   P. Kaye and R. Jackson, "Randol Gold Forum"; Cairns Australia, 16-19 April 1991; Randol International Ltd.; 337.

313   C. Rowden, Personal Communication, 1997.

314   D. A. Holtum, *J. S. Afr. Inst. Min. Metall.*, 88 (1988) 67.

315   M. Wills, "Randol Gold Forum"; Cairns Australia, 16-19 April 1991; Randol International Ltd.; 343.

316   D. M. Menne, "Randol Gold Forum 1991"; Cairns, Australia, 16-19 April 1991; Randol International Ltd.; 299.

317   T. P. Lynch, *Analyst*, 109 (1984) 421.

318   C. Pohlandt-Watson ; Mintek, 1986.

319   E. A. Jones, D. Barnes and J. F. Van Staden, *S. Afr. J. Chem.*, 42 (1989) 25.

320   M. J. C. Taylor, D. E. Barnes, G. D. Marshall, D. R. Groot and S. J. S. Williams, *Process Control Qual.*, 3 (1992) 173.

321   D. Barnes In Mintek Bulletin, 1996; Vol. October 1996.

322   F. K. Crundwell and J. O. Jensen, *Source Journal of the South African Institute of Mining & Metallurgy*, 94 (1994) 103.

323   V. N. Kiryushov, A. G. Obushenkov, G. A. Galkin, V. S. Khotsei and Y. B. Kletenik, *Tsvetn. Met.*, (1987) 99.

324   V. N. Kiryushov and Y. B. Kletenik, *Industrial Laboratory*, 60 (1994) 145.

325   B. Corden, "Perth International Gold Conference (1988 Randol Gold Forum)"; 28 October - 1 November 1988, Perth, Western Australia, 1988; Randol International Ltd.; 183.

---

326   C. Pohlandt ; Council for Mineral Technology (MINTEK), 200 Hans Strijdom Rd., Randburg, South Africa: Randburg, South Africa, 1984, pp 30 pages.

327   R. C. Mallett, "Extraction Metallurgy '85"; London, UK, 9-12 Sept. 1985; The Institution of Mining and Metallurgy, 44 Portland Place, London W1N 4BR, UK; 1075.

328   P. Marion, M. C. Rouillier, V. Blet and M. N. Pons, *Anal. Chim. Acta*, 238 (1990) 117.

329   G. T. W. Ormrod and S. L. Lombard ; National Insitute of Metallurgy (NIM): Randburg, South Africa, 1974, Report 1647.

330   M. Z. Martin, A. A. Garrison, P. D. Hall and C. F. Moore, *Process Control and Quality*, 5 (1993) 187.

CHAPTER TWO

Experimental and General

2.1 Summary of hardware and HPLC columns

The HPLC instrumentation and columns used in this thesis is described in each chapter. However, summaries of the various hardware components and columns used at various stages of this project are listed in Tables 2.1 and 2.2, respectively.

Hardware	Manufacturer
M510 HPLC pump	Waters
M 600E quaternary gradient HPLC pump pump	Waters
U6K injector	Waters
M 717 Plus Autosampler	Waters
M 441 fixed wavelength detector	Waters
M484 variable wavelength detector	Waters
M486 programmable variable wavelength detector	Waters
M996 Photo diode array detector	Waters
Dual post column reaction pumping unit	Waters
Column heater	Waters
Baseline, Maxima and Millennium data stations	Waters

Table 2.1: List of hardware components used throughout this thesis. Waters: Waters Ltd. (Milford, MA, U.S.A.). Waters was previously the Waters Chromatography Division of Millipore.

Column	Manufacturer
Nova-Pak C18 (15 and 5 cm)	Waters
Delta-Pak C18 (15 cm)	Waters
Fast-Fruit Juice ion exclusion (10 cm)	Waters
IC-Pak A (Standard and High capacity)	Waters
PRP-100 (25 cm)	Hamilton, Reno, Nevada, USA.
Hypercarb (10 cm)	Shandon, U.K.

Table 2.2: List of HPLC columns used throughout this thesis.

2.2 Post-column reaction coils

The post-column reaction system for derivatisation of free cyanide consisted of a dual-pump post-column pumping system and two sets of knitted open tubular reaction coils. The reaction coils were knitted on stainless steel (SS) mesh according to the method reported by Englehardt [1], as shown in Fig. 2.1. Various internal dimensions of tubing were used: 0.25, 0.30 and 0.50 mm. Reactions coils were prepared with various lengths of tubing. A picture of a finished reaction coil (5 m length, 0.30 mm ID) is shown in Fig. 2.2. Tape was placed around the edges of each reaction coil to prevent damage to other tubing (and fingers) by the ends of the SS mesh.
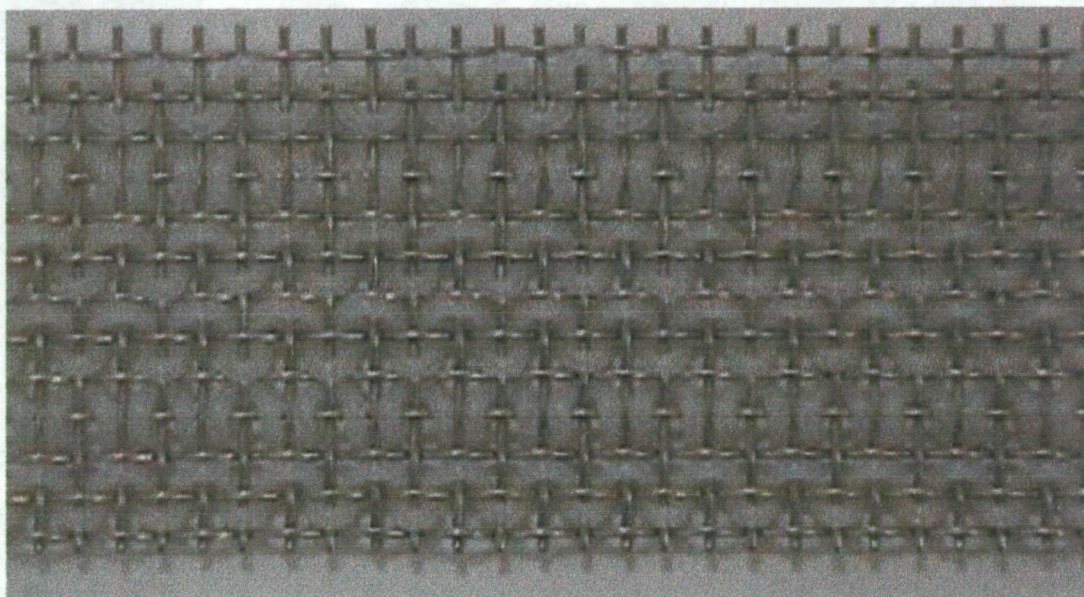
Fig. 2.1: Reaction coil prepared by knitting on SS mesh.
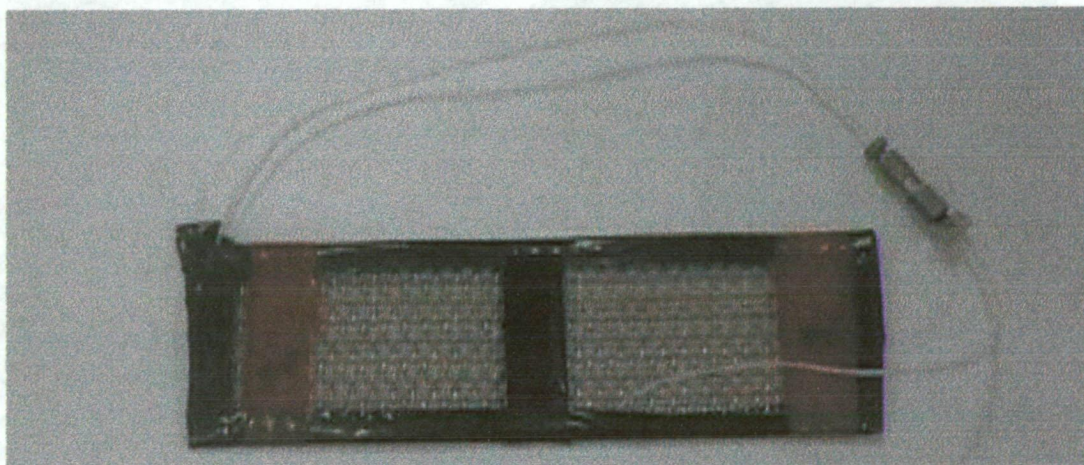
Fig. 2.2: Completed reaction coil (5 m x 0.30 mm ID). Ends joined with a HPLC connector.

The performance of each reaction coil was assessed by comparing the plate count obtained for thiocyanate before and after each reaction coil was placed between the column outlet and UV detector.

2.3 Reagent list

A summary of the reagents and suppliers used in this thesis is shown in Table 2.3.

Reagent	Supplier	Grade
Acetonitrile	Waters, Merck	HPLC
Methanol	Waters	HPLC
THF	Waters	HPLC
Low UV PIC A	Waters	HPLC
Tetrabutylammonium hydroxide	Aldrich	AR
H_3PO_4	Ajax	AR
H_2SO_4	Ajax	AR
KH_2PO_4	Ajax	AR
$(NH_4)_2SO_4$	Ajax	AR
NaOH	M & B	AR
NaCN	Aldrich	AR
CuCN	Aldrich	AR
AgCN	Aldrich	AR
KSCN	Ajax	AR
NaCNO	Aldrich	AR
$K_4[Fe(CN)_6]$	M & B	AR
$K_3[Fe(CN)_6]$	M & B	AR
$K[Au(CN)_2]$	Aldrich	AR
$NiCl_2.6H_2O$	Aldrich	AR
$Ni(NO_3)_2$	Ajax	AR
$CoCl_2.6H_2O$	Aldrich	AR
Camphorsulphonic acid	Aldrich	AR
Anthranilic acid	Aldrich	AR
Benzoic acid	Ajax	AR

Table 2.3: List of reagents used throughout this thesis. (Continued next page)

Reagent	Supplier	Grade
KHphthalate	Ajax	AR
Na_2S	Ajax	AR
Na_2CO_3	Ajax	AR
$NaNO_3$	Ajax	AR
$NaNO_2$	M & B	AR
KI	M & B	AR
5-(4'-Dimethylaminobenzyliden)-rhodanin	Merck	AR
$AgNO_3$	Ajax	AR
Isonicotinic acid	Sigma	AR
Barbituric acid	Aldrich	AR
3-Methyl-1-phenyl--2-pyrazolin-5-one	Aldrich	AR
N-Chlorosuccinimide	Aldrich	AR
Succinimide	Aldrich	AR
Succinic acid	Aldrich	AR
Na_2EDTA	Ajax	AR

Table 2.3: List of reagents used throughout this thesis. (Continued from previous page) Ajax: Ajax Chemical Co., Auburn, NSW, Australia. M & B : May and Baker, UK

The potassium salts of the Ni(II) and Co(III)-cyanide complexes were prepared using standard methods by Kalambaheti [2].

2.4 References

1   H. Engelhardt and U. D. Neue, *Chromatographia*, 15 (1982) 403.

2   C. Kalambaheti PhD Thesis, University of NSW, 1991.

CHAPTER THREE

Initial development of methods for the chromatographic determination of cyanide in gold cyanidation samples

3.1 Introduction

Most of the metallo-cyanide complexes can be separated using reversed phase ion interaction chromatography (RPIIC), as discussed in Chapter one. The majority of these complexes also display strong UV absorption, enabling photometric detection at 214 nm [1]. However, an alternative detection technique is required for cyanide as it is UV transparent [2]. In addition, preliminary studies indicated that free cyanide was unretained during the RPIIC separation of the metallo-cyanide complexes. This placed an additional demand on the detection of free cyanide as other anions would also be co-eluted with cyanide in the void volume.

The first part of this Chapter describes the development of a PCR detection system (based on the König reaction) suitable for cyanide and compatible with the RPIIC separation. Three approaches for coupling the PCR detection system to the chromatographic system were examined.

The second part of this Chapter briefly describes a field trial conducted at the Rothsay Gold Mine in Western Australia. Some major problems were experienced with the analytical methods developed in the first part of this Chapter during the field trial. Some solutions to these problems and some results are presented.

3.2 Experimental

3.2.1 Instrumentation

The HPLC instrumentation used in this work was manufactured by Waters Chromatography Division of Millipore (Milford, MA, U.S.A.). The basic hardware consisted of a model 510 pump, model U6K injector, model 441 fixed wavelength

absorbance detector operated at 214 nm, and a model Baseline 810 data station. A Nova-Pak C-18 column (150 x 4.6 mm, ID) was used for separation of the metallo-cyanide complexes with an ion interaction eluent.

3.2.2 Post-column reaction system

The post-column reaction system for derivatisation of free cyanide consisted of a Waters dual-pump post-column pumping system and two knitted open tubular reaction coils containing 40 cm x 0.22 mm ID and 30 m x 0.22 mm ID PTFE tubing. Further details of this system are given later. The derivatised free cyanide was then passed to a Waters model 484 variable wavelength absorbance detector operated at 500 nm. The output of this detector was recorded by the data station.

3.2.3 Hardware configurations

The basic ion-interaction system and the post-column reaction system were interfaced in several ways, as shown in Fig. 3.1. In the simplest case, shown in Fig 3.1(a), the effluent emerging from the UV detector in the ion-interaction system was passed directly into the post-column reactor (PCR). This approach will be referred to as a "tandem" system. The second approach (Fig. 3.1(b)) involved passing the effluent from the UV detector in the ion-interaction system through a 6-port rotary valve fitted with a 100 µL loop, as shown in Fig. 3.2. This valve could direct the effluent either to waste or to the post-column reactor. In this way, a selected portion (or heart-cut) of the effluent could be transferred to the post-column reactor. A second model 510 pump was employed to carry the sample to the post-column reactor. Rotation of the 6-port valve was accomplished by pneumatic pressure, under the control of the computer data station. This method will be referred to as a "cut" system. The third configuration (Fig. 3.1(c)) was identical to the "cut" system, except that a Millipore Waters Fast Fruit Juice ion-exclusion column (150 x 7.8 mm, ID) was inserted prior to the post-column reactor as a means of separating free cyanide from any components co-eluted from the ion-interaction system. This approach will be referred to as a "coupled" system.
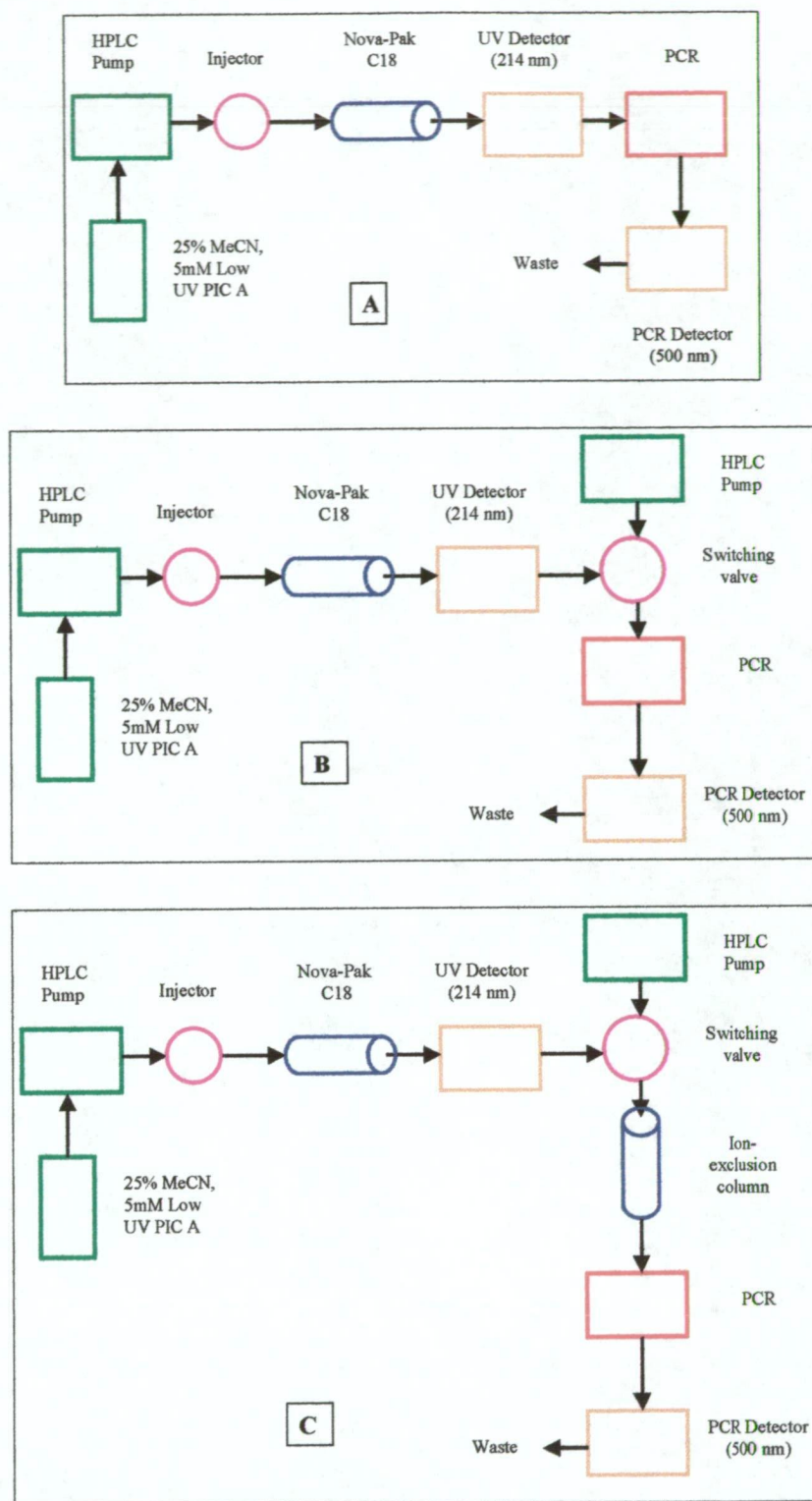
Fig. 3.1: Chromatographic hardware configurations used in this study. The post-column reactor (PCR) configuration is shown in Fig. 3.2. **(A)** "Tandem" system; **(B)** "Cut" system; **(C)** "Coupled" system.
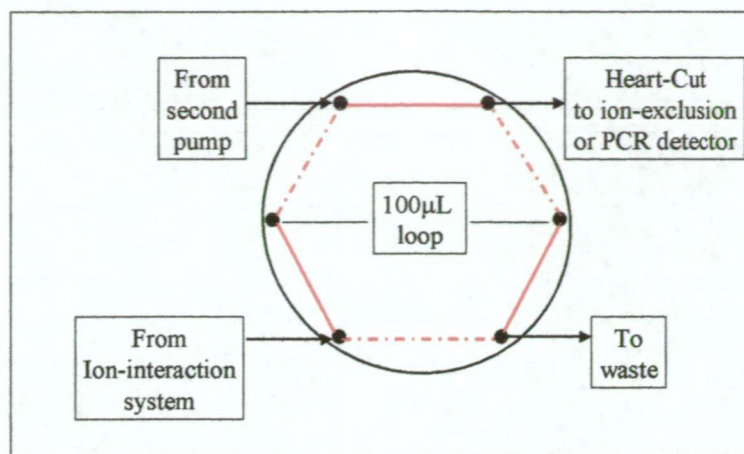
Fig. 3.2: Switching valve configuration used for obtaining a heart-cut from the ion-interaction system.

3.2.4 Reagents and procedures

All reagents used were of Analytical Reagent grade. N-chlorosuccinimide, succinimide, barbituric acid and isonicotinic acid were obtained from Aldrich (Milwaukee, WI, U.S.A.). $KAu(CN)_2$ was purchased from Johnson and Matthey Chemicals (London), whilst potassium salts of the cyano complexes of Ag(I), Cu(I), Fe(II) and Fe(III) were synthesised by Kalambaheti [3] using published methods. Chromatographic grade acetonitrile (UV cut-off 190 nm) was obtained from Waters. The mobile phase used in the ion-interaction chromatographic system comprised a 25% (v/v) solution of acetonitrile in 5 mM low UV PIC A, which was obtained from Millipore Waters. The carrier fluid used in the "cut" system shown in Fig. 3.1(b) was 25:75 (v/v) acetonitrile-water, and water served as the eluent for the ion-exclusion column used in the coupled system shown in Fig. 3.1(c). All eluents were filtered through a 0.45 μm membrane filter and degassed in an ultrasonic bath prior to use. The flow-rate was 1 ml/min in all cases.

Two reagents were used in the post-column reactor, as shown in Fig. 3.3. The first reagent consisted of 0.1% (w/v) N-chlorosuccinimide and 1% (w/v) succinimide. This reagent was prepared daily. The second post-column reagent consisted of 0.5% (w/v) isonicotinic acid and 0.25% (w/v) barbituric acid dissolved in dilute NaOH solution, after which the solution was buffered to pH 7.0 with H_3PO_4. Addition of the buffer was essential to maintain stability, and under the conditions described, the reagent was stable for 3 weeks. Both of the post-column reagents were filtered

through a 0.45 µm membrane filter before use. The flow rate of the N-chlorosuccinimide/succinimide reagent was 0.4 ml/min, and the same flow-rate was used for the isonicotinic acid/barbituric acid reagent. Further details on the post-column reactor are shown in Fig. 3.3.
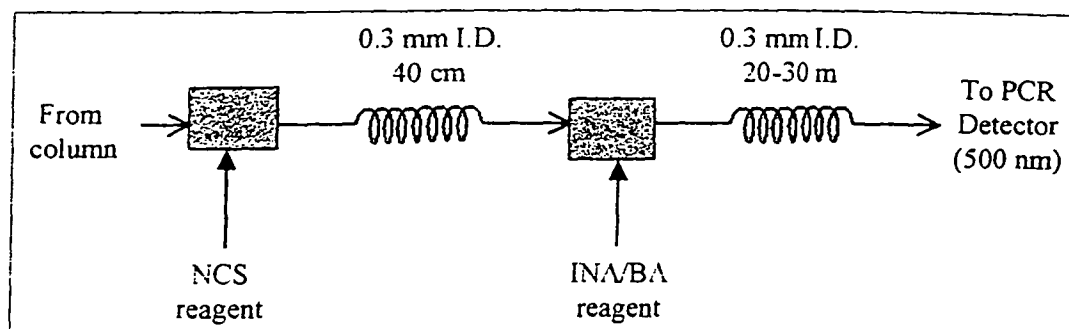
Fig. 3.3: Details of the post-column reactor used for derivatisation of cyanide. NCS reagent contained 0.1% N-Chlorosuccinimide (NCS) and 1% succinimide. INA/BA reagent contained 0.5 % isonicotinic acid (INA), 0.25% barbituric acid (BA) and phosphate buffer (pH 7). Flow rate of both PCR reagents: 0.4 ml/min.

Comparative cyanide analyses were conducted with AgNO$_3$ titrations. A silver-sensitive dye, p-dimethylaminobenzylidine rhodanine, was used as the indicator for these titrations in a specified manner [4].

3.2.5 Procedures at the Rothsay gold mine

Samples were collected and filtered immediately with disposable 0.45 mM Millipore HA cartridge filters prior to HPLC analyses. Silver nitrate (AR grade) titrations for cyanide analysis were mostly performed by plant operators with a KI indicator. Cu and Au analyses were performed by both HPLC and atomic absorption spectroscopy (AAS). AAS analyses were performed by laboratory personnel at the gold mine. It was found that the K[Au(CN)$_2$] standard used for HPLC analyses reported a lower gold concentration when analysed by AAS than was specified on the K[Au(CN)$_2$] reagent bottle.

3.3 Results and Discussion

3.3.1 Selection of separation conditions

The first step in the development of a chromatographic procedure for the determination of free cyanide in CIP leach liquors was to identify chromatographic conditions under which free cyanide could be separated from as many of the components of the leach liquor as possible. Coupled with this requirement was the desire to resolve those key components of the leach liquor which might yield important analytical information to the CIP plant operator. The key components were thiocyanate and the cyano complexes of silver(I), copper(I), iron(II), iron(III) and gold(I). Based upon the work of Kalambaheti [3], several combinations of organic modifiers (methanol (MeOH), acetonitrile (MeCN) and tetrahydrofuran (THF) were possible for the separation of the above metallo-cyanide complexes. While MeOH/THF combinations were feasible, it was found that they were impractical due to the volatility and chemical instability of THF. Consequently, an eluent containing 25% acetonitrile and 5mM Low UV PIC A was selected for the separation of the metallo-cyanide complexes. The separation achieved using this mobile phase with a Nova-Pak C-18 column is shown in Fig. 3.4(a). This chromatogram illustrates the separation of species typically found in cyanidation leachates. It can be seen that all components are well resolved and that the Au(I) peak can be quantified readily by appropriate scale expansion (Fig. 3.4(b)). Calibration plots constructed for all the species shown in Fig. 3.4 were linear (correlation coefficients $\geq$ 0.99) up to the maximum concentrations tested, which were as follows: 300 ppm for thiocyanate and copper(I), 50 ppm for iron(II) and 20 ppm for iron(III), silver(I) and gold(I). It should be noted that these concentrations refer to the metal ions rather than to the complexes themselves.

3.3.2 Selection of post-column reaction conditions

The free cyanide eluted from the column is not detected at 214 nm, but collection and derivatisation of mobile phase fractions revealed that this species was unretained on the column and was eluted at the void volume. It was therefore feasible that the small volume of mobile phase containing the free cyanide could be further analysed
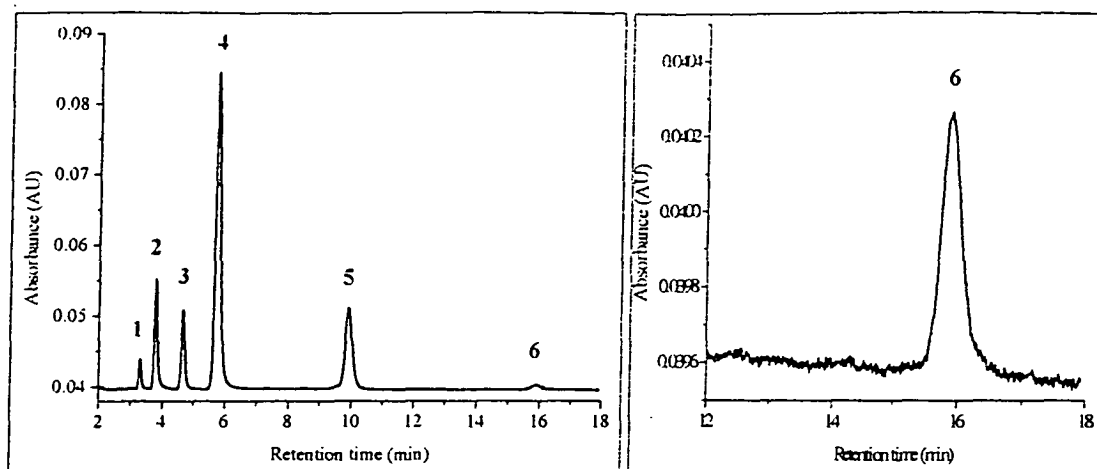
Fig. 3.4: (a) (LHS)UV detector chromatogram illustrating the separation of several cyano species. (b) RHS: Expanded chromatogram showing the Au(I) complex. Legend: (1) SCN$^-$ (3 ppm); (2) Cu(I) (1.5 ppm); (3) Ag(I) (2 ppm); (4) Fe(II) (2ppm); (5) Fe(III) (2 ppm); (6) Au(I) (1 ppm). Column: Waters Nova-Pak C-18. Eluent: 25% acetonitrile, 5 mM Low UV PIC A.

to determine the free cyanide concentration. To accomplish this, it was necessary to select appropriate analytical methodology to permit the determination of the eluted free cyanide in the presence of the mobile phase components and of any co-eluted components of the leach liquor. Moreover, any analytical technique used should be amenable to on-line operation so that the analysis could be automated. After consideration of these constraints, several possibilities existed, including the use of ion chromatography with conductometric or amperometric detection, and spectrophotometry using a flow-through reactor.

The use of ion chromatography with anion-exchange columns was initially investigated, but this approach was abandoned because of interferences caused by acetonitrile and tetrabutylammonium ions (from the low UV PIC A). In addition, it was found that common inorganic anions present in the leach liquor, such as chloride and sulfate, were co-eluted with free cyanide on the ion-interaction system and these either eluted from the ion-exchange column at the same time as cyanide or were so strongly retained that excessive run times were necessary.

A selective spectrophotometric reaction appeared more suitable, provided that any interfering species present in the free cyanide band could be removed. For this reason, several spectrophotometric procedures for cyanide were examined which

could be adapted to a continuous flow system. The simplest approach is to react the cyanide with a transition metal cation to form a metallo-cyanide complex. The metallo-cyanide complex is then monitored either by direct or indirect spectrophotometric detection. Examples of both these detection alternatives are the reaction of Ni^{2+} in an ammoniacal buffer with direct detection at 267 nm [5] or reaction with a highly coloured Cu^{2+} solution (such as citrate) and indirect detection at the λ_{max} for Cu^{2+} [6].

One of the simplest complexation methods utilised a Ni^{2+} reagent. However, a precipitate was formed when this reagent was mixed with the eluent. The reason for this was unknown at the time of these experiments. It was later found that the cause of this precipitation was due to the formation of very insoluble Ni^{2+} salts with the phosphate buffer present in the ion interaction reagent, Low UV PIC A (see Chapter five, section 5.3.7).

It was noted in Chapter one that the most common group of spectrophotometric methods for cyanide analysis involves variations of the König reaction [7]. These reactions were chosen for investigation in view of their high selectivity towards cyanide and because they have been utilized in continuous-flow, flow-injection (FIA) and post-column reaction (PCR) analysis systems on numerous occasions [8-14]. A review of the König reaction was presented in chapter one (section 1.6). The following discussion outlines the reasons for selection of reagents and conditions used in this chapter.

The most commonly used chlorination reagent, chloramine-T, caused formation of a precipitate in the PCR coils on several occasions. An alternative chlorination reagent, N-chlorosuccinimide (NCS), was used because its reaction product, succinimide, was soluble in water. In addition, Lambert et al. [15] reported that a 10-fold excess of succinimide in a 0.1% NCS reagent was stable for several months.

Isonicotinic acid was selected for the pyridine substitute as it is odourless and has minimal toxicity. Barbituric acid was selected for use, based on toxicity considerations and ease of reagent preparation.

The reaction scheme for the INA/BA variant of the König reaction is relevant to the following discussion (see Chapter one). Barbituric acid (VI) condenses with the dialdehyde (V) to produce an intermediate dye species (VII), which on standing condenses with a further molecule of barbituric acid to give a second and final polymethine dye (VIII) [16]. Several authors have noted that there are two distinct wavelengths of maximum absorbance associated with this reaction [17]. The first absorbance maximum appears rapidly at 525 nm and is due to formation of the intermediate dye species (VII). The second maximum occurs at 600 nm and is attained after approximately 15 min. This maximum is due to formation of the final polymethine dye (VIII) and is of greater magnitude than the first absorbance maximum. Under flow-through reaction conditions, the first maximum is the most useful because of its rapid formation and was therefore applied in this work. Other workers have used the same criteria for selection of the intermediate dye [10, 18].

The λ_{max} observed for the intermediate INA/BA dye was 515 nm in the PCR system. However, a λ_{max} of 527 nm was observed when no acetonitrile was present, which is similar to the value (525 nm) reported by Nagashima [17]. This difference was attributed to the solvent effect of acetonitrile in the reaction mixture. The acetonitrile concentration in the effluent from the PCR detection system was calculated to be 19% for an eluent concentration of 25%.

The reaction conditions (i.e. reagent concentrations and reaction coil length) were then optimized to provide suitable response to the range of cyanide concentrations expected in the samples to be analysed. The detection wavelength was altered to 500 nm to reduce sensitivity, the length of the second reactor was decreased and the isonicotinic acid and barbituric acid concentrations were varied until linearity of the cyanide calibration plots was achieved. The method was further modified by buffering the INA/BA reagent to pH 7.0 with H_3PO_4. This avoided the requirement to add a phosphate buffer as a post-column reagent (as used by Toida et al.. [13]), improved the stability of this reagent, and provided a suitable pH for dye formation. A phosphate buffer was used in the INA/BA reagent since it has been shown that this was more suitable than other common buffers [17, 19].

3.3.3 Evaluation of hardware configurations

As can be seen from Fig. 3.1, there are three possible ways in which the post-column reactor can be coupled to the ion-interaction chromatographic system. The simplest configuration is the "tandem" system (Fig. 3.1(a)). A series of samples from different gold mines was analysed with each configuration in order to assess and compare each configuration. Chromatograms obtained from the analysis of leach samples with the "tandem" system are shown in Fig. 3.5. The concentrations of the various components determined by these analyses are shown in Table 3.1. It should be recognised that concentrations of all the species shown in Table 3.1, except cyanide, were identical for each hardware configuration shown in Fig. 3.1.

Sample	Sample No.	[CN] (ppm)	[SCN] (ppm)	[Cu(I)] (ppm)	[Fe(II)] (ppm)	Co(III) (ppm)	[Fe(III)] (ppm)	[Au(I)] (ppm)
Mt. Magnet LD	1	57	1.9	1.7	3.6	0.4	0.2	1.9
You Anmi LT3	2	157	1.2	< 0.5	1.2	0.5	< 0.1	1.9
Reedy LD	3	201	40	9.5	20	1.1	0.5	3.7
Rothsay LT3	4	154	64	139	15	1.3	2.1	1.3

Table 3.1 : Concentrations of cyanide, thiocyanate and the metallo-cyanide complexes found in cyanidation leach samples from four gold mines. LD and LT3 refer to Leach Discharge and Leach Tank # 3. Sample No. refers to the chromatograms of these samples shown in Fig. 3.4.

Fig. 3.4: UV and PCR detector chromatograms of samples (next two pages). Chromatograms labeled 1(a,b &c); 2 (a,b &c); 3 (a,b &c) and 4 (a,b &c) refer to samples 1-4 in Table 3.1. "(a,b &c)" refers to UV (214 nm) detector chromatogram; expanded UV detector chromatogram (showing minor peaks) and PCR (500 nm) detector chromatogram, rerspectively. Peak legend: (1) Cyanide; (2) Thiocyanate (3) Cu(I); (4) Fe(II); (5) Co(III); (6) Fe(III); (8) Au(I); (7) and (9) Unidentified components. The peak labeled "?" in Chromatogram 2b was also unidentified. The tailing on the Fe(III) peak (#6) in chromatogram 3b was due to Ni(II).

Concentration of thiocyanate and the metallo-cyanide complexes are shown in Table 3.1.

Chromatographic conditions as for Fig. 3.4. PCR conditions as for Fig. 3.3.
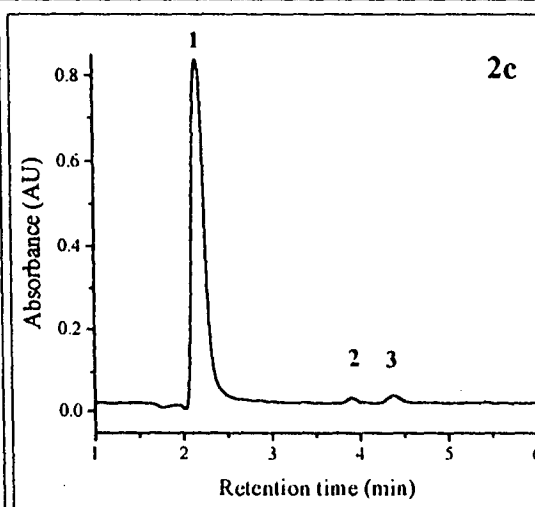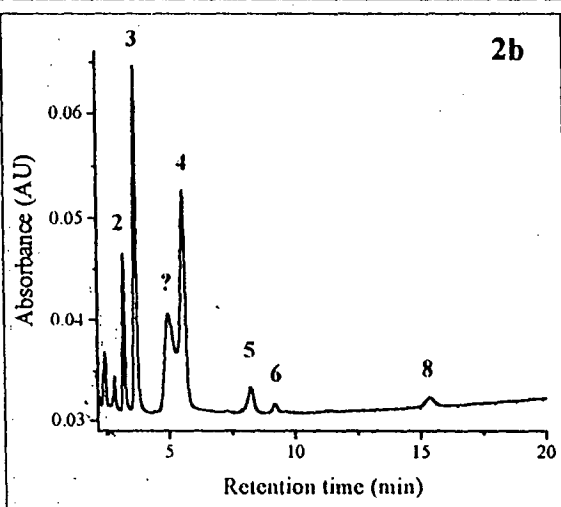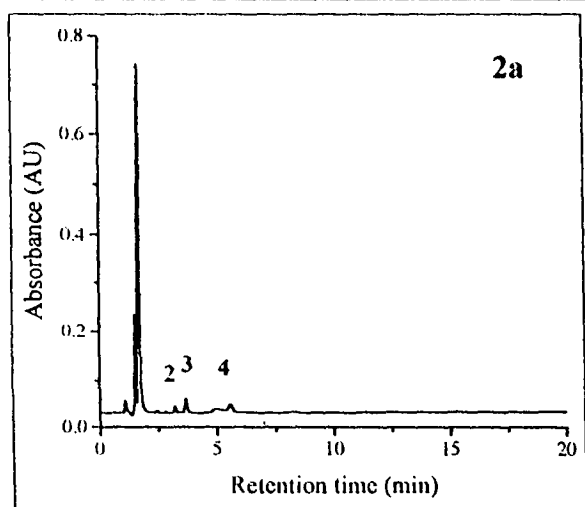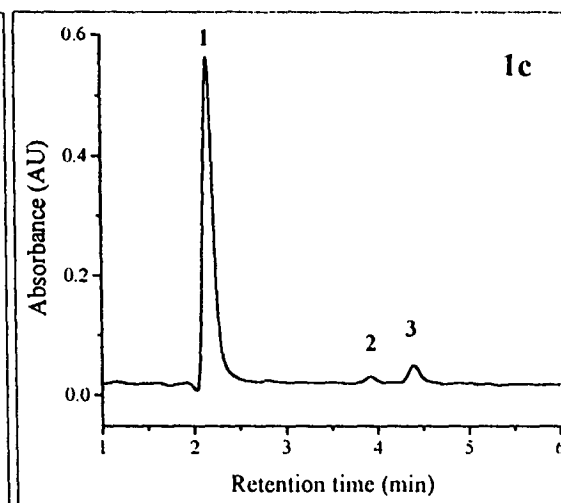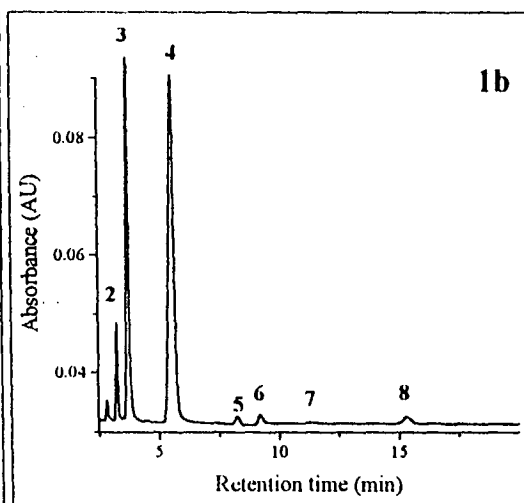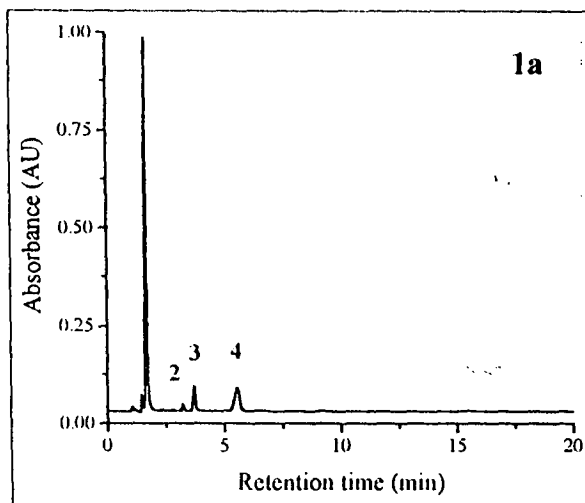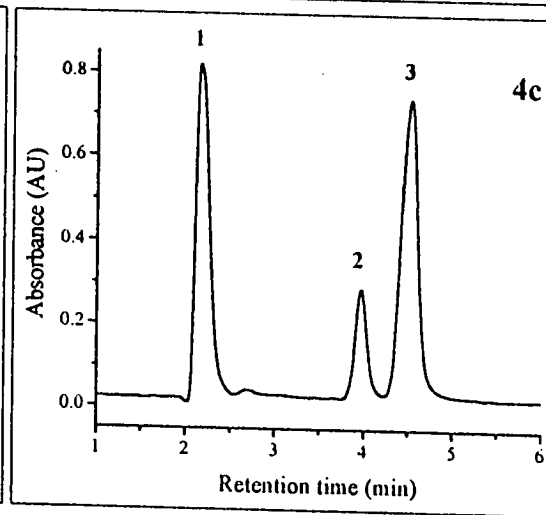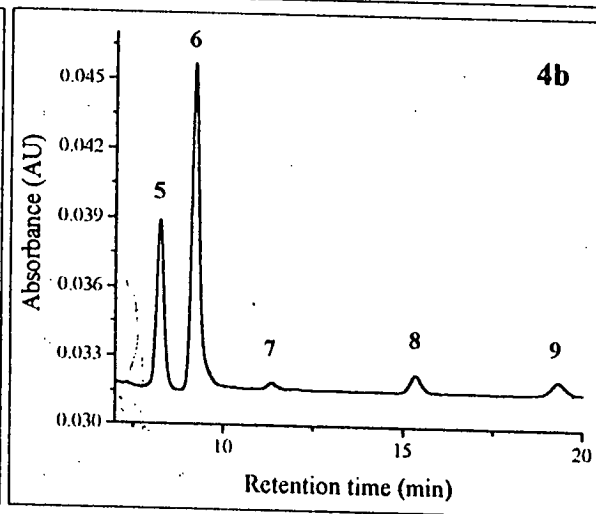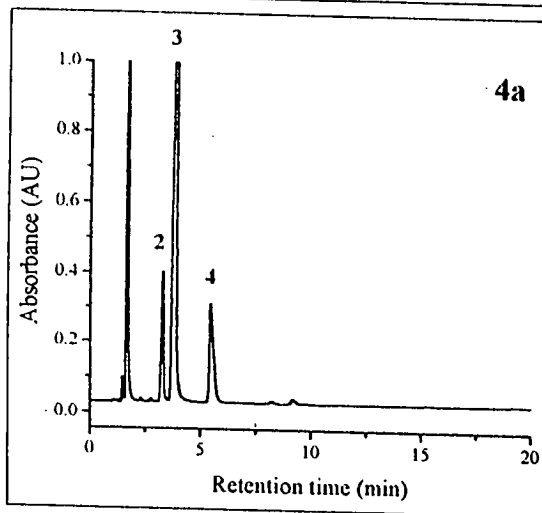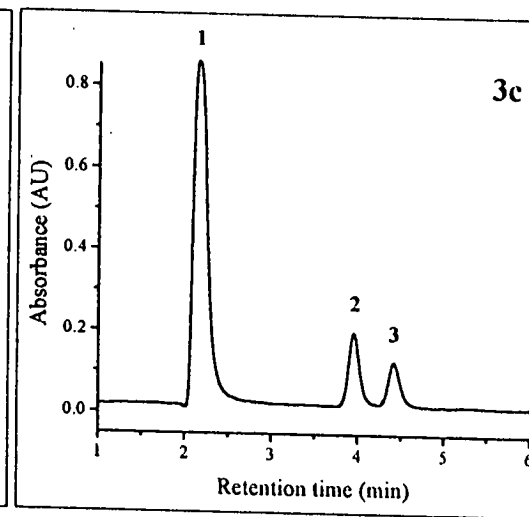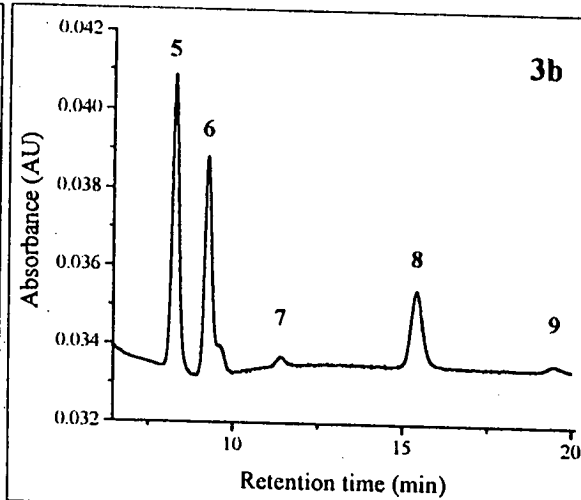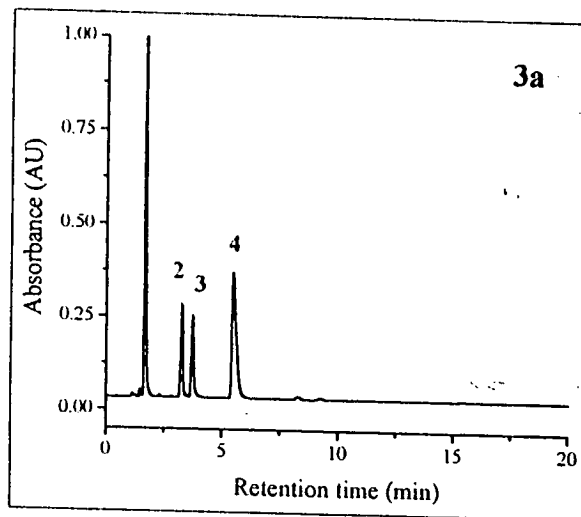
The "tandem" approach described above (Fig. 3.1(a)) is the simplest hardware configuration, but has the disadvantage that all components of the leach liquor, including those that are co-eluted with free cyanide, are passed to the reactor. The use of a switching valve to select a desired portion of the free cyanide band (*i.e.*, the "cut" system shown in Fig. 3.1(b)) partly avoids this disadvantage but introduces the further problem of deciding which portion of the cyanide band should be passed to the post-column reactor. It was found that there were differences between standards and some samples, as shown in Fig. 3.5 for a 150 ppm cyanide standard and a Rothsay sample containing a relatively high copper concentration (140 ppm). Fig. 3.5 shows that a heart-cut from 1.5-1.6 min contained the highest cyanide concentration for both sample and standard. However, due to the difference between the standard and sample, the apparent cyanide concentrations were 116, 135 and 206 ppm in heart-cuts 1, 2 and 3, respectively, for the Rothsay sample {Fig 3.5(d)}. These concentrations were determined with separate calibration plots prepared for each heart-cut interval (Fig. 3.6) and are obviously incorrect due to the difference between the standards and Rothsay sample. When the cyanide concentration in each heart-cut from the leach sample was determined with the same calibration plot ("Cut 2" in Fig 3.6), the cyanide concentrations were 70, 135 and 22 ppm in heart-cuts 1, 2 and 3, respectively. The order of magnitude of these latter values agrees with the PCR detector chromatogram (Fig. 3.5(d)).

It should be noted in passing that the heart-cuts shown in Fig. 3.5 provide an estimation of the extent of band broadening occurring for the cyanide peak after PCR derivatisation. The volume cut from the ion-interaction system was 100 µL. This was equivalent to a 0.1 min time interval since the flow rate was 1.0 ml/min. The total flow rate after the PCR detection system was approximately 1.8 ml/min. The peak width of the derivatised CN peak varied from approximately 0.2 to 0.3 min (Fig. 3.5(c)), which is equivalent to a volume of 360-540 µL. This indicated that a significant degree of band broadening occurred to the CN peak in the PCR detection system. The extent of band broadening induced by the PCR detection system was also calculated by comparing the plate counts of the thiocyanate peak obtained from both detectors in the tandem system (Fig. 3.4). The plate count (calculated at 4.4% peak height) decreased from approximately 4000 for the UV detector to

peak height) decreased from approximately 4000 for the UV detector to approximately 3000 for the PCR detector, indicating less band broadening than was observed for the CN peak in the cut system. The reason for this difference in band broadening was unknown.
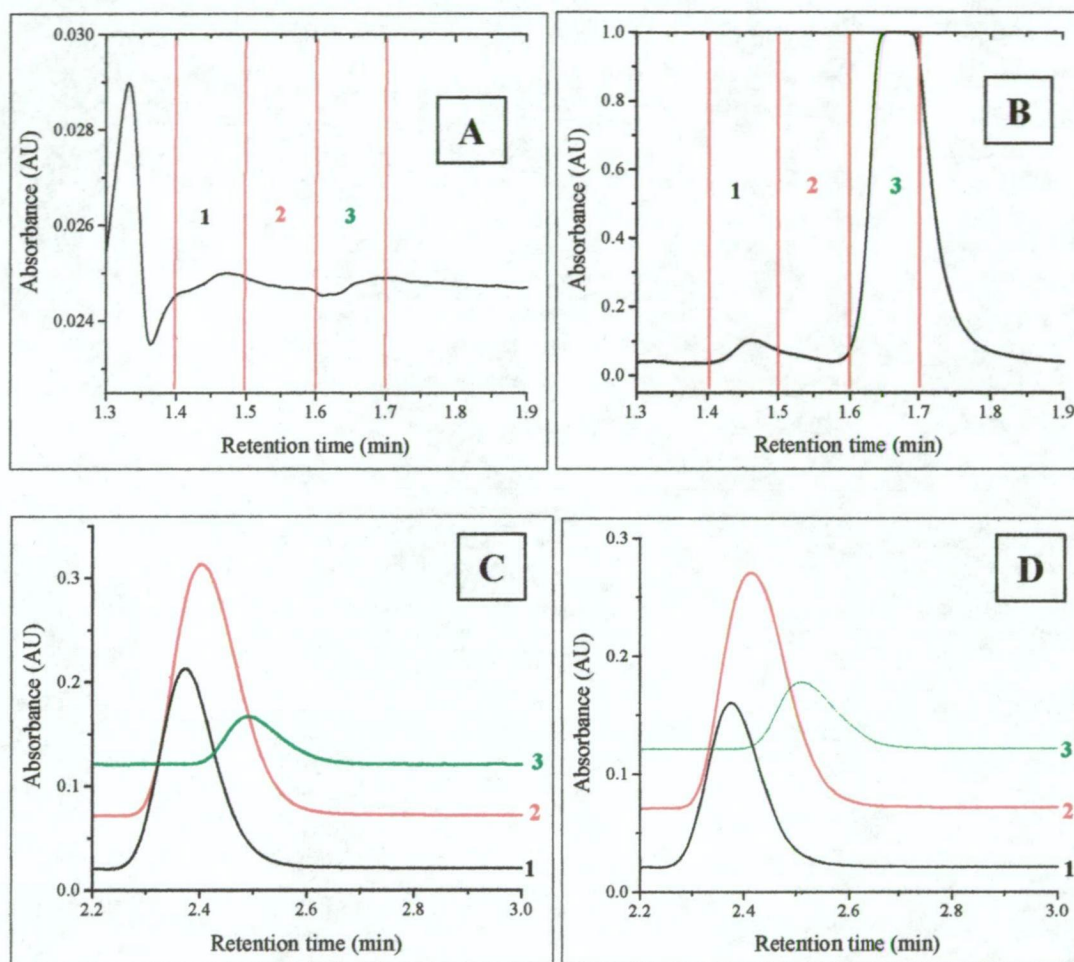
Fig. 3.5: Comparison of cyanide peaks (PCR detector) obtained from 100 µL heart-cuts from the ion-interaction system at three sequential times. **(A)** Top LHS and **(B)** Top RHS: UV detector chromatograms showing the time intervals from where each heart-cut was taken for the 150 ppm CN standard and Rothsay LT3 sample, respectively. **(C)** Bottom LHS and **(D)** Bottom RHS: PCR detector chromatograms showing the cyanide peaks obtained by heart-cuts for the 150 ppm CN standard and Rothsay LT3 sample. Heart-cuts at **(1)** 1.4-1.5 min; **(2)** 1.5-1.6 min and **(3)** 1.6-1.7 min. Note: The Rothsay sample contained 140 ppm Cu as the Cu(I)-cyanide complex).
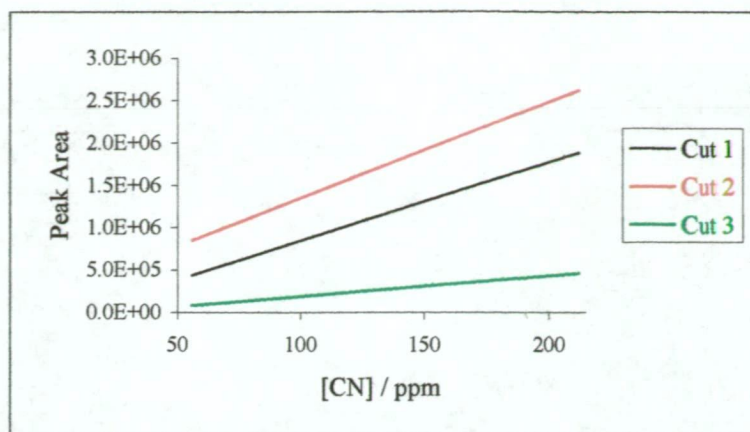
Fig. 3.6: Calibration plots obtained for each heart-cut shown in Fig. 3.5.

Complete separation of the cyanide from any co-eluted species can be achieved by passing the cut fraction through a suitable chromatographic column (*i.e.*, the "coupled" system shown in Fig. 3.1(c)), but again, the timing of the cut is critical for the reasons discussed above. Preliminary experiments showed that free cyanide could be resolved from most common inorganic anions by use of an ion-exclusion column with water as eluent. Under these conditions, the cyanide is present predominantly as undissociated HCN, which is moderately well retained on the ion-exclusion column used (Millipore Waters Fast Fruit Juice column). In contrast, all fully ionized inorganic species are unretained. Sulfide is the most significant and problematic interference for most analytical methods (including the König reaction) developed for cyanide [20]. It was found that sulfide was retained on the ion-exclusion column, presumably as H_2S, with a retention time of 8.86 min, while the retention time of cyanide (HCN) was 6.93 min. This indicated that the ion exclusion column enabled complete separation of cyanide and sulfide. It was also noted that the ion exclusion separation, combined with the PCR detection scheme, afforded an excellent method for the analysis of cyanide and thiocyanate as shown in Fig. 3.7. Recently, Hiroki *et al.* [21] have extended this separation and detection system to include cyanogen chloride (CNCl) in addition to thiocyanate and cyanide. The neutral CNCl was eluted after HCN in this separation.

Comparison of chromatograms obtained from injections of a cyanide standard with each of the possible hardware configurations showed that the best shaped peaks were obtained from the "cut" system. The peak produced in the "cut" system was smaller

than that from the "tandem" system since the total amount of cyanide entering the post-column reactor was less. The peak obtained for the "coupled" system in which the heart cut was injected onto the ion-exclusion column prior to derivatisation displayed some peak tailing as shown in Fig. 3.7. The reason for this tailing was unknown, but may have been due to column damage. It should also be recognised that this tailing may have been, in part, due to the use of an unbuffered eluent (Milli-Q grade water) for this separation.
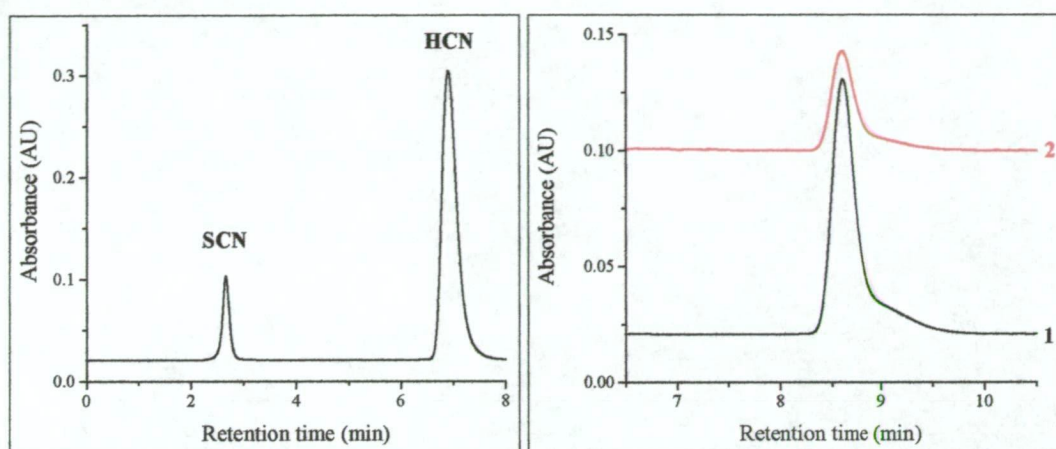
Fig. 3.6 (LHS): Separation of thiocyanate and cyanide by ion exclusion chromatography combined with PCR detection. Column: Waters Fast Fruit Juice ion exclusion. Eluent: Milli-Q-grade water. PCR detection as for Fig. 3.5.

Fig. 3.7 (RHS): Separation of cyanide on an ion exclusion column after a heart-cut from the ion-interaction system using the hardware configuration shown in Fig. 3.1(c). Legend: **(1)** Rothsay sample; **(2)** Mt. Magnet sample. Column: Waters Fast Fruit Juice ion exclusion. Eluent: Milli-Q-grade water. PCR detection as for Fig. 3.5.

Calibration plots were constructed for each hardware configuration over the range 0-300 ppm of cyanide, using 10 µl injections onto the ion-interaction chromatographic system. These plots are shown in Fig.3.8, from which it can be seen that all hardware configurations yielded linear calibrations. Precision was less than 5% RSD for each system.

The cyanide concentration in each of the four samples shown in Fig. 3.4 and Table 3.1 was determined using the three hardware configurations (Fig. 3.1). The samples were also analysed by titration with silver nitrate using p-dimethylaminobenzylidine

rhodanine as the indicator [4]. The results for these four sets of analyses are shown in Table 3.2. The results indicate that there were some differences between the analytical methods for three samples. There was good agreement for the Mt. Magnet sample with all four methods.

The cyanide concentrations determined by the "Cut" and "Coupled" methods for the other three samples were similar. However, these concentrations were quite different from those obtained by the "Tandem" method. The major reason for this was due to the differences in cyanide elution time for standards and samples as discussed above with respect to the Rothsay sample (Fig. 3.5). It should also be noted that these analyses were performed over several days. Consequently, some of the differences were also due to loss of cyanide from the samples.
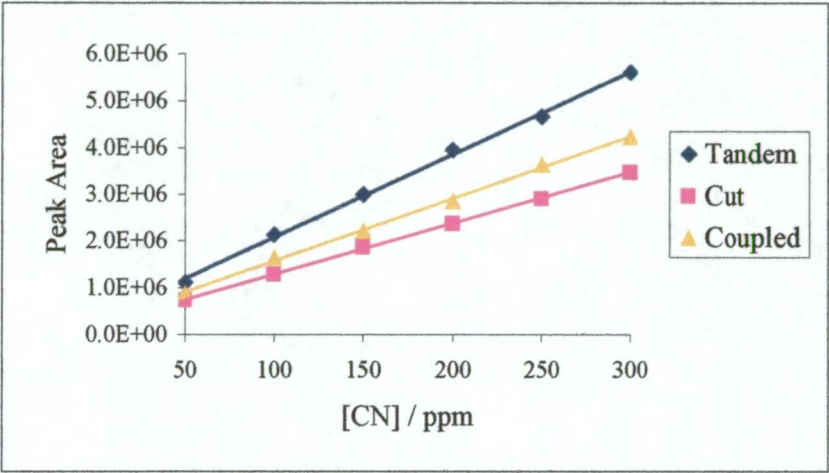
Fig. 3.8: Comparison of the cyanide calibrations obtained for the three hardware configurations.

Sample	Sample No.	Tandem	Cut	Coupled	Titration
Mt. Magnet LD	1	57	56	53	57
You Anmi LT3	2	157	188	210	98
Reedy LD	3	201	138	145	126
Rothsay LT3	4	154	172	178	145

Table 3.2 : Cyanide concentration (expressed in ppm) found in cyanidation leach samples using the three hardware configurations shown in Fig.3.1 and by titration with silver nitrate. Sample No. refers to the chromatograms of these samples shown in Fig. 3.4.

Sample	Sample No.	Tandem	Cut	Coupled	Titration
Mt. Magnet LD	1	57	56	53	57
You Anmi LT3	2	157	188	210	98
Reedy LD	3	201	138	145	126
Rothsay LT3	4	154	172	178	145

Table 3.2 : Cyanide concentration (expressed in ppm) found in cyanidation leach samples using the three hardware configurations shown in Fig.3.1 and by titration with silver nitrate. Sample No. refers to the chromatograms of these samples shown in Fig. 3.4.

Significant differences between the titrimetric and "Tandem" results were observed for the You Anmi and Reedy samples. While the reason for this was uncertain, it should be noted that both these samples had high Total Dissolved Solids (TDS) values and significant sulfide concentrations, both of which would have interfered in the titrimetric analysis.

Common inorganic anions, including sulfide, are partially co-eluted with cyanide. The interference effects of these ions were examined by preparing 100 ppm cyanide standards containing 1000 ppm of each potential interferent. These analyses were performed on the "Tandem" system. The peak area for cyanide was altered by less than 1% for chloride, sulfate, nitrate, nitrite and phosphate, whilst sulfide caused a moderate interference (20%) at this level. A more detailed study of the interference effects of sulfide was undertaken and showed that this interference was not evident for sulfide concentrations up to 500 ppm. Sulfide interference can be overcome using the "coupled" chromatographic system as discussed above, but this was not considered necessary for the samples analysed because the sulfide levels were below the interference threshold.

Evaluation of the results presented in this section indicated that the tandem system was favoured. The increased mechanical complexity of a "cut" or "coupled" system and the necessity to sample a large volume from the ion-interaction system (at least 400 μL, based on the Rothsay sample) were serious disadvantages to a system incorporating a heart cut. For these reasons, such a system should only be considered if the co-eluting species cause significant interferences.

3.3.5 Field trial at Rothsay Gold mine

A short field trial was conducted on an operational gold mine to evaluate the performance of the HPLC method for the analysis of cyanide species. The Rothsay Gold Project was selected for this field trial. The consumption of NaCN per tonne of ore processed at Rothsay was very large (> 8 kg/tonne) due to high concentrations of Fe, S and especially cyanide-soluble Cu in the ore. The ore body was quite variable, consisting mainly of chalcopyrite ($CuFeS_2$), bornite(Cu_5FeS_4), chalcocite (Cu_2S), azurite ($Cu_3(OH)_2(CO_3)_2$) and malachite($Cu_2(OH)_2(CO_3)$). Consequently, very high solution concentrations (1200-2500ppm) of Cu(I)-cyanide complexes were encountered and these levels could vary greatly from day to day. This presented problems for the routine monitoring of cyanide through the leach and CIP circuits where the cyanide was determined titrimetrically with $AgNO_3$. Allowance had to be made for the labile cyanide bound to Cu(I) and this necessitated that a Cu determination by AAS be performed on a twice-daily basis. Thus, a major goal of this field trial was to determine if the HPLC method could improve the analysis of cyanide available for leaching gold.

3.3.5.1 Initial results

The concentrations of most of the cyano species were considerably higher than anticipated from samples analysed prior to the field trial. Injection of undiluted samples resulted in several large peaks for the UV and PCR detector chromatograms and peak shapes were indicative of column overloading. This was confirmed upon dilution of the samples. The cyanide results obtained by HPLC were similar to those obtained by titration, which further indicated that some of the Cu(I) cyano complexes were dissociating on the column.

The PCR conditions had to be modified to accommodate the high cyanide concentrations present in the samples. The PCR reagent concentrations were initially reduced to produce linear calibration plots. However, the response of the PCR detection system varied more rapidly with time than at the University. The drift in the PCR detection response was improved when the reagent concentrations were

increased and the reaction time was reduced. Even so, the detection drift was noticeable and required frequent re-calibration.

3.3.5.2 Relationship between the cyanide and Cu(I)-cyanide peaks

An experiment was conducted to determine the effect of high Cu concentrations on the cyanide peak. NaCN was added to cuprous chloride (CuCl) in molar proportions until the CN:Cu mole ratio was 6. Dissolution of the CuCl was not complete until the CN:Cu mole ratio was 3, with a final copper concentration (as the Cu(I)-cyanide complex) of 100 ppm. Samples were taken at regular intervals, filtered and injected into the HPLC. It was observed that the cyanide peak was very small until the CN:Cu mole ratio was 3.

On the advice of a senior metallurgist [22], the ratio of the cyanide and Cu(I)-cyanide peak areas obtained from the PCR detector were examined. A linear relationship was found when the CN:Cu(I) peak area ratio was plotted against the CN:Cu(I) mole ratio, as shown in Fig. 3.9. This relationship did not apply when the CN:Cu(I) mole ratio was below 3.0 since not all the CuCl had dissolved and the cyanide peak was very small. This linear relationship indicated that the CN:Cu mole ratio could be determined from the CN:Cu(I) peak area ratio obtained from the PCR detector. The total Cu(I) could be simultaneously determined with the UV detector (214 nm) since the molar absorptivities of the three Cu(I)-cyanide complexes are similar at this wavelength [23, 24]. It was reasoned that the CN:Cu(I) mole ratio and Cu(I) concentration would allow the total cyanide concentration in the Cu(I)-CN system to be calculated.
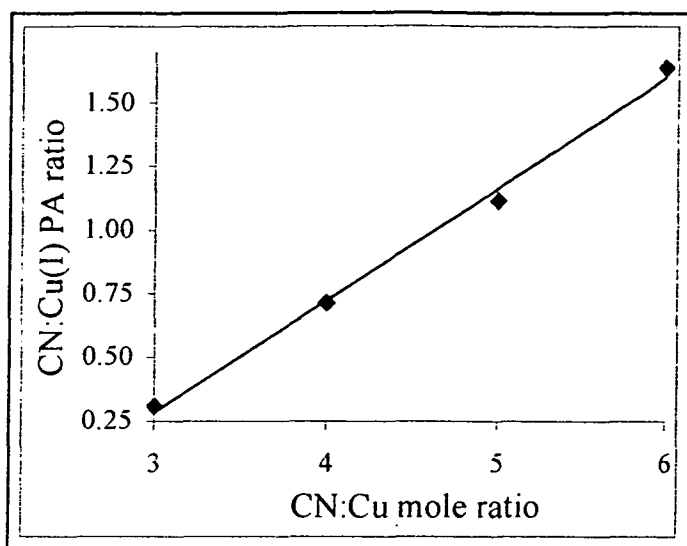
Fig. 3.9: Linear relationship observed between the CN:Cu mole ratio and the CN:Cu(I) peak area (PA) ratio. Total [Cu] = 100 ppm. Eluent: 25% acetonitrile, 5mM Low UV PIC A.

3.3.5.3 Modifications to the eluent

Application of this method to leach samples at Rothsay was further complicated due to the presence of high concentrations of thiocyanate. It was observed that the thiocyanate and Cu(I)-cyanide peaks were not resolved at Rothsay with the same chromatographic conditions used at the University. The reason for this was unknown at the time. However, later studies (see Chapter five, section 5.3.1) identified the cause of the difference due to the use of different sources of acetonitrile. Since the separation of the thiocyanate and Cu(I)-cyanide peaks was critical for a method involving the CN:Cu mole ratio as described above, it became necessary to modify the chromatographic conditions.

Varying the concentrations of either acetonitrile or ion interaction reagent (Low UV PIC A) in the eluent or increasing the column length did not improve the separation of thiocyanate and Cu(I)-cyanide. However, it was known from previous studies that addition of KCN to the eluent stabilised the Cu(I) peak [1]. It was found that an eluent comprising 20% ACN, 5 mM PIC A and 5 ppm CN (as KCN) enabled complete separation of thiocyanate and Cu(I). Since the addition of KCN to the eluent increased the eluent pH above 8, it was necessary to also add KH_2PO_4 to maintain an eluent pH $\leq$ 8 in order to prevent damage to the ODS column.

The addition of KCN to the eluent had a dramatic effect on the Cu(I) and cyanide peaks, as shown in Fig. 3.10. Firstly, the retention time of the Cu(I) was increased significantly compared to the thiocyanate. Secondly, the shape of both the Cu(I) and cyanide peaks was improved, with the tailing of the cyanide peak and fronting of the Cu(I) peak being diminished greatly. These effects were attributed to the partial stabilisation of the eluted Cu(I)-cyanide complex, which would have resulted in the decreased dissociation of the Cu(I) complex, and thereby increased the average anionic charge of the eluted Cu(I)-cyanide complex.

Three unavoidable consequences, which resulted from the addition of KCN to the eluent were the large baseline absorbance, increased baseline noise and reduced sensitivity of the PCR detector (Fig. 3.10). The baseline noise of the PCR detector resulted from visualisation of the pump pulsations. The decreased sensitivity was not considered a problem due to the large analyte concentrations present in the Rothsay samples.
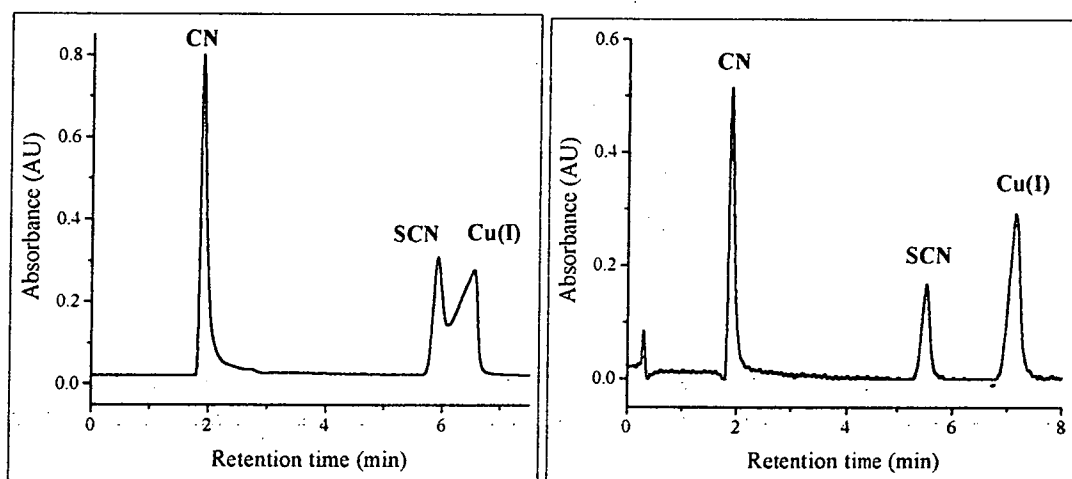
Fig. 3.10: Effect of KCN addition to the eluent at Rothsay (PCR detector chromatograms). Standard: 100 ppm NaCN, SCN⁻ and Cu(I). (a, LHS): Eluent: 20% acetonitrile, 5mM Low UV PIC A (b, RHS): Eluent: 20% acetonitrile, 5mM Low UV PIC A, 5 ppm CN, KH_2PO_4, pH = 7.7.

3.3.5.4 Pilot leach test

A pilot leach test was conducted at Rothsay with leach pulp collected prior to the first leaching tank. Regular cyanide dosing over 12 hours was conducted to simulate plant practice and the leachate was monitored for 24 hours. Samples were collected at regular intervals and prior to each cyanide addition to the leach tank. The samples were filtered immediately and stored in a cool place out of light prior to analysis. Samples were analysed titrimetrically (for cyanide), by HPLC and by ICP-AES. The ICP-AES analyses were performed a week later in order to provide comparative data for the metals and sulfur. Both pH and dissolved O_2 levels were monitored during the leaching test to ensure that they remained within plant specifications.

The first leach sample was taken before the addition of NaCN to the leach tank. There were significant concentrations of thiocyanate and the Cu(I) and Fe(II) cyanide complexes in this sample since the make-up water used in the leaching process was mostly return water from the tailings dam. A negative CN peak was observed for this sample, due to removal of cyanide from the eluent by the sample components, and especially Cu(I) with a low CN:Cu mole ratio. No cyanide was detected titrimetrically in this sample.

The variation in the concentrations of the major cyano species (determined by HPLC) for the other samples (Nos. 2-12) is shown in Fig. 3.11 as a function of the amount of NaCN added to the leaching tank. Table 3.3 shows the cyanide concentrations found in the leach test samples by both titration and the HPLC method. It is noteworthy that the cyanide concentrations determined by HPLC were appreciably lower than those determined titrimetrically. This was in contrast to the results obtained earlier in the field trial when no cyanide was present in the eluent.

The concentration of the Au(I) and Cu(I) cyanide complexes are also shown in Table 3.3. The CN:Cu(I) peak area ratio (PAR) (obtained from the PCR detector chromatograms as described above) was used to calculate the CN:Cu mole ratio (R). The product of the Cu(I) concentration and R was used to calculate the total cyanide concentration in the CN-Cu(I) system, $[CN-Cu]_T$. The values for PAR, R and $[CN-Cu]_T$ are also shown in Table 3.3.

The sum of the CN moieties attached to all the cyano species determined by HPLC were calculated for samples 2 and 12, thereby allowing a mass balance to be performed. The total amount of cyanide calculated by this mass balance was found to be 1.23 kg NaCN. This was considerably less than the total amount of cyanide added between these samples (1.43 kg). However, it should be recognised that a considerable amount of cyanide would have been oxidized to cyanate during the dissolution of cyanide-soluble Cu(II) minerals (see Chapter one, section 1.3.3). Cyanate was not determined by this HPLC method. Later work developed a method for cyanate that enabled quantitative mass balances to be achieved during the leaching of gold ores containing cyanide-soluble Cu(II) minerals (see Chapter seven).
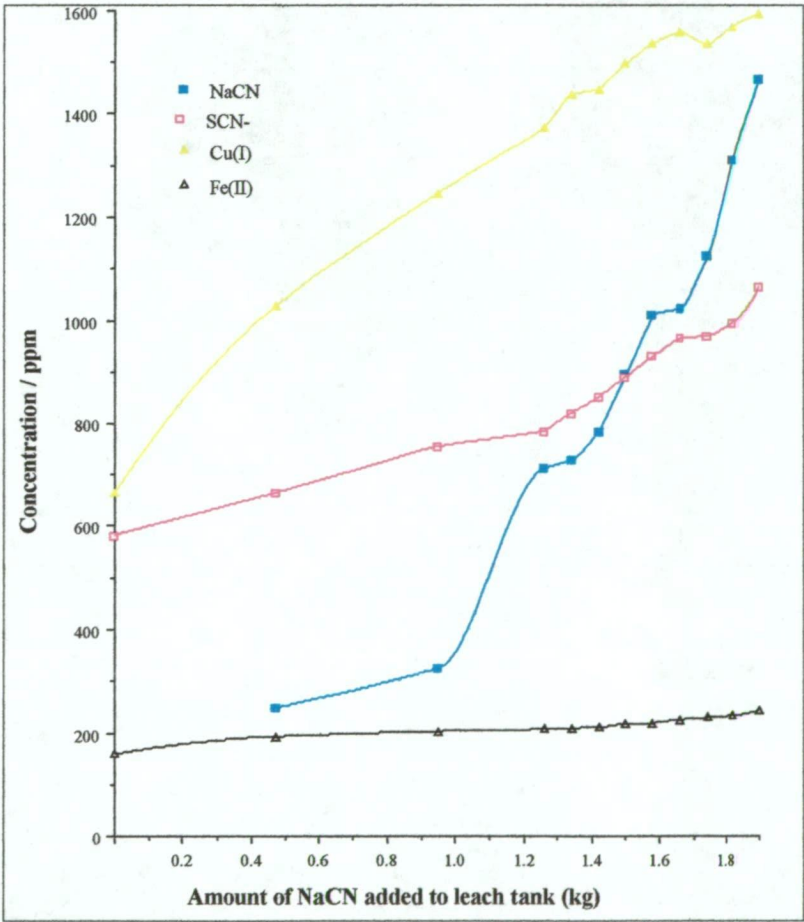
Fig. 3.11: Variation in the major cyano species as a function of NaCN added during the leach test.

Sample No.	Total NaCN added (kg)	[Au(I)] (ppm)	[NaCN] / ppm AgNO₃ titration	[NaCN] / ppm HPLC	CN:Cu(I) PA ratio	CN:Cu Mole ratio	[Cu(I)] (mM)	[CN-Cu]ᴛ (mM)
2	0.47	4.3	346	249	0.117	3.18	16.1	51.2
3	0.95	5.3	385	326	0.127	3.21	19.6	63.0
4	1.26	6.1	817	713	0.256	3.61	21.6	78.1
5	1.34	6.7	885	729	0.266	3.65	22.6	82.4
6	1.42	7.6	942	785	0.275	3.67	22.8	83.8
7	1.50	8.7	1000	897	0.291	3.72	23.5	87.5
8	1.58	9.8	1135	1011	0.318	3.81	24.2	92.2
9	1.66	10.8	1091	1023	0.326	3.83	24.5	93.9
10	1.74	11.2	1250	1128	0.363	3.95	24.2	95.6
11	1.82	11.8	1279	1244	0.399	4.06	24.7	100.3
12	1.90	12.5	1553	1469	0.423	4.14	25.1	103.8

Table 3.3: Concentrations of cyanide, gold and Cu(I) as the amount of total NaCN added to the leaching test was increased. The total solution volume of the leach test was 390 L. The CN:Cu(I) peak area (PA) ratio was used to determine the CN:Cu mole ratio (R). The total cyanide concentration in the CN-Cu(I) system was calculated as follows: [CN-Cu]ᴛ = [Cu(I)] x R. Samples were diluted by a factor of 5 prior to HPLC analysis (10μL injection). Eluent: 20% acetonitrile, 5 mM Low UV PIC A, 5 ppm CN, pH 7.92.

Comparison of the ICP-AES data for S, Cu and F with the HPLC data for thiocyanate and the Cu(I) and Fe(II) complexes revealed a good correlation, indicating that most of these elements were present as their respective cyano species.

One final comment on the results presented for the leach test was the relationship between the gold concentration in solution and the CN:Cu mole ratio, as shown in Fig. 3.12. This shows that gold leaching rate was significantly increased when the CN:Cu mole ratio reached a value of approximately 3.6. This is similar to early observations reported by Hedley and Kentro [25].
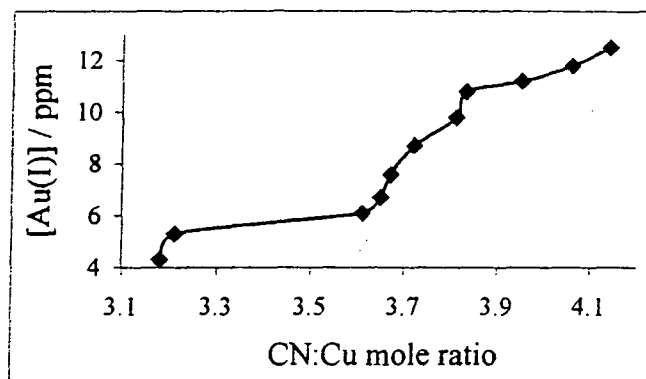
Fig. 3.12: Gold dissolution compared to the CN:Cu mole ratio calculated for each sample during the leach test.

3.4 References

1   P. R. Haddad and C. Kalambaheti, *Anal. Chim. Acta*, 250 (1991) 21.

2   E. A. Simpson and G. M. Waind, *J. Chem. Soc.*, 1958 (1958) 1746.

3   C. Kalambaheti PhD, University of NSW, 1991.

4   W. J. Williams, *Handbook of Anion Determination*; Butterworths: London, 1979, pp. 70-87.

5   A. T. Haj Hussein, *Anal. Lett.*, 21 (1988) 1285.

6   R. J. M. Wyllie, *Engineering and Mining Journal*, 188 (1987) 32.

7   W. Konig, *J. Prakt. Chem.*, 70 (1905) 19.

8   P. Casapieri, R. Scott and E. A. Simpson, *Anal. Chim. Acta*, 49 (1970) 188.

9   J. L. Royer, J. E. Twichell and S. M. Muir, *Anal. Lett.*, 6 (1973) 619.

10   Z. Zhu and Z. Fang, *Anal. Chim. Acta*, 198 (1987) 25.

11   R. B. Roy, *Int. Lab. (Aust. Ed.)*, (1988) 47.

12   A. Tanaka, K. Deguchi and T. Deguchi, *Anal. Chim. Acta*, 261 (1992) 281.

13   T. Toida, T. Togawa, S. Tanabe and T. Imanari, *J. Chromatog.*, 308 (1984) 133.

14   Y. Inoue, Y. Suzuki and M. Ando, *Bunseki Kagaku, Oct*, 42 (1993) 617.

15   J. L. Lambert, J. Ramasamy and J. V. Paukstelis, *Anal. Chem.*, 47 (1975) 916.

16   J. F. Lui and H. C. Ma, *Talanta*, 40 (1993) 969.

17   S. Nagashima, *Intern. J. Environ. Anal. Chem.*, 10 (1981) 99.

18   H. C. Ma and J. F. Liu, *Anal. Chim. Acta*, 261 (1992) 247.

19   C.-C. Chien, F.-C. Chang and S.-C. Wu, *Mikrochimica Acta*, 2 (1980) 9.

20   J. C. Wilmot, S. Ljiljana, E. B. Milosavljevic, J. L. Hendrix and W. Rader, S., *Analyst*, 121 (1996) 799.

21   K. Hiroki, Y. Inoue, T. Sakai and Y. Date, Japanese patent JP 06,229,926 [94,229,926], (1993).

22   R. Keating, Development Metallurgist, Metana Minerals, Personal Communication, 1991.

23   C. Kappenstein and R. Hugel, *Rev. Chim. Miner.*, 6 (1969) 1107.

24   J. C. Pierrard, C. Kappenstein and R. Hugel, *Rev. Chim. Miner.*, 8 (1971) 11.

25   N. Hedley and D. M. Kentro, *Trans. Can. Inst. Min. Metall.*, 48 (1945) 237.

CHAPTER FOUR

Improvements to the PCR detection system and understanding the reversed-phase ion-interaction chromatography of the Cu(I)-cyanide complexes

4.1 Introduction

This chapter is concerned with resolving the problems observed during the analysis of cyanide leachates using the HPLC methods developed in the previous Chapter. The two major problems concerned the stability of the PCR detection system and the partial dissociation of the Cu(I)-cyanide complexes on the chromatographic column. Solutions to these problems were partially interlinked since both involved the PCR detection system. Resolving these problems resulted in a significantly improved understanding of the reversed-phase ion interaction chromatography (RPIIC) of the Cu(I)-cyanide complexes.

The field studies at the Rothsay gold mine demonstrated that partial dissociation of the Cu(I)-cyanide complexes occurred on the column. The extent of this dissociation was similar to that observed when samples were analysed titrimetrically. It was also shown at Rothsay that the addition of a low concentration of cyanide to the eluent had a significant effect on the retention of the Cu(I)-cyanide peak. The initial reason for the addition of cyanide to the eluent at Rothsay was to enable the separation of thiocyanate and the Cu(I) peaks. However, it was also found that the shape of the Cu(I) cyanide peak was improved significantly. Previous studies have noted that the retention characteristics of the Cu(I)-cyanide complexes can be altered considerably by the addition of cyanide to the ion-interaction eluent [1-3]. These observations indicated that the partial chromatographic dissociation of the Cu(I)-cyanide complexes can be controlled by the addition of cyanide to the eluent.

Due to the importance of the Cu(I)-cyanide complexes in the gold mining industry, a series of studies investigating the ion-interaction chromatography of the Cu(I)-cyanide complexes was performed. The latter part of this chapter examines the

degree of the dissociation of these complexes which occurs during the separation process and the manner in which this dissociation effect can be controlled by the addition of cyanide to the eluent.

4.2 Experimental

4.2.1   Instrumentation

The instrument consisted of a Waters (Milford, MA, USA.) M510 isocratic HPLC pump, a Waters 717 auto-sampler, a Waters M441 fixed wavelength ($\lambda = 214$ nm) absorbance detector and a post-column reaction (PCR) detection system. The PCR system consisted of two Eldex pumps, two stitched open tubular reactors, a Waters column heater to maintain the reactors at a constant temperature (usually 40 $^{\circ}$C) and a photometric detector operated at 515 nm. The first reactor was a coil 1.4 m in length with an I.D. of 0.025 mm and the second reactor consisted of three 5 m coils with an I.D. of 0.025 mm, connected in series. The reaction coils were prepared using the method described in Chapter two. The PCR detector was a Waters M484 variable wavelength absorbance detector operating at 515 nm for the isonicotinic acid/barbituric acid (INA/BA) PCR reagent. A detection wavelength of 546 nm was used for the INA/pyrazolone (INA/PZ) PCR reagent.

The photodiode array (PDA) investigation used a Waters 996 PDA detector. Data were acquired and processed with a Waters Millennium data system. A Waters Model 430 Conductivity detector was briefly used. A Bruker IFS-66 FTIR instrument fitted with a demountable micro FTIR flow cell (Spectra-Tech, Stamford, Conn.) with CaF$_2$ windows and 25 - 50 mm Pb spacers was used for the FTIR investigation.

Chromatographic data was acquired on either a Waters Maxima data station or a Waters Millennium data station. Chromatographic parameters (such as peak width, peak asymmetry and resolution) were calculated with the Millennium data system.

4.2.2 Preparation of the eluents

All the reagents used in this work were obtained from Aldrich (Aldrich Chemical Co. Inc., Castle Hill, NSW, Aust.), unless otherwise stated. The eluents were prepared with Grade 1 water from a Milli-Q system (Millipore, MA, USA), acetonitrile (Waters, Lane Cove, NSW, Aust.), a tetrabutylammonium (TBA$^+$) salt and a NaCN stock solution. A NaOH solution was used to adjust the apparent pH of these eluents to 7.95 ± 0.05. All eluents were filtered (0.45 μm) and degassed under vacuum in an ultrasonic bath prior to use.

The nature of the TBA$^+$ salt varied during these experiments. The eluents used during the PDA experiments were prepared from TBAOH (Aldrich) and H_3PO_4, with a TBA$^+$ concentration of 5 mM. The eluents used for the PCR study were prepared with a proprietary reagent, Low UV PIC A (Waters) containing a TBA$^+$ concentration of 5 mM. The acetonitrile concentration in the eluents was 20% for the PDA experiments and 25% for the PCR experiments.

4.2.3 Preparation of the post-column reaction reagents

The two PCR reagents were prepared as follows and kept in the dark at less than 4°C. Both reagents were filtered (0.45 μm) under vacuum prior to use each day.

Reagent 1 : N-chlorosuccinimide (0.1%, w/v) was added to a succinate buffer (0.1 M, pH 5.6) containing succinimide (2% w/v).

Reagent 2: This reagent contained the sodium salts of isonicotinic acid (INA, 0.3 M), barbituric acid (BA, 4 mM) and EDTA (10 mM) and was prepared by dissolving the INA and BA in excess NaOH prior to the addition of Na$_2$EDTA. The final reagent pH was 7.8.

4.2.4 Standards

Cyanide standards were prepared from a 0.1 M stock solution of NaCN in 0.1 M NaOH. Cu(I) and Ag(I)-cyanide stock solution (10 mM) were prepared from CuCN or AgCN and NaCN in a 10 mM NaOH solution, such that the CN:Metal mole ratio of this stock solution was 3.0. These solutions were kept alkaline to improve their

stability. The metal-cyanide standards used for analysis were prepared from the stock solutions of metal-cyanide and NaCN.

Thiocyanate standards were prepared from a 0.1 M stock solution of KSCN. Both the NaCN and KSCN 0.1 M stock solutions were standardised potentiometrically with a standardised $AgNO_3$ solution. The copper concentration in the 10 mM Cu(I)-cyanide stock solution was checked using atomic absorption spectrometry, while the cyanide concentration was checked by total cyanide distillation. Both the copper and cyanide concentrations were within 1% of expected values.

4.2.5   Operation of the instrument

All separations were performed on a 150 x 3.9 mm I.D. Waters Nova-Pak C-18 analytical column fitted with a Waters guard column. The eluents were pumped through the column at a constant flow rate of 1.0 ml/min. An injection volume of 10 μL was used throughout this work. The UV absorbing metallo-cyanide complexes were detected immediately after elution from the column with a fixed wavelength detector set 214 nm.

The PCR detection system involved modifications to the system developed in Chapter three. The flow-rates of the first and second PCR reagent pumps were approximately 0.1 and 0.2 ml/min, respectively. The derivatised cyanide and Cu(I)-cyanide peaks were detected after the PCR unit with a variable wavelength detector operated at 515 nm.

4.3 Results and Discussion

4.3.1 Some preliminary investigations

While the addition of low concentrations of cyanide to the eluent solved the problem concerning separation of thiocyanate and the Cu(I)-cyanide peaks, other problems were created. The major problem was due to the large baseline absorbance of the PCR detector and the visualisation of pump noise in the PCR detector

chromatograms. The following experiments were conducted in attempt to circumvent this problem.

An attempt was made to determine if alternative complexation reagents could be added to the eluent to enable selective manipulation of the retention of the eluted copper. Ligands such as 1,10-phenanthroline and ammonia were used in this work. However, these attempts were unsuccessful due to either no effect on the eluted Cu peak (in the case of ammonia) or a very broad Cu peak (in the case of 1,10-phenanthroline). In addition, 1,10-phenanthroline caused a large baseline absorbance in the UV detector at the wavelength used for monitoring the metallo-cyanide complexes.

An addition of NaCN (1 mM) to the eluent had no effect on the Cu(I) peak when the eluent was buffered at pH 7. This demonstrated that the CN⁻ ligand was responsible for the effect on the Cu(I) peak. Since the pKa of HCN is 9.2, the concentration of CN⁻ at pH 7 is almost zero, while only approximately 6% of the total cyanide exists as CN⁻ at pH 8.

Since the PCR detection system responded to the total cyanide concentration in the eluent, an obvious way of decreasing this concentration (and thereby reducing the PCR detector baseline absorbance) was by use of an eluent with a pH > 8. However ODS columns cannot be used at these pH values due to dissolution of the silica material, eventually resulting in column destruction. Consequently, several columns suitable for high pH ranges were tried. These were the Hamilton PRP-1, SGE C18-P-8/5 (a polymer coated silica column with the C18 functionality attached to the polymer surface) and the Shandon Hypercarb column. None of these alternative columns was satisfactory in providing adequate separation of the metallo-cyanide complexes, which is in agreement with the findings of previous workers [4, 5]. Consequently, the remainder of this work was conducted with the Waters Nova-Pak C-18 column and eluents were maintained at ≤ 8.0.

Brief attempts were made to determine if amperometric or conductivity detection would provide additional information concerning the eluted Cu(I) complex. Amperometric detection resulted in a very tailed Cu peak, indicating the

unsuitability of this detection mode for this analysis. The tailing may have been due to the formation of precipitates such as CuCN on the working electrode surface.

Previous workers have used both suppressed and non-suppressed conductivity detection for the metallo-cyanide complexes [2, 6]. In order to reduce the background conductivity, a TBA^+ concentration of 1-2 mM was used in these studies. Pohlandt [6] observed that the eluted Cu(I) cyanide complex was precipitated in the suppressor, presumably due to formation of species such as CuCN. Padarauskas et al [2] used non-suppressed conductivity detection by using a counter anion (butyrate) with a low limiting ionic conductance. The reason for the selection of butyric acid over other carboxylic acids with similarly low limiting ionic conductances was not given. Based upon this work, an eluent was prepared with 2mM TBAOH neutralised with camphorsulphonic acid (CSA). CSA was selected as it allowed both conductivity and UV detection modes to be used. The chromatograms of various standards injected separately are shown in Fig. 4.1. While significant information concerning the eluted Cu(I)-cyanide complex was not obtained with this experiment, some interesting points were noted. The conductivity detector chromatograms showed that the response was greater for the singly charged thiocyanate and cyanate anions compared to the Cu(I) and Ag(I) complexed anions, with the lowest response being observed for the Cu(I) anion. Two possible explanations to account for this result are:

(i) The limiting ionic conductance of the two complexed anions was lower than for the pseudo halides.

(ii) A partial ion pair was formed with the TBA^+ in the eluent, thereby lowering the conductance of the complexed species. This is a reasonable assumption since the metallo-cyanide complexes are well known for their ability to form ion pairs with quaternary ammonium groups such as TBA^+ [7].

An additional point demonstrated in this experiment was that cyanate was virtually unretained. This indicated that both cyanide and cyanate are almost co-eluted in the void volume during the RPIIC separation of the metallo-cyanide complexes. Cyanide was not observed in either the UV or conductivity detector chromatograms

since it was both UV transparent and almost completely undissociated at the eluent pH (7.5) used in this experiment.
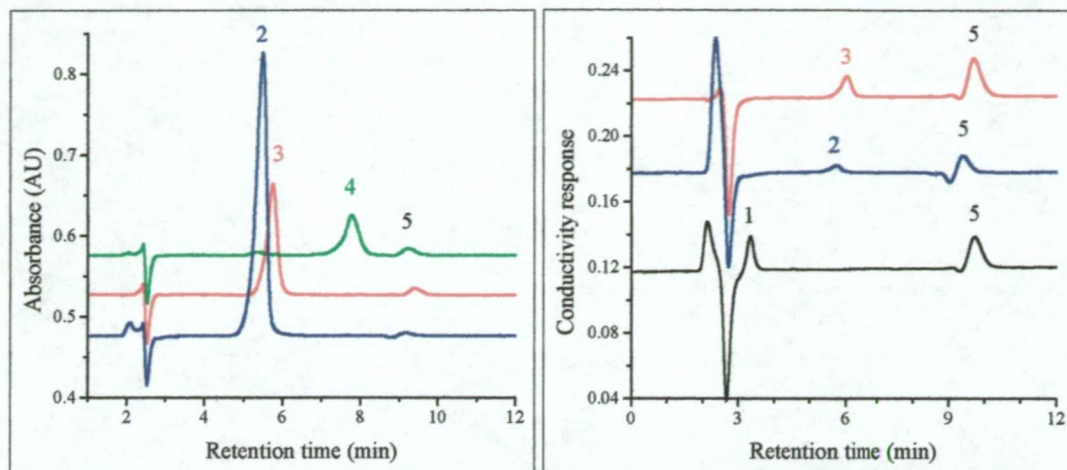
Fig. 4.1: Analysis of standards with an eluent containing camphorsulphonic acid (CSA) using conductivity and UV detection. UV (LHS) and conductivity (RHS) detector chromatograms. Legend: (1) OCN^-; (2) Cu(I); (3) SCN^-; (4) Ag(I); (5) System peak. Eluent: 25%acetonitrile, 2mM TBAOH neutralised with CSA to pH ~ 7.5. Chromatograms offset for clarity.

The retention of cyanide during the RPIIC separation was further investigated by use of a reversed phase eluent (25% acetonitrile) for the determination of cyanide, thiocyanate and the Cu(I) and Ag(I) complexes. The PCR detection system was used in this experiment as it enabled all the above species to be monitored. Some interesting observations were made. Under the eluent conditions used in this experiment, cyanide existed almost entirely in the undissociated form, thereby allowing retention of cyanide as the neutral HCN molecule, as shown in Fig. 4.2. Conversely, the charged anions were all unretained. Slight retention and tailing of the Cu(I) complex indicated that a dissociation effect also occurred during this separation. The cyanide peak shape for the NaCN standard was also improved. This improvement in peak shape was attributed to the PEEK column body used for this experiment. It was noted in a separate experiment that there was a slight improvement in the cyanide peak shape when a PEEK column body was utilised. This indicated that the Stainless Steel (SS) frits in SS body may have chemically affected the cyanide by interaction with the transition metals (in particular Fe) present in the SS.

The implication of the result obtained from this experiment was that cyanide was eluted at the tail end of the void volume during the RPIIC separation. This would appear reasonable to assume since cyanide is predominantly in the HCN form at the pH of the RPIIC eluents. This would account for the surprisingly high tolerance of the PCR detection system to sulfide, which is well known for its acute interference in the König reaction [8].
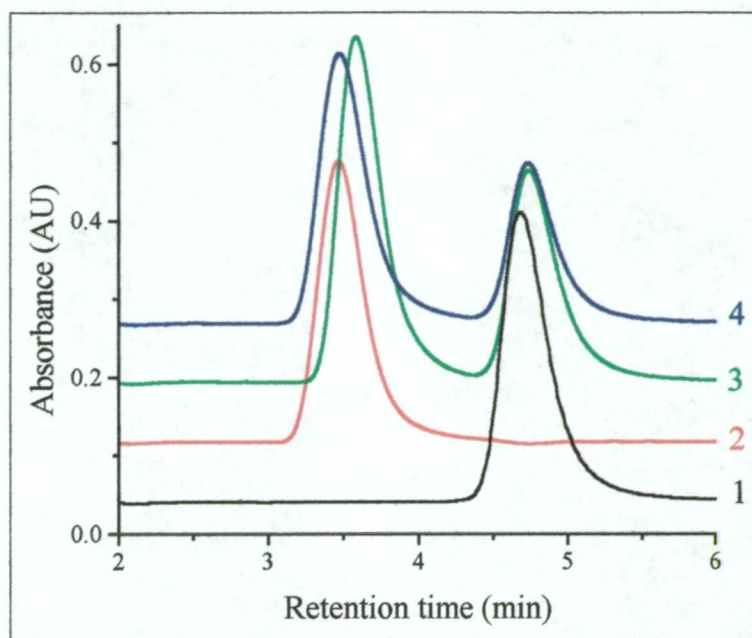
Fig. 4.2: Analysis of standards using reversed phase separation conditions with PCR detection. Legend: **(1)** 1.0 mM NaCN; **(2)** 1.0 mM KSCN; **(3)** 0.5 mM Cu(I), CN:Cu mole ratio = 2.3; **(4)** 0.5 mM Ag(I), CN:Ag mole ratio = 3.0. Column: Waters PEEK C-18 column. Eluent: 25% acetonitrile. Chromatograms offset for clarity.

An attempt was made to use alternative organic modifiers (methanol and tetrahydrofuran (THF)) with the modified PCR conditions to determine the effect of acetonitrile on the cyanide mass balance (see sections 4.3.4 and 4.3.5). In addition, there was the possibility that acetonitrile may contain trace amounts of cyanide (see Chapter five, Section 5.3.1). However, it was found that both methanol and THF were unsuitable for this analysis. The methanol based eluent produced very tailed CN peaks and fronted Cu(I) peaks, as shown in Fig. 4.3. The THF eluent resulted in a split CN peak in the PCR chromatogram. The cause of this peak splitting was unknown and was not investigated any further. In addition, the combined cyanide concentration in the CN and Cu(I) peaks (determined using the method described in

section 4.3.5) was considerably greater than that injected. Due to these problems, all subsequent studies employed acetonitrile (20-25% v/v) as the organic modifier.
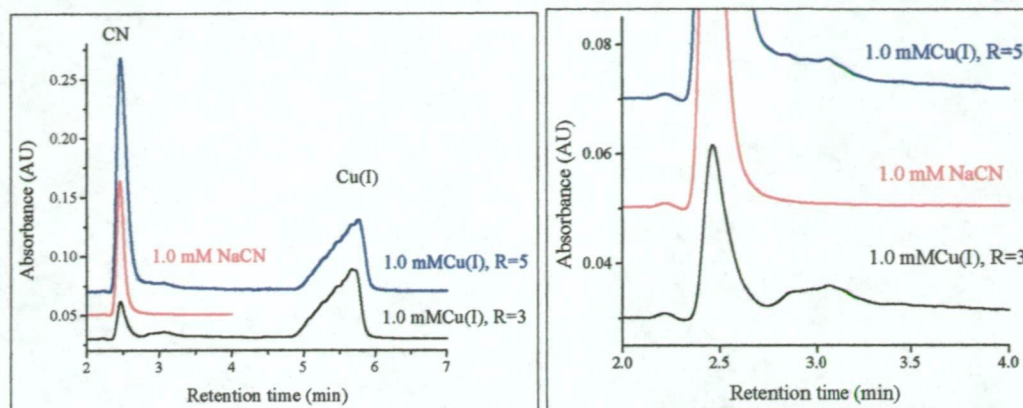
Fig. 4.3: PCR detector chromatograms of 1.0 mM Cu(I)-cyanide standards (R = 3 & 5) analysed with an eluent containing methanol as the organic modifier. 1.0 mM NaCN standard is shown for comparison with the CN peak resulting from the Cu(I)-cyanide standards. LHS: Expanded view of the CN peaks. Chromatograms offset for clarity. Eluent: 28% methanol, 5 mM Low UV PIC A.

4.3.2 Chromatographic behaviour of the Cu(I)-cyanide complexes

When a series of Cu(I)-cyanide standards with a constant copper concentration and increasing CN:Cu mole ratios, R, was analysed in an eluent containing no added cyanide, one peak was observed with the UV detector and two peaks were observed with the PCR detector, as shown in Fig. 4.4. The peak labeled as Cu(I) in both the UV and PCR detector chromatograms was due to the eluted Cu(I)-cyanide species and its retention time and peak area did not change with the value of R injected, provided the injected amount of copper was constant. The cyanide peak in the PCR chromatogram (which corresponded to the void peak in the UV detector chromatogram) increased almost proportionally with R.

Close examination of the peak shapes obtained on the PCR detector in Fig. 4.4 reveal that the cyanide peak showed considerable tailing, and the Cu(I)-cyanide peak exhibited considerable fronting (this was also evident on the UV detector, Fig. 4.4(a)). The cyanide peak tailing was apparent when the PCR detector chromatograms of NaCN, Ag(I) and Cu(I) standards were compared, as shown in Fig. 4.5. The extent of the fronting of the Cu(I) peak increased at higher copper

concentrations, as shown in Fig. 4.6. The value of R was maintained at 3.0 for the standards shown in Fig. 4.6.
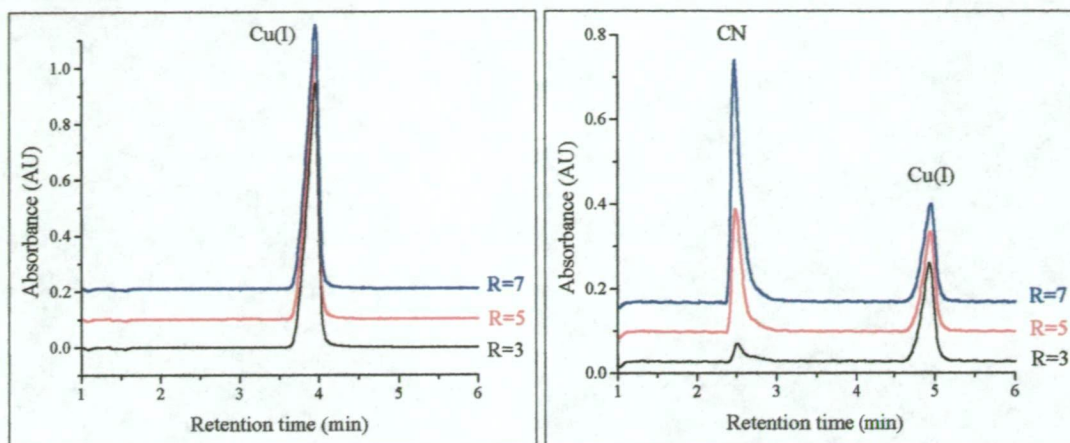
Fig. 4.4: (a) UV (LHS) and **(b)** PCR (RHS) detector chromatograms of Cu(I)-cyanide standards with CN:Cu(I) mole ratios of 3, 5 and 7. The total [Cu] in each standard was 1.0 mM.
Column: Waters Nova-Pak C-18 column. Eluent: 25% acetonitrile, 5 mM Low UV PIC A. Chromatograms offset for clarity.
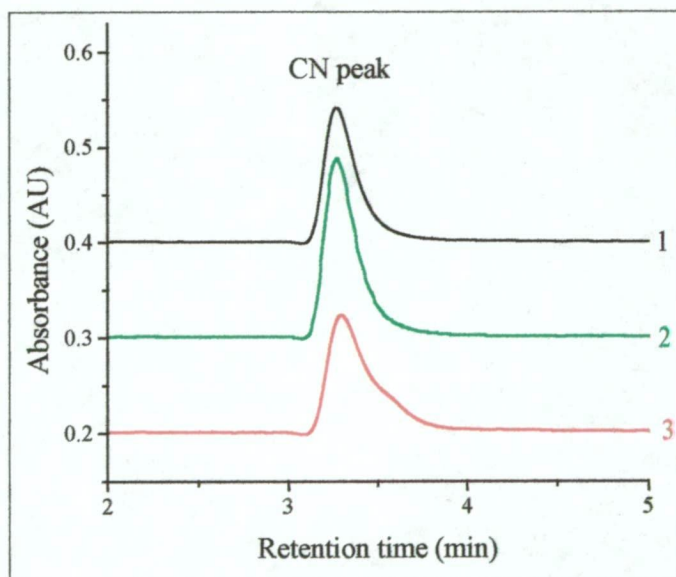
Fig. 4.5: Comparison of cyanide peaks obtained from the analysis of NaCN, Cu(I) and Ag(I) standards. Legend: **(1)** 0.3 mM NaCN; **(2)** 0.4 mM Ag(I), CN:Ag mole ratio = 3.0; **(3)** 0.5 mM Cu(I), CN:Cu mole ratio = 3.0. Column: Waters Nova-Pak C-18 column. Eluent: 25% acetonitrile, 5 mM Low UV PIC A. Chromatograms offset for clarity.
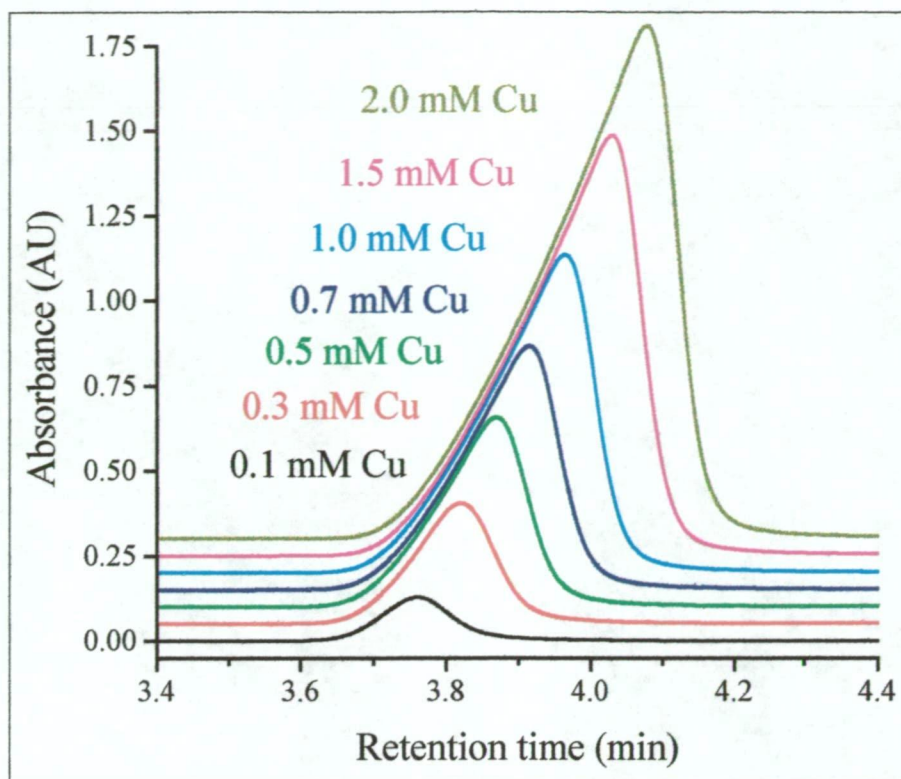
Fig. 4.6: UV detector chromatograms of Cu(I)-cyanide standards (all R = 3) with total [Cu] varying from 0.1 mM to 2.0 mM. Same conditions as for Fig. 4.3. Chromatograms offset for clarity.

The above behaviour can be attributed to the on-column dissociation of the Cu(I)-cyanide complexes. As discussed in Chapter one (Section 1.4), vibrational spectroscopic studies have shown that three monomeric Cu(I)-cyanide complexes, $[Cu(CN)_2]^-$, $[Cu(CN)_3]^{2-}$, $[Cu(CN)_4]^{3-}$, exist in aqueous solution [9, 10]. Radiochemical studies have shown that the cyanide ligands are kinetically very labile [11]. The concentrations of the three complexes are governed by the equilibria shown in Chapter one (Section 1.4.4). These equilibria depend on the value of R and are also pH dependent over the approximate pH range of 7-11 (since the pKa for HCN is 9.2). The changes in the concentrations of the three complexes and uncomplexed cyanide when the R value is varied can be calculated using equilibrium calculations. Fig. 4.7 shows these changes when R is varied from 2.6 to 5.0 at pH 8 with a total copper concentration of 1.0 mM. This pH value was used for these calculations, as this was the eluent pH. It is apparent from Fig. 4.7 that the tri-cyano complex is predominant when R exceeds 3, with the average number of complexed CN ligands increasing only slowly when R exceeds 3.8. Most of the uncomplexed

cyanide occurs as HCN at pH 8. There is an almost linear increase of the HCN concentration when the CN:Cu mole ratio exceeds 3.8.
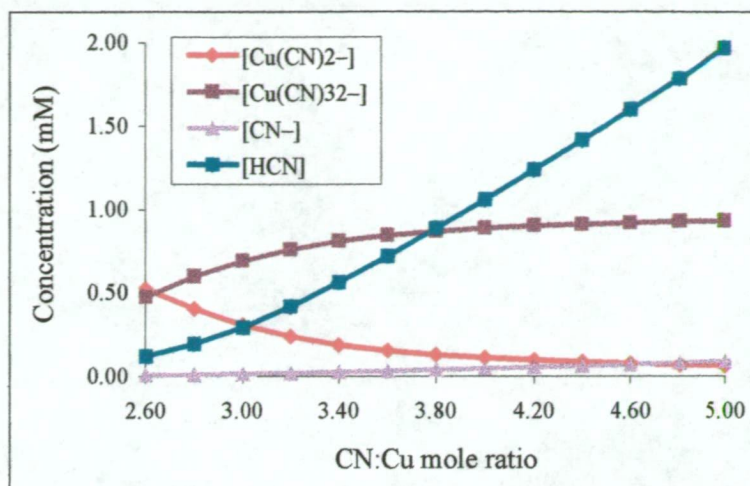
Fig. 4.7: Plots of calculated equilibrium concentrations of $[Cu(CN)_2]^-$, $[Cu(CN)_3]^{2-}$, CN^- and HCN. The constants (obtained from [12, 13]) and parameters used for these calculations were : pk_a HCN = 9.2 ; Log β_2, β_3 and β_4 = 14.4, 19.8 and 21.6, respectively. Solution pH = 8; Total [Cu] = 1 mM; [CN]:[Cu] ratio varied from 2.6 to 5.0.

The effect of acetonitrile has been taken into account in these calculations (Fig. 4.7) by use of the recently published stability constants for the Cu(I)-CN system in aqueous acetonitrile [14]. However, it should be recognised that Fig. 4.7 is only a guide to the equilibrium conditions occurring in the eluent at pH 8. This is because the acetonitrile present in the eluent will also affect the "true" pH value of the eluent. In addition, the ionic strength of the eluent will be affected by the various components of the ion interaction reagent.

To account for the observed chromatographic behaviour, it is worthwhile considering, as an example, a sample having an R value of 3.0, which contains an equilibrium mixture composed mostly of the di and tri-cyano Cu(I) complexes, with small concentrations of cyanide and the tetra-cyano Cu(I) complex. It is assumed that this aqueous sample is alkaline (pH 12) and that all the cyanide is completely dissociated. For a sample containing a total copper concentration of 1 mM, the concentrations of the di, tri and tetra cyano Cu(I) complexes were calculated to be 0.069, 0.929 and 0.002 mM respectively, with a total complexed cyanide

concentration of 2.933 mM, giving by difference that the uncomplexed cyanide concentration was 0.067 mM. These calculations were performed with the constants recommended in the most recent IUPAC review of the stability constants of the metallo-cyanide complexes [12].

The first effect expected to occur following sample injection would result from the changed solution matrix of the sample due to dispersion in the eluent. The two most significant changes in the solution matrix are the lower pH of the eluent (pH 8) and the presence of acetonitrile in the eluent. The eluent pH would result in a decrease of the total complexed cyanide concentration, while the acetonitrile in the eluent would alter the stability constants. The calculated concentrations of the di-, tri- and tetra-cyano complexes, CN^- and HCN under these conditions were 0.308, 0.691, 0.001, 0.013 and 0.294 mM, respectively with a total complexed cyanide concentration of 2.693 mM. The calculated total cyanide concentration for both situations is shown in Fig. 4.8.
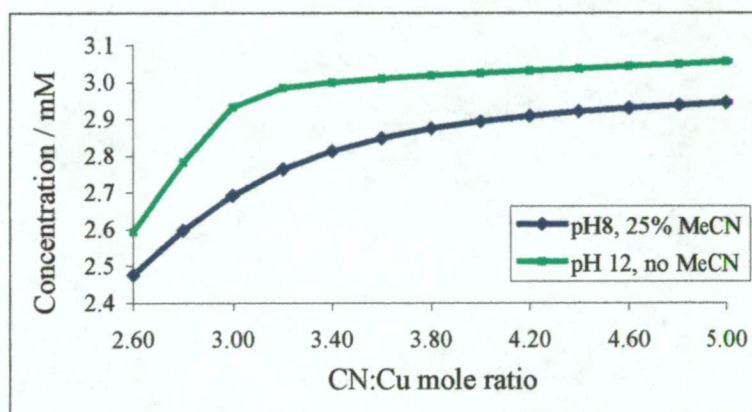
Fig. 4.8: Plots of calculated total complexed cyanide for varying R values at pH 12 (aqueous solution) and pH 8 (25:75 MeCN:H$_2$O). The constants and parameters used for these calculations are described in the text.

The role played by the retention differences between the cyano species and the subsequent perturbations of the composition of the equilibrium mixture traversing the column will now be examined. The most pronounced retention difference occurs between the uncomplexed cyanide, which is unretained, and the Cu(I) cyanide complexes, which are retained. Due to the kinetic lability of the cyanide ligands, as

the cyanide is separated from the Cu(I) cyanide complexes, the tetra- and tri-cyano complexes will undergo dissociation to produce cyanide and the tri- and di-cyano complexes. This process will continue until a kinetically stable mixture results and this mixture will be represented in the eluted Cu(I) peak.

Fronting of the Cu(I) peak can be expected due to increased dissociation at low copper concentrations, leading to increased proportions (relative to the main body of the peak) of the dicyano species in the lower concentration regions. The dicyano species is eluted more rapidly than the tricyano species, so that the eluted band of Cu(I) cyanide complexes comprises a faster moving, low concentration band relatively rich in the dicyano species (which reaches the detector first), followed by a slower moving, higher concentration band relatively rich in the tricyano species (which reaches the detector last). A fronted peak shape results (Fig. 4.4) and this fronting becomes more pronounced as the total amount of Cu injected is increased (Fig. 4.6). This mechanism is identical to that used to explain the fronted peaks observed for ion-exclusion chromatography of carboxylic acids when water is used as eluent [15]. The same explanation can be proposed to account for the observed tailing on the cyanide peak (Fig. 4.5). These mechanism are identical since the equilibria used to describe the dissociation of a weak acid is analogous to the equilibria used to describe the dissociation of the labile Cu(I)-cyanide complexes [16].

Some insight into the validity of the above mechanism can be gained when small amounts of cyanide are added to the eluent. The concentration-dependent dissociation should be reduced, leading to improved peak shape for the Cu(I)-cyanide and cyanide peaks, and the equilibrium position of the eluting band of mixed Cu(I) cyanide complexes should be shifted towards higher levels of the tricyano complex, leading to increased retention. Both of these trends were evident as can be seen from Fig. 4.9 and from the data shown in Table 4.1 (which for comparison also includes data for thiocyanate). An eluent containing 150 μM NaCN produced an almost Gaussian Cu(I)-cyanide peak (Fig. 4.10) having a significantly longer retention time than that obtained using an eluent without cyanide (Table 4.1) In addition the peak shape remained almost the same for all copper concentrations (Fig.

4.10). In contrast, there was very little change to either the retention time for the closely eluted species, SCN⁻, also shown in Table 4.1. An unavoidable side-effect resulting from the addition of NaCN to the eluent was an increase in the baseline absorbance of the PCR detector and a consequent decrease in the signal-to-noise (S/N) ratio due to pump pulsations, as shown in Table 4.1.
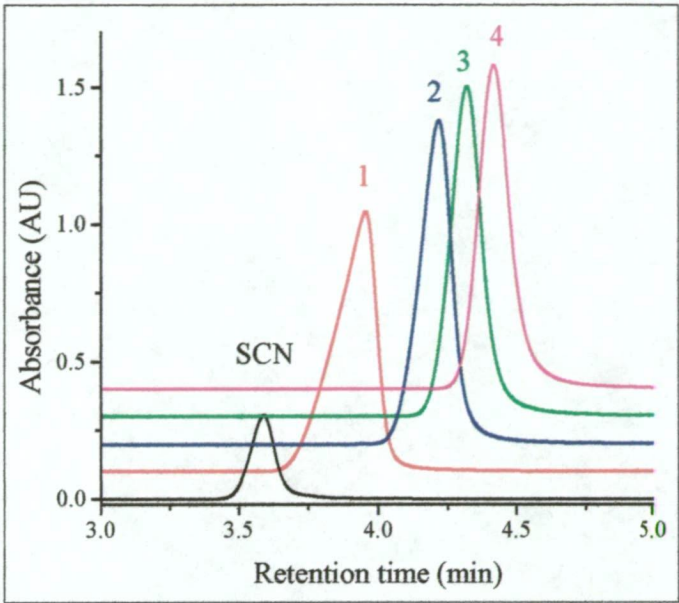
Fig. 4.9: UV detector chromatograms of thiocyanate (1 mM) and Cu(I)-cyanide (1 mM, R=3) standards analysed in eluents containing 0 – 150 µM NaCN. Legend: Cu(I) peak in eluents containing **(1)** 0 µM NaCN; **(2)** 50 µM NaCN; **(3)** 100 µM NaCN and **(4)** 150 µM NaCN. All the eluents contained 25% acetonitrile and 5 mM Low UV PIC A. Chromatographic data for these standards is shown in Table 4.1.

[NaCN] in eluent (µM)	Retention time (min)		Peak width (min)		Peak asymmetry		Resolution of Cu(I) & SCN	S/N ratio
	SCN	Cu(I)	SCN	Cu(I)	SCN	Cu(I)		
0	3.59	3.97	0.198	0.325	0.921	0.372	1.56	131
50	3.53	4.22	0.191	0.254	0.842	0.764	3.33	36
100	3.53	4.32	0.191	0.253	0.911	1.104	3.83	24
150	3.56	4.42	0.191	0.256	0.885	1.243	4.14	12

Table 4.1: Effect of eluent cyanide concentration on the chromatography of the Cu(I)-cyanide species. Peak width, peak asymmetry and resolution calculated at 10% peak height.
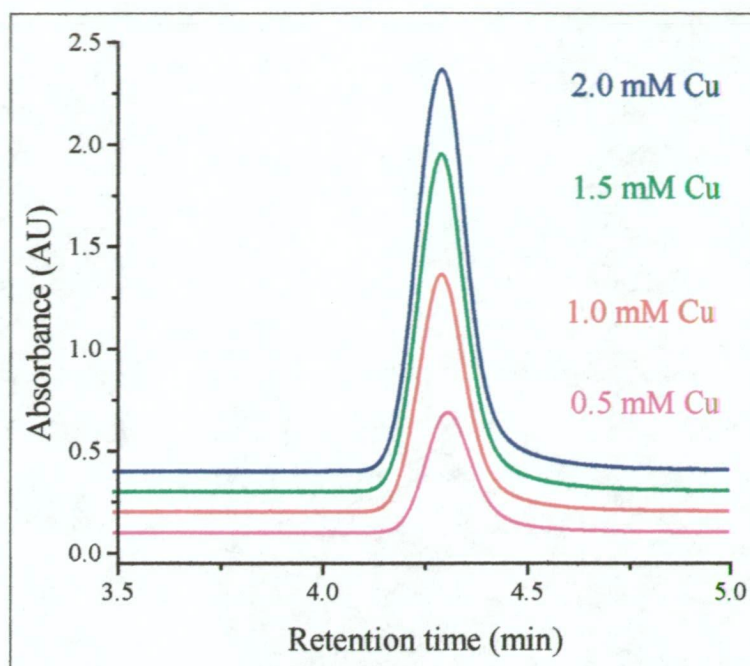
Fig. 4.10: UV detector chromatograms of the some of the Cu(I)-cyanide standards shown in Fig. 4.5. Note that the Cu(I) peak shape is virtually the same for all copper concentrations. Eluent : 25% acetonitrile, 5 mM Low UV PIC A and 150 μM NaCN.

4.3.3 Elucidation of the nature of the eluted Cu(I)-cyano complexes using spectroscopic methods

Prior to reading this section, the interested reader may wish to refer to Section 1.4 for a discussion of the various spectroscopic methods available for examining the Cu(I)-cyanide complexes in aqueous solution. In order to confirm the above mechanism and to determine quantitatively the composition of the eluted complexes under various eluent conditions, two alternative spectroscopic detection techniques were employed, namely Fourier Transform Infrared (FTIR) spectrometry, and photodiode array (PDA) detection. The vibrational spectrum of an aqueous solution of the Cu(I)-cyanide complexes can potentially provide characteristic information concerning the speciation of these complexes since the di-, tri- and tetra-cyano complexes have C-N stretching frequencies of $2125 cm^{-1}$, $2094 cm^{-1}$ and $2076 cm^{-1}$ respectively [9]. However, it was found that the Cu(I)-cyanide complexes could not

be detected by FTIR, even at concentrations 100-times greater than those expected to be eluted from the column. This was considered to be due to the high background IR absorbance of the eluent and the short residence time in the flow cell. It should be noted that a recent study employing FTIR to monitor the metallo-cyanide complexes (in particular the Fe complexes) in environmental samples reported reasonably high detection limits, even with a 10-minute data acquisition time [17]. These detection limits prevented the applicability of FTIR spectroscopy for the analysis of environmental samples.

There have been several studies of the UV spectra of the Cu(I)-cyanide complexes which have shown that spectral changes occur as R is increased [18-21], although there is no clear spectral discrimination between the three complexes as discussed in Chapter one (section 1.4.2). Unlike many other metal-ligand systems, it is not possible to obtain a spectrum of a solution of any of the pure Cu(I)-cyanide complexes for the reasons discussed in Chapter one (section 1.4.4). Consequently, mathematical deconvolutions of the Cu(I)-cyanide spectra are required in order to calculate the spectra of the individual complexes [18, 20-22]. It should therefore be possible to discriminate between spectrally different components in a single chromatographic peak using a PDA detector coupled with a computational package. Some of the computational approaches are described by Frei [23].

Ten 0.5 mM Cu(I)-cyanide standards with R values ranging from 3 to 13 were analysed with the PDA detector in six eluents containing 0-200 μM NaCN. The spectrum of the eluted Cu(I)-cyanide peak was constant in the same eluent, but altered as the NaCN concentration in the eluent was increased. The largest spectral change occurred between the eluents containing no added cyanide and 10 μM NaCN, as shown in Fig. 4.11. The isosbestic points at 207 and 234 nm observed in Fig. 4.11 are similar to the reported values in spectrophotometric studies [22].

To provide a contrast to the Cu(I)-cyanide standards, a series of six 0.5 mM Ag(I)-cyanide standards with CN:Ag mole ratios ranging from 3 to 10 was also analysed with the PDA detector using the above eluents. There was no change in the normalised spectra of the Ag(I) cyanide standards between the eluents. A typical spectrum of the eluted Ag(I)-cyanide peak is shown in Fig. 4.12. It is interesting to

note that literature reports indicate that the Ag(I)-cyanide complexes display a continuous spectrum (as observed) to 260 nm [24-26]. Fig. 4.12 shows that virtually no absorption was recorded by the PDA detector at wavelengths > 225 nm. This was presumably due to the low molar absorptivity at longer wavelengths.
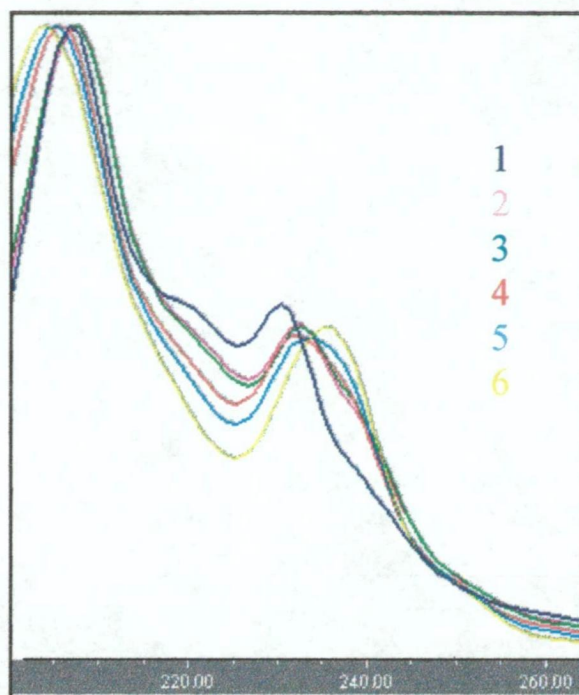
Fig. 4.11: Normalised spectra of Cu(I)-cyanide peak maxima in eluents containing various NaCN concentrations. These spectra were obtained with the PDA detector. All the eluents were prepared with 20% acetonitrile, 5 mM TBAOH and buffered to pH 8 with H_3PO_4. The spectrum labeled (1) was obtained in an eluent containing no added NaCN. The spectra labeled (2) to (6) were obtained in eluents that contained 10, 20, 40, 80 and 200 μM NaCN respectively.
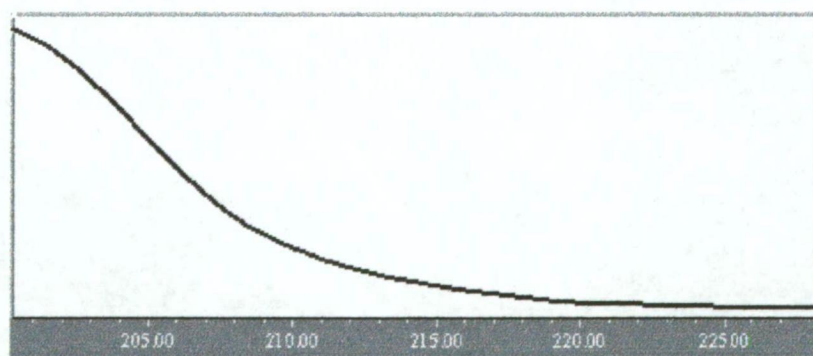
Fig. 4.12: Normalised spectrum of a Ag(I)-cyanide peak. The chromatographic conditions were the same as for Fig. 4.10. There was no change in the normalised spectra between the six eluents.

The six eluents mentioned above each contained 20% acetonitrile and 5 mM TBAOH neutralised to pH 7.95±0.05 with H_3PO_4. This series of eluents contained the same acetonitrile concentration (20%) as the eluents developed at Rothsay. For comparison, the Cu(I) and Ag(I) standards were also analysed in an eluent containing 25% acetonitrile, 5 mM Low UV PIC A. No cyanide was added to this eluent. There were considerable chromatographic differences between the eluents as shown in Figs. 4.13-4.15 and Table 4.2. The most pronounced differences occurred between the eluents containing no added cyanide and 10 μM NaCN, as well as between the two eluents containing no added cyanide and containing either 20% or 25% acetonitrile. It was assumed at the time of the PDA study that the latter differences were due to the variation in acetonitrile concentration between these two eluents. However, later work in this project (see Chapter five) found that the nature and concentration of the counter anion(s) also exerted a considerable effect on both the peak shape, retention time and retention order of the metallo-cyanide complexes. Consequently, some of the differences noted between the two eluents containing no added cyanide were undoubtedly due to the difference in counter anions in these eluents, arising from the different ion interaction reagents used.
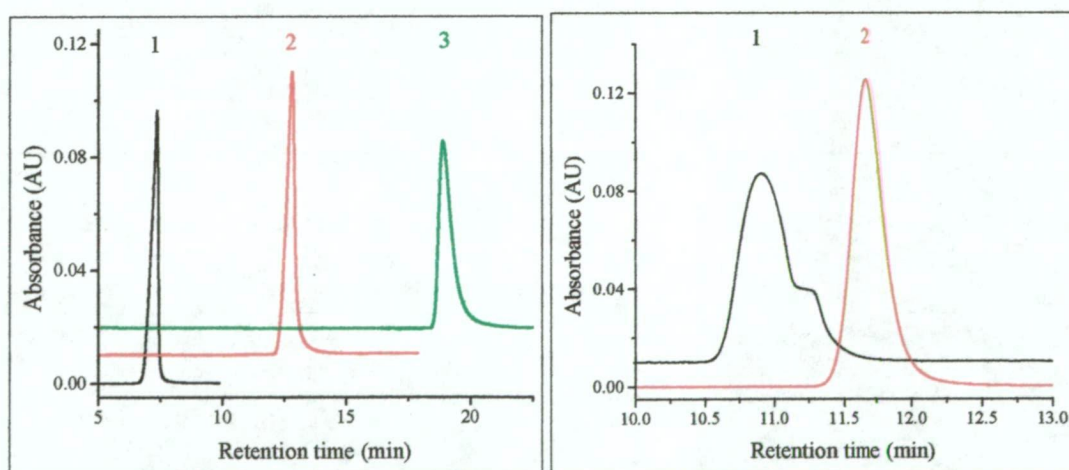
Fig. 4.13: Examples of chromatograms extracted from the PDA study. (a) (LHS) Cu(I)-cyanide peaks in eluents containing (1) 0, (2) 40 μM and (3) 200 μM cyanide. Cu(I) chromatograms extracted at 208 nm. (b) (RHS) Ag(I)-cyanide peaks in eluents containing (1) 0 and (2) 200 μM cyanide. Ag(I) chromatograms extracted at 200 nm. Eluents contained 20% acetonitrile, 5 mM TBAOH, neutralised to pH 7.9 with H_3PO_4. Chromatograms offset for clarity.

[NaCN] in eluent (μM)	Cu(I) standards			Ag(I) standards		
	Rt (min)	Peak asymmetry	Peak purity	Rt (min)	Peak asymmetry	Peak purity
0	7.56	0.16	1.09	11.00	1.93	1.62
10	11.31	0.39	1.09	11.59	1.43	1.15
20	12.90	0.59	1.11	11.91	1.42	1.35
40	15.1	1.53	1.13	12.06	1.42	1.27
80	18.39	1.77	1.21	12.85	1.42	1.27
25% MeCN, 5mM PIC A	4.12	0.57	1.04	5.50	1.66	1.31

Table 4.2 : Data collected from the PDA study. The mean value of each parameter obtained for the series of Cu(I) and Ag(I) cyanide standards analysed with each eluent is shown. Peak asymmetry values are reported for 10% peak height. Peak purity data were calculated by the Waters Millennium PDA software. Apart from the last eluent, all the eluents contained 20% acetonitrile and 5 mM TBAOH. The eluents containing TBAOH and various concentrations of NaCN were neutralised to pH 7.95 ± 0.05 with H_3PO_4. No NaCN was added to the last eluent.
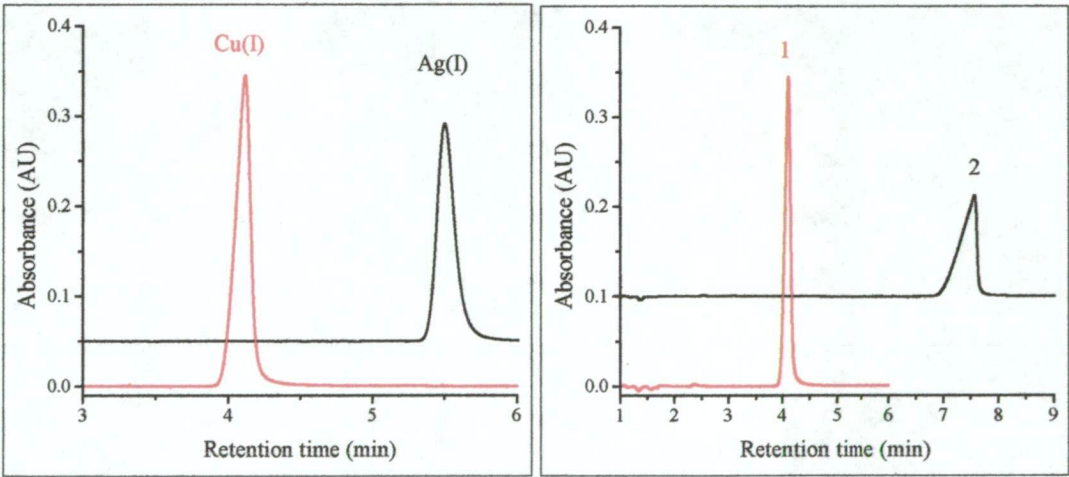
Fig. 4.14 (LHS): Chromatograms of Cu(I) and Ag(I) cyanide complexes obtained with an eluent containing 25% acetonitrile and 5 mM Low UV PIC A. Cu(I) and Ag(I) chromatograms extracted from the PDA study at 208 and 200 nm, respectively. Note the more Gaussian shape of the Ag(I) peak. Chromatograms offset for clarity.

Fig. 4.15 (RHS): Comparison of Cu(I) chromatograms extracted from the PDA study at 208 nm with eluents containing either **(1)** 25% acetonitrile and 5 mM Low UV PIC A or **(2)** 20% acetonitrile and 5 mM TBAOH, neutralised to pH 7.95±0.05 with H_3PO_4. Chromatograms offset for clarity.

The chromatogram of the Ag(I) cyanide complex was markedly different in the eluent containing 20% acetonitrile, TBA-phosphate and no added cyanide as shown in Fig. 4.13(b). The shoulder peak in this chromatogram disappeared in all the other eluents. It is interesting to note that this peak had the highest peak purity value parameter of all the Cu(I) and Ag(I) peaks, indicating an impurity in this peak (Table 4.2). However, normalised spectra from different parts of this peak were identical when subjected to visual inspection.

The effect of cyanide concentration on the Cu(I) peak in the series of six eluents containing 20% acetonitrile and TBA-phosphate was very pronounced (Fig. 4.13(a)). The effect on retention time was much greater than with eluents containing 25% acetonitrile and 5 mM Low UV PIC A (Fig. 4.9 and Table 4.1). It was also noted that in the eluent containing 20% acetonitrile and TBA-phosphate and no added cyanide, that a small peak eluted near the void volume displayed the Cu(I)-cyanide spectrum, thereby indicating that some Cu(I)-cyanide complex was eluted very early. The reason for this was uncertain. However all the eluents containing cyanide and the eluent containing 25% acetonitrile and 5 mM Low UV PIC A did not display this phenomenon.

There was a significant difference in the peak shape and retention time of the Cu(I) complex between the two eluents containing no added cyanide (Fig. 4.15). There was however only a very slight difference in the normalised spectra of the Cu(I) peak between these eluents as shown in Fig. 4.16.

It should be mentioned in finishing this section that the PDA study was conducted over a limited time at the Waters laboratory in Sydney. Unfortunately, after reviewing the results and noting the questions raised above, it was not possible to gain access to the PDA detector at a later time. However, while the PDA study provided strong evidence that cyanide added to the eluent resulted in the elution of different Cu(I)-cyanide complexes, it was not possible to obtain quantitative data regarding the nature of the eluted complexes. Consequently, all further studies concerning the nature of the eluted Cu(I) species were conducted using the PCR detection system.
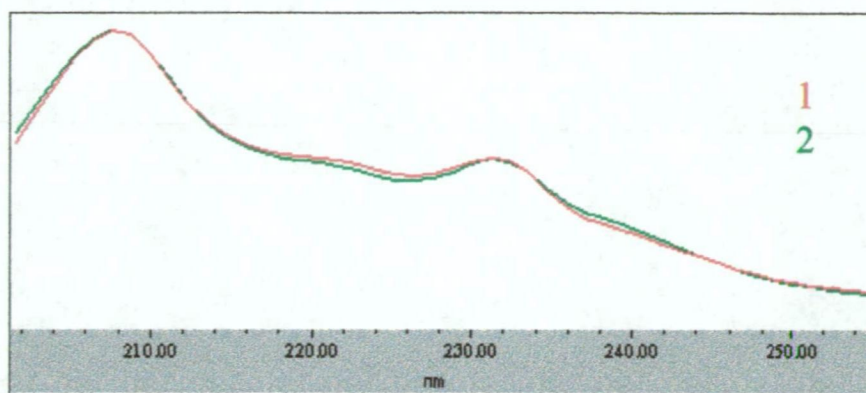
Fig. 4.16: Comparison of Cu(I) spectra with eluents containing either **(1)** 25% acetonitrile and 5 mM Low UV PIC A or **(2)** 20% acetonitrile and 5 mM TBAOH, neutralised to pH 7.95±0.05 with H_3PO_4.

4.3.4 Improvements to the PCR detection system

The first step in the PCR reaction involves the chlorination of cyanide to form cyanogen chloride. This is a very rapid reaction [27-29] and the cyanogen chloride produced subsequently undergoes rapid hydrolysis in the presence of a chlorination reagent. This hydrolysis is base catalysed and accelerated in the presence of excess chlorine [27, 30]. Consequently, to avoid loss of CNCl, it is important that the residence time in the first reactor is small and that the concentration of the chlorinating reagent is not excessive. N-chlorosuccinimide (NCS) was selected as the chlorination reagent for this work since it has been reported that this reagent can be stabilised by the addition of a ten-fold excess of succinimide [31]. However, the results obtained did not show the expected degree of stability reported for the NCS reagent. Alternative chlorination reagents, (hypochlorite and chloramine-T) were examined but were not significantly more stable than the NCS reagent. In addition, hypochlorite was found to have a detrimental effect on the pump seals, while the chloramine-T reagent was not soluble over the range of pH values required for the PCR system. It was therefore decided to continue using the NCS reagent. In order to reduce changes in the NCS reagent, the reagent was prepared freshly every 1-2 days and the NCS reagent bottle was shielded from light and kept in an insulated container packed with ice.

An attempt was made at Rothsay to use the data for thiocyanate from the UV detector as an internal standard for the PCR detector. However, it was found that the derivatisation of thiocyanate varied to a greater extent than for cyanide thereby preventing its use for the this purpose. Several reports exist in the literature concerning the derivatisation of thiocyanate with the König reaction [32-34]. All these studies used chloramine-T as the chlorination reagent. The oxidation of thiocyanate with chloramine-T has been shown to be pH dependent and requiring over 1 hr for complete oxidation [34, 35].

An investigation of the effect of the reaction time and temperature on the chlorination step in the PCR system was conducted with the N-chlorosuccinimide (NCS) reagent. The results shown in Fig. 4.17 revealed that a very long reaction time at 40°C was required for complete derivation of thiocyanate. It should be noted that these reactions times would result in substantial losses of CNCl for the reasons mentioned above. Consequently, it would appear probable that some of the CNCl formed during the chlorination of thiocyanate would have been further oxidised. This proposal was supported by the observation that the absorbance produced when thiocyanate was derivatised was less than for an equimolar concentration of cyanide. The chlorination reaction conditions used for this comparison were different for each species and were those that produced an optimal response for each species. Thus a reaction temperature of 40°C and a reaction time of 90 sec was used for thiocyanate, while ~15°C and ~6 sec was used for cyanide. The shorter reaction time and lower reaction temperature for cyanide were used to prevent oxidation of CNCl.

Consequently, PCR detection conditions optimal for either cyanide or thiocyanate would not be suitable for both analytes. For this reason, it was decided to concentrate on optimisation of the PCR conditions for cyanide. It should be noted in passing that the difference in the reaction rates for thiocyanate and cyanide has been used to develop a König reaction method capable of discriminating between cyanide and thiocyanate [34].
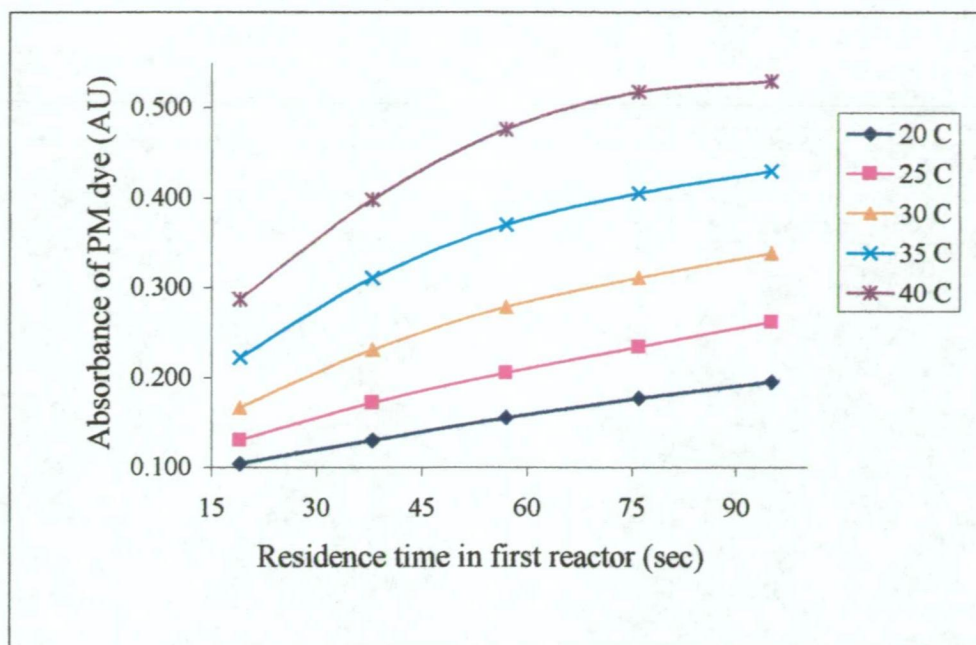
Fig. 4.17: Effect of chlorination reaction time and temperature on the derivatisation of thiocyanate by the König reaction. The effects were determined by the absorbance of the intermediate polymethine (PM) dye, monitored at 515 nm.

It was found that both the residence time and reaction temperature of the second reactor in the König PCR scheme had a significant effect on the formation of the polymethine (PM) dye product as shown in Fig. 4.18. The PCR reagent concentrations used in this study were similar to those used at Rothsay. The spectra of the PM dye were obtained by repeating the analysis at the various wavelengths (Fig. 4.18). This study showed that a maximum reaction temperature of 40°C was suitable for the König PCR. A decrease in the absorbance of the PM dye was observed when the reaction temperature was further increased to 45°C. This temperature dependence was in close agreement with the findings reported by other workers [36, 37] when barbituric acid was used as the coupling reagent. It should be noted that other workers have reported a maximum temperature of 60°C for similar König reagents [38, 39]. Tanaka *et al.* [38] also noted that the cyanide calibrations became convex above 40°C.
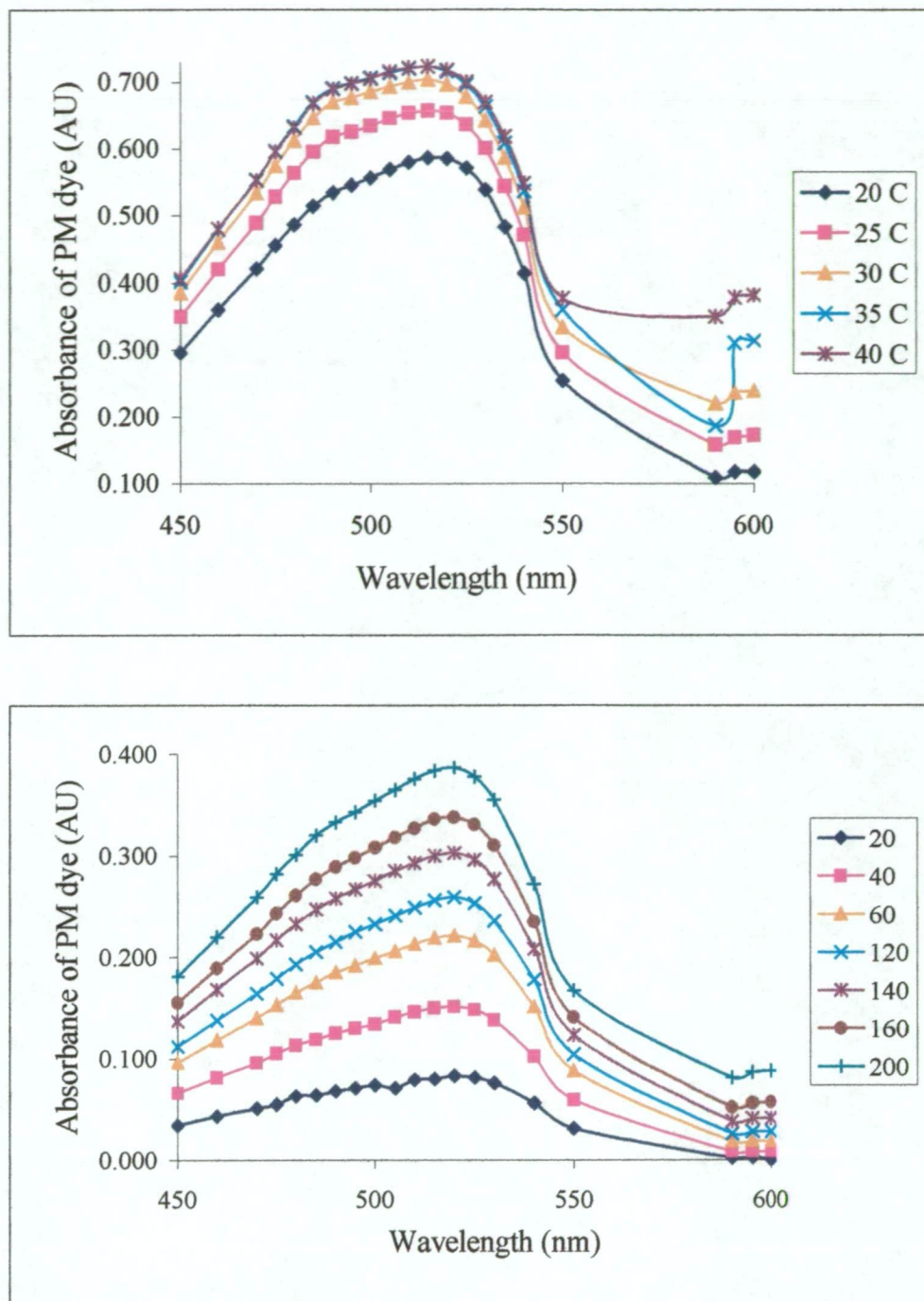
Fig. 4.18: Effect of **(a)** (Top) reaction temperature and **(b)** (Bottom) reaction time on the derivatisation of cyanide by the König reaction. The reaction temperature was set at 20°C for the variation in reaction times, while the reaction time was set at 200 sec for the variation in reaction times temperatures. The effects were determined by the absorbance of the intermediate polymethine (PM) dye, monitored at different wavelengths.

The NCS reagent used in Chapter three was prepared as described by Lambert *et al.*. [31], i.e., an aqueous solution containing 0.1 % NCS and 1.0% succinimide. Several authors have noted that the König reaction is pH dependent. This problem has been overcome by use of a phosphate buffer to prevent sample composition affecting the final absorbance. In the PCR detection system developed in Chapter three, a phosphate buffer was included with the INA/BA reagent. In addition, the sample would have also undergone some buffering due to the presence of a phosphate buffer in the ion interaction reagent (Low UV PIC A). To further improve the buffering capacity of the PCR detection system, a phosphate buffer (pH 2.1) was added to the NCS reagent. Furthermore, literature reports suggested that the reaction of chloramine-T with thiocyanate was catalysed at low pH or by the use of $FeCl_3$ (which would also lower the pH) [34, 40]. The use of a phosphate buffer was not satisfactory due to formation of a precipitate when the NCS reagent was placed in a refrigerator (< 4°C). In addition, there did not appear to be an increase in the derivatisation of thiocyanate with the low pH phosphate buffer. A succinate buffer was then used with the NCS reagent. It was immediately observed that the succinate buffer (pH 5.6) in the NCS reagent enabled the complete derivatisation of the cyanide complexed to the eluted Cu(I)-cyanide peak. This was a major breakthrough as it allowed a cyanide mass balance to be used to determine changes in composition of the eluted Cu(I) complex. This will be discussed in the following section.

The reason for the effect observed with the succinate buffer was probably due to complexation of Cu(II) (with succinate) liberated by the chlorination of the Cu(I)-cyanide species. It has been reported previously that the addition of EDTA to a similar König reagent (pyridine/pyrazolone) was necessary in order to prevent interference from Cu(II) in the colour formation [41]. The stability constant for the Cu(II)-succinate complex ($K_1 = 10^{3.3}$) supports this proposal [42]. However it should be noted that one of the examiners of this thesis questioned whether the relatively low value for the stability constant for the Cu(II)-succinate complex would be the reason for the effect of the succinate buffer.

The effect of reagent selection and reagent concentration in the second PCR reagent was then examined. An important paper by Kuban [43], published after the Rothsay

---

field trial had been completed, reported on a series of investigations dealing with this issue. Kuban found that a large concentration of pyridine or its analogue, isonicotinic acid, and a low concentration of the coupling reagent were required for rapid formation of a relatively stable intermediate PM dye. This was in contrast to earlier reports that had used high concentrations of the coupling reagent to achieve rapid formation of the intermediate PM dye [39, 44]. An advantage of the approach taken by Kuban was that these reagent concentrations were considerably more stable than those reagents using high concentrations of the coupling reagent. Kuban reported that the optimum reagent combination consisted of 240 mM isonicotinic acid (INA) and 1.2 mM pyrazolone (PZ). After several concentrations of the INA and PZ reagents were tried (including the optimum concentrations reported by Kuban), it was decided that the INA/PZ reagent was unsuitable for this project for two reasons:

(i)   The INA/PZ reagent was not very stable even when stored in a refrigerator ($< 4^\circ C$). Noticeable colour changes were observed within one day of preparation of the reagent. By contrast, an INA/BA reagent prepared with similar concentrations of INA and BA and stored under the same conditions was stable for approximately one month.

(ii)   The INA/PZ is very sensitive, which is not suitable for the relatively high cyanide concentrations in the samples examined in this project.

4.3.5   Elucidation of the nature of the eluted Cu(I)-cyano complexes using PCR

In order to further explore the nature of the eluted complexes, modifications were made to the PCR conditions to ensure that all cyanide entering the reactor, either as free or complexed cyanide, would be derivatised. In this way, quantitative measurements of the eluted cyanide species would be possible. Various reaction conditions in a flow-injection mode (i.e. the separation column was removed for these analyses) were tested on three 1 mM Cu(I)standards with R values of 3, 4 and 5. The results obtained from this study are shown in Table 4.3. The concentrations of cyanide present in the standards were determined from calibration plots prepared with NaCN standards. The implicit assumption in this procedure is that the

derivatisation of cyanide was equivalent for the NaCN standards and Cu(I)-cyanide standards. This is particularly relevant to the chlorination reaction for the reasons discussed above with respect to the derivatisation of thiocyanate. Due to the on-column dissociation of the Cu(I)-cyanide complexes, it was realised that the eluted Cu(I) peak would have an R value between 2 and 4. Consequently, the results obtained for the Cu(I)-cyanide standards with R values of 3 and 4 were considered more important than for the standard with R value of 5. For this reason, the conditions that were selected (shown in red in Table 4.3) used a very short reaction time for the chlorination reaction (4 s), with the NCS reagent pH controlled at 5.6. The extent of derivatisation of the Cu(I)-cyanide standards was not significantly altered when the temperature of the first reaction coil was increased from ambient (15±5°C) to 40°C. Thus, for convenience, both reaction coils were placed in the column heater at 40°C. The second (INA/BA) reagent contained 0.3 M INA, 3 mM BA and 2% EDTA.

The following points should also be noted:

(i)   The succinimide concentration in the N-chlorosuccinimide/succinimide reagent was increased to a 20-fold excess and the combined reagent was kept in the dark at less than 4°C.

(ii)   EDTA was added to the INA/BA reagent to further prevent interference by the liberated Cu(II). There was a slight improvement in the performance of the INA/BA reagent when EDTA was present. It was found that the optimal EDTA concentration was 2%.

(iii)   Addition of Na_2EDTA to the INA/BA reagent resulted in the formation of a precipitate when the reagent was stored in a refrigerator. Consequently, the INA/BA reagent were containing EDTA were prepared without a phosphate buffer.

(iv)   The residence time in the reactors was calculated from the length of the reaction coils. The length of the first and second reaction coils was 1.4 m and 15 m, respectively.

NCS reagent pH and NCS reaction conditions			INA / BA reagent composition			[CN] found in 1mM Cu(I) standards		
pH	Temp (°C)	Reaction time (s)	[INA] (M)	[BA] (mM)	EDTA (%)	R=3 (mM)	R=4 (mM)	R=5 (mM)
5.03	Amb	20	0.2	4	0	2.76	3.82	4.65
5.03	Amb	20	0.25	3	0	2.94	3.85	4.69
5.03	Amb	20	0.2	5	0	2.73	3.78	4.62
5.03	Amb	20	0.2	5	1	2.86	3.88	5.02
5.03	Amb	20	0.3	3	0	2.78	3.83	4.68
5.66	Amb	20	0.3	3	0	2.86	3.8	4.65
5.66	Amb	20	0.3	3	2	3.23	4.14	4.88
5.66	Amb	4	0.3	3	2	3.06	3.99	4.73
6.13	Amb	4	0.3	3	2	3.03	3.91	4.8
6.13	40	4	0.3	3	2	3.00	3.90	4.66
6.13	40	20	0.3	3	2	3.14	4.09	4.86
6.13	40	40	0.3	3	2	3.16	4.12	4.93
6.13	40	40	0.3	3	4	3.11	4.15	5.15
6.13	40	40	0.3	3	0	3.18	4.10	4.94
5.03	Amb	20	0.2	4	0	2.76	3.82	4.65
5.03	Amb	20	0.2	5	0	2.73	3.78	4.62
5.03	Amb	20	0.2	5	1	2.86	3.88	5.02
5.66	Amb	20	0.3	3	0	2.86	3.80	4.65
5.66	Amb	20	0.3	3	2	3.23	4.14	4.88
5.66	Amb	4	0.3	3	2	3.06	3.99	4.73
6.13	Amb	4	0.3	3	2	3.03	3.91	4.8
6.13	40	4	0.3	3	2	3.00	3.90	4.66
6.13	40	20	0.3	3	2	3.14	4.09	4.86
6.13	40	40	0.3	3	2	3.16	4.12	4.93
6.13	40	40	0.3	3	4	3.11	4.15	5.15
6.13	40	40	0.3	3	0	3.18	4.10	4.94

Table 4.3: PCR reaction conditions for the derivatisation of three 1 mM Cu(I)-cyanide standards with R values of 3, 4 and 5. Amb. = Ambient temperature (15±5°C). The pH of the NCS reagent was controlled with the succinate buffer. The NCS and succinimide concentrations were maintained at 0.1% and 2.0%, respectively, for all these measurements. The temperature of the second reactor (into which the INA/BA reagent was introduced) was maintained at 40°C for all these measurements. The cyanide concentration found for each Cu(I) standard was expressed in mM units.

A series of three 1 mM Cu(I)-cyanide standards with R values of 3, 5 and 7 were analysed with three eluents containing 25% acetonitrile, 5 mM PIC A and 100 µM, 50 µM or no added NaCN. The PCR detection system incorporated the modifications described above. The cyanide concentrations (from the PCR detector) in the cyanide and Cu(I)-cyanide peaks were determined from cyanide calibration plots. The results are shown in Table 4.4. In the eluent without added NaCN, the mean cyanide concentration in the Cu(I)-cyanide peak was 2.53 and showed virtually no change with the R value of the injected standards (which is supported by the constancy of the Cu(I)-cyanide peak in Fig. 4.4(b)). When no cyanide was present in the eluent, the sum of the cyanide concentrations in the cyanide and Cu(I)-cyanide peaks was very similar to the total cyanide concentration in each of the standards. However, when cyanide was present in the eluent, increased complexation of the Cu(I) caused the observed levels of total cyanide in the two peaks to exceed that in the injected standards. The mean cyanide concentration in the Cu(I)-cyanide peak increased as cyanide was added to the eluent, reaching 3.35 mM for an eluent containing 100 µM cyanide. For each concentration of cyanide in the eluent, the amount of cyanide in the Cu(I)-cyanide peak remained almost constant. Since each standard contained a total copper concentration of 1 mM, the mean values of cyanide concentration in the Cu(I)-cyanide peak shown in Table 4.4 are also the average R values in the eluted Cu(I)-cyanide peak. The observed increase in R for the Cu(I)-cyanide peak with addition of cyanide to the eluent is in accordance with the retention model discussed earlier.

Two additional points should be noted. The calculated total complexed cyanide concentrations at pH 12 (aqueous only) and pH 8 (25:75 $MeCN:H_2O$) for this standard are 2.933 and 2.693 mM (Fig. 4.8). The difference between the two sets of conditions is 0.24 mM. This is the calculated amount of cyanide that would be released when the solution was changed from pH 12 (aqueous only) to pH 8 (25:75 $MeCN:H_2O$).

[NaCN] in eluent	R = 3 [CN] (mM)			R = 5 [CN] (mM)			R = 7 [CN] (mM)			Cu(I) peak
(µM)	CN peak	Cu(I) peak	Total	CN peak	Cu(I) peak	Total	CN peak	Cu(I) peak	Total	Mean
0	0.45	2.54	2.99	2.45	2.51	4.96	4.45	2.54	6.99	2.53
50	0.14	3.06	3.20	2.37	2.98	5.35	4.35	3.06	7.41	3.03
100	0.00	3.41	3.41	2.05	3.30	5.35	4.14	3.35	7.49	3.35

Table 4.4: Cyanide concentration in the cyanide and Cu(I)-cyanide peaks of three 1 mM Cu(I)-cyanide standards with R values of 3, 5 and 7. Eluents contained 0-100 µM NaCN. PCR conditions as described in the text. PCR detection wavelength was 515 nm.

The observed cyanide peak for this standard in an eluent without added cyanide was 0.45 mM, while the observed R value of the eluted Cu(I) peak was 2.54 (Table 4.4). This difference between the calculated and observed results indicates that more dissociation occurred than was predicted by the change from pH 12 to pH 8. This is in accordance with the proposed on-column dissociation due to the retention differences between the uncomplexed cyanide and the Cu(I)-cyanide complexes. It can also be noted that the smallest cyanide addition had the largest effect in both the PDA and PCR studies. This is in agreement with the calculated change in the average ligand number at low R values, as shown in Fig. 4.7.

A further prediction of the retention model was that in the absence of cyanide in the eluent, different R values should be observed in the front and back segments of the Cu(I)-cyanide peak. Further, this difference should be minimised when cyanide was added to the eluent. To investigate these hypotheses the Cu(I)-cyanide peaks in both the UV and PCR chromatograms for the 1 mM (R = 3) standards obtained above (Table 4.4) were segmented at the peak maximum, as shown in Fig. 4.19. The cyanide and Cu(I)-cyanide concentrations in the front and back portions of each peak were then calculated from cyanide (PCR detector) and Cu(I)-cyanide (UV detector) calibration plots. The results are shown in Table 4.5, from which it is apparent that there was a significant change in the R value over the Cu(I)-cyanide peak in the first

two eluents and that the peak was homogenous with 100 μM NaCN in the eluent. These results provide quantitative evidence that the Cu(I)-cyanide complexes undergo partial dissociation during the chromatographic process in an eluent without added cyanide, leading to peak asymmetry.
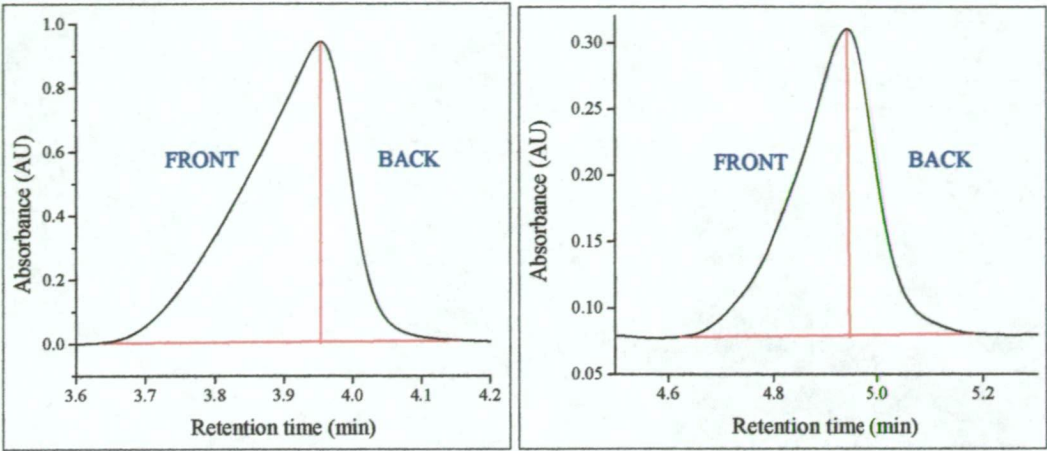
Fig. 4.19: UV (LHS) and PCR (RHS) detector chromatogram of 1.0 mM Cu(I)-cyanide standard (R = 3), illustrating the FRONT and BACK portions of the Cu(I)-cyanide peak. Eluent : 25% acetonitrile, 5 mM Low UV PIC A.

[NaCN] in eluent (μM)	[CN]:[Cu] ratio	
	Front of Cu(I) peak	Back of Cu(I) peak
0	2.28	3.10
50	2.85	3.42
100	3.51	3.50

Table 4.5: [CN]:[Cu] ratio in the front and back of the Cu(I)-cyanide peaks resulting from the injection of 1 mM Cu(I)-cyanide standard (R = 3) in eluents containing 0 - 100 μM NaCN.

4.4 References

1   P. R. Haddad and C. Kalambaheti, *Anal. Chim. Acta*, 250 (1991) 21.

2   A. Padarauskas, I. Stul' gene, R. Kazlauskas and O. Petrukhin, *Zh. Anal. Khim.*, 46 (1991) 1169.

3   E. O. Otu, C. W. Robinson and J. J. Byerley, *Analyst*, 117 (1992) 1145.

4   Pohlandt C., *S. Afr. J. Chem.*, 38 (1985) 110.

5   L. Giroux and D. J. Barkley, *Can. J. Chem.*, 72 (1994) 269 .

6   C. Pohlandt ; MINTEK Rep., no. 3, pp. 47-52, 1986.

7   H. M. N. H. Irving and A. D. Damodaran, *Anal. Chim. Acta*, 53 (1971) 267.

8   F. D. Snell, *Photometric and Fluorometric Methods of Analysis (Non Metals)*; Wiley Interscience, New York, 1981.

9   R. A. Penneman and L. H. Jones, *J. Chem. Physics*, 24 (1956) 293.

10   C. Kappenstein, R. Hugel, A. J. P. Alix and J. L. Beaudoin, *J. Chim. Phys. Phys.-Chim. Biol.*, 75 (1978) 427.

11   A. G. MacDiarmid and F. H. Norris, *J. Am. Chem. Soc.*, 76 (1954) 4222.

12   K. Kurnia, D. E. Giles, P. M. May, P. Singh and G. T. Hefter, *J. Coord. Chem.*, 38 (1996) 183.

13   M. T. Beck, *IUPAC : Pure and Applied Chemistry*, 59 (1987) 1704.

14   K. Kurnia, D. E. Giles, P. M. May, P. Singh and G. T. Hefter, *Talanta*, 43 (1996) 2045.

15   B. K. Glod, *Chem. Anal. (Warsaw)*, 39 (1994) 399.

16   R. Shantz and J. Reich, *Hydrometallurgy*, 3 (1978) 99.

17   A. D. Stuart and R. Van den Heuvel, *Int. J. Environ. Anal. Chem.*, 49 (1992) 171.

18   E. A. Simpson and G. M. Waind, *J. Chem. Soc.*, 1958 (1958) 1746 .

19   J. H. Baxendale and D. T. Westcott, *J. Chem. Soc.*, 1959 (1959) 2347.

20   C. Kappenstein and R. Hugel, *Rev. Chim. Miner.*, 6 (1969) 1107.

21   J. C. Pierrard, C. Kappenstein and R. Hugel, *Rev. Chim. Miner.*, 8 (1971) 11.

22   C. Kappenstein and R. Hugel, *J. Inorg. Nucl. Chem.*, 36 (1974) 1821.

23 R. W. Frei and K. Zech In Journal of Chromatography Library; Elsevier:
Amsterdam, 1988; Vol. 39A.

24 J. Brigando, *Bull. Soc. chim.*, 2 (1957) 503.

25 J. Perumareddi, A. Liehr and A. Adamson, *J. American Chemical Society*, 85
(1963) 249.

26 D. K. Kalani and M. A. Matin, *Lab. Pract.*, 18 (1969) 275.

27 A. I. Gladysheva, A. I. Gutman and I. V. Saramukova, *Uch. Zap. Tsent. Nauch.-
Issled. Inst. Olovyannoi Prom.*, 2 (1969) 3.

28 D. S. Mahadevarappa and B. T. Gowda, *Indian Journal of Chemistry*, 17A (1979)
484.

29 C. M. Gerritsen and D. W. Margerum, *Inorg. Chem.*, 29 (1990) 2757.

30 P. L. Bailey and E. Bishop, *J. Chem. Soc. Dalton Transactions*, 1973 (1973)
912.

31 J. L. Lambert, J. Ramasamy and J. V. Paukstelis, *Anal. Chem.*, 47 (1975) 916.

32 R. I. Botto, J. H. Karchmer and M. W. Eastwood, *Anal. Chem.*, 53 (1981) 2375.

33 S. Nagashima, *Anal. Chem.*, 55 (1983) 2086.

34 S. Nagashima, *Anal. Chem.*, 56 (1984) 1944.

35 D. S. Mahadevappa, B. T. Gowda and N. M. M. Gowda, *Z. Naturforsch.*, 34B
(1979) 52.

36 A. Rios, M. D. Luque de Castro and M. Valcarcel, *Talanta*, 31 (1984) 673.

37 H. C. Ma and J. F. Liu, *Anal. Chim. Acta*, 261 (1992) 247.

38 A. Tanaka, K. Mashiba and T. Deguchi, *Anal. Chim. Acta*, 214 (1988) 259.

39 J. A. Sweileh, *Anal. Chim. Acta*, 220 (1989) 65.

40 J. Epstein, *Anal. Chem.*, 19 (1947) 272.

41 S. Yasuda, K. Tanihara, K. Tanai and H. Kakiyama, *Bunseki Kagaku*, 31 (1982)
545.

42 G. S. Sillen, *Stability Constants of metal-ion complexes*; The Chemical Society:
London, 1964.

43 V. Kuban, *Anal. Chim. Acta*, 259 (1992) 45.

44 A. Sharma and Thibert, *Microchimica Acta*, 1 (1985) 357.

CHAPTER FIVE

Development of methods for use at the Telfer Gold Mine

5.1 Introduction

A series of field trials was conducted at the Telfer Gold Mine over a one-year period. The results and methodology developed at Telfer are described in the next three chapters. This chapter is concerned with the determination of cyanide, thiocyanate and the metallo-cyanide complexes in the CIL and dump leach operations. Chapter six continues this work with the development of HPLC methodology suitable for the routine determination of the CN:Cu mole ratio in samples obtained from a new process under development at Telfer. These samples contained high concentrations of Cu(I)-cyanide complexes and presented some interesting analytical challenges. This development was based on the initial work at Rothsay and the subsequent studies on the Cu(I)-cyanide complexes described in Chapter four. Chapter seven is concerned with the development of methods for the analysis of cyanate in the presence of large concentrations of Cu(I)-cyanide complexes.

It should be stressed that the work at Telfer was undertaken following significant developments and improvements to the HPLC methods since the Rothsay field trial. In addition, an Australian Research Council (ARC) Collaborative Grant (awarded to Professor Paul Haddad [1]), provided funding for the project at Telfer. The aim of this ARC funded project was to continue development of a HPLC system suitable for controlling the gold cyanidation process. The two industrial partners in this ARC Collaborative grant were Newcrest Mining and Waters Australia.

The Telfer Gold Mine is owned and operated by Newcrest Mining. At several stages in its 21-year history, Telfer has been either the first or the second largest pure gold mine in Australia, with a total gold production approaching 5 million troy ounces (141 tonnes) [2]. Telfer is located in the Great Sandy Desert, Western Australia and is one of the most geographically isolated mining centres in Australia. The nearest town, Marble Bar, is over 300 km distant by road, while Perth (the capital of Western Australia) is more than 1900 km distant by road. Incidentally, Marble Bar

holds the official record as the hottest place in Australia, with a daily maximum temperature exceeding 100°F (37.8°C) for a six-month period in the 1930's. The daily temperature at Telfer can vary from 5-20°C in winter to 25-50°C in summer. Over a 20 year period, the average annual rainfall at Telfer was under 300 mm, with an average of 39 rain days per year [3]. Telfer's water is supplied completely from underground reserves. Fortunately, this water is potable with relatively low Total Dissolved Solids (TDS) of approximately 2000 ppm [2]. This compares very favourably to gold mines located in the Goldfields region (near Kalgoorlie) in Western Australia, where TDS values can exceed 100,000 ppm [4].

When the field trials mentioned in this thesis were conducted, staff and some families were permanently housed on-site. Since employees had three return trips to Perth per year, most employees were on site for periods of 3-4 months duration. It should be acknowledged that the tremendous support (both technical and social) provided by the laboratory staff and metallurgists on-site at the Telfer contributed to the overall success of this project. Since the field trials have been completed, Telfer has changed over to a fly-in/fly-out roster that allows staff rotations on at least a fortnightly basis. This has allowed families to move to Perth and reduced staff costs. The total number of people employed at the Telfer mining centre, including contractors, is about 800.

The geographical isolation and size of Telfer has enabled the development of a modern, air-conditioned laboratory. The majority of the analyses required by the mine are performed in this laboratory. Over 300,000 ore samples are assayed annually for gold and other elements (such as Cu and S), while the total number of analyses exceeds 1,000,000 per year. The most common ore assays are for gold, total copper, cyanide-soluble copper and total sulfur concentrations. The most common solution assays are for cyanide, pH, gold and copper concentrations.

A sophisticated Laboratory Information Management System (LIMS) is used to keep track of samples and analyses. To prevent errors and increase efficiency, each ore sample is bar-coded on entry to the laboratory. By use of hand-held scanners, each analytical result (eg. sample weight or AAS absorbance) is automatically entered into the LIMS database. The instrumentation in the main Telfer laboratory includes

two AAS instruments used mostly for either Cu or Au, an XRF instrument and a LECO sulfur analyser. Extensive quality control and quality assurance continually assesses the analytical accuracy of the laboratory results.

The majority of the ore mined at Telfer is obtained from open-cut mining operations. The higher grade ore obtained by open-cut mining is crushed and milled prior to treatment in a CIL plant. The lower grade ore obtained by open-cut mining is treated in dump leach operations. A schematic of the Telfer mine site is shown in Fig. 5.1. The Telfer dump leach operation handles approximately 10×10^6 tonnes of ore annually [5]. There are only low concentrations of thiocyanate and metallo-cyanide complexes in the "pregnant" effluent from the dump leach pads as there is very little mineralisation (and hence gold) in this low-grade ore. While only about 63% of the gold is recovered in the dump leach operation (compared to approximately 95-98 % in the CIL operation), the treatment costs of the dump leach operations are approximately only 20% that of the CIL operation. These low treatment costs allow low grade ore (Au concentration as low as 0.7 g/t) to be economically treated.

There are significant occurrences of cyanide soluble cupriferous minerals at Telfer. The most commonly occurring cupriferous mineral found in the open-cut operations at Telfer is chalcopyrite [$CuFeS_2$]. Chalcocite [Cu_2S] and malachite [$CuCO_3.Cu(OH)_2$] are also found in the ore body. There are gradual changes in the mineralogy at Telfer that is not defined by the above minerals. The major gangue minerals present at Telfer are quartz (commonly as sand grains) and clay minerals (kaolinite and sericite) and iron oxide ores. Typical concentration ranges (% by weight) of these gangue minerals are quartz (54-70 %), kaolin (6-27 %), sericite (5-11 %) and iron oxide ores (0-6 %) [3].

About 10 % of the ore mined at Telfer is obtained from underground operations. The underground ore contains relatively high concentrations of copper minerals (3-4 % Cu) and gold (15-20 g/t) [6]. This high grade ore is treated in a flotation plant to produce a concentrate that is transported by road to Port Hedland, for shipment to a smelter. Oxide copper ores (from both the open-cut and underground mining operations) are treated by Controlled Potential Sulfidisation (CPS) prior to flotation.
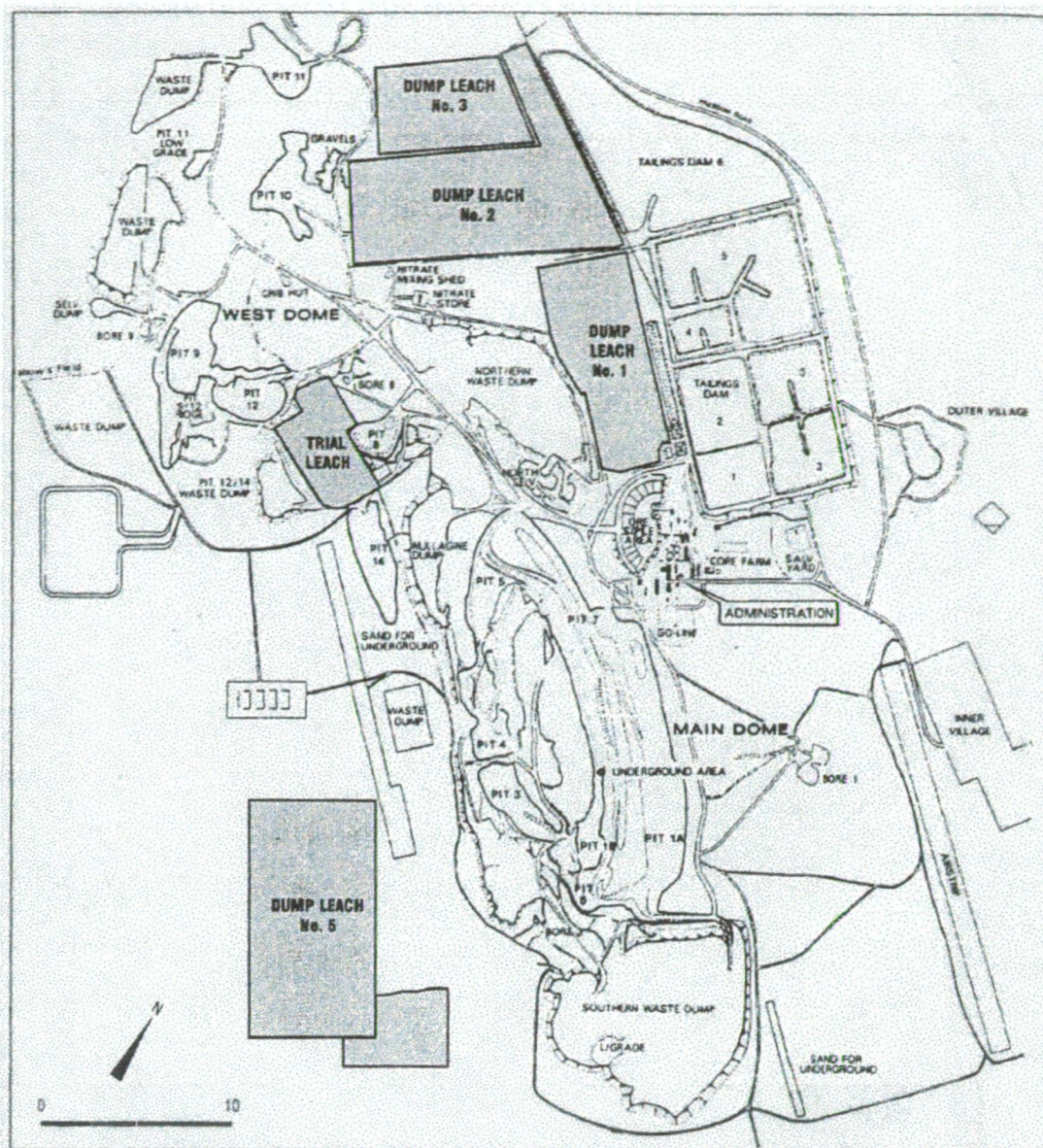
Fig. 5.1 : Schematic of Telfer mine site. Source : Fig. 1 of [5]

The copper and gold levels in the concentrate are approximately 25% and 100 g/t respectively [5]. The flotation tails (referred to as pyrite leach tails) contain copper minerals (~1.1%) and gold (5 g/t). The major copper minerals in the flotation tailings are chalcocite [Cu_2S] and cuprite [Cu_2O]. The pyrite leach tails are treated with excess cyanide prior to addition to the CIL circuit for recovery of [$Au(CN)_2$]⁻. The cyanide leachate obtained from the pyrite leach tails also contains considerable concentrations of thiocyanate and the cyanide complexes of Cu(I) and Fe(II). This will be discussed in the next chapter.

Due to the presence of copper minerals, it has become increasingly important for the Telfer operations to determine the amount of cyanide-soluble copper present in the ore prior to mining. At the moment, there are considerable regions of the Telfer ore body that cannot be treated with conventional cyanidation practices due to the abundance of cyanide-soluble copper minerals in these regions. The application of HPLC analytical methods to a new process suitable for leaching this high copper ore is dealt with primarily in the following chapter. It should be noted that some details of this leaching process and some results couldn't be reported in this thesis due to confidentiality agreements. However, these omissions should not detract from the analytical methodology reported in this thesis.

Prior to the first visit to Telfer, five samples were sent to the University of Tasmania (UTas) for analysis. These samples were also used to investigate improved eluent conditions for separation of the major components in the Telfer samples. These improvements to the eluent conditions were continued during the first visit to Telfer. An investigation into the optimum PCR conditions for the Telfer samples was also performed during the first visit to Telfer.

The cyano species that are of particular interest to the metallurgists at Telfer are cyanide, thiocyanate and the Cu(I) and Au(I)-cyanide complexes. The Fe(II) and Fe(III)-cyanide complexes are present in low concentrations (generally less than 2 ppm) in Telfer samples and are of minor interest. Cyanate is also of interest, especially during the cyanidation of Cu-bearing ores. The development of methods to enable the determination of cyanate in samples containing high concentrations of Cu(I)-cyanide complexes will be dealt with in Chapter seven.

5.2 Experimental

5.2.1 Instrumentation

The HPLC instrument has been described in previous Chapters and consisted of a Waters (Milford, MA, USA.) M510 isocratic HPLC pump, a Waters 717 auto-sampler, a Waters M486 variable wavelength absorbance detector and a PCR detection system. The PCR system consisted of two Eldex pumps, two stitched open

tubular reactors, a Waters column heater to maintain the reactors at a constant temperature (40 °C) and a photometric detector operated at 436 nm. The first reactor was a coil 1.5 m in length with an I.D. of 0.030 mm. The second reactor initially consisted of three 5 m coils with an I.D. of 0.030 mm, connected in series, but was later replaced with a single 5 m coil with an I.D. of 0.050 mm. The reaction coils were prepared using the method described in Chapter three. The PCR detector was a Waters M441 fixed wavelength absorbance detector operating at 436 nm.

5.2.2 Preparation of the eluents

All the reagents used in this work were obtained from Aldrich (Aldrich Chemical Co. Inc., Castle Hill, NSW, Aust.), unless stated otherwise. Acetonitrile was obtained either from Ajax Chemicals (Sydney, NSW, Australia) or from Merck (Kilsyth, Vic., Australia). Eluents were prepared with water either from a Milli-Q water purification system (Millipore, MA, USA) or from a Milli-RO water purification system. The ion-interaction reagent used in the eluents was either Low UV PIC A (Waters) or was prepared from tetrabutylammonium hydroxide (TBAOH), KH_2PO_4 and H_2SO_4. NaCN (0 –160 µM) was added to the eluents. The composition of the final eluent was 25:75 (v/v) acetonitrile:water, TBAOH (10 mM), KH_2PO_4 (10 mM), H_2SO_4 (5 mM) and NaCN (80 - 160 µM), adjusted to pH 8 with NaOH. All eluents were filtered (0.45 µm) and degassed under vacuum in an ultrasonic bath prior to use.

5.2.3 Preparation of the PCR reagents

The two PCR reagents were prepared as described below, filtered (0.45 µm) under vacuum prior to use each day, and stored in the dark at less than 4 °C.

Reagent 1 : N-chlorosuccinimide (0.15%, w/v) was added to a succinate buffer (0.1 M, pH 5.6) containing succinimide (3% w/v).

Reagent 2: The final reagent contained the sodium salts of isonicotinic acid (230 mM), barbituric acid (15.6 mM) and EDTA (54 mM) and was prepared by dissolving

the INA and BA in excess NaOH prior to the addition of Na_2EDTA. The final reagent pH was 7.2.

The Ni^{2+} reagent used for *in-situ* derivatisation of cyanide or by PCR was prepared from $Ni(NO_3)_2$ and $(NH_4)_2SO_4$.

5.2.4 Standard solutions

Cyanide standards were prepared from a 0.1 M stock solution of NaCN in 0.1 M NaOH. A Cu(I)-cyanide stock solution (0.1 M) was prepared from CuCN and NaCN in a 0.1 M NaOH solution, such that the CN:Cu mole ratio of this stock solution was 3.0. These solutions were kept alkaline to improve their stability. The copper concentration in the Cu(I)-cyanide stock solution was checked using AAS, while the cyanide concentration was checked by total cyanide distillation. Both the copper and cyanide concentrations were within 1% of expected values. The Cu(I)-cyanide standards used for analysis were prepared from the stock solutions of Cu(I)-cyanide and NaCN. Thiocyanate standards were prepared from a 0.1 M stock solution of KSCN. Both the NaCN and KSCN 0.1 M stock solutions were standardised potentiometrically with a standardised $AgNO_3$ solution. The $[Ni(CN)_4]^{2-}$ and $[Co(CN)_6]^{3-}$ standards were prepared from their respective potassium salts $K_2[Ni(CN)_4]$ and $K_3[Co(CN)_6]$. These potassium salts had been prepared at the University of NSW by Kalambaheti using published methods [7]. Other metallo-cyanide complexes were used as received.

5.2.5 Operation of the instrument

Separations were performed on either a 50 x 3.9 mm ID or a 150 x 3.9 mm ID Waters Nova-Pak C-18 analytical cartridge column fitted with a Waters guard column. The eluents were pumped through the column at a flow-rate of 1.0 ml/min. The UV absorbing metallo-cyanide complexes were detected immediately after elution from the column with a variable wavelength detector set at an appropriate wavelength between 205 nm and 245 nm. The wavelength was changed to adjust the sensitivity of the detector.

The PCR comprised three reactions and two reagent additions. The first reagent contained a chlorinating reagent (N-chlorosuccinimide) to enable formation of CNCl. A pyridine derivative (isonicotinic acid) in the second reagent combined with the CNCl to form an aldehyde. An *in-situ* condensation reaction then occurred between the aldehyde and barbituric acid to form an intermediate polymethine dye product with a λ_{max} of 515 nm. This polymethine dye further reacted with barbituric acid at a considerably slower rate to form a second polymethine dye with a λ_{max} of 600 nm. A large excess of isonicotinic acid was used since it has been shown that this stabilises the intermediate polymethine dye [8]. The flow-rates of the first and second PCR reagent pumps were approximately 0.1 and 0.2 ml/min, respectively. The derivatised cyanide and Cu(I)-cyanide peaks were detected after the PCR unit with a fixed wavelength detector operated at 436 nm.

5.3 Results and Discussion

5.3.1 Improvements to the eluent

In order to improve the separation of the metallo cyanide-complexes from that previously reported, three factors influencing the separation were examined. These factors were the column length, concentration of the tetrabutylammonium cation (TBA$^+$) and the nature and concentration of the counter anions in the ion-interaction reagent (IIR). The last factor has been shown to have a significant effect on the retention of the metallo-cyanide complexes [9-13].

It should also be recognised that a consideration associated with use of reversed-phase ion interaction chromatography (RPIIC) for a process control application is the cost of the IIR. In particular, the cost of commercially available IIR's such as Waters Low UV PIC A is considerable, especially when it is compared to the cost of bulk (1 Kg) quantities of tetrabutylammonium hydroxide.

Several authors have used Waters Low UV PIC A for preparing eluents for RPIIC [14-16]. Fig. 5.2 illustrates the separation achieved using this reagent in an eluent comprising 25% acetonitrile, 5 mM Low UV PIC A and 75 μM NaCN. It should be noted that the Fe(III) and Ni(II) complexes had almost identical retention times under these separation conditions. An ion chromatographic analysis of a 5 mM solution of Low UV PIC A revealed the presence of both sulfate (5 mM) and phosphate (10 mM) as counter-anions. Several different combinations of these anions with TBA$^+$ were investigated as a means to vary separation selectivity. In view of the practical requirements of the separation as a tool for process monitoring, the separation requirements were as follows:

(i)   Complete resolution of thiocyanate and the Cu(I) complex.

(ii)   The concentration of cyanide in the eluent should be kept as low as possible to enable use of the cyanide PCR detection system.

(iii)   Rapid analysis of mixtures containing SCN, Cu(I) and Fe(II).

(iv)   Rapid analysis for the Au(I) cyanide complex.

Due to the disparity in concentrations of the above analytes in the Telfer samples, a small injection volume (typically 1-10 µL) was required for the analysis of cyanide, thiocyanate and the Cu(I) and Fe(II)-cyanide complexes in the CIL process samples, while a large injection volume (50-100 µL) was required for analysis of the Au(I) complex.

Fig. 5.2 illustrates that thiocyanate and the Cu(I) and Fe(II) complexes can be readily separated within 10 min. on a Waters 15 cm C-18 Nova-Pak column. Consequently, the first requirement was to reduce the retention time of the Au(I) complex to within 10 minutes. It should also be recognised that reducing the retention time will in general result in increased sensitivity due to reduced chromatographic dispersion. This is particularly relevant to the Au(I) complex due to the relatively low concentrations of this species in many cyanidation leachates. The sensitivity of the Au(I) complex could also be increased by altering the detection wavelength to 205 nm (the λ_{max} for $[Au(CN)_2]^-$ [17]).
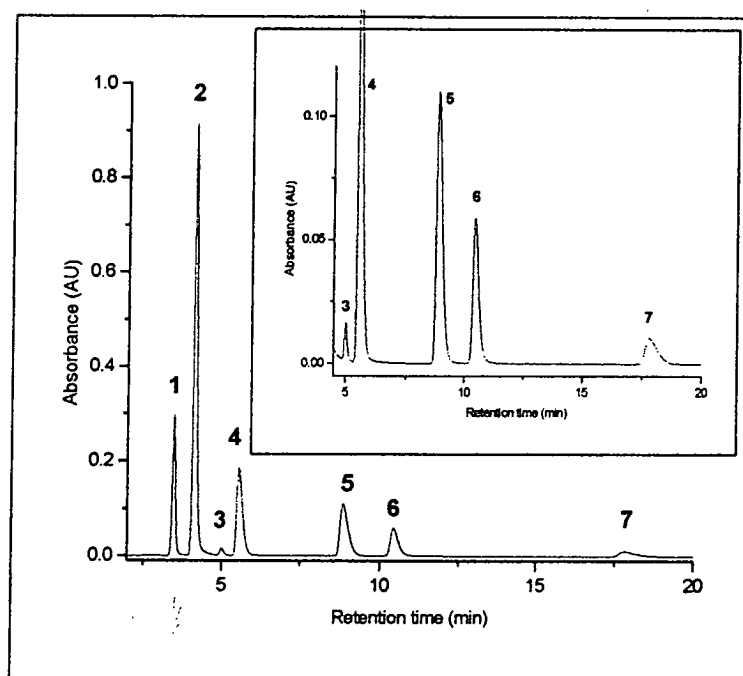
Fig. 5.2: UV detector (214 nm) chromatogram of a standard mixture showing separation of thiocyanate and six metallo-cyanide complexes on a 15 cm Nova-Pak C-18 column.

Legend : (1) SCN; (2) Cu(I); (3) Ag; (4) Fe(II); (5) Co(III); (6) Ni(II); (7) Au(I)

Eluent : 25 % MeCN (Waters), 5 mM Low UV PIC A, 75 µM NaCN; pH 8.0

Two possible approaches were considered for reducing the retention time of the Au(I) complex. The first approach was to alter the eluent composition, while the second approach was to reduce the length of the chromatographic column. In the first approach it was observed that increasing the concentration of acetonitrile in the eluent to 29% eluted the Au(I) complex in 9 minutes on a Waters 15 cm C-18 Nova-Pak column. An alternative method developed by Otu *et al.* [11] was to increase the concentration of the IIR counter-anion to enable rapid elution of the Au(I) complex.

A potential disadvantage of increasing the concentrations of either the organic modifier or IIR counter-anion in the eluent is the increased possibility of precipitation of sample components in the column resulting in column failure. This is a very real possibility when analysing leach samples due to the often high TDS values present in the ground-waters used for leaching.

In addition, this approach also requires different eluent compositions for optimal separation of the various metallo-cyanide complexes. To overcome these problems, the second approach was investigated with a Waters 5 cm Nova-Pak C-18 cartridge column as shown in Fig. 5.3. The Au(I) complex was the last peak eluted, giving an analysis time of less than 10 min.
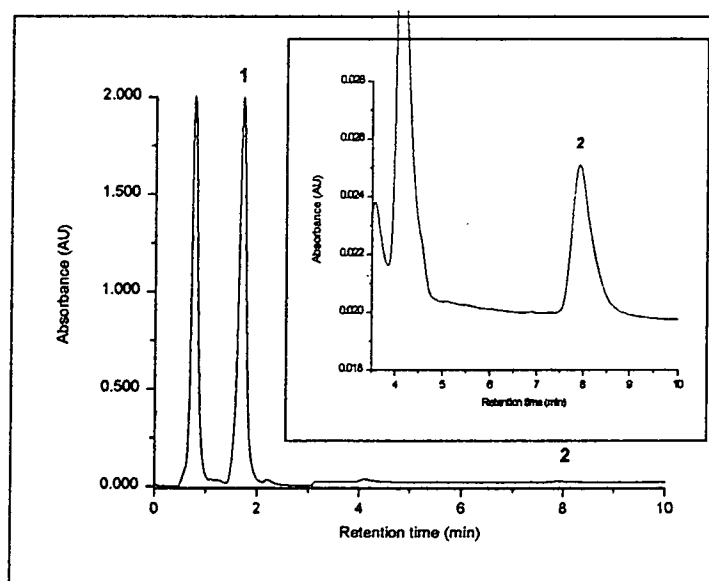
Fig. 5.3: UV detector (205 nm) chromatogram of a CIL sample showing rapid elution of the Au(I) complex on a 5 cm Nova-Pak C-18 cartridge column. Legend : (1) Combined SCN and Cu(I) peaks; (2) Au(I). Concentration of Au(I) complex = 1.32 ppm. Injection vol : 50 µL. Eluent : 25% MeCN (Merck), 5 mM TBAOH, 10 mM KH$_2$PO$_4$, 10 mM Na$_2$SO$_4$, 80 µM NaCN; pH = 8.0

The effects of the IIR counter-anions and cyanide in the eluent were studied using eluents comprising 25% acetonitrile and 5 mM TBAOH at a pH value of 7.95 ± 0.05. Tables 5.1 and 5.2 show retention data for both the 15cm and 5 cm columns under a range of eluent conditions, together with values for the resolution of thiocyanate and Cu(I) on the 15 cm column (Table 5.1). Low concentrations (<160 μM) of cyanide were added to the eluent to improve the Cu(I) peak shape and increase the retention of the Cu(I) complex with respect to thiocyanate for the reasons discussed in chapter four.

The initial eluent developed at the University of Tasmania (UTas) was not able to resolve the thiocyanate and Cu(I) peaks at Telfer. After several tests, it was found that the cause of this difference was due to the acetonitrile. The acetonitrile used at UTas was a Waters product, while the acetonitrile used at Telfer was a Merck product. Both sources of acetonitrile were of HPLC grade quality. Less cyanide was required in the eluent prepared at UTas to enable complete resolution of the thiocyanate and Cu(I) peaks. This suggested that the acetonitrile used at UTas contained a low concentration of cyanide. However, the PCR detection system, which was very sensitive to cyanide, was unable to detect a significant difference between the two sources of acetonitrile. Consequently, it was not possible to be completely certain of the cause of the difference between the two sources of acetonitrile.

It should be noted that other authors have also observed differences between sources of HPLC-grade quality acetonitrile [18]. Furthermore, slight differences in the composition of the acetonitrile were noted towards the end of each reagent bottle (4l (Merck) or 2.5 l (Waters)). These differences were observed as an increase in the PCR detection baseline and increased resolution of the thiocyanate and Cu(I) peaks. Both Day [18] and Berry [19] have reported similar observations concerning the aging of acetonitrile in opened reagent bottles. Berry recommended a shelf life of 2 months for opened bottles of acetonitrile [19].

[Phosphate] (mM)	[Sulfate] (mM)	[Cyanide] (μM)	Retention time (min)					Resolution of SCN and Cu(I)
			SCN	Cu(I)	Fe(II)	Fe(III)	Au(I)	
10	0	40	4.35	5.00	-	-	-	2.21
10	10	80	3.70	4.02	3.85	9.13	-	1.25
8.3	5.0	40	3.52	3.83	6.51	11.38	18.18	1.30
5.0	3.0	60	4.07	4.93	17.05	>20	-	2.94
5.0	5.0	60	3.95	4.62	12.41	17.73	21.89	2.41
5.0 mM Low UV PIC A	-	75	3.47	4.14	5.55	-	17.82	2.50

Table 5.1: Retention data obtained on a 15 cm column. Each eluent contained 25% acetonitrile and the first five eluents contained 5 mM TBAOH. The final eluent pH was 7.95 ± 0.05

[Phosphate] (mM)	[Sulfate] (mM)	[Cyanide] (μM)	Retention time (min)				
			SCN	Cu(I)	Fe(II)	Fe(III)	Au(I)
10	0	40	-	-	4.63	6.31	9.02
10	10	80	-	-	1.53	3.29	7.90
5.0	5.0	60	-	-	4.33	6.49	8.73
5.0	7.0	60	-	-	2.73	4.84	8.23
5.0 mM Low UV PIC A		0	-	-	2.00	3.52	7.46

Table 5.2: Retention data obtained on a 5 cm column. Each eluent contained 25% acetonitrile and the first five eluents contained 5 mM TBAOH. pH = 7.95 ± 0.05.

It was necessary to have a suitable buffer in the eluent to minimise damage to the column by the alkaline samples. A phosphate buffer was selected as it has been used previously in this separation [10] and displays virtually no absorption at the detection wavelengths used in this work.

The first eluent shown in Tables 5.1 and 5.2 (comprising 10 mM phosphate buffer and 40 μM cyanide) gave broad peaks and incomplete separation of the Fe(II) and Fe(III) complexes on a 5 cm Nova-Pak C-18 column as shown in Fig. 5.4. Previous studies have shown that the addition of sulfate to the eluent improved the peak shape of the metallo-cyanide complexes [7]. Consequently, the next eluent shown in Tables 5.1 and 5.2 contained both a phosphate buffer (10 mM) and sodium sulfate (10 mM). This eluent significantly improved the peak shape of the Fe complexes and enabled baseline resolution of the two Fe complexes and the Au(I) complex on a 5 cm Nova-Pak C-18 column, as shown in Fig. 5.5. However, resolution of the thiocyanate and Cu(I) peaks was reduced to the point that these species could not be fully resolved on a 15 cm Nova-Pak C-18 column, even with the addition of more cyanide to the eluent.

The effects of sulfate in the eluent were further investigated and significant changes in the retention times, particularly those of the Fe(II) and Fe(III) complexes, were noted. The concentrations of the phosphate buffer and sulfate were lowered as shown in Tables 5.1 and 5.2. Good separations (resolution greater than 2) of thiocyanate and the Cu(I) species were obtained in the last two eluents. However, the retention time of the Fe(II) complex on the 15 cm Nova-Pak C-18 column was greater than 10 min with these eluents. When the results for the above five eluents shown in Tables 5.1 and 5.2 were compared to those obtained using an eluent containing 5 mM Low UV PIC A, it was apparent that an eluent containing a phosphate buffer (10 mM) and sulfate (5 mM) would be a suitable compromise for the counter anions. This was attributable to the -3 and -4 charges on the Fe(III) and Fe(II) complexes, respectively, compared to the -1 charge on thiocyanate and the Au(I) complex and the variable charge of between -1 and -2 for the Cu(I) complex, depending on the concentration of cyanide in the eluent. High analyte charge results in an increased negative slope of a plot of log k' *versus* log[counter-anion] [13].
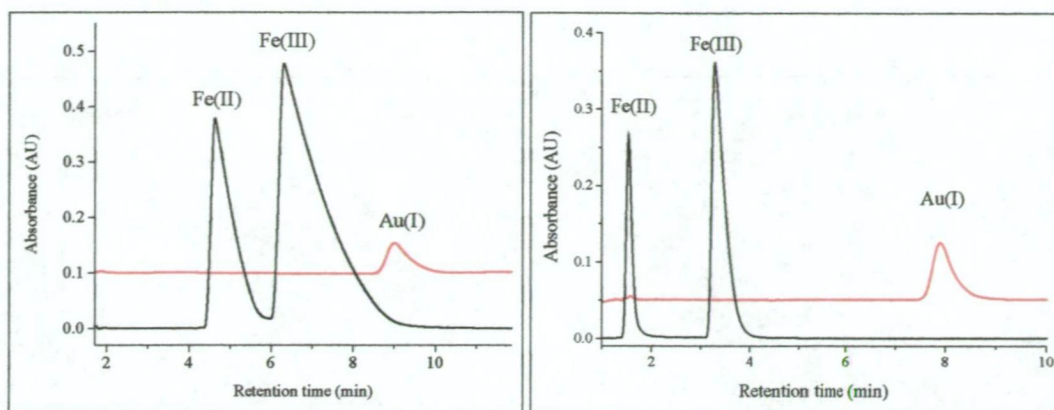
Fig. 5.4 (LHS) and **Fig. 5.5** (RHS): Overlaid (and offset) chromatograms of mixed Fe(II) and Fe(III) standard and Au(I) standard. Column: 5 cm Nova-Pak C-18.

Fig. 5.4: Eluent: 25% MeCN, 5 mM TBA$^+$, 10 mM phosphate buffer, 40 μM NaCN; pH = 7.95

Fig. 5.5: Eluent: 25% MeCN, 5 mM TBA$^+$, 10 mM phosphate buffer, 10 mM sodium sulfate, 75 μM NaCN; pH = 7.95

In view of the desirability of using the 5 cm column because of the rapid analyses possible, further optimisation of the eluent used with this column was undertaken by varying the percentage of acetonitrile and the concentration of TBA$^+$. Table 5.3 shows retention data for a range of eluent compositions, all of which contained phosphate and sulfate at the optimal levels determined above. Increasing the TBA$^+$ or cyanide concentrations, or decreasing the percentage of acetonitrile, were found to improve the resolution of thiocyanate and Cu(I). The optimal eluent composition at Telfer was 25% acetonitrile, 10 mM TBAOH, 10 mM KH$_2$PO$_4$, 5 mM H$_2$SO$_4$ and 160 μM NaCN, adjusted to pH 8.0. The separation of a standard mixture (similar to that used for Fig. 5.2) on a 15 cm Nova-Pak C-18 column with this eluent is shown in Fig. 5.6, while the separation on a 5 cm Nova-Pak C-18 of the major components present in a CIL sample is shown in Fig. 5.7. It is noteworthy that the elution order differed to that obtained in previous studies using an eluent containing 5 mM Low UV PIC A in that the Au(I) complex (not shown in Fig 5.6), which had previously been eluted last was now eluted prior to Fe(III). Again, this can be attributed to the effects of counter-anions on the elution of the highly charged Fe(III) complex.

| [Acetonitrile] | [TBAOH] | [KH$_2$PO$_4$] | [H$_2$SO$_4$] | [NaCN] | Retention time (min) | | | | Resolution of |
(%)	(mM)	(mM)	(mM)	(μM)	SCN	Cu(I)	Fe(II)	Au(I)	SCN and Cu(I)
23	5	10	5	80	-	-	4.03	10.03	-
25	7	10	5	80	1.58	1.87	3.17	7.72	1.81
25	8	10	5	80	1.67	2.00	3.57	-	2.05
25	8	10	5	160	1.65	2.07	3.63	-	2.63
25	9	10	5	160	1.70	2.18	3.93	8.62	2.88
25	9	10	5	0	1.72	1.93	3.88	8.75	Not resolved
25	10	10	5	160	1.78	2.32	4.40	9.07	3.01

Table 5.3: Retention data obtained on the 5 cm column using mobile phases with varying amounts of acetonitrile, TBAOH and NaCN.
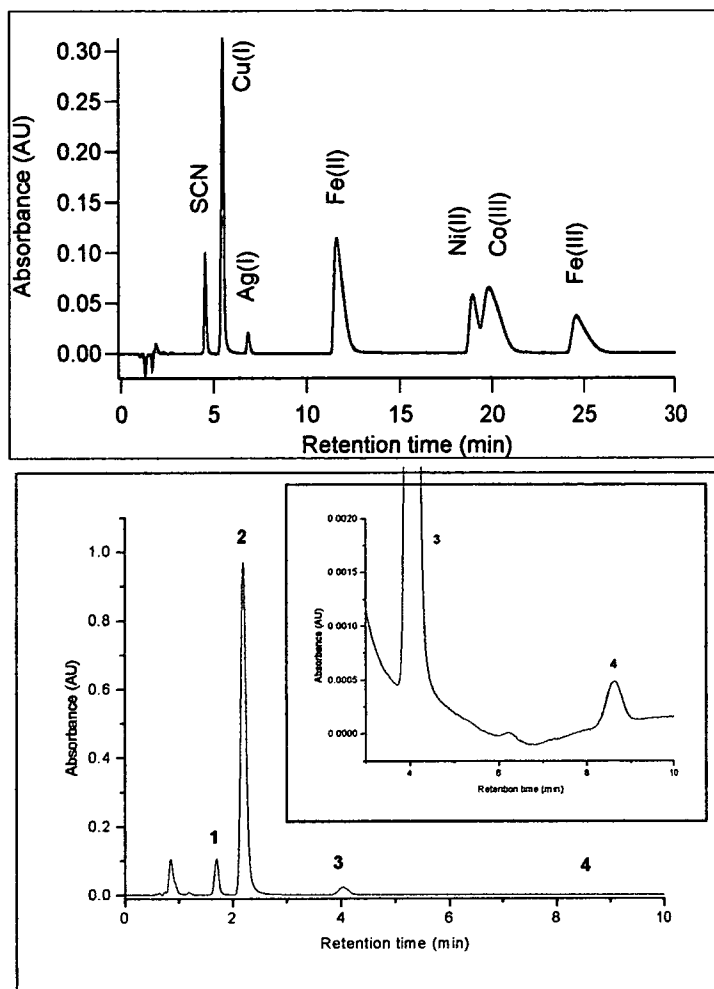
Fig. 5.6 (Top): UV detector (205 nm) chromatogram of a standard mixture analysed on a 15 cm Nova-Pak C-18 column. Eluent : 25% MeCN, 10 mM TBAOH, 10 mM KH_2PO_4, 5 mM Na_2SO_4, 75 μM NaCN; pH = 8.0 (Acetonitrile supplier: Waters)

Fig. 5.7 (Bottom): UV detector (225 nm) chromatogram of a CIL sample analysed on a 5 cm Nov-Pak C-18 column. Legend : (1) SCN; (2) Cu(I); (3) Fe(II); (4) Au(I). Sample concentrations (ppm): SCN (27.5); Cu(I) (103); Fe(II) (1.5); Au(I) (1.2). Eluent : 25% MeCN, 10 mM TBAOH, 10 mM KH_2PO_4, 5 mM Na_2SO_4, 160 μM NaCN; pH = 8.0. (Acetonitrile supplier: Merck)

The columns were inter-changed manually during the initial development of methods employing two column lengths (5 and 15 cm) but this process was automated in later developments by use of a six-port column switching valve. Column manufacturers often state that ODS columns will suffer damage if eluents containing IIR's are left stationary in the column. It is generally recommend that the column is flushed and stored with an aqueous/organic solution to remove the eluent. Since acetonitrile was

---

Chapter Five

generally used in this work, an aqueous acetonitrile solution containing 20-25% acetonitrile was used for column flushing. However, this procedure is not desirable when frequent column changes are occurring. To overcome these problems, a switching valve configuration was designed that minimised the time that the eluent would remain stationary in either column. The switching valve configuration enabled selection of either the two columns (15 and 5 cm) in tandem or the 5 cm column only, as shown in Fig. 5.8. In this arrangement, the Au(I) complex would be analysed on the 5 cm column only, while the early eluting species (thiocyanate and the Cu(I) and Fe(II) complexes) would be analysed on the 15 and 5 cm columns in tandem. The 15 cm column length was selected as although a 10 cm column length was available, it was considerably more expensive than the 15 cm column length. It was envisaged that this configuration would allow the eluent to remain stationary in the 15 cm column only for periods of less than 30 min. The retention data obtained on the 15 and 5 cm columns in tandem is shown in Table 5.4.
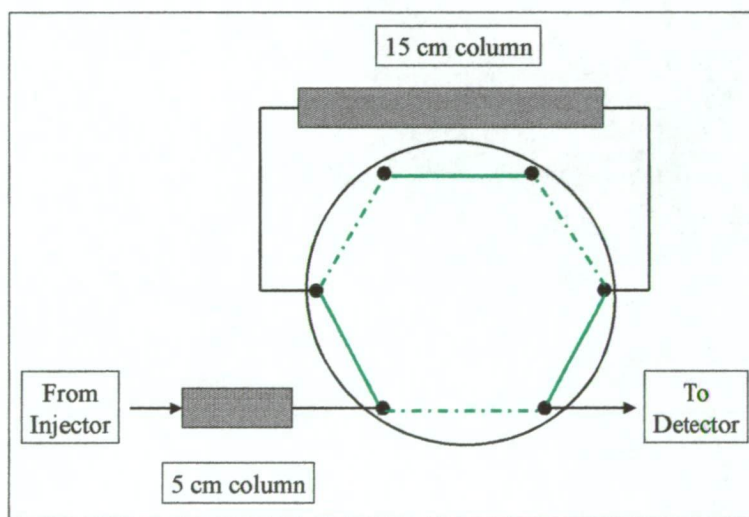
Fig 5.8: Switching valve configuration for selection of either 15 and 5 cm columns in tandem or 5 cm column only.

| [Acetonitrile] | [TBAOH] | [K_2PO_4] | [H_2SO_4] | [NaCN] | Retention time (min) | | | Resolution of |
(%)	(mM)	(mM)	(mM)	(μM)	SCN	Cu(I)	Fe(II)	SCN and Cu(I)
23	5	10	5	80	5.5	6.4	13.6	2.87
25	5	10	5	80	4.4	5.0	6.9	2.25
25	5	10	5	120	4.4	5.1	7.1	3.74
25	7	10	5	80	4.8	5.8	10.4	3.67
25	8	10	5	160	5.1	6.6	12.2	5.99

Table 5.4: Retention data obtained on the (15 + 5) cm columns in tandem.

It is well known that the stability of cyanide in aqueous solution decreases with the solution pH. Adams [20] has observed that there was a difference of approximately three orders of magnitude in the rate of cyanide loss from aqueous solution at pH values of 11 and 8. Since the eluent pH has to be maintained below 8.0 to prevent column damage, it is quite reasonable to assume that there will be loss of cyanide from the eluent. It has been shown in the previous chapter that the eluent cyanide concentration plays an important role in the separation of the Cu(I)-cyanide complexes. To investigate the effect of time on eluent stability, a 1.5 litre batch of eluent was prepared and then used over three days. The eluent was stored in three 500 mL glass reagent bottles, with each bottle shielded from light and kept in a refrigerator (0-2°C) when not in use. Even with these precautions, the resolution of thiocyanate and Cu(I)-cyanide species decreased slightly over a three day period. There was also a decrease in the R value (as determined by the PCR detection system) of the eluted Cu(I)-cyanide peak over this period.

In view of these results, the use of a gradient pump to continually prepare an isocratic eluent was considered seriously. It was envisaged that a gradient pump would allow a dilute NaCN solution (pH > 11) to be used, thereby minimising the loss of cyanide from the eluent. In addition, a gradient pump would also allow up to four eluent components to be continuously added, thus providing constant concentrations of the individual components. This is of particular importance for acetonitrile due to the volatility of this solvent (BP: 81.6 °C; Vapour pressure:90 mm Hg at 25°C [21]) and the significant effect of minor variations in the acetonitrile concentration on chromatographic performance [22]. It should be noted that the problem concerning preparation of an isocratic eluent is not trivial with respect to the mining industry. Muir [23] identified the requirement for precise eluent preparation as one of the problems associated with the use of RPIC by the mining industry. An additional advantage of a gradient HPLC pump is that it would enable a more automated HPLC system to be developed and reduce the operator time required for eluent preparation. Ideally, only weekly refilling of the eluent component reservoirs would be necessary. Conversely, an isocratic pump would require a fresh eluent to be prepared every 1-2 days, assuming the eluent is kept at < 2°C.

The major disadvantages concerning the use of a gradient pump are:

(a) An isocratic pump is considerably smaller and cheaper than a gradient pump.

(b) There are less moving parts in an isocratic pump and consequently fewer potential breakdowns, which is an important consideration at remote locations such as Telfer.

(c) Continual de-gassing of the eluent components is required. The two alternatives means of degassing involve either continual helium sparging of the four eluent components or the use of a four channel on-line vacuum degassing module.

Budgetary considerations finally decided the issue. The project supervisors decided that the cost of either helium or an on-line de-gassing module during the development work at Telfer was not warranted. Consequently, only isocratic eluents were used at Telfer.

5.3.2 Improvements to the PCR detection system

These developments were carried out in conjunction with the analysis of various samples from the CIL circuit and dump leach operations. The initial PCR conditions used were similar to those developed at the University of Tasmania, which were for lower cyanide concentrations than for those found at Telfer. Modifications to the PCR detection system were implemented to facilitate good linearity and precision for cyanide in the concentration range present in the process samples under study. The range of cyanide concentrations initially examined was 1-5 mM NaCN. This was later extended to 9 mM NaCN due to the high cyanide concentrations found in some Leach Pad samples. Several different PCR reagent concentrations and reaction times following the second reagent addition were examined to determine the most appropriate combination for the Telfer samples. The reaction temperature was maintained at 40°C. It was observed that altering the reaction temperature to either 35°C or 45°C resulted in a decrease in the absorbance. The results of this study are summarised in Table 5.5. Under the final PCR conditions shown in Table 5.5, a relatively small calibration drift (< 5%) was observed over the course of a 10 hr period, as shown in Fig. 5.9.

Calibration range (mM)	[INA] (mM)	[BA] (mM)	Reaction time (sec)	Peak area and precision			Correlation Coefficient	Equation terms	
				1 mM	5 mM	Highest conc.		$a*x^2$	$b*x$
1 - 5	300	3	19	308; 2.1 %	2420; 1.4 %	-	0.995	13.2	6590
1 - 5	300	3	37	422; 0.4 %	3132; 0.1 %	-	0.995	14.1	9240
1 - 5	300	3	56	437; 0.8 %	3355; 0.4 %	-	0.998	18.3	9010
1 - 5	300	4	19	366; 0.3 %	2814; 1.4 %	-	0.998	14.7	7630
1 - 5	300	4	56	536; 1.2 %	3823; 0.8 %	-	0.998	17.7	11000
1 - 9	200	10	19	632; 3.9 %	3726; 0.3 %	8063; 0.1 %	0.999	15.7	11600
1 - 7	200	10	37	904; 0.8 %	5653; 1.9 %	9358; 0.2 %	0.996	31.2	16200
1 - 6	200	10	56	1031; 3.5 %	6488; 0.1 %	8140; 0.4 %	0.999	28.9	19400
1 - 8	150	30	19	863; 0.2 %	4929; 0.4 %	9139; 0.2 %	0.999	13.7	12800
1 - 9	230	15.6	19	644; 0.5 %	3952; 0.2 %	6839; 0.1 %	0.993	-0.14	13800

Table 5.5 : Summary of further PCR developments at Telfer. [INA] and [BA] refer to the concentrations of isonicotinic acid and barbituric acid in the second reagent. See the text for more details concerning this table.
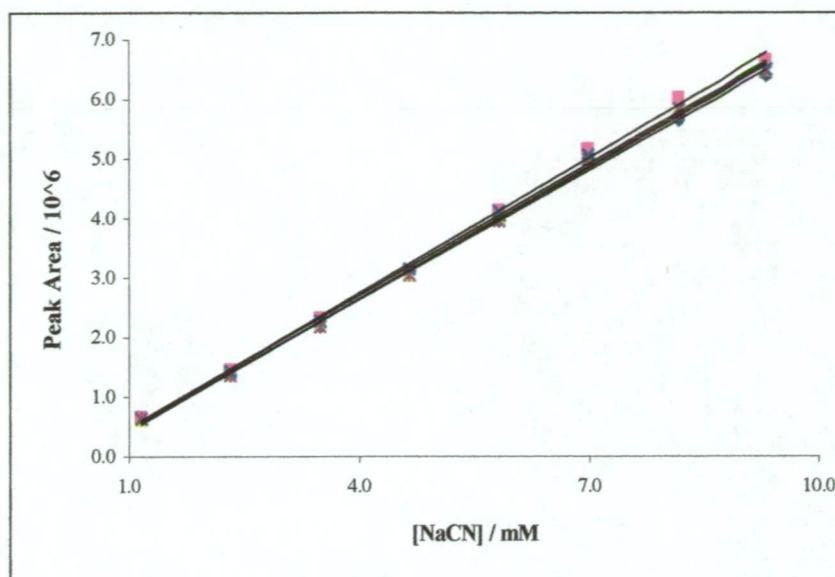
Fig. 5.9(a): Variation in NaCN calibration over a 10 hour period.

PCR Reactor 2 : 5 m x 0.030 mm I.D. stitched reaction coil with a residence time of 19 sec.

Eluent : 25 % acetonitrile, 10 mM TBAOH, 10 mM KH_2PO_4, 5 mM H_2SO_4 , 160 µM NaCN; pH 8.0. Column : 5 cm Nova-Pak C-18.
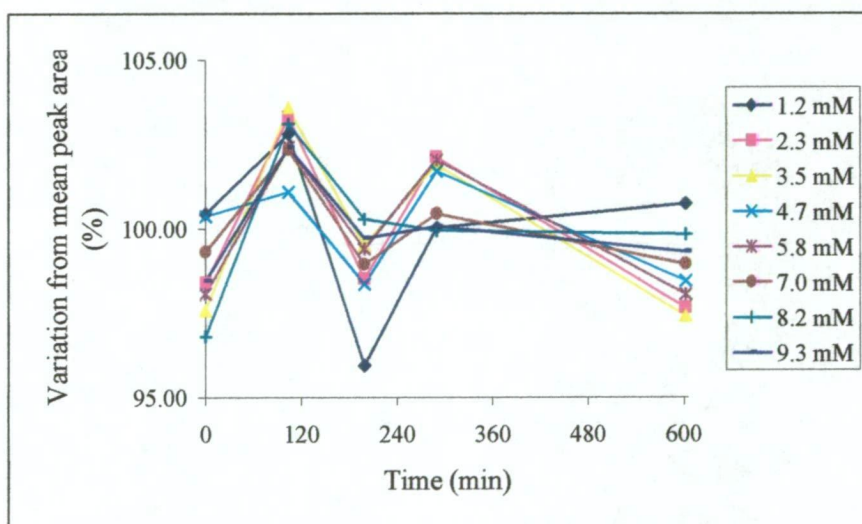
Fig. 5.9(b): Variation in NaCN calibration standards over a 10 hour period. Conditions as for Fig. 5.9(a).

Notes on Table 5.5 :

(i) The peak area and precision data have been mostly reported for three NaCN concentrations (1 and 5 mM and the highest concentration above 5 mM) in order to provide a comparison between the different PCR conditions.

(ii) The peak areas reported have been divided by 1000 for convenience. Since each standard injection was duplicated, the reported peak area is the average of the two values and an estimate of the precision is given by the percentage variation between the mean and actual peak areas.

(iii) All the calibrations were non-linear and could be described by a quadratic equation. The calibrations were all forced through the origin since an injection of a blank produced almost no peak in the PCR detector. An indication of the suitability of each equation is provided by the correlation coefficient, which was greater than 0.990 in all cases. The two constants in each quadratic equation are listed. However, it should be noted that these constants are only for a particular range of concentrations.

(iv) The calibrations were non-linear for a variety of reasons :

- It was found that the linearity of the calibration curve at higher cyanide concentrations was improved by increasing the N-chlorosuccinimide (NCS) concentration from 0.10 % (w/v) to 0.15 % (w/v). These observations are rationalised below.

    - The first reaction, following the addition of the NCS reagent, results in the rapid oxidation of cyanide to form CNCl. The CNCl can be subsequently hydrolysed to form cyanate, which will not undergo reaction with the second reagent to form the polymethine dye product. This hydrolysis is catalysed by excess chlorination reagent. It has been suggested that the component responsible for this catalytic effect is molecular chlorine [24].

    - Consequently, if there is sufficient NCS to react with all the cyanide at the highest NaCN concentration, then some of the CNCl formed at the lower NaCN concentrations will undergo catalytic hydrolysis with excess NCS reagent to form cyanate. This will result in a calibration plot in which the rate of increase of the PCR detector response, ΔRes, will increase with the NaCN concentration. Conversely, if there is insufficient NCS to react with all the cyanide at the highest NaCN concentration, then ΔRes will decrease with the

NaCN concentration. Due to the range of NaCN concentrations and the catalytic hydrolysis of CNCl with excess chlorination reagent, it is not possible to achieve reaction conditions that will enable equivalent conversion of cyanide to CNCl over a large range of NaCN concentrations.

- Due to the very large molar absorptivity values for the polymethine dyes, it is possible to produce a derivatised cyanide peak in which the absorbance is outside the linear range. Two steps were taken in order to decrease the sensitivity of this method so that it could be utilised for the anticipated levels of cyanide.

  - Two detection wavelengths (436 and 546 nm) which were accessible to a fixed wavelength detector and at which the molar absorptivity was less than at the λ_{max} for the polymethine dye were examined. The 436 nm wavelength was selected because the absorbance was less at this wavelength. In addition, the calibration curves were markedly non-linear at higher cyanide concentrations with the 546 nm detection wavelength. This observation was attributed to spectral interference from the final dye ($\lambda_{max} = 600$ nm) at 546 nm. The choice of a fixed wavelength detector enabled the use of a mercury lamp, which is considerably cheaper and more robust than the deuterium lamp in a variable wavelength detector. Both these factors are important in the selection of appropriate instrumentation for a process control application.

  - The second step taken to reduce the large absorption values was by adjusting the INA and BA concentrations and/or the residence time in the second reaction coil(s). However, poor precision resulted, especially at lower cyanide concentrations, if the INA and BA concentrations were too low and/or the reaction time was insufficient.

  - Three reaction times in the second reactor were examined: 19, 37 and 56 sec. These reactions times were achieved by the use of three knitted 5m x 0.30 mm I.D. reaction coils. It was observed that there was a large increase in the PCR absorbance when the reaction time was increased from 19 to 37 sec, while a relatively small increase occurred when the reaction time was increased to 56 secs. This indicated that formation of the intermediate dye was almost

complete after 56 sec. Kuban [8] reported a reaction time of 120 secs for formation of the intermediate dye when using the INA/BA reagent, but the temperature used was not stated. The INA and BA concentrations were optimised to provide the best calibration linearity using the above reaction conditions and a detection wavelength of 436 nm. The final INA and BA concentrations selected were 230 mM and 15.3 mM, respectively. Good calibration linearity for 1-9 mM NaCN was achieved using a reaction time of 19 sec, but increasing the reaction time to 56 sec was required to improve the precision for the derivatised Cu(I)-cyanide peak. This reduced the linearity range to 1-7 mM NaCN due to the large absorbance values generated with the longer reaction time.

- After several problems were experienced using the three 5 m x 0.30 mm I.D. reaction coils, the second reactor was replaced with a 5 m length of 0.50 mm I.D. stitched PFTE tubing reactor. The calculated residence time in this new reactor (47 sec) was similar to the previous reactor (51 sec). The actual difference in residence time between the two reactors was 8.4 sec, presumably due to imperfect connections between the three 5 m coils of the initial reactor. The back-pressure generated by the PCR unit was considerably reduced by use of the wider bore tubing. There was also a considerable increase in the signal:noise (S/N) ratio, as shown in Fig. 5.10. This phenomenon of improved S/N ratio by use of wider bore reactor tubing has also been observed by other workers [25]. The cyanide and Cu(I)-cyanide peaks were noticeably broadened by the use of this wider bore tubing (Fig. 5.10), leading to reduced peak heights and detection sensitivity. This was not considered a disadvantage for this application since these methods were developed for process samples containing relatively large cyanide concentrations.
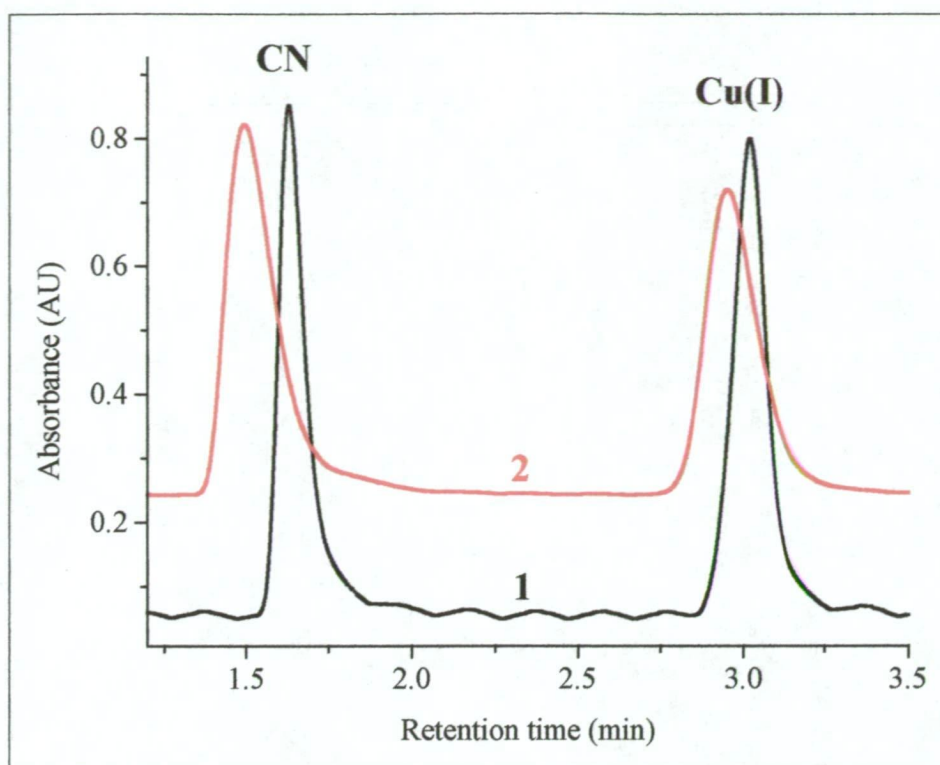
Fig. 5.10: Effect of tubing diameter on PCR reactor 2. (**1**) PCR reactor 2 : 15 metre x 0.3 mm I.D. Calculated volume = 1.09 mL (**2**) PCR reactor 2 : 5 metre x 0.5 mm I.D. Calculated volume = 0.98 mL. Chromatogram (**2**) offset by +0.2 AU. Eluent for both chromatograms: 25 % acetonitrile, 10 mM TBAOH, 10 mM KH_2PO_4, 5 mM H_2SO_4 and 80 μM NaCN; pH = 8.00. Column: 5 cm Nova-Pak C18.

(v) The NCS reagent was usually prepared and used within 36 hours.   It was observed after two days that the calibrations became significantly more non-linear at higher NaCN concentrations.   This was attributed to a decrease in the oxidation potential of the NCS reagent.   The variation in calibration linearity over a two day period was reduced when the NCS concentration was increased from 0.10 to 0.15 % (w/v).   The succinimide concentration was increased to 2.0% (w/v) to allow at least a 10-fold excess over the NCS concentration.   The succinate buffer concentration was maintained at 0.1 M and pH 5.6.   Further increases in the NCS concentration were not attempted for two reasons :

a) Excess chlorination reagent reduced the calibration linearity for the reasons discussed above.

b) N-chlorosuccinimide is only slightly soluble in water [26].

It became necessary to add Na_2EDTA to the eluent during the analysis of some Dump Leach samples (Refer to section 5.3.6). There was a small difference between the NaCN calibrations at higher NaCN concentrations when EDTA was present in the eluent. This difference may have been due to the oxidation of EDTA by the NCS reagent. The oxidation of EDTA by a similar chlorination reagent (Chloramine-T) has previously been reported [27].

To facilitate rapid preparation of the NCS reagent, a stock solution was prepared which contained all the chemicals in the NCS reagent, except for the N-chlorosuccinimide. The stock solution was composed of a succinate buffer (0.2 M, pH 5.6) and succinimide [4.0 % (w/v)]. The stock solution was kept in a refrigerator (< 4 °C) to minimise bacterial growth and was stable for at least 1 month under these conditions. N-chlorosuccinimide (0.15%) was dissolved in this stock solution on a daily basis and filtered to produce the desired NCS reagent. Generally, 250 mL of NCS reagent was sufficient for a 24 hour period. In order to reduce NCS reagent wastage, the NCS reagent remaining at the end of each day was collected in a separate container. N-chloro succinimide could be added to this waste solution after it was several days old and the resultant NCS reagent was equivalent to freshly prepared NCS reagent.

5.3.3 Performance and comparison of UV and PCR detection systems

The performance of the UV and PCR detection system was evaluated at various times whilst at Telfer. The performance of the PCR detection system was discussed in the previous section. This section examines the performance of the UV detector and compares the performance of both detection systems based on the Cu(I) complex.

Typical Mill samples analysed at Telfer contained up to 120 ppm of Cu (as the Cu(I)-cyanide complexes) and 60 ppm thiocyanate. However, higher concentrations of these two species (especially the Cu(I)-cyanide complexes) were occasionally observed. Consequently, the effect of analyte concentration on the resolution of thiocyanate and Cu(I) and calibration linearity for both species was investigated. Satisfactory separation (Resolution > 2.0) and linear calibration were achieved for

25 - 250 ppm of both analytes when the UV detection wavelength was 225 nm. This wavelength was selected since the UV spectrum of the Cu(I)-cyanide complexes has two maxima at 209 and 235 nm and a minimum occurring at 225 nm, while the UV spectrum of thiocyanate shows decreasing absorbance with increasing wavelength. In addition, the molar absorptivity of thiocyanate is considerably less than that for the Cu(I)-cyanide complexes at all wavelengths. It was possible to extend the above concentration range by using a programmed detection wavelength change from 205 nm to 245 nm between the thiocyanate and Cu(I) peaks.

The two other significant cyanide complexes at Telfer were Fe(II) and Au(I). The highest Fe(II) and Au(I) concentrations observed at Telfer were less than 2 ppm and 4 ppm respectively. Calibrations were linear over the range 0.4 - 10 ppm for both Fe(II) and Au(I) complexes. Utilisation of a large injection volume (100 μL) enabled a detection limit for Au of approximately 10 ppb to be achieved. This allowed the $[Au(CN)_2]^-$ to be determined in most of the samples analysed at Telfer.

The calibration drift observed for thiocyanate, Cu(I) and Fe(II) with the UV detector was a maximum of 3.0 % for thiocyanate over a 7 hr period, as shown in Table 5.6. Consequently, six hourly calibrations for the UV detector should provide sufficient precision for use in a process control instrument.

Analyte	Conc.	Peak Area (PA)			% change in PA
	(ppm)	0 hr	2.5 hr	7 hr	after 7 hrs
SCN	100	3246266	3248145	3349520	+ 3.0
Cu(I)	100	12960758	12863533	13308438	+ 2.7
Fe(II)	10	4016224	-	3974654	- 1.0

Table 5.6: Calibration drift for the UV detector

A series of Cu(I)-cyanide standards was prepared and analysed over a day. The range of Cu concentrations varied from 0.5 - 5.0 mM, whilst R varied from 3.0 - 6.0. The standards analysed were prepared by dilution of 20 mM stock standards. These stock standards were prepared from 100 mM solutions of Cu(I)-cyanide (R = 3.0) and NaCN. A small calibration drift was observed with both detection systems, as shown in Figs. 5.11(a) and 5.12(a). The variation in detector response with time for each Cu concentration is shown in Figs. 5.11(b) and 5.12(b). It should be noted that part of the variation in detector response was due to the use of different standards. These different standards all had the same Cu concentration but different R values. Consequently, slight differences would be expected between the standards of same Cu concentration due to dilution errors. An indication of the magnitude of dilution error was provided by taking the ratio of the UV and PCR detector response, as shown in Fig. 5.13. It is evident from this analysis of the calibration data that the R value of a Cu(I)-cyanide standard is not important with respect to determination of the Cu(I) concentration. It is also evident that both detection systems should provide very similar values for the Cu(I) concentration. To illustrate this point, four Mill samples were analysed and the thiocyanate and Cu(I)-cyanide concentrations were determined in these samples from both the UV and PCR detector chromatograms. These results are shown in Table 5.7.

Mill Sample	[SCN]/ppm UV detector	[SCN]/ppm PCR detector	[Cu(I)]/ppm UV detector	[Cu(I)]/ppm PCR detector
C1	24.9 ppm	23.1 ppm	94.5 ppm	93.9 ppm
C7	17.0 ppm	17.1 ppm	58.3 ppm	57.1 ppm
A1	16.2 ppm	16.9 ppm	74.7 ppm	74.7 ppm
TS1	8.0 ppm	9.0 ppm	41.3 ppm	41.3 ppm

Table 5.7: Analysis of four Mill samples for thiocyanate and Cu(I)-cyanide and comparison of the concentrations determined from both UV and PCR detectors.
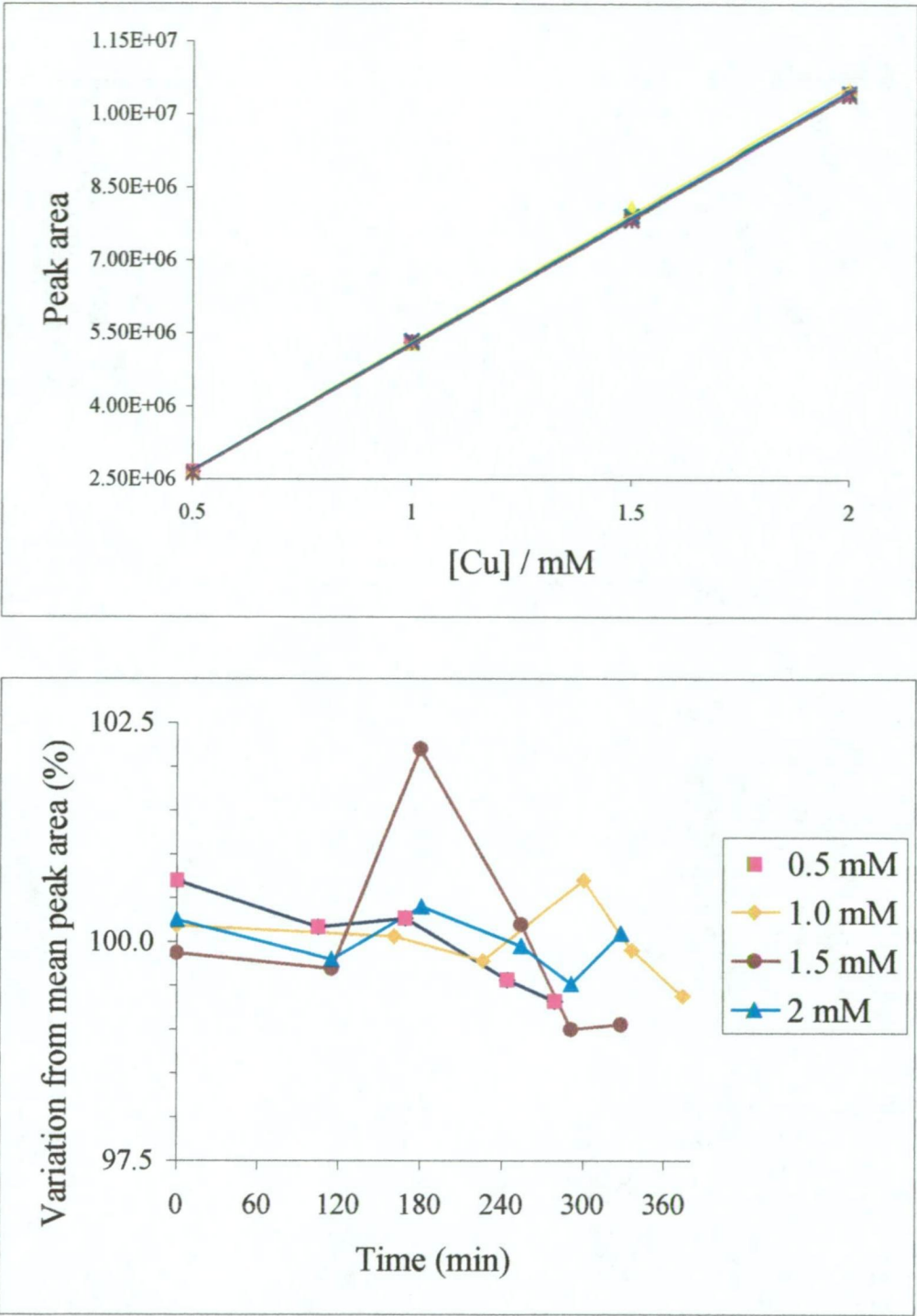
Fig. 5.11: UV detector (235 nm). **(a)** (Top) Calibration drift for Cu(I)-cyanide standards over a 6 hr period. **(b)** (Bottom) Variation in peak response for each standard.
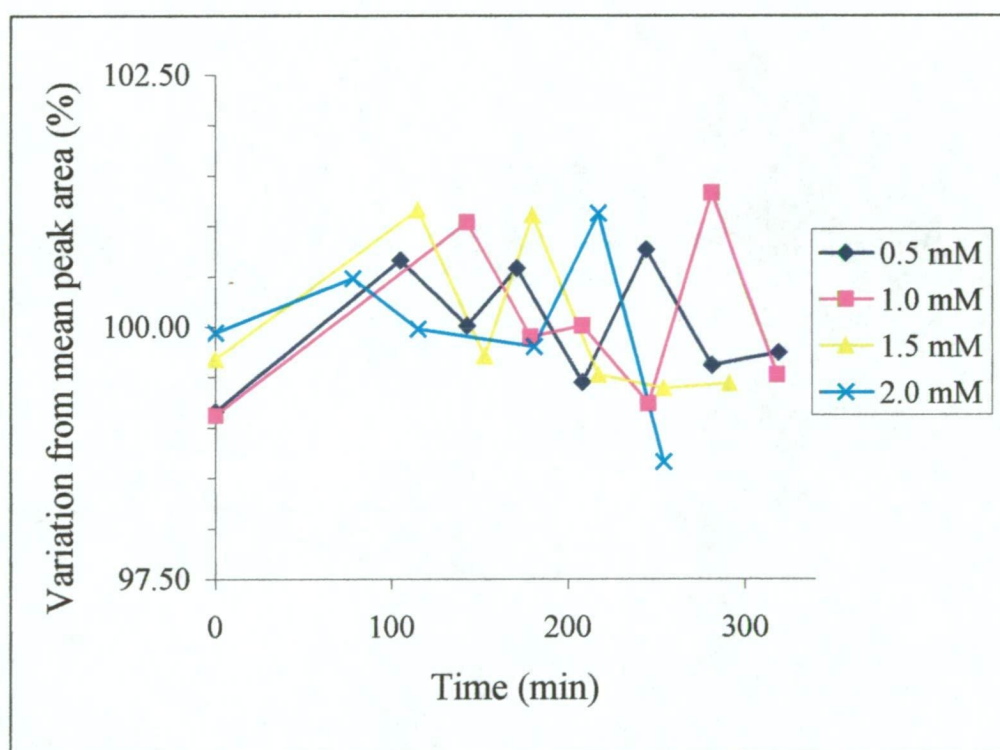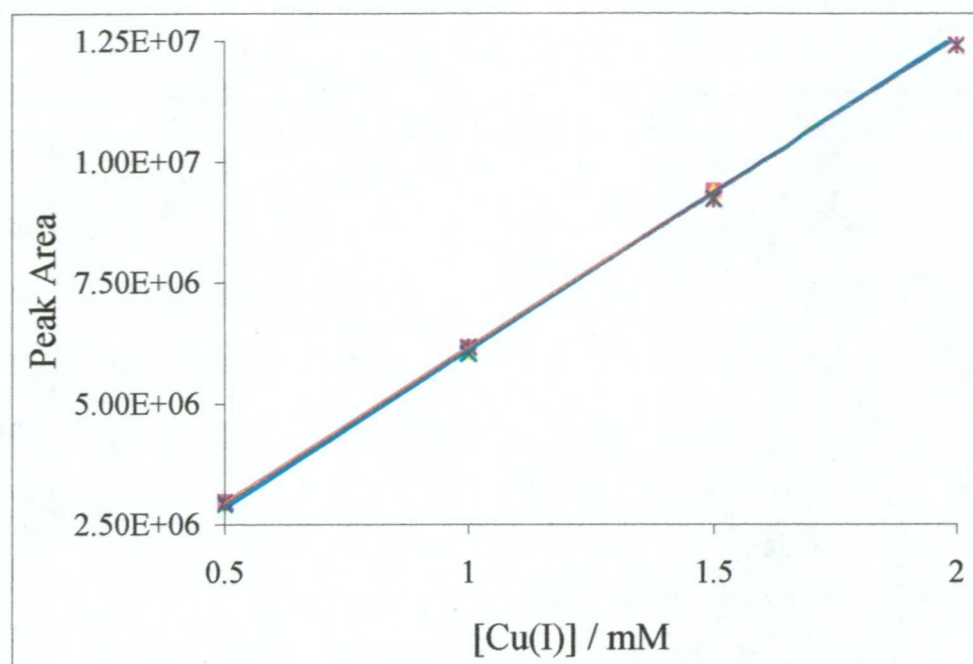
Fig. 5.12: PCR detector (436 nm) **(a)** (Top) Calibration drift for Cu(I)-cyanide standards over a 5 hr period. **(b)** (Bottom) Variation in peak response for each standard.
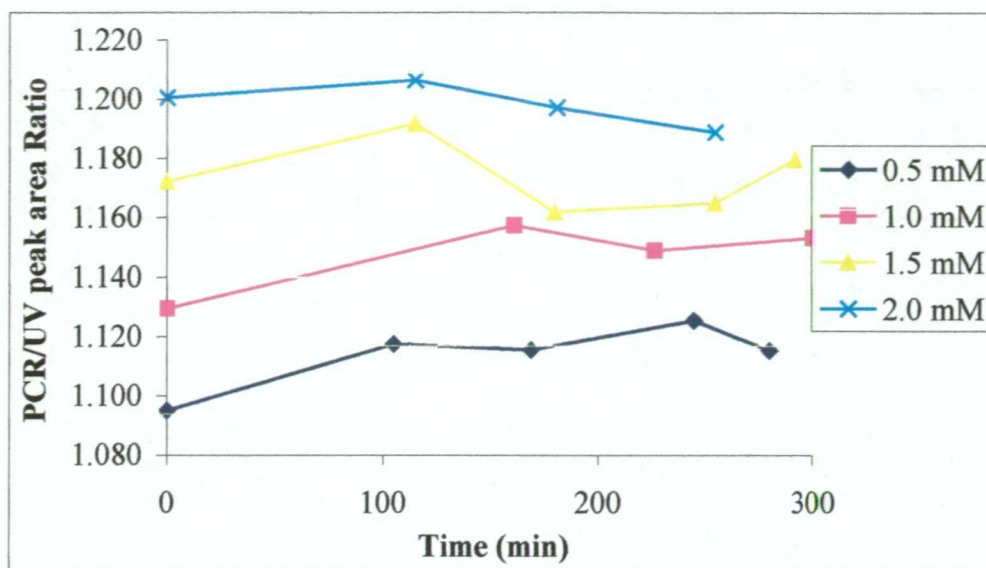
Fig. 5.13: Ratio of PCR and UV detector response. This provides an indication of the degree of dilution errors in standards of equivalent concentration but different R values.

5.3.4   Comparison between HPLC and AAS results for Cu and Au

Cu results

The Cu(I)-cyanide standard was prepared from CuCN and NaCN. The Cu concentration in this standard was checked by AAS and found to be within 1% of the calculated concentration. Mill samples were analysed for Cu by both HPLC and AAS and an excellent agreement between the two sets of results was found, with differences of $\leq$ 1%.

Au results

The HPLC Au standard was prepared from $K[Au(CN)_2]$ dissolved in an alkaline cyanide solution. An aqueous AAS Au standard was prepared from a Au / HCl AAS stock solution and an alkaline cyanide solution. The HPLC standard (4.0 ppm Au) was analysed by AAS and the Au concentration was found to be 3.87 ppm (RSD = 1.3 % for 6 determinations). Mill samples from consecutive shifts were analysed for Au by both techniques. The concentrations of the HPLC Au standards were adjusted by a factor of 3.87 / 4.0 to account for the difference between the HPLC and AAS standards. The HPLC results were up to 8 % greater than those obtained by AAS, as shown in Table 5.8.

5.3.5 Analysis of Mill samples

Cyanide analysis

The development of the eluent for use at Telfer (Section 5.3.1) included the addition of cyanide (160 μM) to the eluent. This concentration of cyanide was required for the separation of thiocyanate and Cu(I)-cyanide on a 5 cm Nova-Pak C-18 column. It has already been discussed that this separation is affected by the concentration of these two analytes. The concentrations of thiocyanate and Cu(I)-cyanide found in typical Telfer mill samples were used as a guide in this development.

Since the addition of cyanide to the eluent partly suppressed the dissociation of the Cu(I)-cyanide complexes, there was a difference in the cyanide concentrations determined titrimetrically and by the HPLC method, as shown in Table 5.9. An eluent without cyanide was also used to analyse the Mill samples on a 5 cm Nova-Pak C-18 column. These chromatographic conditions resulted in the partial merging of the thiocyanate and Cu(I) peaks and significant tailing of the cyanide peak to the extent that the cyanide and Cu(I) peaks were not baseline resolved, as shown in Fig. 5.14.

The cyanide concentrations determined by HPLC with the eluent containing no NaCN were still less than for the cyanide concentrations determined by titration. It is interesting to note that early work in this project (Chapter 3) found that there was reasonable agreement between titrimetric and HPLC results. It should also be noted that the chromatographic conditions were different, with the separation performed on a 15 cm Nova-Pak C-18 column using an eluent containing Waters acetonitrile and Waters Low UV PIC A as the IIR.

Standard addition of NaCN to Mill samples

Since it was not possible to compare the titration and HPLC results directly, the standard addition technique was used to assess the analytical validity of the HPLC analyses. Two NaCN additions were made to three representative Mill samples. The additions were made as follows: 1.0 and 2.0 mL of standardised NaCN (1140 ppm) were added to 10.0 mL of each sample. The results, shown in

Table 5.10, found that recoveries were within 3 % of expected values, indicating that the cyanide analysis of these samples was not suffering from interferences.

Sample	[Au] / ppm (HPLC)	[Au] / ppm (AAS)	HPLC / AAS (% Difference)
CIL D/S	2.41	2.24	108
CIL N/S	1.67	1.64	102

Table 5.8: Comparison of Au analyses by HPLC and AAS for two Mill samples.

Sample	[NaCN] / ppm		
	Titration	HPLC (160 μM CN in eluent)	HPLC (No CN in eluent)
CIL	118	72	104
TAILS	177	126	154

Table 5.9: Comparison of HPLC and titration cyanide results for Mill samples.
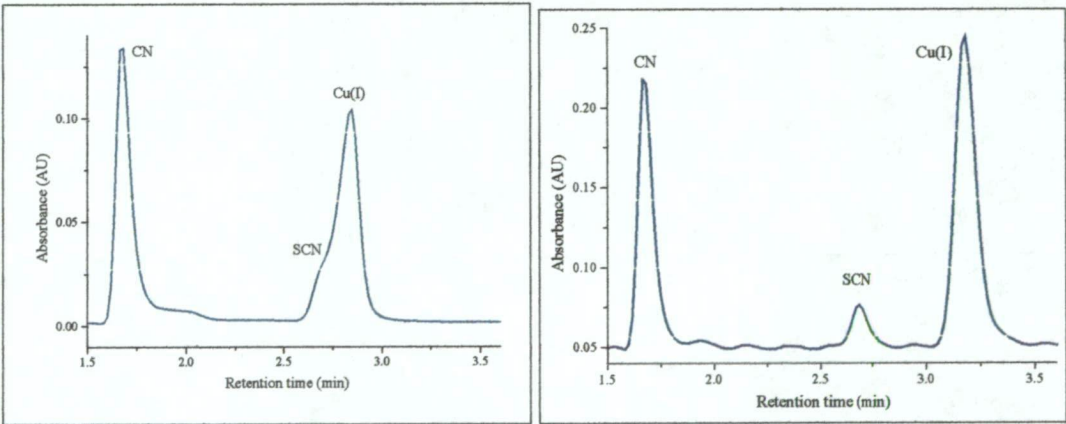
Fig. 5.14: Analysis of a mill tails sample using (a) (LHS) no added cyanide and (b) (RHS) 160 μM cyanide added to the eluent. PCR detector chromatograms. Separation on a 5 cm Nova-Pak C-18 column. Eluent : 25 % acetonitrile, 9 mM TBAOH, 10 mM KH_2PO_4, 5 mM H_2SO_4; pH = 8.0.

Sample	[NaCN] / ppm HPLC analysis	[NaCN] / ppm Calculated	% Recovery
CIL	174	-	-
CIL + 104 ppm NaCN	265	262	101.4
CIL + 190 ppm NaCN	341	335	98.4
C7	78	-	-
C7 + 104 ppm NaCN	171	175	102.5
C7 + 190 ppm NaCN	256	255	99.6
TAILS	76	-	-
TAILS + 104 ppm NaCN	175	173	98.6
TAILS + 190 ppm NaCN	248	253	102.1

TABLE 5.10 : Recoveries for NaCN Standard Additions to Mill samples

5.3.6 Analysis of Dump Leach Samples

During the field trial at Telfer, the dump leach operations consisted of four leach pads (Leach Pads (LP) 1,2, 3 and 5) with a fifth pad under construction. The total annual capacity of all the leach pads rose from 10×10^6 tonnes in 1994 to 16×10^6 tonnes in 1996, before being reduced to 9×10^6 tonnes in 1997 for economic reasons [5, 28]. A schematic of the flowsheet in LP1, LP2 and LP3 is shown in Fig. 5.15. Important sampling points are at the pumps for the Barren Pond, Recycle pond, Intermediate pond and Pregnant pond.

Some Telfer LP samples were analysed at UTas prior to the first field trial. These studies focussed on the analysis of metallo-cyanide complexes and thiocyanate. The LP samples contained only low concentrations of thiocyanate (<3 ppm), Cu(I) (<10 ppm) and Fe(II) (<1 ppm). The Au(I) concentrations were as large as 1 ppm in some pregnant LP samples examined. Since the analyte concentrations were all low, the method development for the LP samples was performed on a 5 cm Nova-Pak C-18 column. There was a problem with the analysis of the $[Au(CN)_2]^-$ species in some samples due to the presence of late eluting peaks, as shown in Fig. 5.16. These components may have been due to some organic material in the ore, leach pad liner or anti-scaling agent. While the components responsible for these peaks were never

identified, the following observations are noteworthy. There was considerable variation in the concentration of the unidentified components and there was no correlation between the concentrations of the unidentified components and the Au(I) complex, as indicated in Fig. 5.16(a). It was also found that increasing the detection wavelength from 205 nm (the λ_{max} for $[Au(CN)_2]^-$) to 215 nm significantly reduced the interference from the unidentified components, as indicated in Fig. 5.16(b). Unfortunately, this change in detection wavelength also reduced the sensitivity for the Au(I) complex, with the peak area being reduced by 50%.

Typical chromatograms obtained from LP samples are shown in Figs. 5.17-5.19. The large void peak in the UV detector chromatograms shown in Figs. 5.17 and 5.18 was typical of all leach pad samples. This large peak was attributed, in part, to the anti-scaling agent used in all the leach pads to prevent fouling with calcium and magnesium salts.
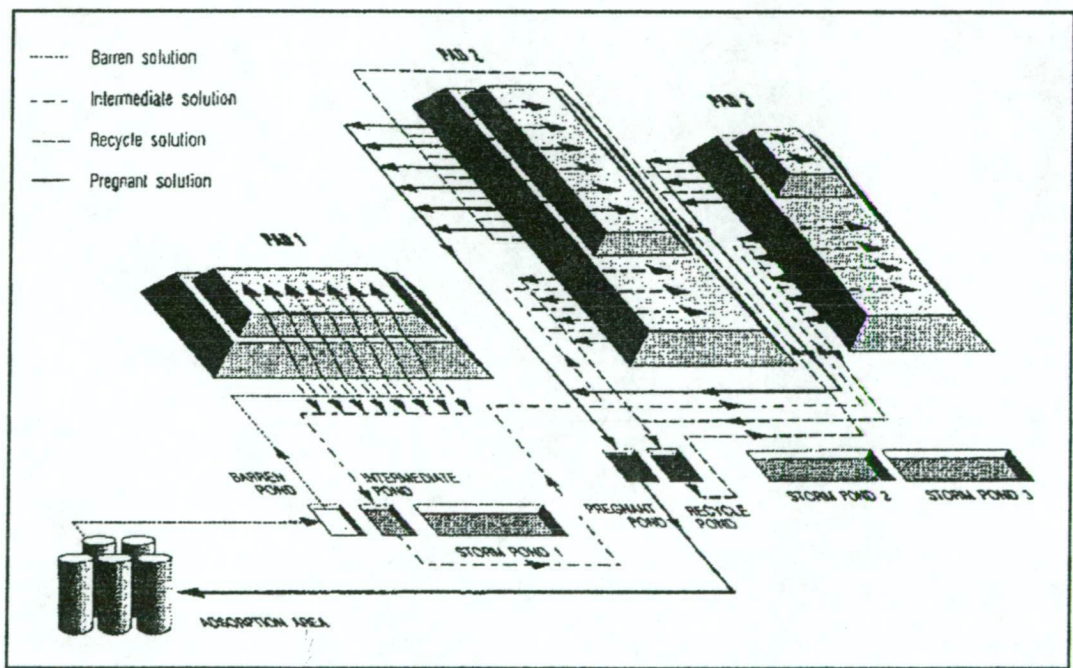
Fig. 5.15: Schematic flow-sheet for dump leach operations at the Telfer gold mine. Only LP1, LP2 and LP3 are shown. Source: Fig.3 from [5].
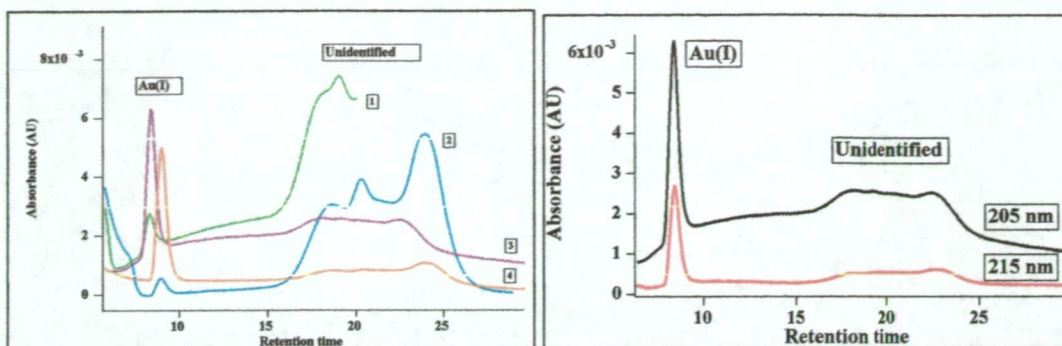
Fig. 5.16: Analysis for [Au(CN)$_2$]$^-$ in LP samples. UV detector chromatograms showing late eluting peaks. **(a)** (LHS) Detection wavelength: 205 nm. Legend: (1) Intermediate pump; (2) Barren Pump; (3) LP5 Pregnant pump; (4) LP3 Pregnant pump. **(b)** (RHS) LP5 Pregnant pump sample analysed at two detection wavelengths. Injection volume: 100 μL. Column: 5 cm Nov-Pak C-18. Eluent: 25% acetonitrile, 5 mM TBAOH, 5 mM H$_3$PO$_4$, 7 mM Na$_2$SO$_4$; pH = 8.0
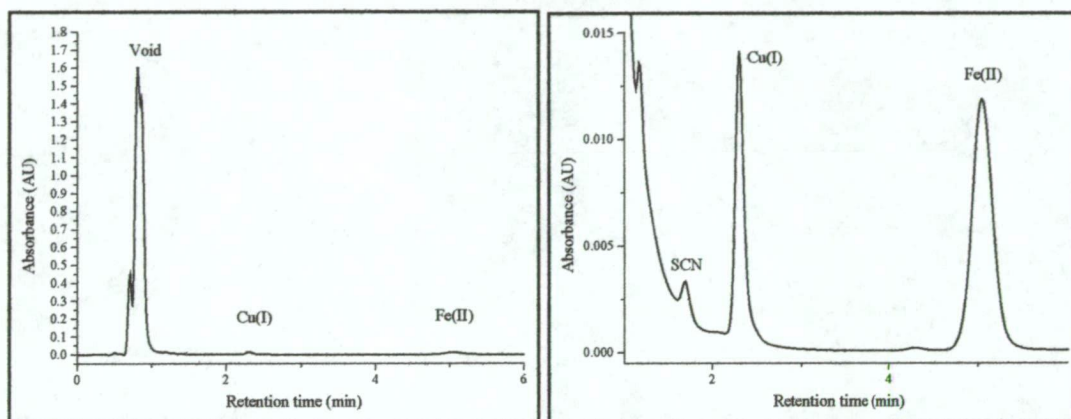
Fig. 5.17: UV (225 nm) detector chromatogram of LP#1 Pregnant sample. RHS: Enlarged section. Column: 5 cm Nov-Pak C-18. Eluent: 25% acetonitrile, 10 mM TBAOH, 10 mM H$_3$PO$_4$, 5 mM Na$_2$SO$_4$, 160 μM NaCN; pH = 8.0. Injection volume: 10 μL.
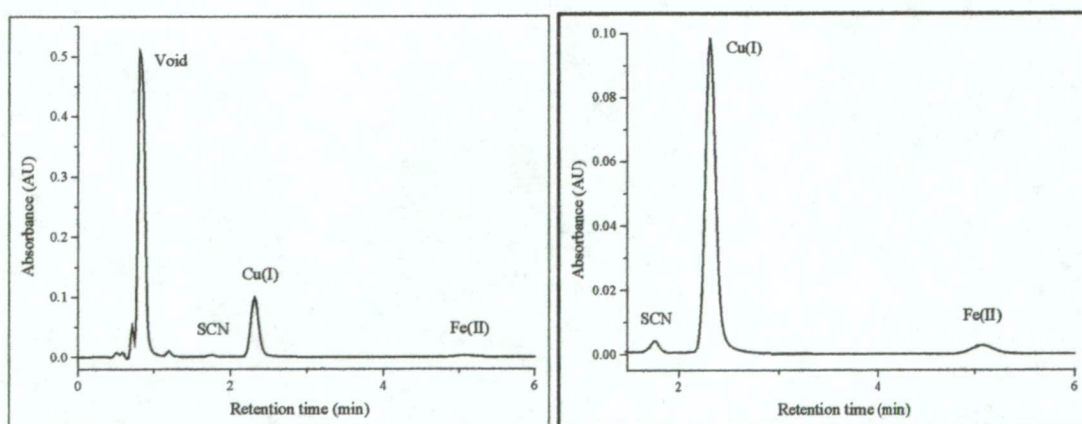
Fig. 5.18: UV (225 nm) detector chromatogram of LP#5 Pregnant sample. RHS: Enlarged section. Chromatographic conditions as for Fig. 5.16.
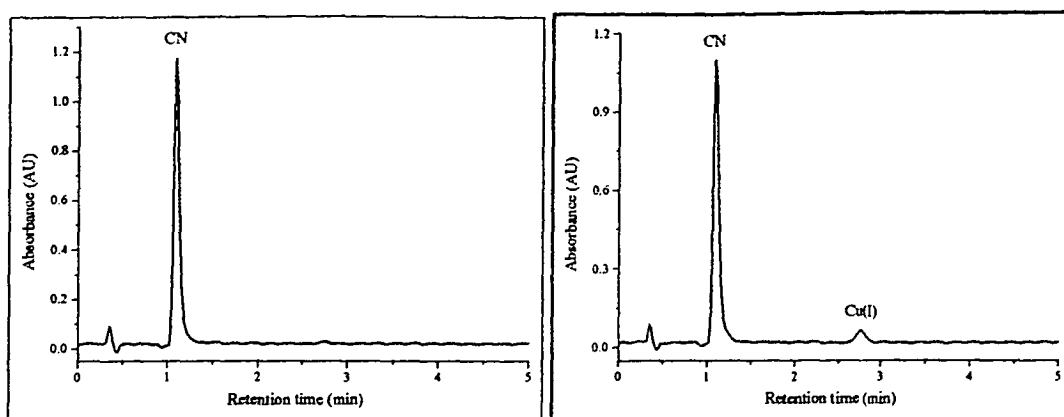
Fig. 5.19: PCR detector chromatograms. LHS: LP1 Pregnant sample; RHS: LP5 Pregnant sample. Chromatographic conditions as for Fig. 5.16.

Since there were only low Cu(I) concentrations in all the LP samples, it was expected that the titrimetric and HPLC cyanide analyses would show good agreement. A comparison of cyanide analyses performed by these two techniques for a variety of LP samples is shown in Table 5.11. While there was good agreement for some samples, there was significant variations found for some LP5 samples. The reproducibility for the HPLC cyanide analyses was less than 1%.

Significant tailing of the cyanide peak was observed in the LP5 Intermediate and LP5 Pregnant Pump samples. The cyanide peak tailing was not a concentration effect since NaCN standards with the same cyanide concentrations, as found in these two samples, did not show the same degree of peak tailing evident in Fig.5.20. None of the LP1 samples displayed cyanide peak tailing. There was a definite correlation between cyanide peak tailing and significant variation between the titrimetric and HPLC cyanide analyses. It was noted that repeated injections of the LP samples resulted in column damage. Since the pH of the LP samples was reasonably low (pH 9 ± 0.8), the column damage was probably the result of precipitation of sample components within the column. When a new 5 cm Nova-Pak C-18 column was installed in the HPLC instrument, similar results were obtained when fresh LP samples were analysed.

Sample name	[NaCN] / (ppm)		
	Titration	HPLC	Difference
LP #1 Barren Pump	140	165	25
LP #1 Intermediate Pump	250	269	19
LP #1 Recycle Pump	240	263	23
LP #5 Barren Pump	340	343	3
LP #5 Intermediate Pump	280	380	100
LP #5 Pregnant Pump	140	241	101

Table 5.11: Comparison of titrimetric and HPLC cyanide analyses of LP samples.
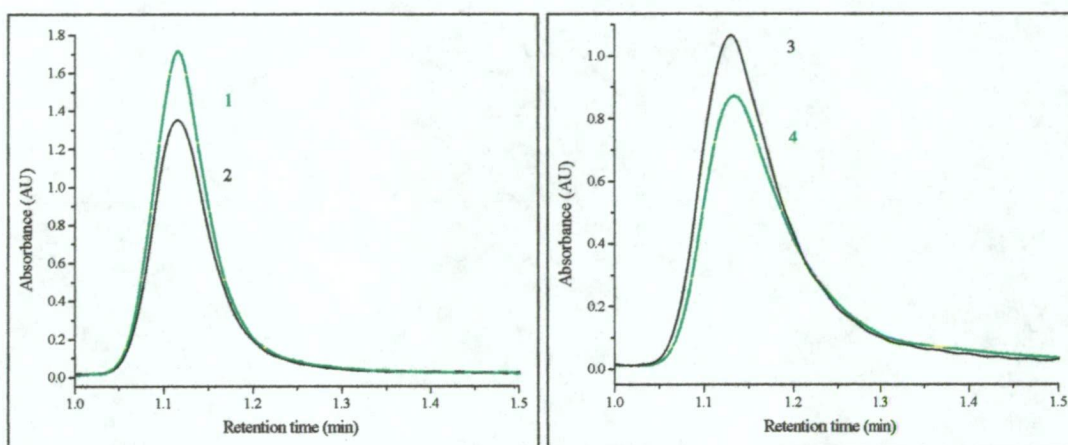
Fig. 5.20: PCR detector chromatograms comparing cyanide peak tailing for NaCN standards (LHS) and LP samples (RHS). Legend: (1) 440 ppm NaCN standard; (2) 390 ppm NaCN standard; (3) LP5 Intermediate Pump sample; (4) LP5 Barren Pump sample.

Addition of EDTA to the eluent

Since the LP samples, and in particular the LP5 samples, contained up to 1000 ppm of Mg^{2+} and Ca^{2+}, the effect of these cations on cyanide standards was investigated. Three standards were prepared which contained 200 ppm NaCN alone or with either 120 ppm Mg^{2+} or 120 ppm Ca^{2+}. Comparison of the cyanide peaks of these standards showed that both these cations caused some tailing of the cyanide peak.

The effect of a complexing agent on the cyanide peak shape was then investigated. EDTA was selected, as it is a very effective complexing agent for both Mg^{2+} and

Ca^{2+} [29]. It was found that the addition of EDTA to the LP5 Intermediate pump sample prior to analysis significantly improved the cyanide peak shape, as shown in Fig.5.21. Major changes to the early eluting peaks in the UV detector chromatograms were observed after the addition of EDTA to the sample. These changes were partly due to the strong UV absorption of EDTA. The second large peak in the UV detector chromatogram was possibly due to metal-EDTA complexes. Further evidence for this hypothesis is discussed below.

Consequently, it was decided to investigate the effects of EDTA in the eluent on the cyanide peak shape, thereby allowing *in-situ* complexation of both Mg^{2+} and Ca^{2+}. The initial EDTA concentration in the eluent was 1 mM. This eluent prevented the cyanide peak tailing, as shown in Fig 5.21. In addition, there was no change in the cyanide peak of a NaCN standard between the eluents containing no EDTA and 1 mM EDTA. There was, however, a large increase in the baseline absorbance for the UV detector with the eluent containing 1 mM EDTA, indicating that the shorter detection wavelengths could not be used, as shown in Table 5.12. This meant that the use of EDTA in the eluent significantly reduced the sensitivity of the UV detector. This is especially important with respect to analysis of the Au(I) complex in LP samples.
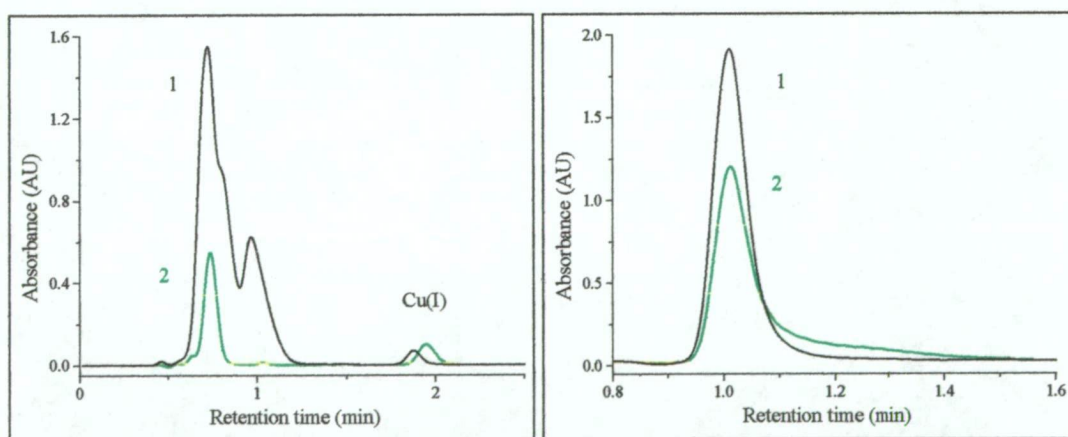
Fig. 5.21: UV (225 nm) and PCR detector chromatograms of a LP Intermediate pump sample (1) with and (2) without the addition of EDTA to the sample prior to analysis. PCR detector chromatogram (LHS) shows the effect on the cyanide peak tailing. Column: 5 cm Nova-Pak C-18. Eluent: 25 % acetonitrile, 10 mM TBAOH, 10 mM KH$_2$PO$_4$, 5 mM H$_2$SO$_4$, 160 µM NaCN, pH = 8.0

A large negative peak was observed in the UV detector chromatogram about 30 sec after the void peak, as shown in Fig. 5.22. Since cyanide is eluted very close to the void volume, these observations suggest that the Mg^{2+} and Ca^{2+} EDTA complexes are slightly retained. A possible mechanism for this separation is cation ion-interaction since the major EDTA species in the eluent (at pH = 8) are $EDTA^{3-}$ and $EDTA^{4-}$ and the large negative peak indicates the elution of a non-UV absorbing species. Further evidence of this possible mechanism is provided later in this section.

[EDTA] /mM	Baseline absorbance (AU)		
	205 nm	214 nm	225 nm
0	- 0.041	- 0.086	- 0.099
0.1	+ 0.245	-	- 0.032
0.2	+ 0.409	+ 0.161	+ 0.045
0.4	+ 0.736	+ 0.407	+ 0.196
1.0	+ 1.982	+ 1.294	+ 0.693

Table 5.12: Effect of EDTA concentration in the eluent on baseline absorbance of the UV detector at 205, 214 and 225 nm.
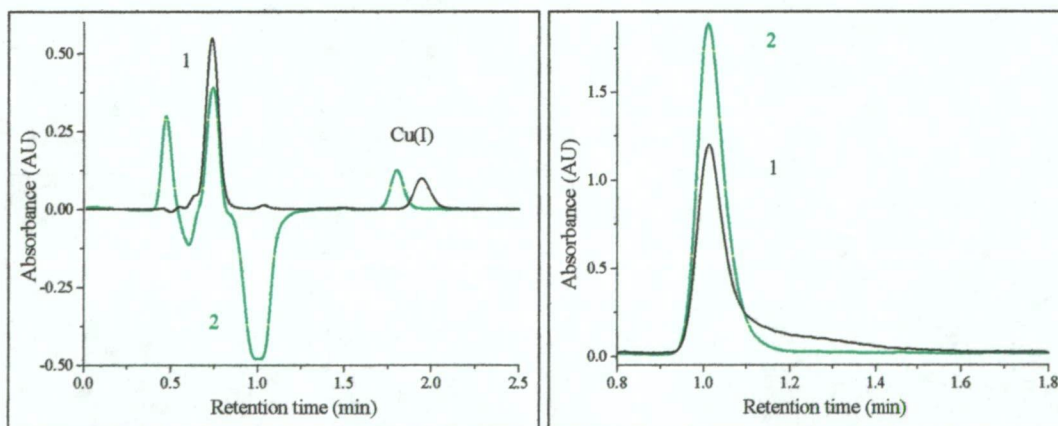
Fig. 5.22: Effect of EDTA in the eluent on cyanide peak tailing. Legend: (1) No EDTA in eluent; (2) 1.0 mM EDTA in eluent. Sample: LP5 Intermediate pump. LHS: UV (225) detector chromatogram. RHS: PCR detector chromatogram. Other conditions as for Fig. 5.18.

The effect of various concentrations of EDTA in the eluent was then studied with a series of eluents containing 0.1, 0.2 and 0.4 mM EDTA. The main purpose of these experiments was to determine if an eluent with an EDTA concentration lower than 1 mM could reduce the cyanide peak tailing, thereby improving the UV detection sensitivity. An eluent containing no EDTA was also used to allow a comparison to be made with the same samples. The cyanide concentrations in the LP5 Barren and Intermediate Pump samples were beyond the calibration range, requiring a two-fold dilution for each sample. These diluted samples were not analysed in the eluents containing 0 and 0.4 mM EDTA. However, a four-fold dilution of the LP5 Barren and Intermediate Pump samples was analysed with the eluent containing 0.4 mM EDTA. The results for these analyses are shown in Table 5.13. The two samples that had significant cyanide peak tailing in the eluent without EDTA (LP5 Intermediate and Pregnant Pump samples), showed significant reduction of peak tailing with even 0.1 mM EDTA in the eluent. The UV detector chromatograms for these eluents showed that the retention times of the Cu(I) and Au(I) complexes generally decreased as the EDTA concentration in the eluent increased, as shown in Table 5.14. An exception occurred with the eluent containing 0.2 mM EDTA, due probably to the loss of acetonitrile during preparation of this eluent.

Examination of the results in Table 5.13 revealed that once again that there was little difference between the titration and initial HPLC results (i.e. No EDTA in the eluent) for the LP1 samples. However, the subsequent analyses with 0.1 and 0.2 mM EDTA in the eluent showed the HPLC cyanide concentrations to be decreasing, while the HPLC cyanide concentration for LP1 Intermediate Pump sample had increased with 0.4 mM EDTA. The most likely cause for these discrepancies was the NCS reagent, which was two days old for the eluents containing 0-0.2 mM EDTA and freshly prepared for the eluent containing 0.4 mM EDTA. The result for the LP5 Intermediate Pump sample with 0.2 mM EDTA in the eluent may also have been affected by the aged NCS reagent. By contrast, the HPLC results for the LP5 Pregnant Pump sample were almost the same in all four eluents. All three LP5 samples had cyanide concentrations of between 120 and 180 ppm NaCN greater than the titration results, regardless of the EDTA concentration in the eluent. Although

the reason for these large differences remains unknown, it should be noted that these experiments demonstrated that the cause was not due to the high concentrations of Mg^{2+} and Ca^{2+} in the LP5 samples.

In order to determine if any changes occurred on dilution of the samples with RO-grade water, three dilutions of the LP1 Intermediate Pump sample were made, as shown in Table 5.15. The slight differences in the cyanide concentrations between the dilutions were possibly due to dilution errors.

Sample name	NaCN concentration (ppm)				
	Titration	HPLC No EDTA	HPLC 0.1 mM EDTA	HPLC 0.2 mM EDTA	HPLC 0.4 mM EDTA
LP1 Barren Pump	190	199	180	171	NA
LP1 Intermediate Pump	290	285	264	249	276
LP1 Recycle Pump	280	296	281	263	NA
LP5 Barren Pump	410	NA	532	517	501
LP5 Intermediate Pump	330	NA	518	545	515
LP5 Pregnant Pump	170	295	292	289	296

Table 5.13: Cyanide analysis of LP1 and LP5 samples with eluents containing 0, 0.1, 0.2 and 0.4 mM EDTA. NA: Sample was not analysed in this eluent.

Eluent [EDTA] (mM)	Retention time (minutes)			
	SCN-	Cu(I)	Fe(II)	Au
0	1.77	2.32	5.08	10.15
0.1	-	2.22	4.75	9.10
0.2	-	2.22	4.60	9.30
0.4	-	2.15	3.90	8.70
1.0	1.50	1.80	3.12	ND

Table 5.14: Effect of various EDTA concentrations in the eluent on retention times.
ND = Not Detected.

mL sample	4	3	2	1
mL RO water	0	1	2	3
Dilution factor	1.0	0.75	0.50	0.25
[NaCN] (ppm)	271	275	268	264

Table 5.15: Dilution of LP1 Intermediate Pump sample with RO-grade water

The large negative peak that was observed in the UV chromatogram when using 1 mM EDTA in the eluent was present in all three eluents with EDTA. An interesting phenomenon observed with this negative peak was that the peak width decreased as the eluent EDTA concentration was increased. When the UV chromatograms of the LP1 Intermediate Pump sample and its three dilutions (from Table 5.15) were examined, it was found that the large negative peak decreased with the sample concentration, as shown in Fig. 5.23. No negative peak was observed when the UV detector chromatograms of a series of NaCN standards were examined. These observations provide additional evidence for the cation ion-interaction mechanism proposed earlier in this section.
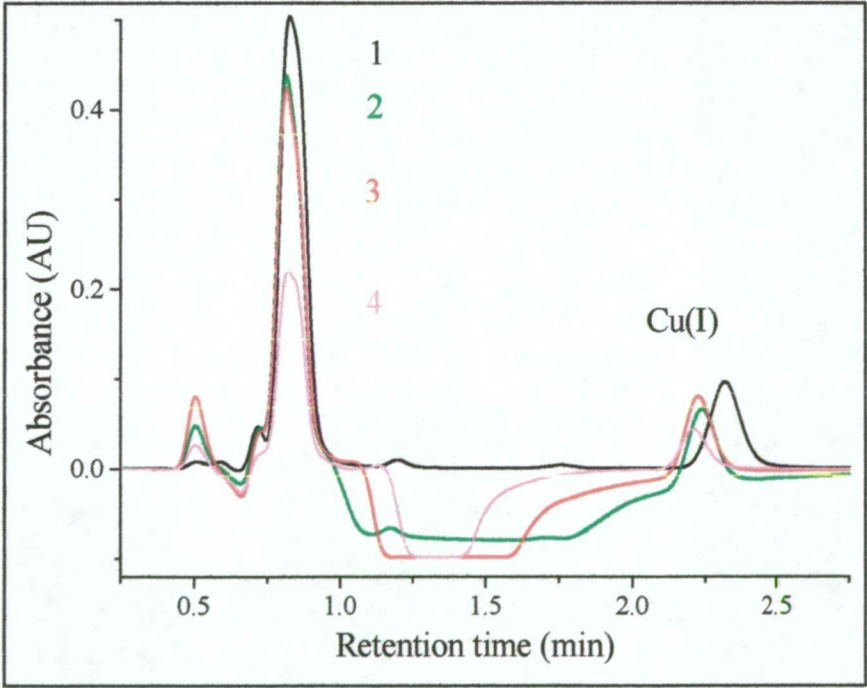
Fig. 5.23: UV(225 nm) detector chromatograms of LP5 Intermediate sample analysed with (1) No EDTA; (2) 0.1 mM EDTA; (3) 0.2 mM EDTA and (4) 0.4 mM EDTA in eluent.
Other chromatographic conditions as for Fig. 5.18.

Due to the broad negative peak with lower eluent EDTA concentrations, the baseline under the Cu(I) peak was sloping, potentially causing some peak integration problems. However, it should also be recognised that only low Cu(I) concentrations were present in the LP samples and consequently routine analysis for Cu(I) was not important for these samples.

Some LP samples were analysed for [Au(CN)$_2$]$^-$ in the eluents containing 0.1 and 0.4 mM EDTA. These analyses used a 100 µL injection with a detection wavelength of 205 nm. The [Au(CN)$_2$]$^-$ peak data and Au concentrations in these samples are shown in Table 5.16. Comparison of the data for the LP1 Intermediate Pump and LP5 Intermediate Pump samples reveals that the eluent containing 0.4 mM EDTA reduced the detection sensitivity for [Au(CN)$_2$]$^-$ to about 1/6 of that in the eluent containing 0.1 mM EDTA. In addition, the separation of the [Au(CN)$_2$]$^-$ peak from earlier eluting peaks was reduced in the eluent containing 0.4 mM EDTA. Because of these effects, it would not be possible to routinely and automatically integrate the [Au(CN)$_2$]$^-$ peak with reasonable precision in the eluent containing 0.4 mM EDTA for samples containing less than 0.20 ppm Au. The lower limit for analysis in the eluent containing 0.1 mM EDTA was estimated to be 0.03 ppm Au from extrapolation of the Peak Height / Au concentration data for the above samples.

Sample	Eluent [EDTA]	Peak Height	Peak Area	[Au(I)] (ppm)
LP1 Barren Pump	0.1 mM	2781	88129	0.07
LP1 Intermediate Pump	0.1 mM	4184	114002	0.11
LP1 Recycle Pump	0.1 mM	15073	427440	0.30
LP5 Barren Pump	0.4 mM	396	10204	0.09
LP5 Intermediate Pump	0.4 mM	1214	35705	0.20

Table 5.16: [Au(CN)$_2$]$^-$ peak data and Au(I) concentrations in some LP samples. Eluents contained 0.1 mM EDTA and 0.4 mM EDTA.

Standard additions of NaCN were made to LP samples in order to verify the analytical accuracy of the HPLC method. These standard additions should also have revealed if there was interference in the HPLC cyanide determinations. These analyses were performed with eluents containing no EDTA and 0.4 mM EDTA.

0.4 mM EDTA in the eluent

Standard additions were performed to the LP1 Intermediate, LP5 Intermediate, LP5 Barren and LP5 Pregnant Pump samples. The dilutions were freshly prepared from the samples. These standard additions were prepared as follows: 1.0 mL of each sample (2.0 mL for the LP5 Pregnant Pump sample) was diluted to 4.0 mL with 1.0, 2.0 or 3.0 mL of RO water or 171 ppm NaCN. The determined and calculated cyanide concentrations and recoveries are shown in Table 5.17.

No EDTA in the eluent

Standard additions of NaCN were made to the LP5 Flume 1, 2 and 3, LP5 Intermediate Pump and LP5 Pregnant Pump samples. No standard additions were made to any LP1 samples since these samples showed no cyanide peak tailing. In addition, the titration and HPLC results agreed reasonably well for the LP1 samples. These standard additions were prepared as follows : 1.0 mL of 1140 ppm NaCN was added to 10.0 mL of each sample (20.0 mL for the first standard addition to the LP5 Pregnant Pump sample). The preparation of these standard additions differed from that listed in Table 5.17 in order to minimise dilution of possible interfering species. The determined and calculated cyanide concentrations and recoveries are shown in Table 5.18. The titrimetric results for these samples are also shown, revealing that the cyanide concentrations as determined by the HPLC results were once again in excess of the titration results by 55 - 170 ppm NaCN.

LP Pump Sample	Added [NaCN]	Found [NaCN]	Calculated [NaCN]	Recovery (%)
LP1 Intermediate / 4	0	68.2	-	-
LP1 Intermediate / 4	42.8	109.3	111.0	101.6
LP1 Intermediate / 4	85.5	151.1	153.8	101.8
LP1 Intermediate / 4	128.3	195.6	196.6	100.5
LP5 Intermediate / 4	0	130.5	-	-
LP5 Intermediate / 4	42.8	178.0	173.3	97.4
LP5 Intermediate / 4	85.5	220.1	216.1	98.2
LP5 Intermediate / 4	128.3	257.9	258.9	100.4
LP5 Barren / 4	0	131	-	-
LP5 Barren / 4	42.8	169.4	173.8	102.6
LP5 Barren / 4	85.5	216.6	216.6	100.0
LP5 Barren / 4	128.3	254.0	259.4	102.1
LP5 Pregnant / 2	0	157.2	-	-
LP5 Pregnant / 2	42.8	197.3	200.0	101.4
LP5 Pregnant / 2	85.5	236.1	242.8	102.8

Table 5.17: Standard additions of NaCN to LP samples with an eluent containing 0.4 mM EDTA. NaCN concentrations are expressed in ppm.

LP5 Sample	Titration [NaCN]	Added [NaCN]	Found [NaCN]	Calculated [NaCN]	Recovery (%)
Flume 1	180	0	235.3	-	-
Flume 1	-	103.6	306.6	317.5	103.6
Flume 3	210	0	382.3	-	-
Flume 3	-	103.6	458.0	451.1	98.5
Flume 5	240	0	399.3	-	-
Flume 5	-	103.6	481.6	466.6	96.9
Pregnant Pump	200	0	273.9	-	-
Pregnant Pump	-	54.3	304.3	315.2	103.6
Pregnant Pump	-	103.6	342.7	352.6	102.9
Intermediate Pump	430	0	519.0	-	-
Intermediate Pump	-	103.6	567.8	575.4	101.3

Table 5.18: Standard additions of NaCN to LP5 samples with an eluent containing no EDTA. NaCN concentrations are expressed in ppm.

Comparison of the results listed in Tables 5.17 and 5.18 showed that slightly better recoveries were achieved with the eluent containing 0.4 mM EDTA. However, it is uncertain if this observation is due to the dilution of interfering species, the effect of EDTA in the eluent, or dilution errors. Some samples were sent to Perth for analysis by an independent laboratory. Unfortunately, the results obtained from the use of blind samples revealed that the Perth laboratory results were not reliable.

5.3.7 Detection of cyanide using a Ni^{2+} reagent

Ni^{2+} reagent in the eluent

Due to the differences between the titrimetric and HPLC results for cyanide in the LP5 samples, an alternate detection system for cyanide was investigated. The reaction of Ni^{2+} with cyanide to form $[Ni(CN)_4]^{2-}$ was selected in part because the necessary reagents were available at Telfer. In addition, this derivatisation reaction had been previously used by other workers to determine cyanide by FIA, HPLC and CZE techniques [30-35]. The $[Ni(CN)_4]^{2-}$ complex has absorption maxima at 267, 284 and 310 nm with molar absorptivities of 11,600; 4,600 and 690 $M^{-1}.cm^{-1}$, respectively [30]. The UV spectrum of the $[Ni(CN)_4]^{2-}$ complex in the range 250-360 nm is shown in Fig. 5.24. While more intense absorption bands occur at shorter wavelengths, previous methods have used 267 nm to reduce the interference from other species and to allow sufficient sensitivity. The major interference in the determination of cyanide using a Ni^{2+} reagent is caused by sulfide [30, 31]. Thiocyanate, thiosulfate, sulfite and some organic acid anions have also been reported to cause moderate interference with detection at 267 nm [31]. The effect of detection wavelength on the $[Ni(CN)_4]^{2-}$ peak response is shown in Fig 5.25.

It was decided to initially investigate the *in-situ* complexation of Ni^{2+} with cyanide and the subsequent separation of the $[Ni(CN)_4]^{2-}$ complex from potential interferences on a 5 cm Nova-Pak C-18 column using similar separation conditions to those described earlier in this chapter. In order to verify that the product of this *in-situ* complexation was $[Ni(CN)_4]^{2-}$, a standard was prepared from $K_2[Ni(CN)_4]$.

Since only the $Ni(NO_3)_2$ salt was available at Telfer, a preliminary test confirmed that nitrate would not seriously interfere in the detection of $[Ni(CN)_4]^{2-}$ at 267 nm.
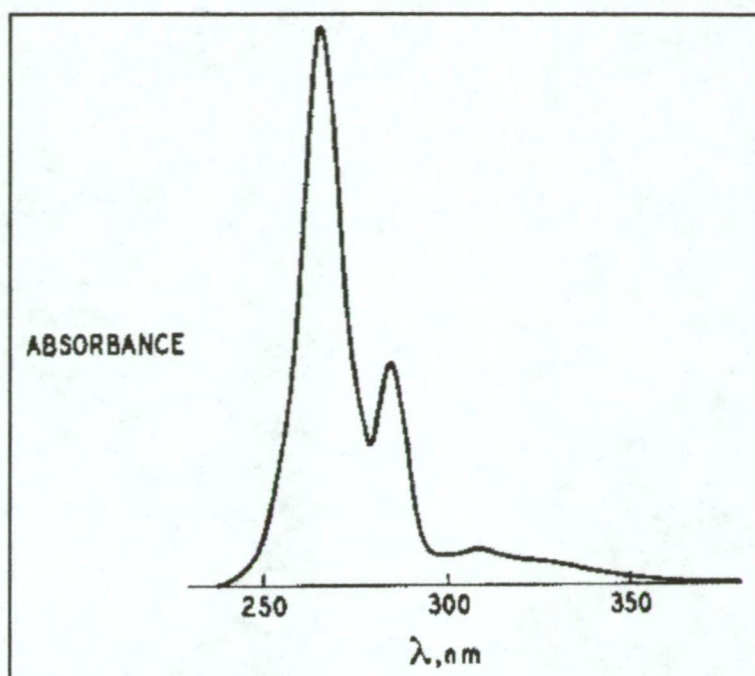
Fig. 5.24: UV spectrum of $[Ni(CN)_4]^{2-}$. Source: Fig. 1 from [30]
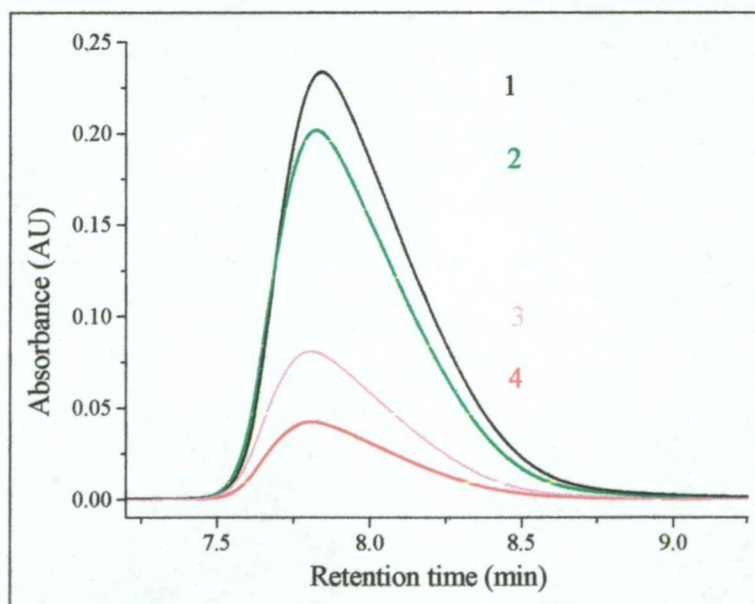
Fig 5.25: Effect of detection wavelength on $[Ni(CN)_4]^{2-}$ peak response.

Standard: 1.2 mM $[Ni(CN)_4]^{2-}$ (80 ppm Ni). Detection wavelengths: (**1**) 205 nm; (**2**) 268 nm; (**3**) 280 nm; (**4**) 254 nm. Eluent: 23% acetonitrile, 8 mM TBAOH, 8 mM $(NH_4)_2SO_4$, 3.2 mM H_2SO_4, 200 µM NaCN; pH 8.0. Column: 5 cm Nova-Pak C-18

Addition of $Ni(NO_3)_2$ to an eluent containing 25% acetonitrile, 10 mM TBAOH, 10 mM KH_2PO_4 and 5 mM H_2SO_4 at pH 8 resulted in the immediate formation of a pale green precipitate. In earlier experiments when an ammoniacal buffered Ni^{2+} solution was used as a PCR reagent for the derivatisation of cyanide, it was observed that the reaction coil became blocked due to formation of a precipitate. Addition of $Ni(NO_3)_2$ separately to each eluent component found that the precipitation was due to the phosphate buffer. This result is understandable since the solubility product of $Ni_3(PO_4)_2$ is very low ($K_{SP}=10^{-32}$ [29]).

A new eluent that did not contain a phosphate buffer was then developed. The initial focus of this development was to determine if it was possible to achieve *in-situ* derivatisation of cyanide in an eluent containing a Ni^{2+} reagent. The composition of the eluents prepared in this development work is shown in Table 5.19.

The first eluent shown in Table 5.19 resulted in a very broad $[Ni(CN)_4]^{2-}$ peak with a peak width greater than 10 minutes. Since this eluent was completely unbuffered, the subsequent eluents contained $(NH_4)_2SO_4$. This reagent was selected since an ammonia buffer has been used previously in the determination of cyanide with a Ni^{2+} reagent [30, 31]. $(NH_4)_2SO_4$ was selected over aqueous ammonia solutions since it was more convenient to handle.

While an ammonia buffer is far from ideal at pH 8, alternative buffers such as tris(hydroxymethyl)-aminomethane (Tris) were not available at Telfer. The second eluent in Table 5.19 produced a very narrow $[Ni(CN)_4]^{2-}$ peak with a retention time of 2.35 minutes with no pre-column reaction time. The effect of pre-column reaction time was investigated with this eluent by placing up to three knitted 5m x 0.30 mm I.D. reaction coils between the injection valve and column. These reaction coils created pre-column reaction times of 66, 43 and 20 seconds for three, two and one 5 m reaction coils respectively. A series of cyanide standards was injected with each pre-column reaction time. The detection wavelength initially used was 268 nm. Since it was envisaged that two detectors would eventually be required, the detection wavelength was changed to 254 nm, thus allowing use of the fixed wavelength detector fitted with a Hg lamp. The absorption at 254 nm was 10.5% that at 268 nm.

The calibration plots at 268 and 254 nm were almost linear, as shown in Fig. 5.26. A quadratic line of best fit provided the best fit with regression coefficients greater than 0.9998.
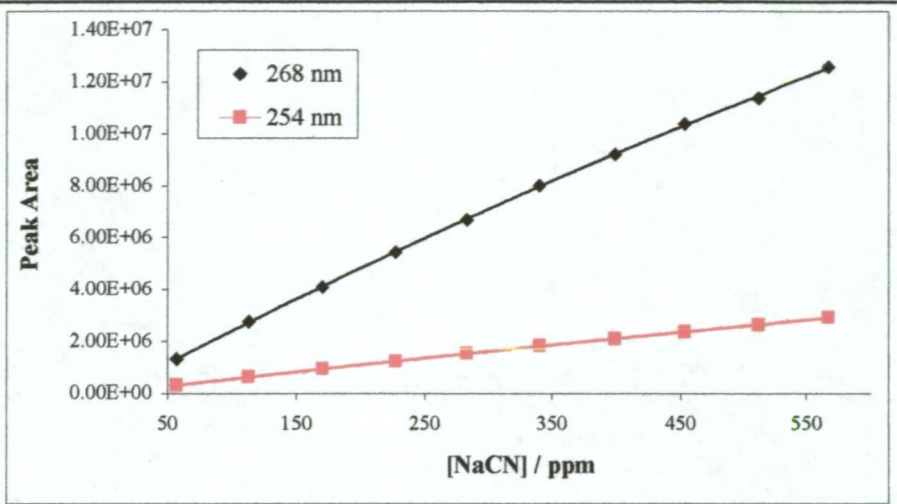
Fig. 5.26: Cyanide calibration at two detection wavelengths (254 and 268 nm) after *in-situ* derivatisation with a Ni^{2+} reagent.

Eluent #	[MeCN] (%)	[TBAOH] (mM)	[H$_2$SO$_4$] (mM)	[(NH$_4$)$_2$SO$_4$] (mM)	[Ni(NO$_3$)$_2$] (mM)	[Ni(CN)$_4$]$^{2-}$ Rt (min)
1	25	10	10	-	1	12
2	25	5	5	25	2	2.35
3	25	5	5	20	4	2.16
4	22.5	5	5	20	6	2.82

Table 5.19: Development of eluents for the *in-situ* derivatisation of cyanide with a Ni^{2+} reagent.

Comparison of the peak areas of the NaCN standards with the different pre-column reaction times showed that these values were very similar, indicating that the reaction was almost complete with no pre-column reaction time. This is not surprising since it is known that the formation of $[Ni(CN)_4]^{2-}$ is very rapid, especially when the pH is greater than 7 [31, 36]. However, the peak heights of the NaCN standards were greatest when there was no pre-column reaction coil. This was due to the increased peak dispersion created by using the pre-column reaction coils.

The cyanide calibrations were used to determine the cyanide concentration in a 1.23 mM $[Ni(CN)_4]^{2-}$ standard. The results were 4.47, 4.49 and 4.51 mM NaCN with the 43, 20 and 0 second pre-column reaction times using a detection wavelength of 254 nm. The mean cyanide concentration determined at 254 nm was 4.49 ± 0.02 mM NaCN. The detection wavelength had no effect on the cyanide result. This was shown by use of a 43 second pre-column reaction time with a detection wavelength of 268 nm. Under these conditions, the cyanide concentration in the $[Ni(CN)_4]^{2-}$ standard was 4.49 mM NaCN. Since the calculated cyanide concentration in the $[Ni(CN)_4]^{2-}$ standard was 4.92 mM, the reaction efficiency was 92% with each pre-column reaction time. This almost constant value for all three reaction times further indicated that the reaction was almost complete and that either the NaCN standards had lower concentrations than determined by $AgNO_3$ titration and/or the $K_2[Ni(CN)_4]$ standard was not pure.

Since the $[Ni(CN)_4]^{2-}$ species was eluted too early with the second eluent, the $(NH_4)_2SO_4$ concentration was reduced to 20 mM in the third eluent with the aim of increasing the retention time of the Ni(II) complex. However, the retention time of $[Ni(CN)_4]^{2-}$ was reduced to 2.16 minutes with this eluent.

The reaction coil(s) were initially removed from between the injection valve and column, as they appeared to have only a minimal effect on the extent of derivatisation. The peak areas of the NaCN standards were almost the same as with the second eluent. The 1.23 mM $[Ni(CN)_4]^{2-}$ standard was re-analysed and the cyanide concentration found was 4.51 mM NaCN, i.e., almost the same value as previously determined. Eight LP5 samples were then analysed using these conditions. The cyanide concentrations in these samples are shown under the column labelled HPLC #1 in Table 5.20. The titration results for these samples are presented for comparison.

A 5 m reaction coil was then placed between the column and injection valve to determine if a pre-column reaction time altered the results for the LP5 samples. While the peak areas for the NaCN standards remained almost the same, the peak areas for the samples decreased following merging of the sample void peak with the

$[Ni(CN)_4]^{2-}$ peak because of increased dispersion. These results are presented under the column labelled HPLC #2 in Table 5.20.

A fourth eluent was then prepared with the same composition as for the previous eluent, except that the acetonitrile concentration was reduced to 22.5% and the $Ni(NO_3)_2$ concentration was increased to 6 mM. The aim of these changes was to increase the retention time of the $[Ni(CN)_4]^{2-}$ and to improve the linearity of the calibration. The 5 m pre-reaction coil was removed for this eluent. The retention time of the $[Ni(CN)_4]^{2-}$ peak was increased to 2.82 minutes and the calibration was more linear. However, the peak width of $[Ni(CN)_4]^{2-}$ was increased more than for the previous two eluents. Consequently, there was some merging of the sample void peak with the $[Ni(CN)_4]^{2-}$ peak. The results for LP5 samples analysed with this eluent are presented under the column labelled HPLC #3 in Table 5.20. Figs. 5.27 and 5.28 illustrate the separation of the void and $[Ni(CN)_4]^{2-}$ peaks with the conditions used in Table 5.20 for a sample and a standard containing similar cyanide concentrations.

LP5 Sample	NaCN concentration (ppm)			
	Titration	HPLC #1	HPLC #2	HPLC #3
Barren Pump	380	569	555	533
Intermediate Pump	360	571	559	536
Pregnant Pump	180	330	327	311
Flume 1	180	315	293	254
Flume 2	220	373	349	300
Flume 3	210	380	358	303
Flume 4	200	375	355	307
Flume 5	240	398	380	329

Table 5.20: Analysis of LP5 samples by HPLC using Ni^{2+} in the eluent. The titration results were obtained a day later. HPLC # 1 and # 2 refers to the third eluent (Table 5.19) with no pre-column reaction coil and with a 5 m reaction coil respectively. HPLC # 3 refers to the fourth eluent (Table 5.19) without a pre-column reaction coil.

Comparison of the three sets of results given in Table 5.20 shows that the cyanide concentration in most of the samples decreased in each successive set, with the exception of the Pregnant Pump sample, which remained almost the same between

the first and second result sets. The largest decrease was observed for the Flume samples. The reason for these changes is unclear - however it is obvious that the changes are related to the samples. A similar observation was made earlier when LP samples were successively analysed on the one day with eluents containing 0, 0.1 and 0.2 mM Na_2EDTA. (See Table 5.13) While the changes in Table 5.13 were attributed to the NCS reagent, there may have been other factors involved as well, such as more rapid cyanide loss in some samples than other samples.

The samples shown in Table 5.20 were analysed by HPLC on the sampling date and analysed by titration on the following day. The samples were stored in a refrigerator overnight to minimise cyanide loss between the HPLC and titration analyses. It is interesting to note that the titration and HPLC #1 values are very similar to those listed in Table 5.17.
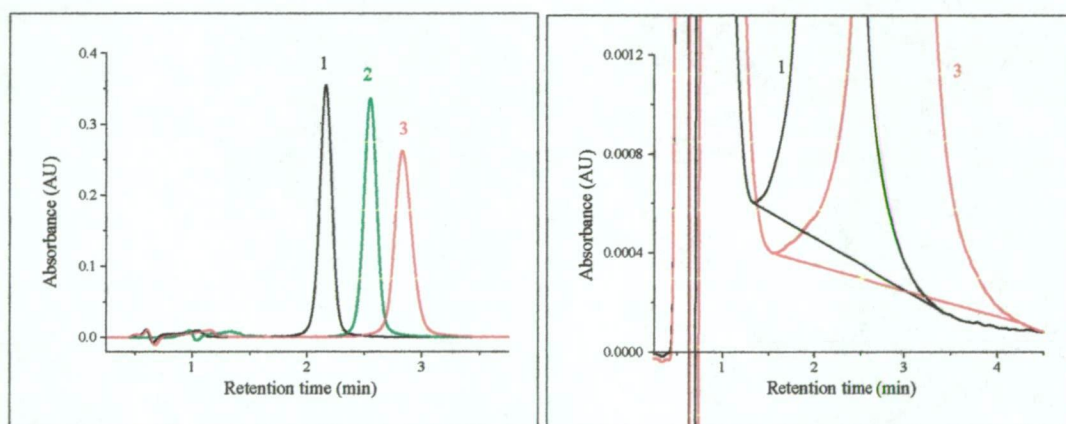
Fig. 5.27: Comparison of the derivatised cyanide peak (as the Ni(II) complex) for a LP5 Intermediate Pump sample under different conditions. Detection at 254 nm. The full-scale chromatograms are shown on the LHS, while expanded chromatograms illustrating the merging of the void and derivatised cyanide peaks are shown on the RHS. **(1)**, **(2)** and **(3)**: Conditions as for HPLC #1, HPLC #2 and HPLC #3, respectively in Table 5.20.
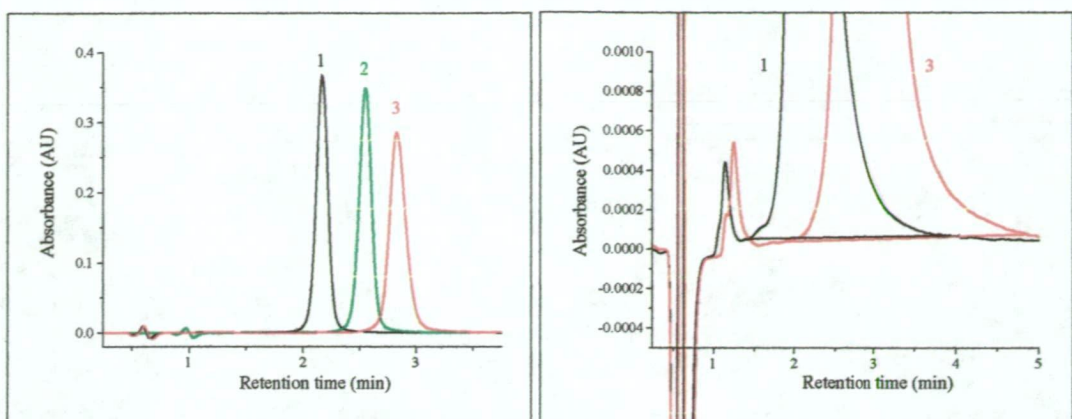
Fig. 5.28: Comparison of the derivatised cyanide peak (as the Ni(II) complex) for a NaCN standard under different conditions. Details same as for Fig. 5.24.

The samples shown in Table 5.17 were collected and analysed four days earlier than the samples shown in Table 5.20. There were only relatively small changes in the cyanide concentrations (as determined by titration) over this four-day period, as shown in Table 5.21. Consequently, it appeared as though the detection of cyanide in LP samples using a Ni^{2+} reagent in the eluent provided similar results to those obtained with the post-column reaction used in section 5.3.6.

LP5 Sample	Cyanide concentration (ppm NaCN)			
	Day 1	Day 2	Day 3	Day 4
Barren Pump	340	390	400	380
Intermediate Pump	430	420	430	360
Pregnant Pump	200	210	180	180
Flume 1	180	210	200	180
Flume 3	210	220	220	210
Flume 5	240	250	260	240

Table 5.21: Titration results for some LP5 samples over a four day period.

In concluding this section, it should be recognised that the significant difference observed by both HPLC methods may have been due to unknown interference(s). The effect of this interference may have been reduced as the retention time of the derivatised cyanide peak (i.e. the Ni(II) complex) was increased. Unfortunately,

time did not permit this important issue to be further addressed. In addition, there was some scepticism on the part of the Telfer Laboratory management with respect to the HPLC results for the LP samples. Finally, the HPLC instrument was only at Telfer for a limited time. Thus, from a process control viewpoint, it was considered more important to have a consistent (and possibly incorrect) analytical method (i.e. argentometric titration) than a method that may provide a more correct analysis but would not always be available.

Development and optimisation of an eluent containing ammonia buffer for the separation of thiocyanate and the metallo-cyanide complexes

In order to incorporate the developments described in the previous section into a chromatographic system for the simultaneous determination of cyanide, thiocyanate and the metallo-cyanide complexes, the most suitable configuration would be a coupled system, as shown in Fig. 5.29(a). This instrumental configuration would allow the separation of cyanide, thiocyanate and the metallo-cyanide complexes on a Nova-Pak C-18 column with an eluent containing cyanide (to stabilise the Cu(I) complex). The void volume from this first column (which contains the cyanide analyte) would be loaded into a sample loop connected to a column switching valve (SV). When the SV was operated, the cyanide would be injected onto a second Nova-Pak C-18 column. The eluent for the second column would contain a Ni^{2+} reagent to allow *in-situ* complexation and subsequent separation of $[Ni(CN)_4]^{2-}$ in a manner similar to that described in the previous section.

An instrumental configuration employing a flow-through system (as used with the NCS and INA/BA reagents) is shown in Fig. 5.29(b). The advantage of a coupled system over a flow-through system is that the derivatised cyanide peak (i.e., the Ni(II) complex) can be separated from any chemical or spectroscopic interference. The latter interference is a significant possibility with the Ni^{2+} reagent as detection is in the UV region (eg. 267 nm).
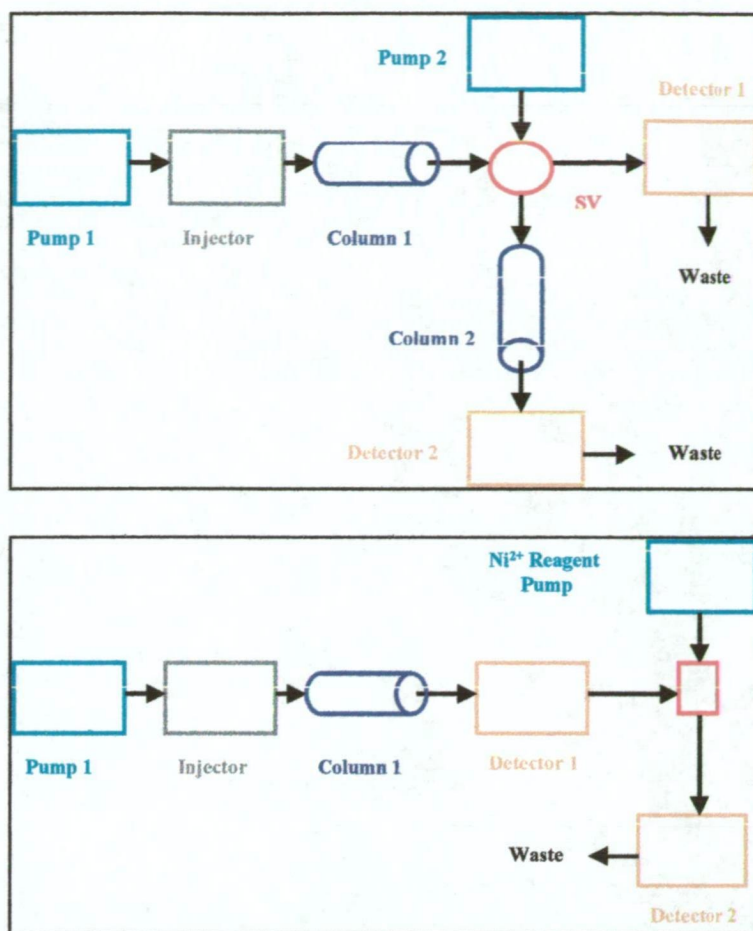
Fig. 5.29: (**a**) (Top): Coupled instrumental configuration.
(**b**) (Bottom) Flow-through instrumental configuration.

For either a coupled or a flow-through system, an eluent without a phosphate buffer would be required to prevent formation of a nickel precipitate. This necessitated the development of an eluent that contained an ammonia buffer for the separation of the metallo-cyanide complexes. It should be stated again that ammonia is not an ideal buffer for ODS columns due to the pH limitation of these columns. In terms of buffering capacity, Tris would be more suitable as it has a pKa of 8.1 [29]. However, a major disadvantage with Tris is that it displays considerable UV absorption in the low-UV region. For this reason, Waters recommend that a detection wavelength below 230 nm is not suitable when a Tris buffer is present in the eluent [37].

Initially, an eluent was prepared with 25% acetonitrile, 10 mM TBAOH and 10 mM $(NH_4)_2SO_4$. The pH of this eluent was 9.15. Increasing the $(NH_4)_2SO_4$ concentration

to 26 mM only reduced the pH to 8.78. From these observations, it was obvious that lower TBAOH and $(NH_4)_2SO_4$ concentration were required and that H_2SO_4 would have to be added to reduce the eluent pH to ≤ 8.

The eluent composition was optimised to enable separation of thiocyanate and the Cu(I), Fe(II), Fe(III), Ni(II) and Au(I)-cyanide complexes within approximately 10 min. and the separation of the first three analytes within approximately 5 min. All the separations were performed on a 5 cm Nov-Pak C-18 column. Six eluents in all were prepared. The composition of these six eluents and the retention times of above analytes are shown in Tables 5.22 and 5.23. The retention data were obtained by the injection of each analyte separately.

A CIL sample was analysed with eluent #6 shown in Table 5.22. The Cu and Au concentrations in this sample, as determined by AAS, were 1.28 and 107 ppm, respectively. A 50 μL injection of this sample with programmed detection wavelength changes during the run enabled quantitative analysis of thiocyanate, Cu(I), Fe(II), Fe(III) and Au(I)-cyanide complexes, as shown in Fig. 5.30. The wavelength changes are shown in Table 5.24.

Eluent #	[MeCN] (%)	[TBAOH] (mM)	$(NH_4)_2SO_4$ (mM)	[H_2SO_4] (mM)	[NaCN] (μM)
1	25	5	5	2	0
2	25	5	3	2	0
3	22	5	3	1.9	160
4	24	7.5	3	3.5	160
5	24	5	5	1.9	160
6	23	8	8	3.2	200

Table 5.22: Composition of eluents with an ammonia buffer for the separation of thiocyanate and the Cu(I), Fe(II), Fe(III), Ni(II) and Au(I)-cyanide complexes. Retention data for these eluents are shown in Table 5.23.

Eluent #	Retention time (min)					
	SCN	Cu(I)	Fe(II)	Fe(III)	Ni(II)	Au(I)
1	1.43	1.52	4.73	6.13	4.55	6.65
2	1.55	1.75	5.57	8.32	5.37	7.28
3	2.02	3.05	>15	>15	9.97	12.32
4	1.87	2.72	13.02	14.10	8.42	10.42
5	1.60	2.13	5.73	7.52	5.48	8.08
6	1.88	2.60	5.47	10.13	7.85	11.23

Table 5.23: Retention times of thiocyanate and metallo-cyanide complexes with eluents described in Table 5.22.

Run time (min)	Wavelength (nm)	Species detected
0	205	SCN
2.2	245	Cu(I)
4.8	205	Fe(II), Fe(III), Au(I)

Table 5.24: Programmed detection wavelength changes to allow quantitative analysis of all the species shown.
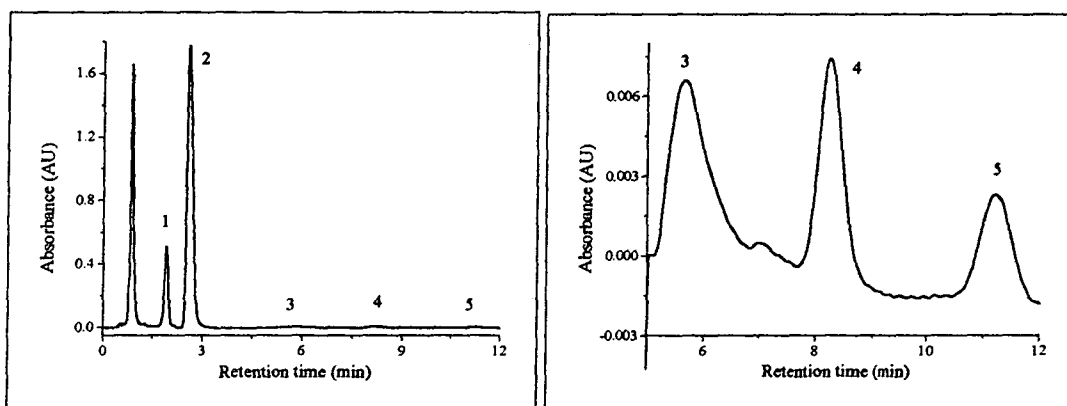
Fig. 5.30: Analysis of a CIL sample with an eluent containing an ammonia buffer.

UV detector chromatogram. Programmed wavelength changes (see Table 5.24)

LHS: Full scale chromatogram. RHS: Enlarged chromatogram

Legend: (1) Thiocyanate; (2) Cu(I); (3) Fe(II); (4) Fe(III); (5) Au(I).

Eluent : 23% acetonitrile, 8 mM TBAOH, 8 mM $(NH_4)_2SO_4$, 3.2 mM H_2SO_4, 200 μM NaCN;

pH = 8.0. Column: 5 cm Nova-Pak C-18. Injection volume: 50 uL

The instrumental configuration shown in Fig. 5.29(b) was used for the determination of cyanide by post column reaction (PCR) with a Ni^{2+} reagent. The PCR detection system used a $Ni(NO_3)_2$ solution (100 mM) for the derivatisation of cyanide. A reaction time of approximately 20 secs was provided by placing a 5m reaction coil between the T-junction and the PCR detector. A fixed wavelength detector, set at 254 nm, was used as the PCR detector. The cyanide calibration was linear in the range 30 - 150 ppm NaCN, with a regression co-efficient of 0.9992.

A mixed thiocyanate and Cu(I)-cyanide (R=3) standard was analysed with this instrumental configuration. The PCR detector chromatogram showed a cyanide peak, almost no peak for thiocyanate and a very large Cu(I) peak. It was then realised that this Cu(I) peak was mainly due to absorption by the Cu(I) complex at 254 nm. This was confirmed by changing the detection wavelength of the first detector (before the Ni^{2+} reagent addition) also to 254 nm and re-injecting the standard. There was a small difference between the two detector chromatograms for the height and area of the Cu(I) peak, with the PCR detector chromatogram having the larger peak. From the difference in the detector response, it was calculated that the cyanide concentration detected in the Cu(I) peak by reaction with the Ni^{2+} reagent was only 48 ppm NaCN. This was equivalent to a CN:Cu(I) mole ratio of 0.64, which is considerably less than the actual CN:Cu(I) mole ratio in the eluted Cu(I) peak. Consequently, only the most labile cyanide in the Cu(I) was complexed by the Ni^{2+} reagent.

The CIL sample analysed in the previous section (Fig. 5.30) was also analysed with the PCR instrument configuration. The resultant PCR detector chromatogram is shown in Fig. 5.31. The cyanide concentration was determined from the 50 μL injection to be 78 ppm NaCN, which is similar to a result obtained with the PCR detection system employing the König reaction scheme reagents used in section 5.3.5.

The above preliminary results showed that a HPLC system, incorporating a programmable wavelength UV detector and a PCR detection unit using a Ni^{2+}

reagent, could be used to enable analysis of cyanide, thiocyanate and the important metallo-cyanide complexes. This work also demonstrated that an analysis time of 12 min. was feasible. Unfortunately, limited time did not permit further development of this flow-through system or the coupled system shown in Fig. 5.29(a).
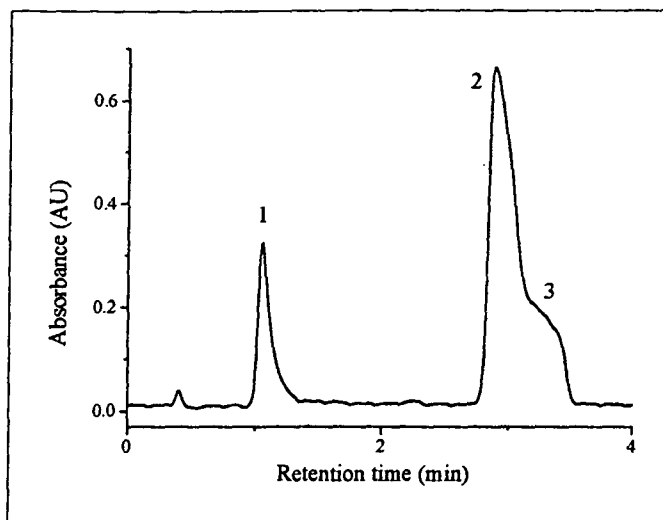
Fig. 5.31: Analysis of a CIL sample with an eluent containing an ammonia buffer. PCR detector (254 nm) chromatogram. Legend: (1) Cyanide; (2) Cu(I); (3) Tailed part of Cu(I) peak. Most of the Cu(I) peak response is due to absorbance by the Cu(I)-cyanide complexes at 254 nm. The reason for the peak tailing is uncertain, however, it is possibly due to the most labile CN ligands in the eluted Cu(I) peak. Chromatographic conditions as for Fig. 5.30.

5.4   References

1   P. R. Haddad, Australian Research Council (ARC) Collaborative Grant (1994).

2   Newcrest, *Australia's Mining Monthly*, (1992) 41.

3   Australian Bureau of Meteorology, National Climate Centre: Melbourne, 1994.

4   T. W. Trofe, S. J. Galegher, C. O. Reuter and S. Findley, "Perth International Gold Conference (1988 Randol Gold Forum)"; 28 October - 1 November 1988, Perth, Western Australia; Randol International Ltd.; 206.

5   A. Lawry, P. Gelfi, I. Mitchell, R. Pyper and R. Dunne, "Recent Trends in Heap Leaching"; Bendigo, Vic., 1994; The Australasian Institute of Mining and Metallurgy; 89.

6   R. Dunne, "Randol Gold Forum 1991"; Cairns, Australia, 16-19 April 1991; Randol International Ltd.; 239.

7   V. Kuban, *Anal. Chim. Acta,* 259 (1992) 45.

8   Pohlandt C., *S. Afr. J. Chem.,* 38 (1985) 110.

9   C. Pohlandt-Watson and M. J. Hemmings, *S. Afr. J. Chem., Dec,* 41 (1988) 136.

10   E. O. Otu, C. W. Robinson and J. J. Byerley, *Analyst,* 118 (1993) 1277.

11   L. Giroux and D. J. Barkley, *Can. J. Chem.,* 72 (1994) 269 .

12   Q. Huang, B. Paull and P. R. Haddad, *J. Chromatog.,* 770 (1997) 3.

13   B. Grigorova, S. A. Wright and M. Josephson, *J. Chromatogr.,* 410 (1987) 419.

14   P. R. Haddad and N. E. Rochester, *Anal. Chem.,* 60 (1988) 536.

15   P. R. Haddad and N. E. Rochester, *J. Chromatogr.,* 439 (1988) 23.

16   W. Mason, *J. American Chemical Society 1973, 95(11): 3574,* 95 (1973) 3574.

17   P. R. Haddad and C. Kalambaheti, *Anal. Chim. Acta,* 250 (1991) 21.

18   W. R. Day In Analytical Testing Technology, 1998, pp 28.

19   V. V. Berry, *J Chromatogr,* 290 (1984) 143.

20   M. D. Adams, *J. S. Afr. Inst. Min. Metall.,* 90 (1990) 37.

21   S. Ohe, *Computer aided data book of Vapour Pressue;* Data Book Publishing Company: Tokyo, Japan, 1976.

22   D. F. Hilton and P. R. Haddad, *J. Chromatogr.,* 361 (1986) 141.

23   D. M. Muir, *Chemistry in Australia,* (1994) 582.

24   P. L. Bailey and E. Bishop, *J. Chem. Soc. Dalton Transactions,* 1973 (1973) 912.

25   Dr. P. Jones , Personal Communication 1994.

26   R. C. Weast and J. G. Grasselli, *CRC Handbook of data on Organic Compounds,* Second ed.; CRC Press: Boca Raton, Florida, USA, 1989.

27   R. Sanehi, R. M. Mehrotra and S. P. Mushran, *Z. Naturforsch.,* 28B (1973) 483.

28   Dr. R. Dunne , Personal Communication 1998.

29   D. G. Peters, J. M. Hayes and G. M. Hieftje, *Chemical separations and measurements: The theory and practice of analytical chemistry;* W.B. Saunders Company: London, U.K., 1974.

30   M. W. Scoggins, *Anal. chem.,* 44 (1972) 1294.

31   A. T. Haj Hussein, *Anal. Lett.,* 21 (1988) 1285.

32   J. A. Sweileh, *Anal. Chim. Acta*, 220 (1989) 65.

33   K. Kurnia and D. E. Giles, Poster presented at "11th Australian Analytical Chemistry Symposium"; Hobart, 1991 .

34   P. Kuban, W. Buchberger and P. R. Haddad , *J. Chromatogr.*, 770 (1997) 329

35   J. A. Cox, H. L. Novak and R. M. Montgomery, *J Chromatogr, A*, 739 (1996) 229.

36   H. Perrson and C. G. Ekstrom, *Acta Chem. Scand. A*, 30 (1976) 31.

37   Waters, *486 Detector manual.*

CHAPTER SIX

Determination of the CN:Cu(I) mole ratio with ion chromatography

6.1 Introduction

This chapter continues the development of RPIIC methodology for the analysis of cyanide, thiocyanate and the metal-cyanide complexes. The emphasis of this chapter is on the development of methods suitable for the analysis of Cu(I)-cyanide leachates. The most significant development was the routine determination of the CN:Cu mole ratio, R. The importance of R during the cyanidation of gold-copper ores and during the electrowinning of copper and cyanide has been described in Chapter one.

The methodology described in this chapter and the following chapter was developed to provide analytical support for a new leaching process undergoing trials at Telfer. Detailed information of this project cannot be revealed in this thesis due to a confidentiality agreement. However, some information is public knowledge and can be discussed freely. The project was based on DuPont's Augment process [1] and a related process developed by Dreisinger [2]. These processes were discussed in Chapter One (section 1.3.4.5). Newcrest Mining was considering this process as one of several options for the recovery of gold from large low grade copper/gold deposits at the Telfer Gold Mine. These deposits cannot be treated economically with normal cyanidation processes. The Augment process is designed for the economic recovery of copper and gold from cupriferous ores with the use of a Cu(I)-cyanide lixiviant containing a CN:Cu mole ratio of 4.

Part of the evaluation of the Augment process at the Telfer Gold Mine involved leaching an oxide ore containing in excess of 1500 g/t total copper. A substantial leaching test was performed at Telfer in a large column test facility that had been previously constructed for the purpose of conducting heap leaching tests [3]. The large columns were assembled from three 2.4 m sections of 1.2 m diameter concrete sewer pipes, stacked atop one another. Each column rested on a reinforced concrete slab and the pipe segments were coated with a silicone waterproof paint. The joint

---

between each segment was sealed with a thick layer of Silastic (a commercial silicone sealant). The final dimensions of each column were 7.2 m (Height) x 1.2 m (Diameter) and each had a total capacity of approximately 15 tonnes. Pictures of the large column test facility and a schematic of the flowsheet for the large column leaching assembly are shown in Figs. 6.1 and 6.2(a).

A lixiviant prepared from CuCN and NaCN was continually circulated through two of the large columns. Samples were collected at the following five points. The sample names are shown in brackets.

(i)   Effluent from Column A (Column A).

(ii)   Effluent from Column B (Column B).

(iii)   Leachate prior to passage through the Carbon Column (CC Feed).

(iv)   Leachate after passing through the Carbon Column (CC Product).

(v)   Lixiviant prior to input into Column A (Barren).

The effluent from Column A was transferred to Column B without any reagent additions. A cyanide solution was generally added to the effluent from Column B. The resultant solution (CC Feed) was passed through a column packed with activated carbon (typically 1500 g) to remove the Au(I) complex leached from the ore. Cyanide was added to the effluent from column B prior to passage through the carbon column (CC) to increase the CN:Cu mole ratio and thus prevent adsorption of $[Cu(CN)_2]^-$ on the activated carbon. The effluent from the CC was referred to as the CC Product. Concentrated cyanide solution and/or more Cu(I)-cyanide concentrate and/or water were added as required to the CC Product to form the new Barren solution. The water addition was to increase the solution volume due to losses resulting from leaks, etc. The Barren solution was then added to Column A. A schematic illustrating these procedures is shown in Fig. 6.2(b).
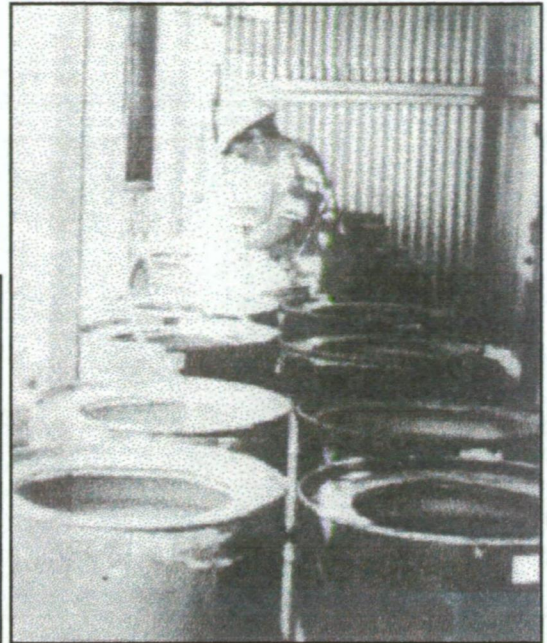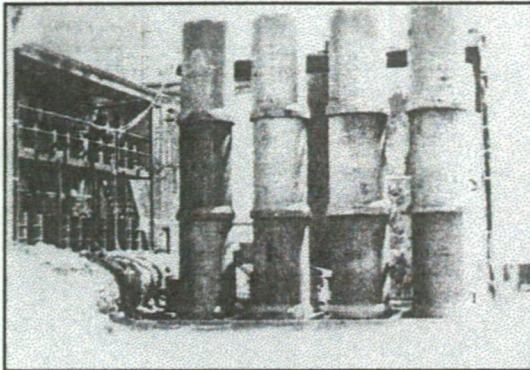
Fig. 6.1: Pictures of large column leaching facility at Telfer. LHS: Completed 7.2 m x 1.2 m columns with cyanide reagents building on left side. RHS: Cyanide reagents building with 200 litre drums. Note carbon column above drums. Source : Figs. 1 & 2 from [3].
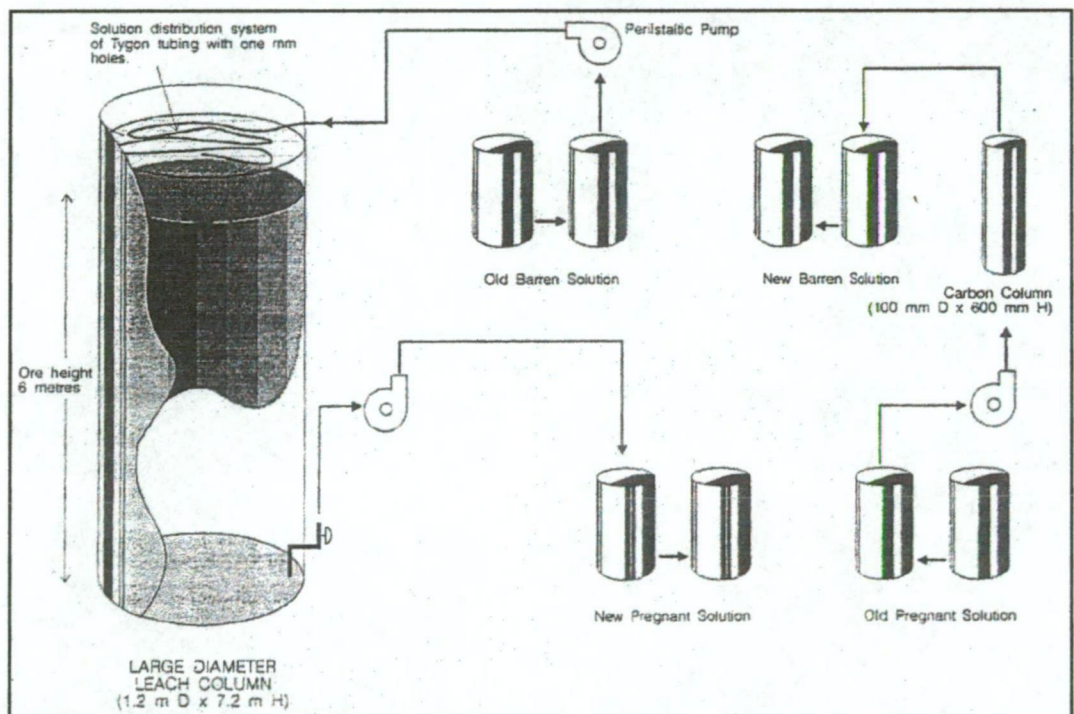
Fig. 6.2(a): Schematic flow-sheet for large column leaching system at Telfer. Source: Fig. 5 from [3].
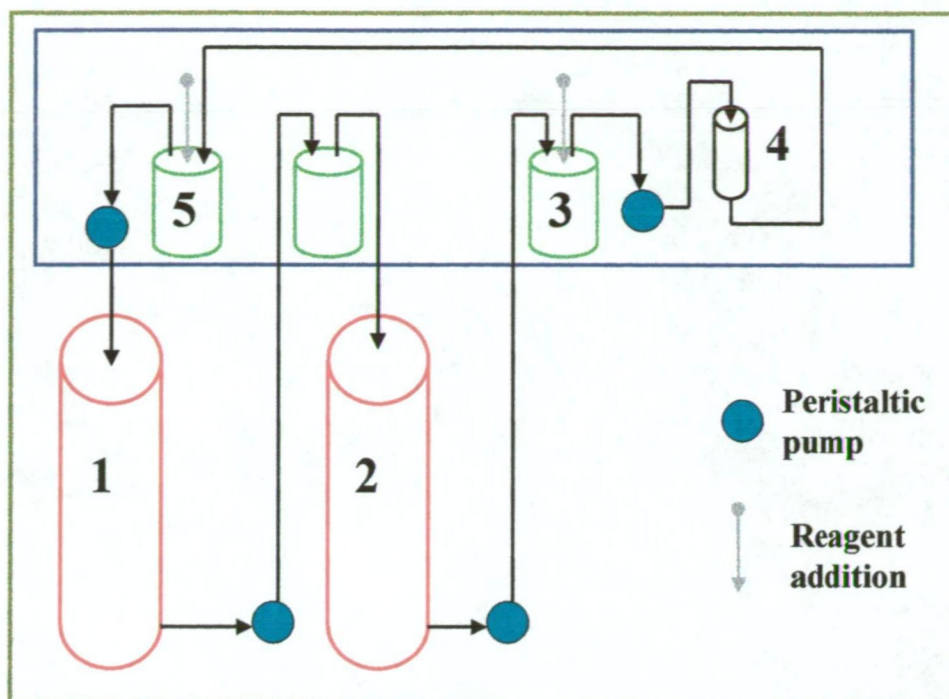
Fig. 6.2(b): Schematic diagram illustrating sampling points and reagent additions used during the Cu(I)-cyanide leach tests. Legend: **(1)** Column A; **(2)** Column B; **(3)** CC Feed sampling point after NaCN addition to effluent from column B; **(4)** Carbon column; **(5)** CC Product and Barren sampling points. Barren sample collected after reagents added. 200 litre drums (green cylinders in diagram) used for collecting effluents from columns and reagent additions.

An important part of the evaluation of the Augment process was the accurate monitoring of the total cyanide and cyano species so that cyanide losses could be determined and the economic feasibility assessed. It was intended to maintain the copper concentration at 5000 ppm Cu, with an R value of 4 during the leaching test. In actuality, the leach samples typically contained between 2000 and 4000 ppm Cu as the Cu(I) complex. Low concentrations of thiocyanate and the cyano-complexes of Co(III), Fe(II), Ni(II) and Au(I) were also present. Significant concentrations of cyanate were observed using the methods developed in the following Chapter.

Since the predominant cyano species were the Cu(I)-cyanide complexes, it was essential that the copper concentration and total cyanide were monitored over the duration of the leaching trials (approximately 8 months). This was an ideal test application for the HPLC instrument, since the product of the CN:Cu mole ratio and Cu(I) concentration should, in this instance, provide a very good estimate of the total

cyanide concentration. Furthermore, a comparison of the results obtained by standard metallurgical analytical methods and the HPLC methods would allow further evaluation of the HPLC instrument as a process control instrument.

Previous test-work on the Augment process had been conducted for Newcrest Mining by several independent metallurgical laboratories, including the Lakefield Research Centre (LRC) at Ontario, Canada. The standard acid distillation technique (see Fig. 1.6) was employed at the LRC to determine the total cyanide concentration in samples. The titrimetric method for cyanide analysis was not suitable due to the presence of large concentrations of the Cu(I)-cyanide complexes as discussed in Chapter one (Section 1.3.4.3).

In order to provide comparable data, an acid distillation system handling 10 samples simultaneously was purchased for use at the Telfer Gold Mine. Unfortunately, due to several technical problems, the acid distillation unit was inoperable for part of the time that the HPLC instrument was located at the Telfer gold mine. The Cu concentration in the samples was determined at the LRC by AAS allowing the CN:Cu molar ratio to be estimated on the basis that most of the total cyanide was derived from the Cu(I)-CN system.

The analytical methodology developed for the Cu(I)-cyanide leach samples was also applied to samples obtained from the pyrite leach plant which operated on an intermittent basis while the HPLC instrument was located at the Telfer gold mine. The source of the pyrite leach samples was discussed in the previous Chapter (Section 5.1).

6.2 Experimental

The same instrumentation as described in Chapter five was used for this work. The eluents and PCR reagents were prepared as described in Chapter five.

6.2.1 Standard solutions

The Cu(I)-cyanide standards were prepared from stock solutions of both Cu(I)-cyanide (R = 3) and NaCN. The concentration of the working Cu(I)-cyanide standards for determination of the CN:Cu mole ratio was initially 1.0 mM. This was subsequently increased to higher concentrations after further method development. A micro autosampler syringe (25 µL volume) was used in conjunction with the higher concentrations to enable small and reproducible injection volumes. The Cu(I)-cyanide and NaCN stock solutions were standardised as discussed in the previous Chapter.

The standards for thiocyanate and other metallo-cyanide complexes were prepared from their respective potassium salts without standardisation. The sources of these standards were discussed in the previous Chapter. The study of the cobalt cyanide species was conducted using $CoCl_2.6H_2O$ (Anal R grade, BDH, England) and NaCN.

6.2.2 Comparative metallurgical analyses

The standard method for determination of copper used AAS. The standard method for total cyanide determination used boiling sulfuric acid digestion of a sample followed by collection of the evolved HCN gas in a receiving vessel containing a NaOH solution, as shown in Fig. 1.7. A one hour period was used for the acid digestion/distillation step. The cyanide concentration in the NaOH solution was subsequently determined by titration with $AgNO_3$. A multi-cyanide distillation unit (Activon, Sydney, Australia) allowed up to 10 samples to be treated simultaneously.

6.3 Results and Discussion

6.3.1 Determination of the CN:Cu mole ratio

In Chapter four it was shown that the Cu(I)-cyanide complexes undergo partial dissociation during the chromatographic process. This dissociation was studied by monitoring the two peaks observed with the PCR detector. The first peak was due to uncomplexed cyanide in the sample, together with any further cyanide produced by dissociation of the Cu(I) complex during its passage through the chromatographic column. The second peak was due to the derivatisation of cyanide in the Cu(I) complex. The peak area of the Cu(I) peak did not change with the value of R in the injected sample, while the cyanide peak increased with R.

The above studies suggested that a linear relationship should exist between the R value and the ratio of the peak areas for the cyanide and Cu(I) peaks from the PCR detector chromatograms. Furthermore, since the composition of the Cu(I) peak is constant, regardless of the composition of a sample, the CN:Cu(I) peak area ratio should be a direct reflection of the CN:Cu(I) mole ratio of a sample. Thus a plot of the CN:Cu(I) peak area ratio against the R value should allow determination of the R value of an unknown sample. It was also reasoned that use of the peak area ratio would eliminate errors from long term drifts in the PCR detection system. To facilitate a linear PCR detector response, the PCR conditions developed in Chapter five were used for this work. These PCR conditions provided a linear response over the range 1-7 mM NaCN.

The chromatographic conditions developed in Chapter five were initially employed, viz. separation on a 5 cm Nova-Pak C-18 column with an eluent containing 160 µM NaCN. A series of Cu(I)-cyanide standards with equimolar (1.0 mM) copper concentration and increasing CN:Cu mole ratios, R, was injected onto the ion interaction separation system. The resultant PCR detector chromatograms are shown in Fig. 6.3(a). A linear relationship was obtained when the CN:Cu(I) peak area ratio was plotted against the CN:Cu mole ratio as shown in Fig. 6.3(b).

When the plot shown in Fig. 6.3(b) was extrapolated to a CN:Cu(I) peak area ratio of zero, the intercept on the R axis indicated that the CN:Cu mole ratio of the eluted Cu(I) peak was 2.79 under the chromatographic conditions used. The concentration of cyanide in the CN and Cu(I) peaks was determined using a calibration of NaCN standards. For a 1.0 mM Cu(I)-cyanide standard with a CN:Cu mole ratio of 4.0, the concentrations of cyanide in the CN and Cu(I) peaks was found to be 1.18 and 2.78 mM, respectively, providing a total cyanide concentration of 3.96 mM, which compared very well with the expected total cyanide concentration of this standard (4.0 mM). Since the concentration of the Cu(I)-cyanide standard injected onto the column was 1 mM, the CN:Cu mole ratio of the eluted Cu(I) peak was 2.78, which compared very favourably with the CN:Cu mole ratio (2.79) found from extrapolation of the CN:Cu calibration plot as discussed above. This result provided further confirmation of the studies described in Chapter four concerning the nature of the eluted Cu(I)-cyanide complex.
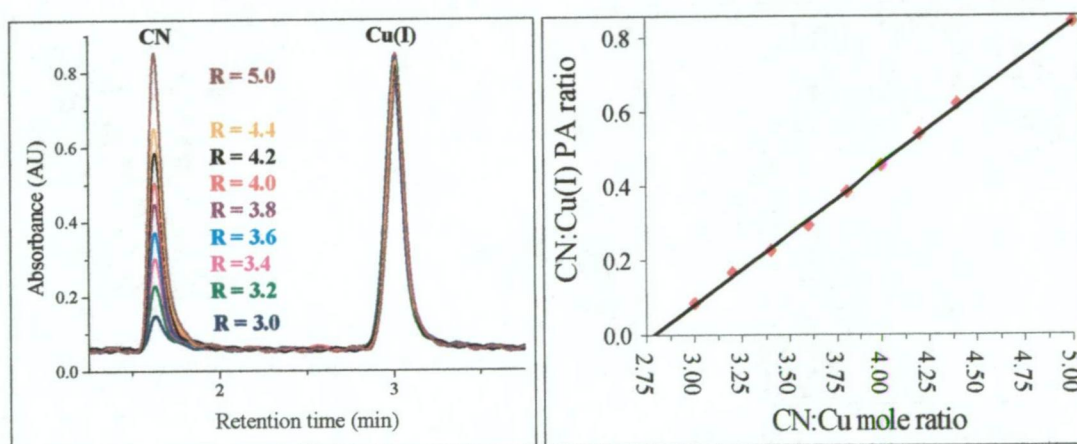
Fig. 6.3 (a) (Top) Overlaid PCR detector chromatograms of equimolar (1.0 mM) Cu(I)-cyanide standards with R values ranging from 3.0 - 5.0. (b) (Bottom) CN:Cu(I) peak area ratio plotted against the CN:Cu mole ratio for the standards shown in Fig. 6.3(a).

6.3.2 Analysis of Cu(I)-cyanide leachate

The Cu(I)-cyanide lixiviant was analysed prior to the commencement of leaching operations with the calibration shown in Fig. 6.3(b). While the actual CN:Cu mole ratio of the lixiviant was 4.0, the mole ratio determined from the calibration plot was 4.02. This result provided a high level of confidence in this analytical method.

An injection volume of 10 µL was initially used for the Cu(I)-cyanide leach samples. A typical sample dilution factor of 40 was required with this injection volume. Following the purchase of a micro 25 µL syringe for the autosampler, reproducible (≤ 1% RSD) injection volumes as low as 1.0 µL were possible, thereby allowing a typical dilution factor of 4. This was possible since the absolute mass (and not concentration) of the analyte was important.

This small injection volume also allowed samples to be diluted in 4.0 mL autosampler vials as follows: 1.0 mL of sample diluted with 3.0 mL RO water. This procedure considerably reduced the time required for sample preparation. An additional advantage of a small injection volume was the increased stability of both standards and diluted samples. Other workers have previously noted that the metallo-cyanide complexes are more stable at higher concentrations [4].

The pre-dominant peak in the UV detector chromatogram was due to the Cu(I) complex. Since the thiocyanate concentration in these samples was very low when compared to the Cu(I) concentration, it was possible to reduce the NaCN concentration in the eluent from 160 to 80 µM and still achieve baseline resolution of thiocyanate and Cu(I) peaks, as shown in Fig. 6.4.
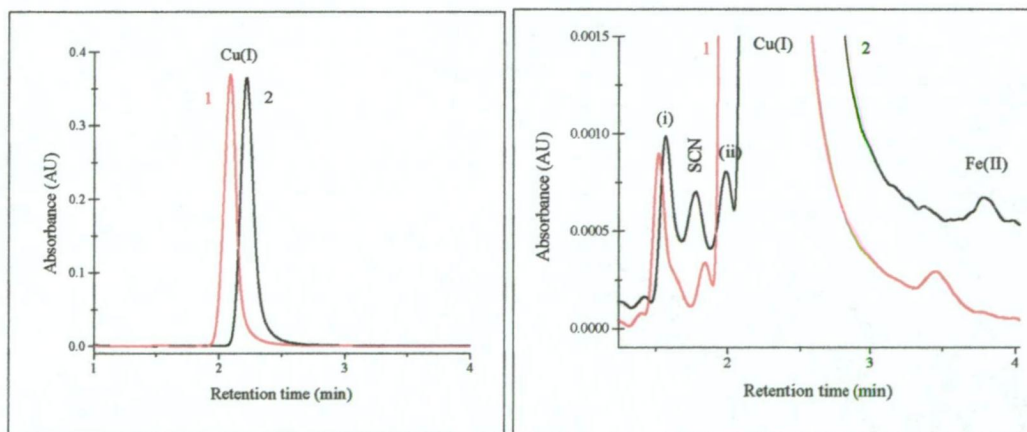
Fig. 6.4: Analysis of an early Column A sample. [Cu(I)] = 2700 ppm. Peaks (i) and (ii) unidentified at the time of analysis. UV (245 nm) detector chromatograms. 40-fold dilution. 10 µL injection volume. Column: 5 cm Nova-Pak C-18. Eluents: 25% acetonitrile, 10 mM TBAOH, 10 mM KH_2PO_4, 5 mM H_2SO_4 and either (**1**) 80 µM NaCN or (**2**) 160 µM NaCN; pH 8.0.

Two unidentified peaks {labelled (i) and (ii) in Fig. 6.4(b)} did affect accurate quantitative analysis of the thiocyanate peak in early samples. The identification of these unknown components was subsequently tentatively assigned to intermediate cobalt-cyanide complexes for reasons discussed later in this chapter (Section 6.3.6). It was observed over a 9-day period shortly after the commencement of leaching operations that the magnitude of the unidentified peak (i) was considerably reduced relative to the thiocyanate peak, as shown in Fig. 6.5.

Several other effects were observed when the concentration of cyanide in the eluent was reduced. The retention time of the derivatised Cu(I) complex was reduced from 2.97 min to 2.86 min, as shown in Fig. 6.6 (a&b). The PCR detector noise was also reduced, as shown in Fig. 6.6(c).

The slope of the calibration plot for the CN:Cu(I) mole ratio in the eluent containing 80 μM NaCN was almost identical to that for the eluent containing 160 μM NaCN, but as expected gave a smaller R value for an extrapolated peak area ratio of zero, as shown in Fig. 6.6(d). The reason for the slight difference in the slopes of these plots was uncertain.
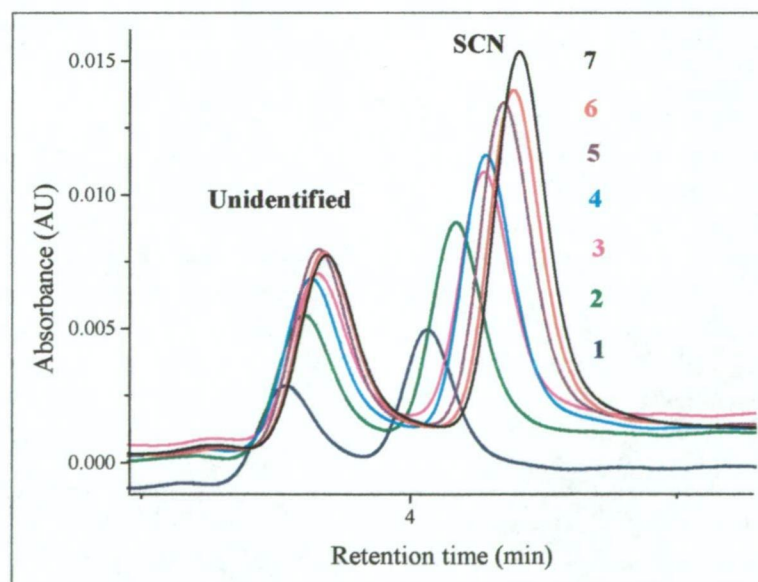
Fig. 6.5: Variation in thiocyanate and unidentified peak (i) in Column A samples with sampling date. Legend: (**1**) Day 1; (**2**) Day 4; (**3**) Day 5; (**4**) Day 6; (**5**) Day 7; (**6**) Day 8; (**7**) Day 9. UV (205 nm) detector chromatogram. Column: 15 cm Nova-Pak C-18. Eluent: 25% acetonitrile, 10 mM TBAOH, 10 mM KH_2PO_4, 5 mM H_2SO_4 and 160 μM NaCN; pH 8.0.
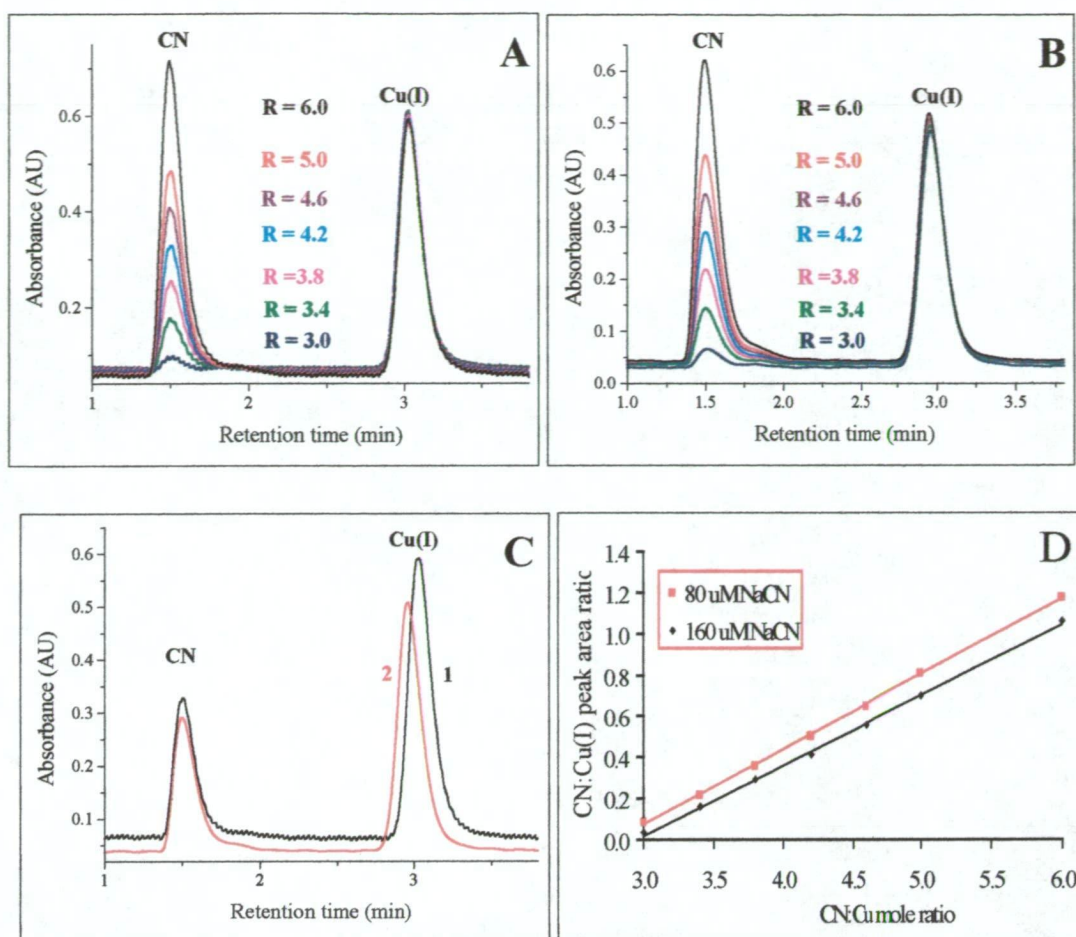
Fig. 6.6: Effect of cyanide concentration in the eluent on the CN and Cu(I) peaks (PCR detector chromatograms). **(a)** (Top LHS) and **(b)** (Top RHS): 160 and 80 μM NaCN in eluent respectively. **(c)** (Bottom LHS): Comparison of 1 mM Cu(I)-cyanide standard (R=4.2) in eluents containing either **(1)** 80 μM NaCN or **(2)** 160 μM NaCN. **(d)** (Bottom RHS): Comparison of CN:Cu mole ratio calibration plots derived from the 1 mM Cu(I)-cyanide standards shown in Fig. 6.6 (a & b). Column: 5 cm Nova-Pak C-18. Eluents: 25% acetonitrile, 10 mM TBAOH, 10 mM KH_2PO_4, 5 mM H_2SO_4 and (80 μM or 160 μM) NaCN; pH 8.0.

The UV detector chromatogram shown in Fig. 6.4(b) revealed that the large concentration of Cu(I) complex in these samples resulted in partial co-elution of the Cu(I) and Fe(II) peaks when analysed on a 5 cm Nova-Pak C-18 column. For this reason it was necessary to use a 15 cm Nova-Pak C-18 column to enable separation of thiocyanate and all the metallo-cyanide complexes when the level of Cu(I) was very high, as shown in Fig.6.7.
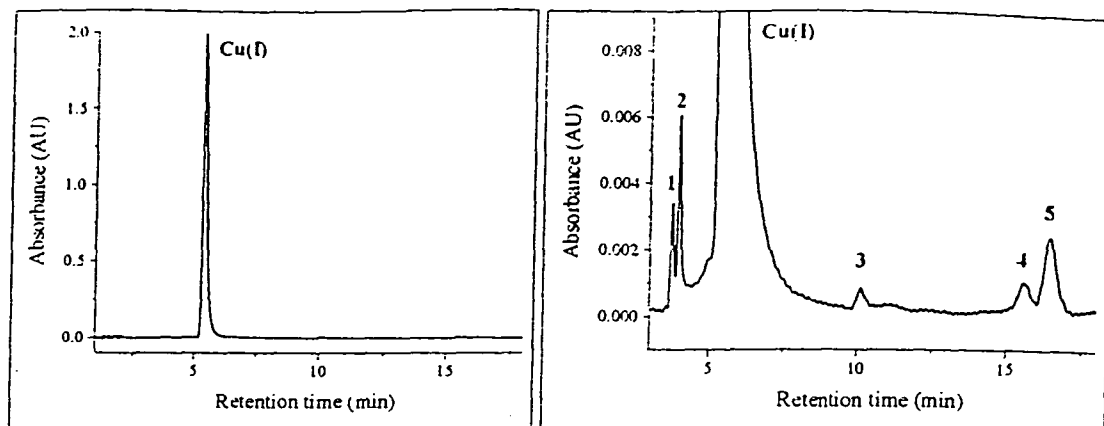
Fig. 6.7: Analysis of an early Column A sample on a 15 cm Nov-Pak C-18 column. 20-fold dilution. 10 µL injection volume. UV (205 nm) detector. [Cu] = 3230 ppm. Legend: (1) Unidentified; (2) Thiocyanate; (3) Fe(II); (4) Ni(II); (5) Co(III). Chromatographic conditions as for Fig. 6.5.

The effect of detection wavelength on the minor components was investigated. It was found that 230 nm was an optimal detection wavelength when only the analysis of thiocyanate and the Cu(I) and Fe(II) complexes was required, as shown in Fig. 6.8. At this detection wavelength, there was still sufficient sensitivity to allow quantitative analysis of thiocyanate and the Fe(II) complex. However, the Ni(II) and Co(III) peaks observed in typical leach samples were very small at a detection wavelength of 230 nm. This allowed sample injections after the elution of the Fe(II) complex as the Ni(II) and Co(III) peaks would not interfere in the subsequent injection.

When analysis of all the leach components was required, programmed UV detection wavelength changes were used to optimise detection sensitivity for each component, as shown in Fig. 6.9. A detection wavelength of 230 nm was used from the injection time until after the Cu(I) peak was eluted. The detection wavelength was then changed to 215 nm (λ_{max} for the Fe(II) complex), before being changed again to 205 nm to allow maximum sensitivity for the Ni(II) and Co(III) complexes.
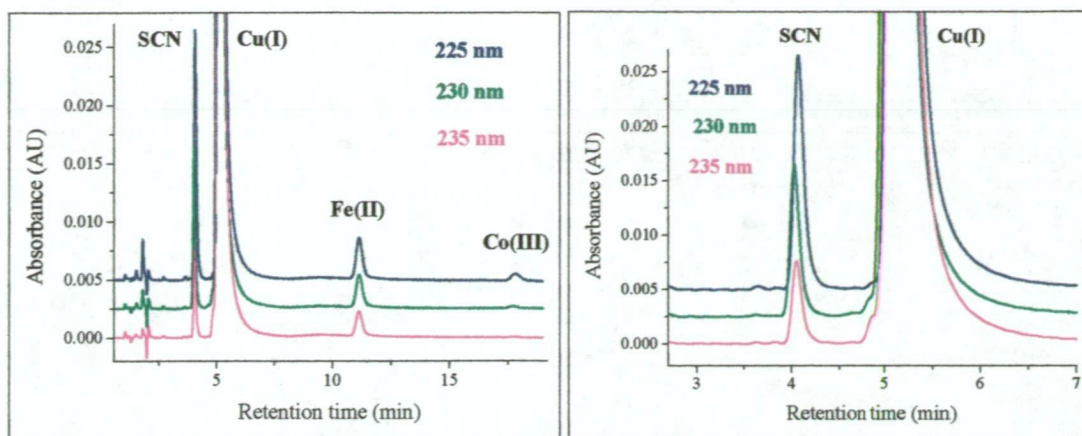
Fig. 6.8: Column A sample analysed on a 15 cm Nov-Pak C-18 column at different UV detection wavelengths. Chromatographic conditions as for Fig. 6.7
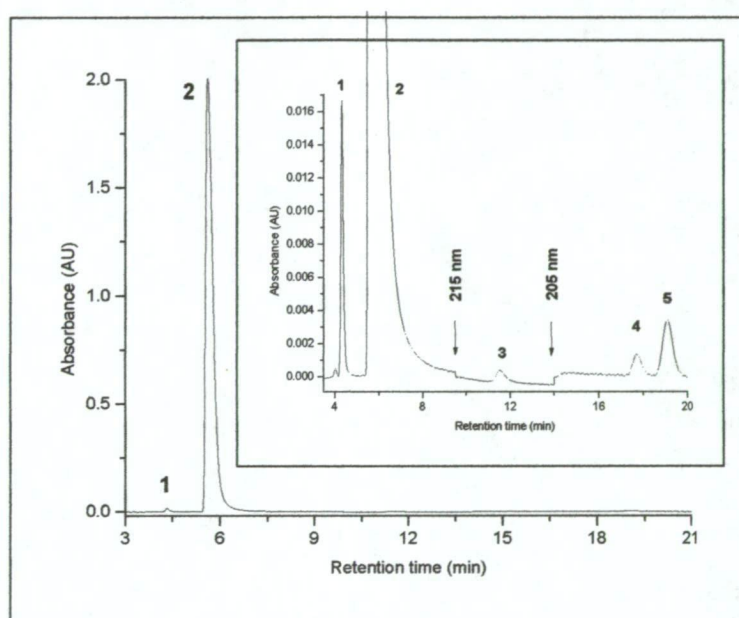
Fig. 6.9: Column A sample analysed on a 15 cm column. Legend : **(1)** SCN; **(2)** Cu(I); **(3)** Fe(II); **(4)** Ni(II); **(5)** Co(III). Sample concentrations : SCN (94.4 ppm); Cu(I) (4616 ppm); Fe(II), Ni(II) and Co(III) (< 1 ppm). UV absorbance detector: Programmed wavelength changes : t=0 min, λ=230 nm; t=9.5 min, λ=215 nm; t=14.0 min, λ=205 nm. Four-fold dilution. 1.0 μL Injection volume. Eluent: 25% acetonitrile, 10 mM TBAOH, 10 mM KH_2PO_4, 5 mM H_2SO_4 and 150 μM NaCN; pH 8.0.

Typical PCR detector chromatograms of equimolar (1.0 mM) Cu(I)-cyanide standards analysed on a 15 cm Nova-Pak C-18 column are shown in Fig. 6.10(a). The CN:Cu mole ratio calibration plot for these standards is shown in Fig. 6.10(b).

Comparison of the calibration plots obtained on the 5 cm and 15 cm Nova-Pak C-18 columns with identical eluents revealed that the plots were almost identical, as shown in Fig. 6.11. The slight difference between the two plots was attributed to slight variations in eluent composition due to errors that occurred during preparation or as a result of loss of cyanide and/or acetonitrile.
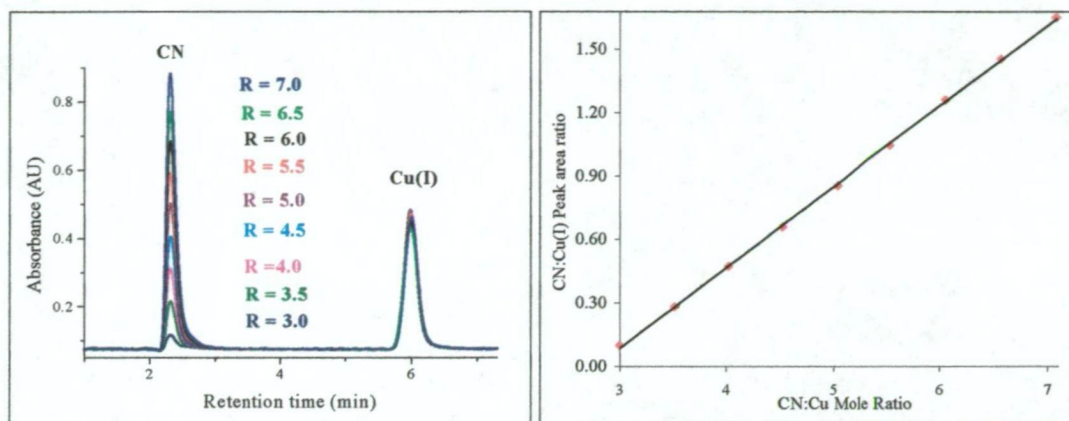
Fig. 6.10: (a) (LHS) Overlaid PCR detector chromatograms of equimolar (1.0 mM) Cu(I) standards with R values ranging from 3.0 - 7.0 analysed on a 15 cm Nova-Pak C-18 column. (b) (RHS) CN:Cu mole ratio calibration plot for the standards shown in (a). Chromatographic conditions as for Fig. 6.7.
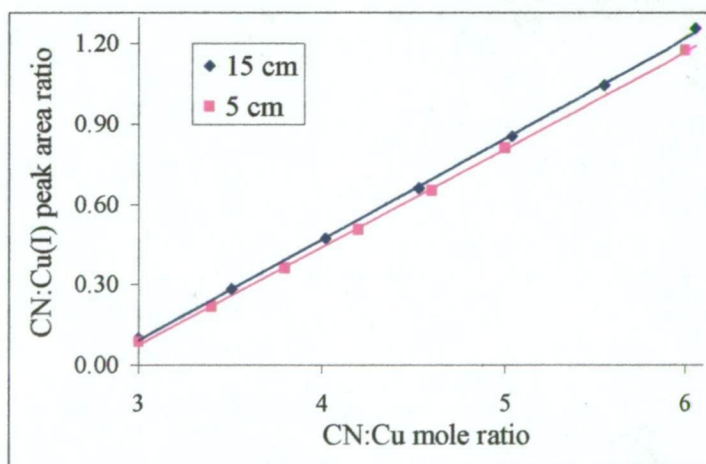
Fig. 6.11: Comparison of CN:Cu mole ratio calibration plots obtained on 5 cm and 15 cm Nova-Pak C-18 columns. Eluent for both columns contained 80 µM NaCN.

6.3.3 Stability of CN:Cu mole ratio calibration

The stability of the CN:Cu(I) mole ratio calibration was determined over 4 non-consecutive days with a series of eluents of constant composition. The eluents were freshly prepared on a daily basis. There was a gradual change in the CN:Cu mole ratio calibration over the course of each day as illustrated for a 14 hr period [Fig. 6.12(a)]. This variation was attributed to the loss of cyanide and acetonitrile from the eluent. It has already been shown that altering the cyanide concentration in the eluent alters the CN:Cu mole ratio calibration (Fig. 6.11). The loss of acetonitrile from the eluent would also affect the CN:Cu mole ratio calibration since it is an excellent ligand for the Cu(I) oxidation state and significantly alters the thermodynamic stability constants of the Cu(I)-cyanide complexes [5, 6].

The loss of both cyanide and acetonitrile from the eluent was minimised by shielding the eluent from light and placing the eluent container in an insulated box (an "Esky") packed with ice. It was observed that over the 4 day period, each calibration point varied by less than 5% RSD, as shown in Table 6.1 and Fig. 6.12(b). The values for the intercept and slope for each linear calibration plot over the 4 days are shown in Table 6.1. In order to further compare the calibration plots, the R value for a typical CN:Cu(I) peak area ratio (0.35) was calculated for each calibration plot. The calculated R value varied by less than 1% RSD, as shown in Table 6.1. The variation in the calculated R value was less than the variation in the CN:Cu(I) peak area ratio (PAR) because the slopes of the calibration plots were 0.385 ± 0.011.

The variation between the first calibrations for each day [Fig. 6.12(b)] was attributed to slight differences in each eluent, resulting from errors that occurred during preparation. The variation in the CN:Cu mole ratio calibration could be further reduced in a process control instrument by use of a gradient HPLC pump to continually prepare an isocratic eluent. It should also be noted that there may have been slight variations in the standards used on each day as these were also prepared on a daily basis. Subsequent work (see Section 6.3.4) found that the use of a small injection volume (1 μL) and more concentrated standards negated the need for daily preparation of the standards.

The variation in the calibration plots over the 4 days was greatest for the standard with the lowest CN:Cu mole ratio (R = 3). The reasons for this were twofold. First, this standard had the smallest cyanide peak, resulting in the largest relative errors in peak integration due to the inherently noisy baseline. Secondly, the loss of cyanide from this standard was greater than from an equimolar Cu(I) standard with a higher R value.
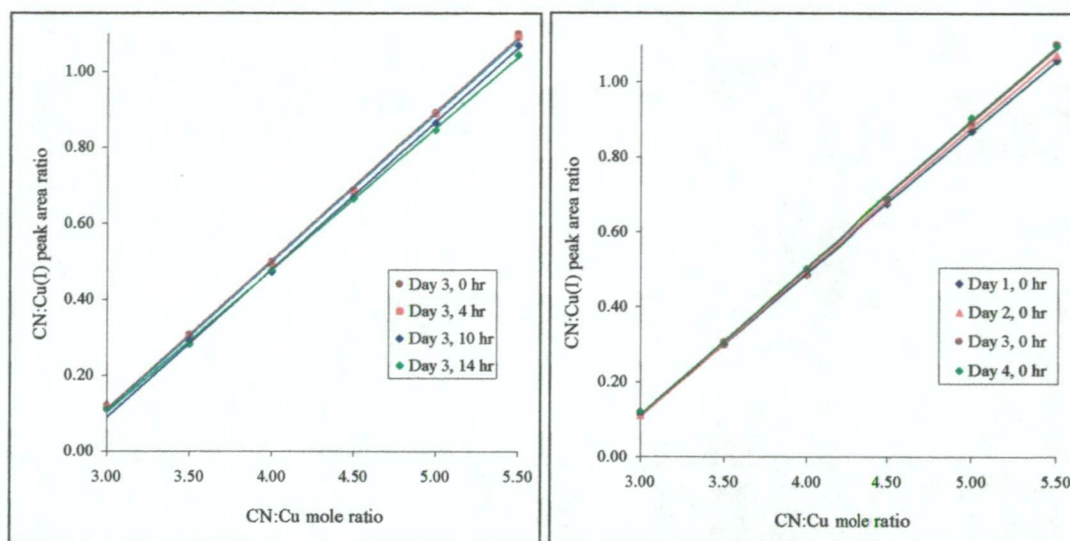
Fig. 6.12: Variation in CN:Cu mole ratio calibration over (**a**) (LHS) 14 hrs (**b**) (RHS) 4 days. The same eluent composition was used over this period, with the eluents prepared on a daily basis. Column: 15 cm Nova-Pak C-18. Eluent: 25% acetonitrile, 10 mM TBAOH, 10 mM KH_2PO_4, 5 mM H_2SO_4 and 80 µM NaCN. See text and Table 6.1 for further details.

6.3.4   Effect of Cu(I) concentration on determination of R

It was known from the studies presented in Chapter four that the Cu(I) concentration in the samples had an effect on the CN:Cu(I) peak area ratio. This would have a detrimental influence on the determination of the CN:Cu mole ratio in samples with varying Cu(I) concentrations. To overcome this problem, samples were initially diluted such that the Cu(I) concentration in the sample was approximately equivalent to that of the Cu(I) standards, i.e. 1.0 mM. This required samples to be re-diluted on several occasions when sudden changes in the leach samples occurred. Since it was desirable to develop a more rugged method, the effect of Cu(I) concentration on the CN:Cu mole ratio calibration plot was further investigated.

Day & time	Peak area ratio for Cu(I) standards						Slope	Inter-cept	PAR 0.35
	R=3.0	R=3.5	R=4.0	R=4.5	R=5.0	R=5.5			
Day 1; 0 hr	0.114	0.300	0.486	0.675	0.869	1.058	0.378	-1.023	3.63
Day 1; 5 hr	0.110	-	0.477	-	0.852	-	0.371	-1.004	3.65
Day 2; 0 hr	0.111	0.301	0.488	0.682	0.886	1.071	0.386	-1.049	3.62
Day 2; 6 hr	0.106	0.292	0.480	0.667	0.873	1.069	0.385	-1.057	3.65
Day 2; 10 hr	0.104	0.291	0.476	0.677	0.867	1.067	0.385	-1.057	3.65
Day 3; 0 hr	0.119	0.306	0.498	0.686	0.891	1.100	0.391	-1.063	3.61
Day 3; 4 hr	0.115	0.300	0.492	0.684	0.889	1.091	0.391	-1.066	3.62
Day 3; 10 hr	-	0.292	0.472	0.668	0.864	1.069	0.389	-1.078	3.67
Day 3; 14 hr	0.111	0.282	0.476	0.665	0.845	1.044	0.374	-1.019	3.66
Day 4; 0 hr	0.120	0.304	0.502	0.691	0.904	1.096	0.393	-1.065	3.60
Day 4; 6 hr	0.114	0.306	0.491	0.694	0.896	1.087	0.391	-1.063	3.61
AVERAGE	0.112	0.297	0.485	0.679	0.876	1.075	0.385	-1.049	3.64
RSD (%)	4.54	2.64	2.03	1.50	2.14	1.66	1.94	2.24	0.63

Table 6.1: Variation in the CN:Cu(I)-cyanide mole ratio calibration over 4 days. The average and RSD (%) of the CN:Cu peak area ratio (PAR) for each standard over the 4 days are shown. The slope and intercept values for each calibration are shown. The calculated R value of a PAR of 0.35 is calculated for each calibration. The average and RSD (%) of the slope, intercept and calculated R value are shown. Chromatographic conditions as for Fig. 6.12.

Initially, the effect of the Cu(I) concentration was determined for an eluent containing 80 µM NaCN. This was performed on a series of Cu(I)-cyanide standards with the Cu(I) concentration ranging from 0.6 to 1.4 mM, but all having a CN:Cu mole ratio of 3.0. The peak area ratios (PAR's), percentage variation of PAR's from the 1.0 mM Cu(I)-standard and the CN:Cu mole ratios calculated from the observed PAR's are shown in Table 6.2. It can be noted that a variation of up to 8% was observed in the PAR for solutions containing Cu(I) in the range 0.6–1.4 mM. However, for the reasons discussed in the previous section, the effect on the calculated CN:Cu mole ratio was less than 1% for this range of Cu(I) concentrations. This permitted a CN:Cu mole ratio calibration prepared with standards containing a

single Cu(I) concentration to be used for solutions containing varying amounts of Cu(I).

Since the on-column dissociation of the Cu(I)-cyanide complexes could be controlled by the addition of NaCN to the eluent, it was reasoned that increasing the cyanide concentration in the eluent would improve the ruggedness of the method with respect to the range of Cu(I) concentrations. This was indeed the case, as shown in Tables 6.3 and 6.4. However, increasing the NaCN concentration in the eluent also had the effect of increasing the PCR detector baseline noise as was shown in Chapter four. Furthermore, because of this noise, accurate peak integration decreased when the R value of the standard was close to 3. This accounts for the larger variation in the PAR for the R = 3 standards shown in Tables 6.1 and 6.4. It should also be noted that increasing the eluent cyanide concentration had the same effect on the CN:Cu calibration plots as for the 5 cm Nova-Pak C-18 column as shown in Fig. 6.13.

[Cu] (mM)	CN:Cu(I) PAR	% Variation in PAR compared to 1.0 mM Cu(I) standard	Calculated CN:Cu Mole ratio
0.6	0.0886	92.48	3.01
0.8	0.0898	93.74	3.02
1.0	0.0958	100.00	3.03
1.2	0.0929	96.97	3.02
1.4	0.0939	98.02	3.03

Table 6.2: Variation in CN:Cu(I) peak area ratio (PAR) with concentration of Cu(I) in the sample. Each standard had a CN:Cu mole ratio of 3.0. Calculated R value determined from the CN:Cu mole ratio calibration plot for 1.0 mM standards. The eluent contained 80 μM NaCN and the analysis was performed on a 15 cm Nova-Pak C-18 column.

[Cu]	80 μM NaCN		100 μM NaCN		120 μM NaCN	
(mM)	PAR	% variation in PAR	PAR	% variation in PAR	PAR	% variation in PAR
0.5	0.5014	105.46	0.4720	103.50	0.4422	100.84
1	0.4755	100.00	0.4561	100.00	0.4385	100.00
1.5	0.4740	99.70	0.4458	97.74	0.4301	98.08
2	0.4670	98.22	0.4537	99.48	0.4274	97.46

Table 6.3: Effect of eluent NaCN concentration on the variation in CN:Cu(I) peak area ratio (PAR) with concentration of Cu(I) in the sample. Each standard had a CN:Cu mole ratio of 4.0. The eluents contained 80-120 μM NaCN and the analyses were performed on a 15 cm Nova-Pak C-18 column.
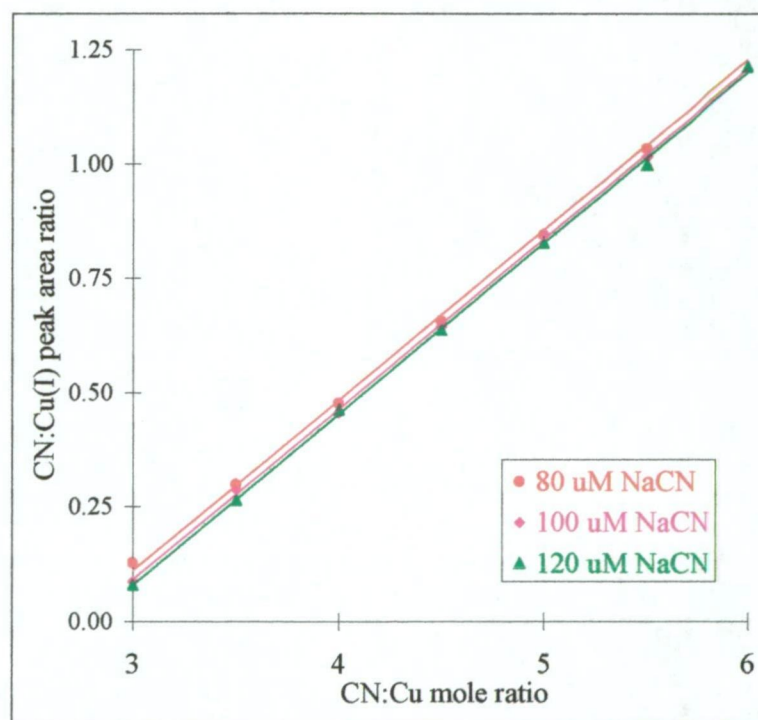
Fig. 6.13: Effect of eluent cyanide concentration on the CN:Cu mole ratio calibration plot. Eluents contained 80-120 mM NaCN. Analyses on a 15 cm Nova-Pak C-18 column.

Actual R value	0.5mM Cu(I) Standard			1.0mM Cu(I) Standard			1.5mM Cu(I) Standard			2.0 mM Cu(I) Standard		
	PAR	% variation in PAR	Calculated R value	PAR	% variation in PAR	Calculated R value	PAR	% variation in PAR	Calculated R value	PAR	% variation in PAR	Calculated R value
3	0.1113	87.41	3.00	0.1273	100.00	3.04	0.1150	90.36	3.01	0.1063	83.49	2.99
4	0.5014	105.46	4.05	0.4755	100.00	3.98	0.4740	99.70	3.98	0.4670	98.22	3.96
5	0.8706	103.21	5.04	0.8435	100.00	4.97	0.8399	99.57	4.96	0.8466	100.36	4.98

Actual R value	0.5mM Cu(I) Standard			1.0mM Cu(I) Standard			1.5mM Cu(I) Standard			2.0 mM Cu(I) Standard		
	PAR	% variation in PAR	Calculated R value	PAR	% variation in PAR	Calculated R value	PAR	% variation in PAR	Calculated R value	PAR	% variation in PAR	Calculated R value
3	0.0777	88.95	2.96	0.0874	100.00	2.99	0.0942	107.81	3.01	-	-	-
4	0.4721	103.50	4.02	0.4561	100.00	3.98	0.4458	97.75	3.95	0.4537	99.47	3.97
5	0.8702	102.78	5.09	0.8467	100.00	5.03	0.8397	99.18	5.01	0.8347	98.59	5.00

Table 6.4 : Effect of (a; Top) 80 and (b; Bottom) 100 μM NaCN in the eluent on the dissociation of Cu(I)-cyanide complexes. Cu(I) standards contained 0.5-2.0 mM Cu(I) and CN:Cu mole ratios from 3.0 - 5.0. Percentage variation in PAR (Peak area ratio) compared to the 1.0 mM Cu(I) standards. Calculated R value determined from the CN:Cu mole ratio calibration plot for 1.0 mM standards.

A calibration plot prepared using 15 mM Cu(I) standards (1.0 μL injection volume) and an eluent containing 140 μM NaCN was found to be applicable for sample solutions containing Cu(I) in the range 7.5–22.5 mM. This is illustrated in Table 6.5 and Fig. 6.14 which show CN:Cu values obtained for a series of standards using calibration plots derived from either a single 15 mM Cu(I) concentration or a series of Cu(I) concentrations. The values obtained using each approach were very similar. From these results it was evident that only five standard solutions (Nos. 1-3, 9 and 10 in Table 6.5) were required for calibration plots for determination of the CN:Cu mole ratio and the concentrations of the Cu(I) complex and thiocyanate in the samples.

Standard No.	[Cu] (mM)	CN:Cu Mole ratio	[SCN] (ppm)	CN:Cu PA ratio	Calculated CN:Cu Mole ratio	
					15 mM Cu stds	Other Cu Stds
1	7.5	5.00	50	0.91	4.98	5.00
2	12	4.25	100	0.62	4.24	4.25
3	15	3.00	150	0.14	3.03	3.03
3	15	3.00	150	0.13	3.00	3.00
4	15	3.50	50	0.32	3.49	3.49
5	15	4.00	100	0.51	3.97	3.98
6	15	4.50	250	0.72	4.49	4.50
7	15	5.00	200	0.93	5.03	5.05
8	7.5	4.00	150	0.54	4.03	4.05
9	19.5	3.77	200	0.41	3.71	3.72
10	22.5	3.33	250	0.25	3.29	3.30

Table 6.5: Standards used for the determination of [Cu(I)], [SCN] and the CN:Cu mole ratio. The CN:Cu peak area ratio (PA) was determined experimentally in an eluent containing 140 μM NaCN and the CN:Cu mole ratios for each standard were then calculated from calibration plots prepared either from standards 3-7or from standards 1-3, 8-10.
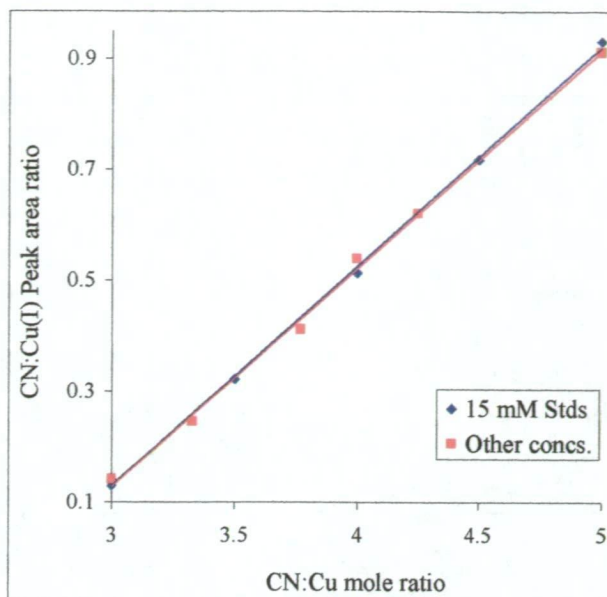
Fig. 6.14: Effect of Cu(I) concentration on the CN:Cu mole ratio calibration plot. Standards as shown in Table 6.4.

6.3.5 Comparison of HPLC results with standard methods

The results obtained by the HPLC methods were compared to those obtained by the standard methods used for determination of copper and total cyanide. The standard method for determination of copper used AAS. The standard method for total cyanide determination used acid digestion of a sample followed by collection of the evolved HCN gas in a receiving vessel containing a NaOH solution, as shown in Fig. 1.7. The cyanide concentration in the NaOH solution was subsequently determined by titration with $AgNO_3$. Since a one hour period was recommended for the acid digestion step, a multi-cyanide distillation unit was used that allowed up to 10 samples to be treated simultaneously. However, due to failure of the cyanide distillation unit on several occasions, only a limited amount of data was obtained for comparison of the HPLC and acid distillation results for total cyanide. The most common problem encountered with the multi-cyanide distillation unit was failure of the thermostat and subsequent failure of the heating elements due to over-heating.

The results obtained from both the UV and PCR detection systems were compared with the standard methods (Table 6.6). The ratio of the HPLC result (UV and PCR detectors) compared to the result obtained by standard methods was expressed as a

percentage, as shown in Table 6.6. Since time did not permit extensive duplicate analyses, an estimation of the variation between the different sets of results was obtained by determining the mean and RSD (%) of the above ratios as shown in Table 6.6. It can be seen that the results obtained by the PCR detector were closer to those obtained by the standard methods than those obtained by the UV detector. A possible reason for this difference is discussed in the following section.

Table 6.6: Following four pages: Comparison of copper and total cyanide determinations obtained by HPLC and standard methods in Cu(I)-cyanide leach samples over twenty consecutive days. Results and comparisons with the standard methods shown for both the UV and PCR detectors. The total cyanide in the Cu-CN system was calculated for the HPLC results as a product of the Cu(I) concentration and CN:Cu mole ratio. The standard methods for determination of copper and total cyanide are discussed in the text.

Col. A Sampling Day No.	HPLC UV Detector		HPLC PCR detector			HPLC [Total CN] CuCN system		Standard methods		Variation between results			
	[SCN] (mM)	[Cu] (mM)	[SCN] (mM)	[Cu] (mM)	CN:Cu Mole ratio	Cu-UV (mM CN)	Cu-PCR (mM CN)	[Cu] (AAS) (mM)	[Total CN] (acid digest) (mM)	[Cu] UV (%)	PCR (%)	[Total CN] UV (%)	PCR (%)
1	4.96	59.83	5.07	58.60	3.485	208.53	204.26	57.99	204.12	103.16	101.05	102.16	100.07
2	4.99	59.29	5.06	57.90	3.459	205.08	200.26	56.99	201.69	104.04	101.60	101.68	99.29
3	5.08	59.63	5.10	58.55	3.525	210.21	206.39	57.40	206.28	103.89	102.00	101.90	100.05
4	4.92	57.13	5.47	56.14	3.507	200.32	196.88	53.78	196.33	106.23	104.40	102.03	100.28
5	4.77	54.87	4.78	53.94	3.464	190.09	186.87	54.03	187.00	101.56	99.84	101.65	99.93
6	5.17	59.05	5.69	57.49	3.517	207.69	202.22	55.67	210.51	106.08	103.28	98.66	96.06
7	5.51	62.72	6.04	60.56	3.420	214.52	207.13	58.95	205.65	106.38	102.72	104.31	100.72
8	5.52	62.61	5.34	60.46	3.533	221.19	213.58	60.39	217.28	103.69	100.12	101.80	98.29
9	5.20	59.94	5.83	59.33	3.523	211.16	209.01	59.00	202.59	101.59	100.55	104.23	103.17
10	4.56	51.92	5.01	52.54	3.507	182.08	184.23	49.64	178.58	104.60	105.84	101.96	103.17
11	4.43	51.00	4.93	51.04	3.590	183.10	183.25	47.67	175.76	106.98	107.07	104.17	104.26
12	4.71	52.72	5.45	54.46	3.544	186.86	193.02	54.44	179.09	96.84	100.03	104.34	107.78
13	5.27	58.51	4.41	53.10	3.609	211.18	191.66	58.59	201.57	99.85	90.62	104.77	95.08
14	5.46	59.01	5.23	58.23	3.567	210.47	207.68	57.82	210.39	102.06	100.71	100.04	98.71
15	5.54	59.93	5.67	58.98	3.603	215.93	212.50	57.40	209.22	104.41	102.75	103.21	101.57
16	5.65	61.11	5.35	60.20	3.598	219.85	216.60	61.17	221.10	99.89	98.41	99.44	97.97
17	5.03	55.17	3.67	55.18	3.645	201.11	201.14	56.85	193.78	97.05	97.06	103.78	103.80
18	5.35	58.18	4.60	56.70	3.625	210.89	205.54	59.16	209.10	98.34	95.84	100.86	98.30
19	4.96	53.18	4.92	52.30	3.630	193.03	189.85	54.93	187.13	96.81	95.22	103.16	101.45
20	4.81	51.18	4.75	50.18	3.717	190.24	186.52	57.54	189.68	88.94	87.20	100.30	98.34
									Average:	101.62	99.82	102.22	100.41
									Standard Deviation:	4.42	4.81	1.77	2.99
									% RSD:	4.35	4.82	1.73	2.97

Table 6.6(a): Comparison of results obtained for Column A samples over a twenty day period.

Col. B Sampling Day No.	HPLC UV Detector [SCN] (mM)	[Cu] (mM)	HPLC PCR detector [SCN] (mM)	[Cu] (mM)	CN:Cu Mole ratio	HPLC [Total CN] CuCN system Cu-UV (mM CN)	Cu-PCR (mM CN)	Standard methods [Cu] (AAS) (mM)	[Total CN] (acid digest) (mM)	Variation between results [Cu] UV (%)	[Cu] PCR (%)	[Total CN] UV (%)	[Total CN] PCR (%)
1	4.68	54.89	5.00	53.65	3.329	182.72	178.61	54.08	177.68	101.50	99.22	102.84	100.52
2	5.15	60.77	4.88	59.28	3.321	201.80	196.87	58.28	195.55	104.27	101.72	103.19	100.68
3	5.20	60.64	5.20	59.63	3.337	202.33	198.99	59.88	202.45	101.26	99.58	99.94	98.29
4	5.37	61.95	6.06	61.20	3.342	207.03	204.55	58.58	207.69	105.75	104.48	99.68	98.49
5	5.26	60.46	5.13	59.76	3.276	198.04	195.77	61.55	196.33	98.22	97.09	100.87	99.72
6	5.27	59.90	5.10	58.93	3.332	199.56	196.32	56.42	196.96	106.17	104.44	101.32	99.68
7	5.58	63.78	5.53	61.31	3.277	209.00	200.90	60.65	212.43	105.16	101.08	98.39	94.57
8	5.72	64.98	6.55	62.06	3.316	215.47	205.78	62.01	207.06	104.79	100.08	104.06	99.38
9	5.68	65.48	6.21	65.14	3.369	220.61	219.47	69.00	216.89	94.90	94.41	101.71	101.19
10	5.65	63.96	4.73	64.18	3.350	214.29	215.03	60.43	206.16	105.83	106.20	103.94	104.30
11	5.24	59.51	5.82	57.95	3.453	205.47	200.08	55.74	181.76	106.75	103.95	113.04	110.08
12	5.21	57.51	4.77	59.77	3.391	195.01	202.66	57.27	188.66	100.42	104.36	103.37	107.42
13	5.24	57.89	2.95	53.12	3.388	196.13	179.98	59.99	187.78	96.50	88.55	104.45	95.85
14	5.63	61.64	5.53	60.82	3.399	209.56	206.76	63.38	202.33	97.26	95.97	103.57	102.19
15	5.77	62.01	5.68	61.97	3.384	209.84	209.69	67.80	195.04	91.46	91.40	107.59	107.51
16	5.74	61.98	5.85	60.20	3.428	212.48	206.38	62.10	206.28	99.80	96.94	103.00	100.05
17	5.95	63.60	4.92	62.97	3.436	218.51	216.34	65.58	213.06	96.98	96.01	102.56	101.54
18	5.67	61.26	4.58	60.82	3.419	209.45	207.94	61.85	199.53	99.05	98.33	104.97	104.21
19	5.78	61.33	5.72	60.60	3.342	204.96	202.49	58.40	203.86	105.01	103.75	100.54	99.33
20	5.58	58.43	5.46	57.20	3.401	198.71	194.53	66.34	188.53	88.09	86.23	105.40	103.18
									Average:	100.46	98.69	103.22	101.41
									Standard Deviation:	5.22	5.51	3.18	3.85
									% RSD:	5.19	5.58	3.08	3.80

Table 6.6(b): Comparison of results obtained for Column B samples over a twenty day period.

CC Feed Sampling Day No.	HPLC UV Detector		HPLC PCR detector			HPLC [Total CN] CuCN system		Standard methods		Variation between results			
	[SCN] (mM)	[Cu] (mM)	[SCN] (mM)	[Cu] (mM)	CN:Cu Mole ratio	Cu-UV (mM CN)	Cu-PCR (mM CN)	[Cu] (AAS) (mM)	[Total CN] (acid digest) (mM)	[Cu] UV (%)	PCR (%)	[Total CN] UV (%)	PCR (%)
1	4.61	54.11	4.61	52.63	3.777	204.36	198.78	58.53	212.30	92.44	89.91	96.26	93.63
2	5.27	61.84	5.50	59.96	3.711	229.50	222.51	53.70	201.69	115.17	111.66	113.78	110.32
3	5.24	61.00	5.61	59.43	3.793	231.36	225.44	56.19	217.65	108.56	105.78	106.30	103.58
4	5.30	61.41	5.17	60.23	3.814	234.25	229.74	60.10	225.44	102.18	100.21	103.91	101.90
5	5.31	60.99	5.47	60.28	3.666	223.58	220.97	59.96	227.63	101.72	100.53	98.22	97.08
6	5.23	59.55	5.29	58.25	3.753	223.50	218.63	59.00	219.06	100.93	98.73	102.03	99.81
7	5.47	63.10	5.70	60.38	3.705	233.76	223.71	57.00	220.73	110.69	105.93	105.90	101.35
8	5.62	63.63	6.17	61.17	3.909	248.71	239.09	57.87	230.79	109.96	105.70	107.76	103.59
9	5.64	64.48	4.12	64.19	3.768	242.96	241.87	59.85	242.56	107.73	107.24	100.16	99.71
10	5.60	63.28	6.22	63.22	3.814	241.35	241.12	65.23	240.40	97.01	96.91	100.40	100.30
11	5.23	59.26	5.78	60.24	3.857	228.57	232.34	56.31	227.12	105.24	106.97	100.64	102.30
12	5.13	56.90	6.04	58.79	3.795	215.96	223.11	59.55	213.18	95.55	98.71	101.30	104.66
13	5.15	57.07	4.03	52.91	3.789	216.23	200.48	58.39	206.28	97.74	90.62	104.82	97.18
14	5.58	61.05	5.63	59.66	3.890	237.52	232.09	58.55	211.26	104.28	101.90	112.43	109.86
15	5.67	61.76	5.50	60.90	3.749	231.56	228.33	57.60	217.53	107.22	105.72	106.45	104.97
16	5.72	61.62	5.59	60.55	3.671	226.19	222.28	61.52	225.08	100.15	98.42	100.49	98.76
17	5.90	63.35	4.65	62.60	3.740	236.93	234.11	64.04	223.91	98.93	97.75	105.81	104.55
18	5.70	61.38	4.22	61.38	3.953	242.60	242.62	63.96	224.81	95.96	95.97	107.91	107.92
19	5.68	60.63	5.96	59.94	3.693	223.88	221.33	63.03	225.83	96.18	95.09	99.13	98.01
20	5.67	59.70	5.70	58.50	3.550	211.92	207.66	60.86	217.02	98.10	96.12	97.65	95.69
									Average:	102.29	100.49	103.57	101.76
									Standard Deviation:	6.09	5.78	4.76	4.53
									% RSD:	5.96	5.75	4.60	4.45

Table 6.6(c): Comparison of results obtained for Carbon Column Feed (CC Feed) samples over a twenty day period.

CC Prod Sampling Day No.	HPLC UV Detector [SCN] (mM)	HPLC UV Detector [Cu] (mM)	HPLC PCR detector [SCN] (mM)	HPLC PCR detector [Cu] (mM)	CN:Cu Mole ratio	HPLC [Total CN] CuCN system Cu-UV (mM CN)	HPLC [Total CN] CuCN system Cu-PCR (mM CN)	Standard methods [Cu] (AAS) (mM)	Standard methods [Total CN] (acid digest) (mM)	Variation [Cu] UV (%)	Variation [Cu] PCR (%)	Variation [Total CN] UV (%)	Variation [Total CN] PCR (%)
1	4.80	57.62	5.15	55.67	3.690	212.61	205.39	57.37	207.69	100.45	97.04	102.37	98.89
2	4.71	55.60	5.08	54.47	3.761	209.12	204.89	52.34	204.53	106.21	104.07	102.24	100.18
3	5.14	61.03	5.79	59.13	3.753	229.08	221.92	57.88	219.71	105.44	102.14	104.26	101.01
4	5.23	60.91	4.98	59.60	3.782	230.41	225.45	59.38	226.10	102.58	100.38	101.91	99.71
5	5.26	60.60	5.44	59.61	3.796	230.04	226.26	60.59	229.91	100.02	98.38	100.05	98.41
6	5.24	60.15	5.14	58.96	3.658	220.01	215.67	57.10	224.57	105.34	103.26	97.97	96.04
7	4.74	53.28	5.20	50.94	3.749	199.75	190.98	55.70	220.34	95.65	91.45	90.66	86.67
8	5.62	63.82	5.54	61.54	3.731	238.11	229.60	60.29	231.59	105.85	102.06	102.82	99.14
9	5.64	64.69	5.79	65.09	3.822	247.24	248.80	64.24	241.93	100.69	101.32	102.19	102.84
10	5.55	64.26	6.12	65.13	3.825	245.78	249.11	61.91	239.24	103.79	105.19	102.74	104.13
11	5.52	62.60	4.50	62.80	3.790	237.25	238.00	57.92	222.97	108.09	108.44	106.40	106.74
12	5.30	59.06	5.70	62.95	3.849	227.31	242.30	58.26	217.79	101.36	108.05	104.37	111.25
13	5.05	53.94	4.53	50.71	3.786	204.25	191.99	56.77	219.83	95.03	89.32	92.91	87.34
14	5.34	58.43	5.16	57.58	3.783	221.05	217.85	57.60	217.53	101.43	99.97	101.62	100.15
15	5.54	60.39	5.06	58.74	3.854	232.75	226.36	59.65	224.30	101.25	98.47	103.76	100.92
16	5.64	60.92	5.46	59.70	3.817	232.55	227.89	62.59	217.02	97.33	95.38	107.16	105.01
17	5.76	62.82	5.54	63.28	3.922	246.38	248.20	64.56	225.20	97.30	98.02	109.41	110.21
18	5.67	62.21	4.15	62.14	3.976	247.35	247.07	63.03	225.20	98.69	98.58	109.84	109.71
19	5.68	60.10	6.18	59.77	3.984	239.44	238.13	58.80	228.26	102.21	101.65	104.90	104.32
20	5.71	61.03	5.65	59.78	3.904	238.24	233.38	66.10	209.22	92.33	90.44	113.87	111.55
Average:										101.05	99.68	103.07	101.71
Standard Deviation:										4.14	5.24	5.31	6.78
% RSD:										4.09	5.25	5.15	6.67

Table 6.6(d): Comparison of results obtained for Carbon Column Product (CC Prod) samples over a twenty day period.

6.3.6 Interference from cobalt cyanide complexes

Analysis of some Cu(I)-cyanide HPLC standards by AAS revealed very little difference between the two analytical methods, as shown in Table 6.7. Since there was good agreement between the PCR detector results and those obtained by the standard methods, this suggested that there was an interfering species which was detectable at the UV wavelength but was not derivatised by the selective PCR reaction.

ICP-AES analysis of some Cu(I)-cyanide leachate samples showed the presence of cobalt and a peak due to the Co(III) complex was also observed in most samples, as shown in Fig. 6.9. The cobalt concentrations determined by ICP-AES were significantly higher than those obtained by HPLC. It was not until after the leaching trials were completed that it was realised that the reaction of Co(II) with cyanide is slow and the final product, $[Co(CN)_6]^{3-}$, is not formed immediately. This slow reaction accounts for the differences between the ICP-AES and HPLC results. Chromatographic analysis of a solution of NaCN added to Co(II)chloride gave a series of peaks, with two major peaks at retention times of 4.0 and 5.9 min, as shown in Fig. 6.15. The first of these had the same retention time as the small, unidentified peak in Fig. 6.5, whilst the second had the same retention time as Cu(I).

HPLC standard [Cu(I)] / (mM)	HPLC standard R value	AAS analysis [Cu] / mM
10	3.0	10.1
5	4.0	4.90
10	4.5	10.0
15	5.0	15.4
20	5.25	19.6

Table 6.7: Analysis of Cu(I) HPLC standards by AAS.
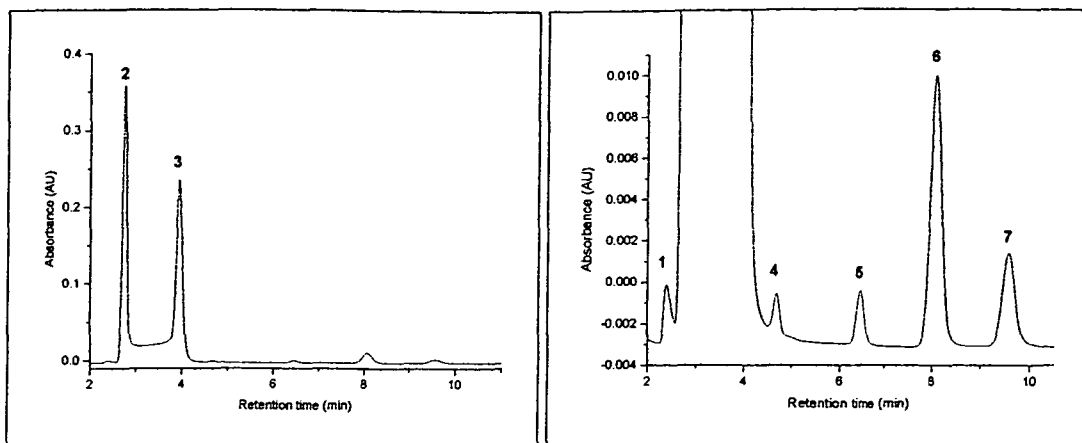
Fig. 6.15 : UV detector chromatogram (205 nm) of solution of CoCl$_2$ mixed with NaCN.

RHS: Enlarged chromatogram showing minor peaks.

Legend: **2, 3** and **6** : Cobalt cyanide complexes **(I)**, **(II)** and **(IV)** (See text for details).

Peaks **1, 4, 5** and **7**: Other metallo-cyanide complexes resulting from contamination and/or impurities. Eluent: 25% acetonitrile, 5 mM Low UV PIC A. Column: 15 cm Nova-Pak C-18

The chromatography of the cyano-cobalt complexes has previously been reported [7] and it has been shown that the first complex formed when cyanide was added to a Co(II) salt was the pentacyano cobalt (II) complex, $[Co(CN)_5]^{2-}$ **(I)**. In the presence of oxygen (which is ubiquitous in the leaching process), **(I)** formed an oxygen bridged complex, $[Co(CN)_5CoOOCo(CN)_5]^{6-}$ **(II)**, which reacted further with **(I)** to form the cobalt (III) pentacyano complex $[Co(CN)_5]^{3-}$ **(III)**. Finally, **(III)** and cyanide reacted to form the hexacyanocobalt (III) complex, $[Co(CN)_6]^{3-}$ **(IV)**.

From the above observations and the conclusions obtained by Thompsen [7], it would appear that the two major peaks noted above in the chromatogram of the mixture of NaCN and Co(II) chloride could be assigned to the intermediate Co-cyanide complexes **(I)** and **(II)**. This suggested that the positive bias in the UV detector results for Cu(I) may have been due to interference from one of the intermediate Co-cyanide complexes. Such a complex would be detectable at low UV wavelengths but would not be derivatised by the PCR reaction. Furthermore, the decrease in the unidentified peak relative to the thiocyanate peak shown in Fig. 6.5 provides further evidence to support this hypothesis.

6.3.7 Analysis of Pyrite Leach samples

6.3.6.1 Initial investigations

Pyrite leach samples were obtained from the cyanidation of the tailings from the CPS/flotation treatment of high grade copper-gold ore. Previous studies have found 5g/t Au in this tailings stream [8]. The operation of the pyrite leach plant was intermittent and only a limited number of samples could be analysed during the first field trial. The PCR detection system was not operational for these analyses, thereby preventing cyanide analyses of these three samples. The concentrations (as determined with the UV detector) of thiocyanate, Cu(I), Fe(II) and Au(I) in three pyrite leach samples are shown in Table 6.8.

A 25-fold dilution of each sample was required to enable quantitative analysis of thiocyanate and the Cu(I) and Fe(II) complexes, as shown in Fig 6.16(a). A large injection volume (100 µL) of the undiluted sample was required for analysis of the Au(I) complex. However, a shoulder peak on the $[Au(CN)_2]^-$ peak prevented accurate quantitative analysis of the Au(I) complex with an eluent containing 25% acetonitrile as shown in Fig. 6.16(b). In addition, a series of small and only partly resolved peaks were eluted off the column 12 minutes after the $[Au(CN)_2]^-$ peak. The appearance of these peaks was similar to those observed with the Dump Leach samples discussed in the previous Chapter (Section 5.3.6).

Sample	[SCN] (ppm)	[Cu(I)] (ppm)	[Fe(II)] (ppm)	[Au] (ppm)	[MeCN]	Retention time (min)			
						SCN	Cu(I)	Fe(II)	Au(I)
#1	3007	3418	93.5	-					
#2	1605	1811	41.2	4.26	25%	4.37	4.78	8.28	6.53
#3	1429	1758	36.7	-	23%	5.47	6.38	13.63	10.05

Table 6.8: Concentrations thiocyanate, Cu(I), Fe(II) and Au(I) in Pyrite Leach samples. Retention time of the four analytes with two eluents used for these samples.

Eluents : 25% or 23% acetonitrile, 5 mM TBAOH, 10 mM KH_2PO_4, 5 mM H_2SO_4 and 80 µM NaCN. Columns (Nova-Pak C-18): 15 + 5 cm tandem combination for analysis of thiocyanate and the Cu(I) and Fe(II) complexes. 5 cm column for analysis of the Au(I) complex.

When the acetonitrile concentration in the eluent was reduced to 23%, it was possible to separate the $[Au(CN)_2]^-$ peak from the shoulder peak observed with the eluent containing 25% acetonitrile, as shown in Fig. 6.16(c). However, the retention times of all the components were significantly increased, as shown in Table 6.8. The concentration of the Au(I) complex was determined in one of these samples by both HPLC and AAS to be 4.26 and 3.79 ppm respectively. This difference in the Au(I) concentrations between the HPLC and AAS determinations was similar to that observed for the CIP samples discussed in the previous Chapter (Section 5.3.4).
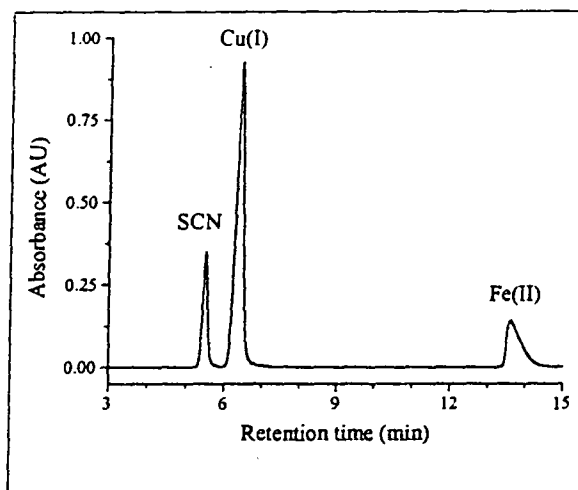
Fig. 6.16 (a): 25-fold dilution of Pyrite leach sample #2 (see Table 6.7) for analysis of thiocyanate and the Cu(I) and Fe(II) complexes. (10 µL injection). UV detector chromatogram (214 nm).
Eluent: 23% acetonitrile, 5 mM TBAOH, 10 mM KH_2PO_4, 5 mM H_2SO_4 and 80 µM NaCN.
Columns: 15 + 5 cm Nova-Pak C-18 in tandem.
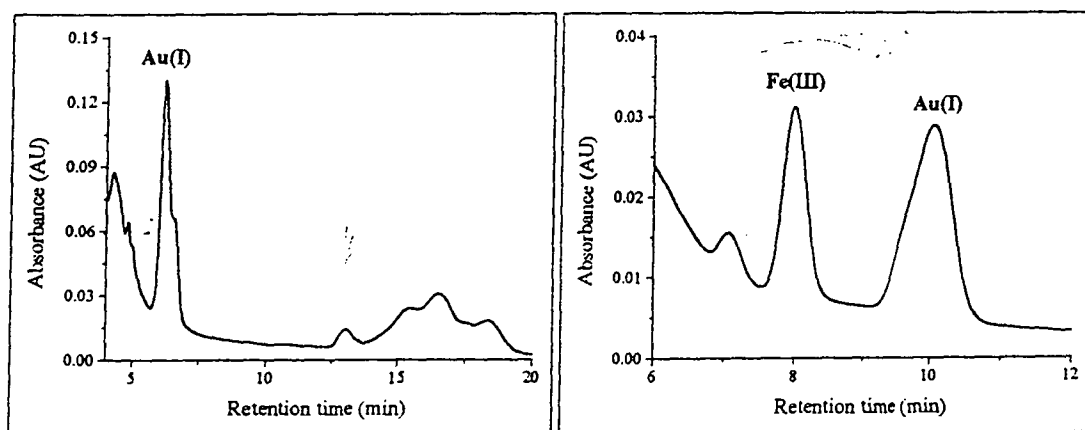
Fig. 6.16 [b (LHS) & c (RHS)]: Undiluted Pyrite leach sample analysed for Au(I) (100 µL injection). UV detector chromatograms (205 nm). Eluents : 25% (LHS) or 23% (RHS) acetonitrile, 5 mM TBAOH, 10 mM KH_2PO_4, 5 mM H_2SO_4 and 80 µM NaCN. Column: 5 cm Nova-Pak C-18.

A new Pyrite Leach (PL) plant became operational during the Cu(I)-cyanide leach trials. This allowed pyrite leach samples to be analysed with the methodology developed for the Cu(I)-cyanide leach samples. The new Pyrite leach plant used three leaching tanks (PLT1, PLT2 and PLT3). The effluent from PLT3 was fed directly into the CIP circuit for subsequent recovery of the Au(I) complex. The major species observed in the PL tank (PLT) samples were cyanide, thiocyanate, cyanate and the complexes of Cu(I) and Fe(II), with concentrations up to 150 mM of Cu(I), 7 mM Fe(II), 93 mM thiocyanate and 23 mM cyanate. Typical examples of chromatograms obtained from PLT1 and PLT3 tanks are shown in Fig. 6.17.

The concentration of cyanide decreased progressively through the pyrite leach circuit, while the concentrations of the other species increased. This led to a situation where many of the PLT3 samples contained R values below 3.0. Due to considerable variation in the flotation tails, large, and sometimes rapid, fluctuations of all species commonly occurred. The concentrations of PLT1 and PLT3 samples over five consecutive days are shown in Table 6.9.

6.3.7 Analysis of samples with CN:Cu mole ratios less than 3.0

Two approaches were investigated for samples having R values below 3.0. The first was to perform standard additions of cyanide to the samples, after which the concentration of cyanide originally present in the sample could be calculated. Initially, it was found that the concentrations of all the cyano species in the PLT samples increased after a NaCN standard addition. This complicated the calculation of the R value of the original sample, since it was necessary to account for changes to the peak areas of all species before and after the addition of cyanide. However, it was subsequently found that filtration of the PLT samples with a 0.45 μM filter prior to the standard addition avoided this problem. This indicated that the PLT samples contained very fine particulate matter which was had not completely reacted with cyanide in the three pyrite leaching tanks. The validity of the standard addition procedure was tested on PLT1 samples as these all had R values greater than 3.0, (i.e. these samples fell within the normal calibration range). The experimentally

determined R values after the NaCN addition were within 5% of the calculated values, as shown in Table 6.9. The mean, standard deviation and %RSD are calculated for the cyanide recovery in the five PLT1 samples (Table 6.9). These statistics further supported the validity of the standard addition procedure.

Fig. 6.17 (a & b): Typical UV detector chromatogram of a pyrite leach sample. Expanded chromatogram shown in (**b**) (RHS).

Fig. 6.17 (c & d): Typical PCR detector chromatograms of (**c**) (LHS) PLT1 sample and (**d**) (RHS) PLT3 sample before (RED) and after (GREEN) NaCN standard addition.

Column: 15 cm Nova-Pak C-18.

Eluent: 25% acetonitrile, 10 mM TBAOH, 10 mM KH_2PO_4, 5 mM H_2SO_4 and 140 μM NaCN.

Name	CN : Cu mole ratio		[Cu] / mM				[SCN] / ppm			[Fe(II)] / ppm			Cyanide Recovery (%)
	Before CN added	After CN added	Before CN added	After CN added	Mean (mM)	Mean (ppm)	Before CN added	After CN added	Mean	Before CN added	After CN added	Mean	
PLT1, Day1	3.10	3.97	111.2	110.4	110.8	7040	3774	3741	3758	62.6	61.6	62.1	96.40
PLT3, Day1	2.65	3.29	156.9	154.9	155.9	9906	6837	6798	6818	92.0	91.7	91.9	
PLT1, Day2	3.16	4.11	104.4	104	104.2	6621	3514	3500	3507	66.6	65.5	66.1	98.99
PLT3, Day2	2.80	3.46	152.5	152.2	152.4	9680	6498	6470	6484	82.0	80.0	81.0	
PLT1, Day3	3.16	4.19	100.8	99.1	100.0	6351	3420	3360	3390	64.0	68.1	66.1	102.95
PLT3, Day3	2.91	3.63	140.1	137.8	139.0	8829	5647	5559	5603	74.0	72.0	73.0	
PLT1, Day4	3.60	4.82	84.89	84.7	84.795	5388	2929	2877	2903	56.0	59.1	57.6	103.45
PLT3, Day4	2.71	3.50	127.5	125.5	126.5	8038	4987	4929	4958	66.0	66.0	66.0	
PLT1, Day5	3.31	4.57	82.66	84.55	83.61	5312	2929	2957	2943	69.5	70.3	69.9	105.34
PLT3, Day5	3.20	4.02	115.1	118	116.6	7406	4412	4515	4464	69.4	70.7	70.1	
												mean=	101.43
												Std. Dev.=	3.64
												%RSD=	3.59

Table 6.9: Analysis of pyrite leach samples over five days, including standard additions of NaCN to Pyrite leach samples. For PLT1 samples, all with R values > 3, the R value was determined before and after the standard addition. The R value of the original PLT1 sample was then calculated from the value determined after the standard addition. This calculated value was compared to the value determined before the standard addition. This allowed the cyanide recovery to be determined and expressed as a percentage. The CN:Cu mole ratios for the PLT3 samples that were less than 3.0 were calculated from the standard addition results.

Sample preparation: 10.0 ml of each sample was diluted to 100.0 ml with RO water prior to analysis. The standard addition consisted of 10.0 ml of 100 mM NaCN to each diluted sample. An analysis was performed on each diluted sample before and after the addition of NaCN. Chromatographic conditions as for Fig. 6.17.

The second approach was to extrapolate the calibration plot for the CN:Cu mole ratio, which was applicable only when a cyanide peak was obtained. However, very small cyanide peaks were difficult to determine accurately due to the baseline pump noise in the PCR detector chromatograms, as shown in Fig. 6.17(d). Injection of a sample with a CN:Cu mole ratio below the intercept value for the calibration plot gave a negative cyanide peak due to removal of cyanide from eluent by the eluted Cu(I)-cyanide complex, as shown in Fig. 6.18. The use of the CN:Cu(I) peak area ratio below the calibration limit was compared to the above standard addition approach, as shown in Table 6.10. Note that the same calibration equation was used when samples had a negative CN peak. These results indicated that extrapolation of the CN:Cu mole ratio below the calibration limit was feasible, so long as there was a CN peak (either positive or negative) of sufficient magnitude to allow accurate quantification. This was encouraging since the standard addition procedure required more sample preparation time.
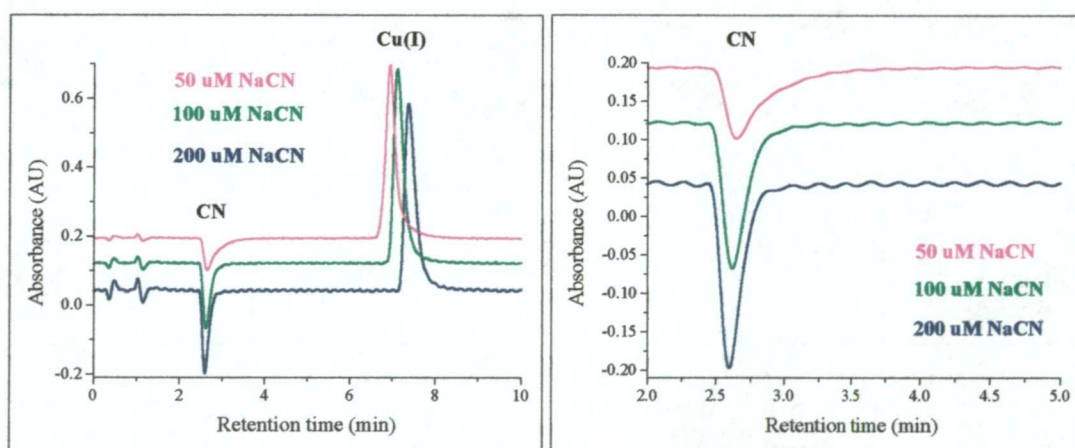
Fig. 6.18: Overlaid (and offset) PCR detector chromatograms of a Cu(I)-cyanide leach sample with a low CN:Cu mole ratio (R = 2.15) analysed in three eluents containing 50 mM, 100 mM or 200 μM NaCN. Enlarged CN peak and baseline shown on RHS.

Some points should be noted with respect to the use of negative CN peaks. For a given sample with a low R value, the magnitude of the negative CN peak increased with the concentration of NaCN in the eluent, as shown in Fig. 6.18. The negative CN peak symmetry also improved with increased NaCN concentration in the eluent.

However, the baseline noise of the PCR detector also increased with the NaCN concentration in the eluent. Furthermore, an increase in the NaCN concentration in the eluent resulted in a decrease in the magnitude of positive CN peaks and a decrease in the CN:Cu(I) peak area ratio as shown in Table 6.11. This led to a situation where samples with an R value close to 3.0 (eg. Samples #7 & #9 in Table 6.11) that could be analysed directly with an eluent containing 50 μM NaCN, would require a standard addition prior to analysis in an eluent containing 200 μM NaCN.

Sample #	Without std addn	With std addn	Sample #	Without std addn	With std addn
1	2.959	3.002	8	2.844	2.893
2	2.925	2.946	9	2.798	2.794
3	2.898	2.931	10	2.571	2.554
4	2.848	2.892	11	2.737	2.716
5	2.735	2.711	12	2.605	2.6
6	2.925	2.945	13	2.513	2.525
7	2.872	2.906	14	2.410	2.388

Table 6.10: Comparison of methods for determining low R values. The R values determined without the standard addition (std addn) procedure were determined by extrapolation of the CN:Cu mole ratio calibration.

Sample	CN:Cu mole ratio	[Eluent NaCN] = 50 µM			[Eluent NaCN] = 100 µM			[Eluent NaCN] = 200 µM		
		Peak area (PA)		CN:Cu	Peak area (PA)		CN:Cu	Peak area (PA)		CN:Cu
		CN	Cu(I)	PA ratio	CN	Cu(I)	PA ratio	CN	Cu(I)	PA ratio
1	4.02	3174188	6295984	0.5042	2888574	6602013	0.4375	2788818	6777199	0.4115
2	3.47	2070146	7055540	0.2934	1808059	7105349	0.2545	1698797	7549627	0.2250
3	3.08	1117940	7750623	0.1442	892851	8291116	0.1077	674582	8319942	0.0811
4	3.44	1983258	7096464	0.2795	1687982	7467496	0.2260	1491092	7636135	0.1953
5	3.04	1003564	7923079	0.1267	703772	8319647	0.0846	501296	8491857	0.0590
6	3.40	1869205	7043857	0.2654	1658191	7745770	0.2141	1506255	7887335	0.1910
7	2.99	876801	8042879	0.1090	588699	8314536	0.0708	332584	8695287	0.0382
8	3.34	1781254	7322981	0.2432	1548585	7772981	0.1992	1262224	7770358	0.1624
9	2.95	771792	8218414	0.0939	438064	8579495	0.0511	-	-	-

Table 6.11: Effect of increasing NaCN concentration in the eluent on the CN and Cu(I) peaks and the CN:Cu peak area ratio. Sample #9 was not analysed in the eluent containing 200 µM NaCN as the CN peak was too small.

6.3.8 Further validation of HPLC method

The results in Table 6.6 showed that the difference between the HPLC method and standard method for determining total cyanide was less than 5%. To further confirm the validity of the HPLC method, a series of controlled leach tests was performed in which the initial amount of cyanide added to the ore sample was known accurately. The initial copper concentration in these leach tests was 500 ppm to reduce the dominating influence of the Cu(I)-cyanide complexes on the final total cyanide results. The various cyano species formed during the leaching process were then determined by HPLC. Cyanide, thiocyanate and the metallo-cyanide complexes were determined by the methods developed in this chapter, whilst cyanate was determined using the chromatographic methods described in the following Chapter . The mass balance of all the cyano species produced during the leaching experiments was within 5% of the cyanide initially added to each leach test.

6.3.9 Problems encountered with the HPLC method

This section summarises the problems encountered during use of the HPLC instrument for analysing the Cu(I)-cyanide leach samples and suggests some possible solutions. There were two major problems, both of which affected the PCR detection system.

The first problem was due to derivatisation of the cyanide in the eluent resulting in the noisy baseline for the PCR detector. This noise reduced the precision, especially when integrating small peaks, and prevented reliable automated integration. The noisy baseline was due to the pump pulsations emanating from the HPLC pump and the two PCR reagent delivery pumps. There are two possible solutions to this problem, which may both be used together to provide maximum benefit.

The first solution involves a software approach to enable removal of the pump noise by various filtering methods. A Fourier Transform (FT) of a typical chromatogram identified three pump frequencies which closely matched the operating frequencies of the three pumps. The largest component of the noise was attributed to the HPLC pump. Engelhardt and Siffrin [9] have employed a similar procedure to identify

problems in a chromatographic system. Removal of the pump frequencies and subsequent inverse FT produced a chromatogram with a significantly improved baseline. This is not a new concept. For example, an identical approach using purpose built software on an Apple II computer was reported in 1985 [10]. However, it should be recognised that this approach is not regarded as Good Laboratory Practice (GLP) since it involves the manipulation of the raw data. An alternative approach to the above FT/inverse FT procedure, which should be GLP compliant, involves the use of an electronic filter to remove the pump frequencies prior to the PCR detector.

Many authors have discussed the use of various filters to improve a chromatographic signal. While it is beyond the scope of this thesis to discuss these issues in detail, an interesting paper by Mittermayr *et al.* [11] should be noted. The authors investigated the use of three filtering programs to allow automated integration of chromatograms with a noisy baseline. They found that a Savitzky-Golay filter was superior to a FT filter. However, the authors noted that special care had to be taken in setting the Savitzky-Golay filter parameters, especially when integrating peaks of highly different peak widths.

The second solution to the problem of a noisy PCR detector baseline involves a hardware approach by use of better quality HPLC and PCR reagent delivery pumps. It is intended to pursue this solution in a new project by use of the new HPLC pump incorporated in the Waters Alliance module. Waters claim that this new pump creates much smaller and more rapid pulsations. The rapid pulsations should be able to be more easily removed with commonly available filtering programs. Furthermore, the Alliance module incorporates a vacuum degassing module and a precise quaternary HPLC pump allowing constant preparation of an isocratic eluent.

The second major problem was due to the drift of the PCR detector response. There were two causes for this drift. The first cause was due to the instability of the chlorination reagent, N-chlorosuccinimide, while the second cause was due to changes in the eluent resulting from losses of cyanide and acetonitrile. The second cause can be overcome with a quaternary HPLC pump as described above. Since all chlorination reagents have shown a similar instability to that of

N-chlorosuccinimide, it may be possible to overcome the first cause by use of an *in-situ* chlorine generator, similar in principle to that used for swimming pools. This chlorine generator would consist of a platinum electrode over which a NaCl solution would flow. Electrolysis of the NaCl solution would produce chlorine which would immediately form a hypochlorite solution. The concentration of hypochlorite should remain constant as long as all the parameters remained constant. The obvious parameters are the NaCl concentration, flow rate of the NaCl solution and the current through the platinum electrode.

Minor, but not trivial, problems encountered with the use of the HPLC instrument at Telfer included power failure on several occasions and dust getting into parts of the instrument. Both these problems are endemic in the mining industry. The problem of power failures can be overcome by use of a battery back-up power supply. A 2 kW unit should be suitable for a HPLC instrument. An additional advantage of a battery back-up power supply is that a "clean" electrical supply (i.e. with no power spikes and abnormal voltages) would be available for the instrument. Large power spikes are not uncommon on mines sites, especially after a power failure. This resulted on one occasion in damage to the electronic circuitry of a HPLC pump, necessitating shipment to Sydney for repair. Fortunately, a second HPLC pump was brought to Telfer for just such an eventuality and enabled analyses to continue for the five week period that the HPLC pump was in transit and undergoing repairs.

The problem due to dust requires that the HPLC instrument should be located in, at least, a dust-free cabinet. Furthermore, the cabinet would need to be temperature controlled if it was located outside a fully air conditioned laboratory. As mentioned in Chapter five, the main Telfer laboratory was fully air conditioned. However, this was the exception to the rule as most mine laboratories have inadequate air conditioning.

Mintek have had similar experiences and consider that a dust-free, temperature-controlled environment and an independent electrical supply are essential for analytical instrumentation [12]. Mintek provided these facilities in a caravan converted to a mobile laboratory to allow use at several mine sites in South Africa.

6.4 References

1   P. D. Chamberlain, "Randol Gold Forum '96"; Squaw Creek, Olympic Valley, California, USA, 1996; Randol International Ltd., Golden, Colorado, USA; 303.

2   D. B. Dreisinger, B. Wassink, F. P. de Kocks and P. West-Sells, "Randol Gold Forum '96"; Squaw Creek, Olympic Valley, California, USA, 1996; Randol International Ltd., Golden, Colorado, USA; 315.

3   I. Mitchell, J. Defilippi and R. Dunne, "International conference on Extractive metallurgy of gold and base metals"; Kalgoorlie, W.A., 1992; The Australasian Institute of Mining and Metallurgy; 153.

4   V. M. McNamara and G. M. Ritcey ; CANMET Report MSL 88-3 (OPJ); Dept. of Energy, Mines and Resources, Canada, 1988.

5   P. Hemmerich and C. Sigwart, *Experientia*, 19 (1963) 488.

6   K. Kurnia, D. E. Giles, P. M. May, P. Singh and G. T. Hefter, *Talanta*, 43 (1996) 2045.

7   J. C. Thompsen and A. B. Carel, *Analyst*, 114 (1989) 1197.

8   D. Muir, S. La Brooy and K. Fenton, "World Gold '91"; Cairns 21-25 April 1991, 1991; The Australasian Institute of Mining and Metallurgy (AusIMM); 145.

9   H. Engelhardt and C. Siffrin, *Chromatographia*, 45(Suppl S): (1997) 35.

10 G. J. de Groot, *Trends Anal. Chem.*, 4 (1985) 134.

11 C. R. Mittermayr, H. Frischenschlage, E. Rosenberg and M. Grasserbauer, *Fresenius Journal of Analytical Chemistry*, 358 (1997) 456.

12 D. A. Holtum, *J. S. Afr. Inst. Min. Metall.*, 88 (1988) 67.

CHAPTER SEVEN

Ion chromatographic analysis of cyanate in gold processing samples containing Cu(I) and other metal-cyanide complexes

7.1 Introduction

Cyanate is formed from the oxidation of cyanide. Two oxidation mechanisms of importance to the gold cyanidation process are due to the catalytic effect of activated carbon and the oxidation of cyanide by cyanide-soluble Cu(II) minerals [1-4]. A more detailed discussion of the chemistry of cyanate formation relevant to the gold cyanidation process was provided in Chapter one (Section 1.3.3).

Unlike cyanide, there are only a limited number of analytical methods available for the analysis of cyanate. Cyanate is commonly determined using the Kjeldahl Nitrogen method [5, 6]. However, this method is very laborious, requiring over one hour per analysis and involves the use of near-boiling concentrated acids. While several electrochemical methods for the analysis of cyanate have been reported [7-9], it was initially intended to monitor cyanate using one of several reported colorimetric methods since a spectrophotometer was available at the Telfer laboratory. The most important colorimetric methods are based on the following chemistries:

(i) Reaction with a $Cu(NO_3)_2$ / pyridine reagent to form the $[Cu(OCN)_2(py)_2]$ complex [10, 11]. This neutral complex is insoluble in water and is extracted into a solvent such as chloroform. The complex has been monitored at both visible (700 nm) and UV (315 nm) wavelengths. The use of the UV wavelength allowed a 30-fold increase in sensitivity [11].

(ii) Reaction with Co(II) to form the neutral $[Co(OCN)_2]$ complex, which is normally extracted into a non-aqueous solvent such as acetone or dimethylformamide [12, 13]. The complex is monitored at a wavelength between 630-645 nm depending upon the solvent. This method suffers from poor sensitivity, with a reported detection limit of 250 ppm [12].

(iii) Reaction with chloramine-T to form ammonia, followed by colour development with a pyridine/pyrazalone reagent [14]. The coloured product has been extracted with carbon tetrachloride and monitored at 450 nm [14]. These reagents are very similar to those used for the analysis of cyanide by the König reaction using the method initially developed by Epstein [15]. As a consequence, cyanide must be removed prior to using this analytical method.

(iv) Reaction with anthranilic acid (2-aminobenzoic acid) followed by acidification with 6M HCl to form a product monitored at 310 nm [16]. This colorimetric method was developed for the determination of low cyanate concentrations in biological samples.

Ion chromatography (IC) has been successfully used for the determination of cyano species in cyanide leachates. Most of the important metallo-cyanide complexes and thiocyanate can be determined by ion-interaction chromatography with UV detection as discussed in previous Chapters. However, cyanide and cyanate are both unretained on such a chromatographic system and are also UV transparent. Therefore, in the case of cyanide, pre- or post-column derivatisation techniques have been used to facilitate detection as discussed in earlier Chapters. There are only three reported methods for the pre- or post-column derivatisation of cyanate [17-19]. The two pre-column derivatisation methods are not compatible with the ion interaction separation of the metal-cyanide complexes and use unstable reagents [17, 19]. The post-column derivatisation method would derivatise both cyanide and cyanate, thereby requiring a second separation column. Furthermore, the reported post-column derivatisation required a very long reaction time resulting in severe peak broadening [18].

Several methods describing the separation and determination of the cyanate anion have been published. Silica based ion-exchangers [20, 21], anion-exchange resins [22, 23] and ion-interaction reversed phase liquid chromatography [24-26], have all been used for the separation of cyanate. Each of these studies have found that cyanate is weakly retained, being eluted shortly after chloride.

Only one of the above papers has described an IC method for the determination of cyanate and other anions which has been developed specifically for the gold processing industry [26]. Here, ion-interaction chromatography was used with a reversed-phase column permanently coated with cetylpyridinium chloride, with 1,3,5-benzenetricarboxylic acid-tris buffer being employed for the mobile phase. However, cyanate and chloride were unresolved and therefore the method was not suitable for the determination of cyanate in samples containing large excesses of chloride. One of the best reported separations of cyanate and chloride was obtained on a Hamilton PRP X100 column with a 4-amino-2-hydroxybenzoic acid (2 mM) eluent [27]. However, the instability of aqueous solutions of 4-amino-2-hydroxybenzoic acid restricted the applicability of this method [28]. In all of the above methods, either suppressed conductivity [22, 23] or indirect UV detection [20, 21, 24, 26, 27] were used for detection of cyanate.

Indirect UV detection was used in the present study since it enabled the same detector to be applied to both this analysis and to the separate analysis of metallo-cyanide complexes using the ion-interaction method mentioned previously. This detection approach necessitated the use of an aromatic carboxylic acid for the eluent in order to provide both a weak eluent and a strong UV chromophore [29].

7.2 Experimental

7.2.1 Instrumentation

The instrumentation used consisted of two HPLC pumps, a Waters M-510 pump for delivering the mobile phase and a Waters M-600E gradient pump for back-flushing the guard column (Waters, Milford, MA, USA). Samples and standards were injected with a Waters M-717 WISP HPLC autosampler fitted with either a standard 250 µL or a micro 25 µL syringe. Injection volumes for the automated, on-line removal of the metallo-cyanide complexes were between 1 and 10 µL. A Waters 6-port, 2-way Automated Switching Valve unit was used for switching the flow direction on the guard column. A Waters M-486 variable wavelength detector set at 355 nm was used for indirect UV detection. Instrument control and data handling

were performed with a Waters Millennium data system. A Waters High Capacity IC-Pak A (150 mm x 4.6 mm I.D.) analytical column and a Waters guard column fitted with Waters IC-Pak A Guard-Pak inserts were used for most of this work. A Hamilton PRP-X100 (300 mm x 2 mm I.D.) analytical column and a Hamilton guard column fitted with Hamilton PRP-X100 inserts were also briefly used (Hamilton Co., Reno, Nevada, USA).

Supelclean LC-SAX (Supelco Inc., Bellefonte, PA, USA) solid phase extraction (SPE) cartridges were used for the manual removal of metallo-cyanide complexes from samples prior to the IC analysis. These SPE cartridges contained 500 mg of a quaternary amine strong base anion-exchanger (SAX) in the chloride form. Prior to use, the SPE cartridges were conditioned with methanol (2 mL) followed by water (2 mL) and then flushed with 5 aliquots (2 mL) of 15 mM Na_2SO_4. Solutions were manually pushed through the SPE cartridge with a syringe at a flow-rate of approximately 2 mL/min.

7.2.2 Reagents

Anthranilic acid (Ajax Chemicals, Auburn, NSW, Australia), benzoic acid (May and Baker, Dagenham, England), o-phthalic acid (BDH, Port Fairy, Vic., Australia), salicylic acid (Aldrich Chemical Co. Inc., Castle Hill, NSW, Australia) and 4-hydroxybenzoic acid (Aldrich Chemical Co. Inc., Castle Hill, NSW, Australia), were used as supplied. These carboxylic acids were all of Analytical Reagent grade quality. Eluents were prepared by dissolving the carboxylic acid in a dilute NaOH solution. The eluent used for most of this work was a 10 mM solution of anthranilic acid (pH 6.7). The eluent prepared with 4-hydroxybenzoic acid contained 4% methanol (Waters, HPLC grade). All the eluents were filtered (0.45 μm) and degassed prior to use. The anthranilic acid eluents were prepared freshly each day.

Sodium cyanate (Aldrich) was used to prepare the cyanate standards. Standardisation was carried out using the Kjeldahl Nitrogen method. The purity of the sodium cyanate was found to be 96.4%. The other standards and reagents were prepared from Analytical Reagent grade salts. The cyanate standards were prepared in 10 mM NaOH solution and stored in a refrigerator. Deionised water obtained

from a Milli-RO water purification system (Millipore, MA., USA) was used for preparing all solutions.

7.2.3 Samples

Samples were obtained from various cyanidation plants at the Telfer Gold Mine. Most of the samples were filtered on collection and the clear filtrates were analysed without further treatment. The samples from the pyrite leach plant contained very fine suspensions and were further filtered with disposable 0.45 μm Millex filters (Millipore).

7.3 Results and Discussion

7.3.1 Preliminary investigations

It was decided to attempt the colorimetric methods for cyanate analysis based upon anthranilic acid and Co(II), due to their simplicity and compatibility with the samples containing high concentrations of cyanide and copper.

To prevent any interference from the Cu(I)-cyanide complexes, commercially available cartridges containing 500 mg SAX were used for sample pre-treatment. Since cyanate is a weakly retained species on an anion exchanger, while the metallo-cyanide complexes (including Cu, Fe and Ni) and thiocyanate are very strongly retained, the SAX cartridges would effectively trap the Cu(I)-cyanide complexes while allowing the elution of cyanate with a suitable eluent.

After the anthranilic acid method conditions were modified for use with the samples, it was found that the cyanate concentrations determined were much higher than expected using this colorimetric method, suggesting an interference. The poor sensitivity of the Co(II) reaction prevented this method from being useful for this application.

Consequently, it was decided to use an ion chromatographic (IC) technique for the determination of cyanate in the samples. This decision followed the work by conducted at Lakefield Research Centre (LRC) to use an ion chromatographic

method for cyanate analysis after it was found that the Cu(I)-cyanide complexes produced cyanate during the standard acid digestion method (Kjeldahl method) for cyanate analysis.

7.3.2 Selection of separation conditions

The process samples for which the methods described in this paper were developed contained large concentrations of cyanide, metallo-cyanide complexes (especially Cu(I)-cyanide complexes), thiocyanate, chloride and sulfate. The typical ranges of chloride and sulfate concentrations in these samples were 43-86 mM and 16-32 mM, respectively. For this reason, a high capacity anion-exchange analytical column was employed to reduce overloading effects due to chloride and sulfate.

Metallo-cyanide complexes are known to have a very strong affinity for anion-exchange resins [30-32]. Consequently, these complexes are very strongly retained on the above anion-exchange columns when a weak eluent is used. This can result in reduced column efficiency and a drifting baseline if the complexes are not flushed off the column after each injection. To avoid this, the metallo-cyanide complexes were removed from the samples prior to injection onto the analytical column with one of two procedures described later in Sections 3.2 and 3.3.

A preliminary investigation examining the separation of 56 mM chloride, 0.6 mM cyanate and 10 mM sulfate was undertaken using eluents prepared from four aromatic carboxylic acids. The four acids investigated were anthranilic, benzoic, o-phthalic and salicylic acids. The best separation of cyanate, chloride and sulfate was achieved with an anthranilic acid eluent, which is consistent with results from a previous comparative study of substituted aromatic monocarboxylic acids in which it was noted that anthranilic acid was a particularly weak eluent [33]. As a result of this investigation, all further work was conducted with an anthranilic acid eluent.

The eluent pH was important for several reasons. The most important consideration was to ensure that the eluent pH was greater than the pKa value of the carboxylic acid in the eluent so that the carboxylate group could act as an eluting anion. It was also necessary to have an eluent pH between 4 and 7 so that cyanate would be

retained whilst cyanide was unretained and eluted as HCN. The pKa values of HOCN and HCN are 3.7 and 9.2, respectively [28]. The carboxylate and amino groups in anthranilic acid have pKa values of 2.14 and 4.92, respectively [34], but although these pKa values indicate that the carboxylate group is fully dissociated at pH 5, no peaks were observed in a 10 mM eluent at pH 4.9. When the eluent pH was increased to 6.0, a large system peak was observed at a retention time of 20 min. When the eluent pH was then further increased to 6.7, an excellent separation was observed, without any system peak. There was also a considerable improvement in sensitivity when the eluent pH was increased from 6.0 to 6.7. The retention times obtained with this final eluent for some common anions and cyanate are shown in Table 7.1. It should be noted that nitrate and sulfate were not completely resolved when large sulfate concentrations were present in the sample. However, this was not considered to be a problem as there were generally only negligible amounts of nitrate in the samples analysed. The presence of nitrate was indicated by a fronted sulfate peak.

Over a 12 hour period a gradual darkening of the eluent was observed, and over 24 hours the eluent pH had increased slightly. These changes were attributed to the oxidation of the amino group in anthranilic acid. Due to these changes, a fresh eluent needed to be prepared each day. It was also noticed that there was a gradual deterioration of the column performance.

Anion	R_t (min)
Carbonate	3.60
Chloride	5.08
Cyanate	6.59
Nitrate	8.88
Sulfate	9.53

Table 7.1: Retention times for some common anions and cyanate. Separation on a Waters High Capacity IC-Pak A column with an eluent composed of 10 mM anthranilic acid (pH 6.7).

This deterioration was attributed to oxidation product(s) of anthranilic acid blocking exchange sites, or to the presence of small residual amounts of the metallo-cyanide complexes remaining on the column after sample analysis, resulting in the gradual loss of exchange sites within the column. There was some recovery in the column performance after the column was flushed with 10 mM HNO_3. However, even with periodic HNO_3 flushes, the column performance was sufficiently reduced after six weeks of operation to render the column unusable for this analysis.

The analytical parameters for the determination of cyanate under the optimal eluent conditions were studied. Calibration linearity was determined for cyanate and the calibration plot was linear at least over the range 10-120 nmol injected onto the analytical column. For an injection volume of 10 µL this corresponded to the concentration range 1-12 mM. The two major anions present in the samples were chloride and sulfate. Consequently, the effect of large concentrations of these two anions on cyanate was examined. The cyanate peak area was the same for a 0.57 mM cyanate standard and another standard containing the same cyanate concentration in the presence of a 100-fold excess of both chloride and sulfate. From this experiment, it was concluded that the optimal separation conditions could tolerate at least a 100-fold excess of both chloride and sulfate. The detection limit was determined at the point where the cyanate peak height was three times the average baseline noise. The observed detection limit for a 50 µL injection volume was 9.5 µM. This is equivalent to an absolute detection limit of 0.48 nmol.

7.3.3 Removal of metallo-cyanide complexes by off-line Solid Phase Extraction

The retention of the Cu(I)-cyanide complexes on the Solid Phase Extraction (SPE) cartridges was examined by conditioning the cartridges with 56 mM NaCl and then flushing the cartridges with successive 2.0 mL portions of a sample containing 3.7 mM Cu(I)-cyanide complexes in 50 mM NaCl. The effluent from the cartridge was collected after each sample portion and analysed for copper using atomic absorption spectroscopy (AAS). The results, shown in Table 7.2, demonstrated that at least 6 mL of the sample (corresponding to 22 µmol of the Cu(I)-cyanide complex) could be

loaded onto the SAX sorbent before breakthrough occurred. Previous studies have suggested that the copper(I) would be retained on the cartridge predominantly as the $[Cu(CN)_2]^-$ complex [32, 35].

Since cyanate from the sample would also be retained on the cartridge and would be required to be eluted before analysis, it was necessary to choose an eluting anion which did not interfere in the cyanate analysis. It was also necessary that cyanate be stripped from the cartridge in a small volume to prevent sample dilution and that no Cu(I)-cyanide complex be eluted with the cyanate fraction. Experiments were conducted with carbonate, chloride or sulfate as the anion in the stripping eluent, with best results (98% recovery of cyanate) being obtained using 15 mM Na_2SO_4. When 2.2 mL of 15 mM Na_2SO_4 was used as the stripping eluent after loading 200, 300 and 400 μL volumes of a sample containing Cu(I)-cyanide complexes (36.7 mM), copper was only detected in the effluent from the SPE cartridge when 400 μL of the sample was used. The injection volume of the SPE effluent onto the analytical column was also investigated. It was observed that a 50 μL injection volume enabled the cyanate peak and the large sulfate peak (from the stripping eluent) to be baseline resolved, as shown in Fig. 7.1. Increasing the injection volume to 100 μL caused the sulfate peak to merge with the cyanate peak.

From the above investigations, the following method was adopted for the SPE removal of Cu(I)-cyanide complexes. The SAX sorbent in the SPE cartridge was conditioned as described in the Experimental section, after which 200 μL of sample was slowly loaded onto the SAX sorbent, followed by 2.2 mL of 15 mM Na_2SO_4. The entire effluent from the SPE cartridge was collected and placed directly into an autosampler vial, from which 50 μL was injected onto the analytical column for analysis.

Sample volume (mL)	[Cu] in effluent	Sample volume (mL)	[Cu] in effluent
Blank	< 15 nM	8.0	47 nM
2.0	< 15 nM	10.0	110 nM
4.0	< 15 nM	12.0	19 μM
6.0	< 15 nM	14.0	1.3 mM

Table 7.2: Breakthrough study of Cu(I)-cyanide complexes on a SPE cartridge containing 500 mg of a SAX sorbent. The SPE cartridge was conditioned prior to use with a NaCl solution (56 mM). The sample contained Cu(I)-cyanide complexes (3.67 mM) in a NaCl solution (50 mM). The blank was a NaCl solution (56 mM).
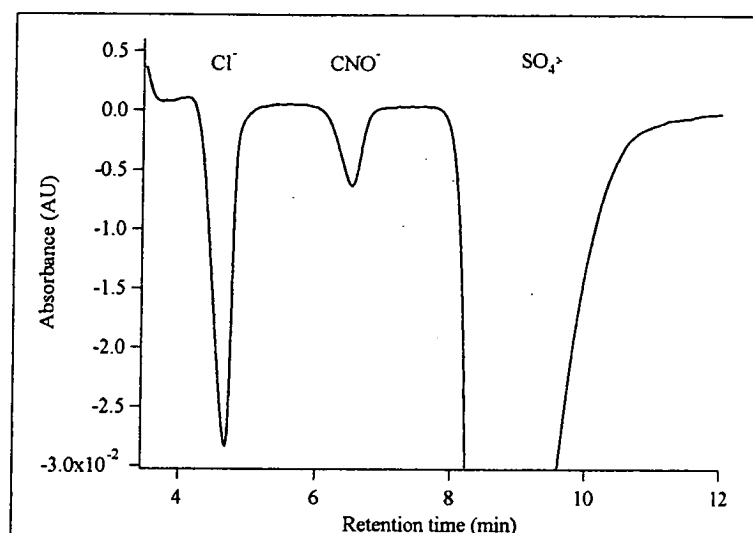

Fig. 7.1: Chromatogram of a Cu(I)-cyanide leach sample after the manual off-line removal of metallo-cyanide complexes with a SPE cartridge containing a strong anion exchanger. The CNO⁻ was eluted from the SPE cartridge with 2.2 mL Na_2SO_4 (15 mM).

Two samples were prepared for analysis using this method, with each sample preparation being performed in duplicate. It was observed that there was up to a 9% variation between the results from the duplicate preparations. This variation was attributed primarily to the SPE step since the variation between duplicate injections of the same sample was approximately 1%. The variation in the SPE method was further investigated. Thirteen samples were prepared by the above method and the mass of eluate collected from each SPE cartridge in the auto-sampler vials was recorded. The mass of eluate collected in the vials varied from 2.250 to 2.435 g with a mean mass of 2.369 g and a standard deviation of 0.057 g. These results indicated

that dilution of each eluate to a constant mass in the autosampler vial would considerably improve the reproducibilty of this method. However, this dilution step would have increased the sample preparation time and thus this approach was not pursued. This decision was taken as a method was required for the analysis of large numbers of samples. However, it should be noted that the SPE method with a dilution step would be useful for the analysis of a small number of samples due to the considerable additional capital costs involved in the following on-line method for the removal the Cu(I)-cyanide complexes.

7.3.4 Removal of metallo-cyanide complexes by an on-line method

Due to the difficulties encountered with the off-line SPE method, an on-line method utilising a 6-port, 2-way, column switching valve and a guard column was developed. In this approach, the metallo-cyanide complexes were retained on the guard column, while cyanate was eluted off the guard column directly onto the analytical column. By operation of the column switching valve, it was then possible to back-flush the guard column and remove the adsorbed metallo-cyanide complexes with a second pump as shown in Fig. 7.2.

7.3.4.1 Retention of Cu(I)-cyanide on guard column

The first step in developing this method was to determine the residence times of the cyanate and Cu(I)-cyanide complexes on the guard column using an anthranilic acid eluent. The elution of the Cu(I)-cyanide complexes was studied by injecting a sample onto the guard column, passing the anthranilic acid eluent through the guard column and collecting aliquots every 30 sec. The Cu concentration was then determined in these aliquots, after dilution, using AAS. When 5 μL of a sample containing Cu(I)-cyanide complexes (57.4 mM) was injected onto the guard column, 91 % of the total Cu injected was recovered in 3 min. No Cu was detected in the effluent from the guard column in the first 30 seconds, 1.7% of the injected Cu was detected in the subsequent 30 sec and 72 % of the Cu was eluted off the guard column in the following minute. When the guard column was dismantled, it was obvious that a noticeable darkening of the packing material in the insert had

occurred with the most pronounced darkening on the front of the insert. This was attributed to the Cu which was not eluted from the guard column. When a dilute HNO_3 (7 mM) solution was used to back-flush the guard column, most of the darkening disappeared indicating that most of the Cu had been removed.

7.3.4.2 Retention of cyanate and other anions on guard column

The guard and analytical columns were then connected to the column switching valve using the configuration shown in Fig 7.2. The time required to completely elute HCO_3^-, Cl^-, CNO^- and SO_4^{2-} off the guard column was then studied. This was achieved by turning the switching valve from the injection position to the back-flush position, at the various switching times shown in Fig. 7.3. These results show that the four anions were completely eluted off the guard column in 30 sec. Consequently the switching valve was set to turn 30 sec after injection.
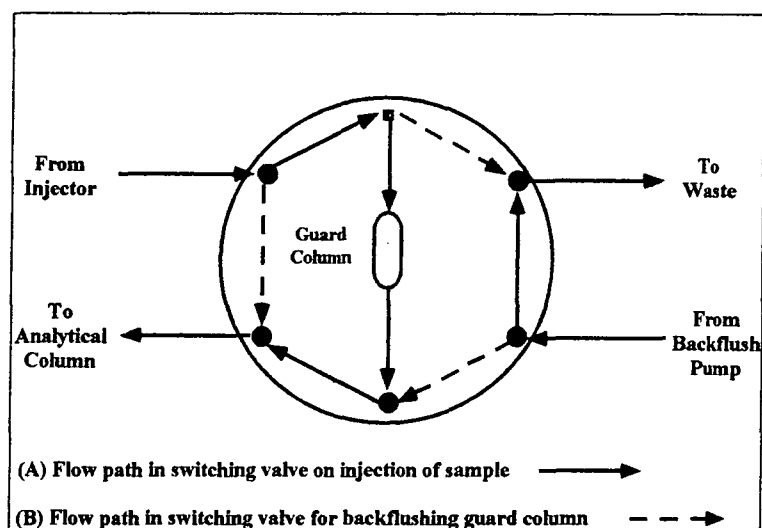

From Injector
To Waste
Guard Column
To Analytical Column
From Backflush Pump

(A) Flow path in switching valve on injection of sample ⟶
(B) Flow path in switching valve for backflushing guard column − − ⟶

Fig. 7.2: Configuration of a column switching valve and guard column for the on-line removal of metallo-cyanide complexes. The complexes are back-flushed off the guard column with the anthranilic acid eluent by a second pump.
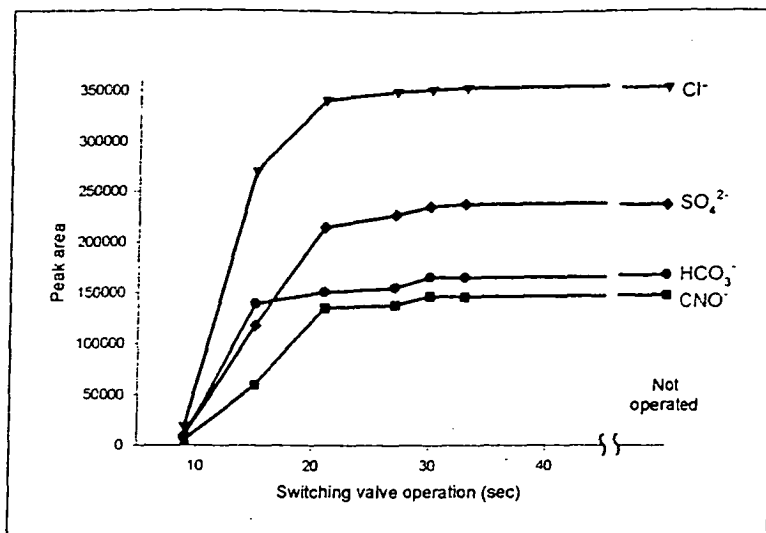
Fig. 7.3 Effect of switching valve operation time on peak areas (arbitrary units) of four anions following injection of sample. The switching valve is turned after the injection of sample to enable back-flush of the guard column. The final point for each anion shows the peak areas obtained when the switching valve was not turned following injection of sample. This comparison shows that these four anions were completely eluted off the guard column in 30 sec.

7.3.4.3 Backflush of Cu(I)-cyanide off the guard column

Regeneration of the guard column was then addressed. Use of HNO_3 solution (10 mM) to back-flush the guard column and thereby remove the bound Cu(I)-cyanide complexes was unsuccessful as only 93% of the Cu was removed from the guard column in 28 min, with most (71%) of the Cu being removed in the first 4.7 min. However, back-flushing of the guard column with the anthranilic acid resulted in complete elution of the Cu in 6 min, presumably due to the ability of anthranilic acid to form Cu(II) complexes [36]. The regeneration cycle consisted of ramping the flow-rate of the back-flush pump from 0 to 1.5 mL/min over a 1.5 min period after the switching valve was turned. This flow-rate was then maintained for 3 min, after which the flow was reduced progressively to zero over an additional 1.5 min. These slow changes in flow-rate were used to minimise damage to the guard column. The switching valve was turned back to the injection position just prior to the commencement of a new analysis.

7.3.4.4 Dilution factor and injection volume

The level of sample dilution to be used was investigated. In order to prevent overloading the guard column with Cu(I)-cyanide complexes and overloading the analytical column with chloride and sulfate, samples were normally diluted four-fold with deionised water in 4.5 mL autosampler vials and 10 μL injection volumes were used. Whilst this approach was used satisfactorily for over 200 samples, the method was adapted to the injection of undiluted samples by replacing the standard autosampler syringe with a 25 μL micro-syringe and reducing the injection volume to 2 μL. The precision for the cyanate peak area was 1.4% RSD for 5 replicate 2 μL injections of a sample.

7.3.4.5 Modification to switching valve arrangement

Since the back-pressure generated by the analytical column was about 600 psi, it was decided to use the effluent from the UV detector for back-flushing the guard column as shown in Fig. 7.4. This was possible as the UV detector flow cell was designed to withstand 1000 psi back-pressure.
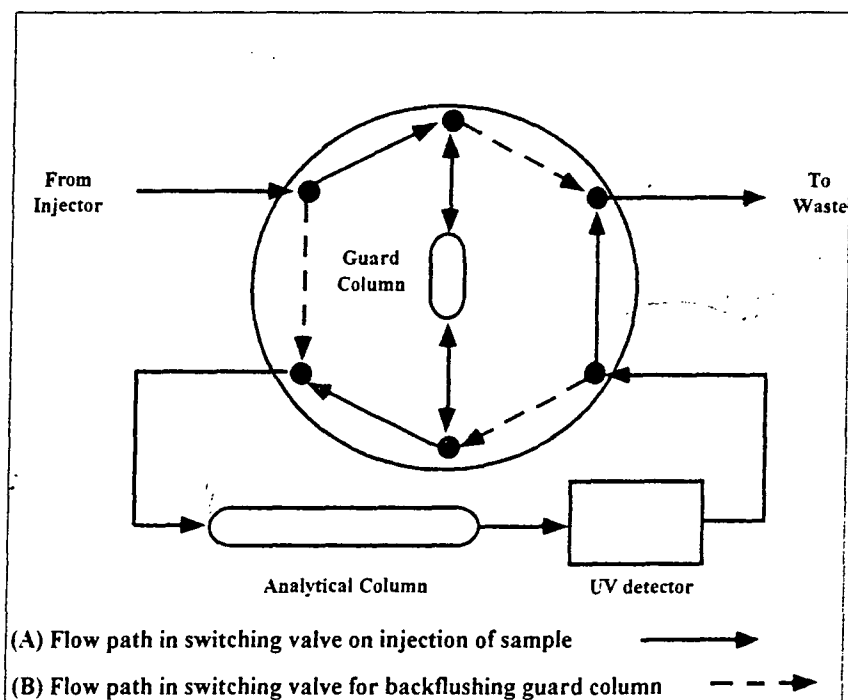

Fig. 7.4: Configuration of a column switching valve and guard column for the on-line removal of metal-cyanide complexes. The complexes are back-flushed off the guard column with the effluent from the UV detector.
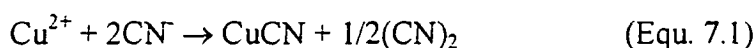
The advantage of this configuration was that a second pump was no longer required for back-flushing the guard column. The disadvantage was that a considerable pressure shock was exerted on the guard column when the switching valve was turned.

This configuration operated well. However, after many injections on three separate occasions, a blockage occurred in the switching valve resulting in a system shutdown due to high back-pressure. On each occasion, the blockage occurred immediately after the switching valve was turned to enable back-flushing of the guard column. This indicated that some solid material was back-flushed from guard column. The nature of this material was not ascertained, although it must have come from either the sample or the polymethacrylate resin of the guard column. Since this problem did not occur when a second pump was used to back-flush the guard column, the most likely source of the blockages was due to damage to the guard column caused by the repeated pressure shocks.

7.3.5   Analysis of samples

7.3.5.1 Verification of on-line method

Prior to the analysis of samples, the reaction between Cu(II) and cyanide was used to test the on-line removal of Cu(I)-cyanide complexes and subsequent IC analysis for cyanate. In this reaction, Cu(II) is reduced and complexed by cyanide to form Cu(I)-cyanide complexes, while the oxidised cyanide forms cyanogen which then undergoes rapid hydrolysis in alkaline solution to form cyanate as shown below [37].

$$Cu^{2+} + 2CN^- \rightarrow CuCN + 1/2(CN)_2 \qquad \text{(Equ. 7.1)}$$

$$(CN)_2 + 2OH^- \rightarrow CN^- + CNO^- + H_2O \qquad \text{(Equ. 7.2)}$$

In this experiment, solid $CuCl_2$ (2.5 mmol) was dissolved in an alkaline solution containing excess NaCN (12.5 mmol). Dissolution occurred in less than 1 min to form a clear solution, which was then diluted to 250 mL and injected immediately

after dilution (5 min after the $CuCl_2$ was added to the NaCN solution) and then at two successive 9 min intervals. The cyanate concentration in these injections was found using the on-line sample treatment method to be 5.00, 4.97 and 4.95 mM, respectively (expected cyanate concentration was 5.00 mM), thereby establishing the validity of the proposed approach for the determination of cyanate in the presence of Cu(I)-cyanide complexes.

7.3.5.2 Analysis of samples containing large concentrations of Cu(I)-cyanide complexes

Samples were collected from the Cu(I)-cyanide leaching trial and the pyrite leach circuit. The samples obtained from the Cu(I)-cyanide and pyrite leach operations contained up to 63 mM and 150 mM of Cu(I)-cyanide complexes, respectively. In addition, the pyrite leach samples contained up to 93 mM thiocyanate and 7 mM $[Fe(CN)_6]^{4-}$. The samples obtained from the pyrite leach operation were diluted by a factor of 10 with deionised water prior to analysis due to the very large concentrations of Cu(I)-cyanide complexes. Typical chromatograms of samples from both leaching operations are shown in Figs. 7.5 and 7.6. The major anions identified in these chromatograms were carbonate, chloride, sulfate and thiosulfate (present in the pyrite leach samples as one of the flotation reagents). Cyanate concentrations were generally in the range 2.4-10 mM for the cupriferous leach samples and up to 45 mM in the pyrite leach samples, indicating considerable cyanide oxidation in these latter samples. Since no thiocyanate was observed in chromatograms of the pyrite leach samples, it was assumed that this strongly retained anion was also trapped on the guard column along with the metallo-cyanide complexes.
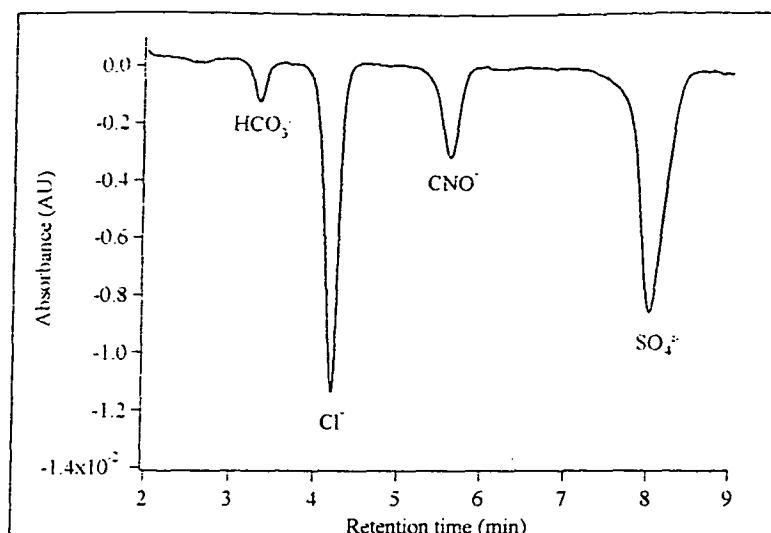
Fig. 7.5: Chromatogram of a Cu(I)-cyanide leach sample after the on-line removal of the metallo-cyanide complexes.
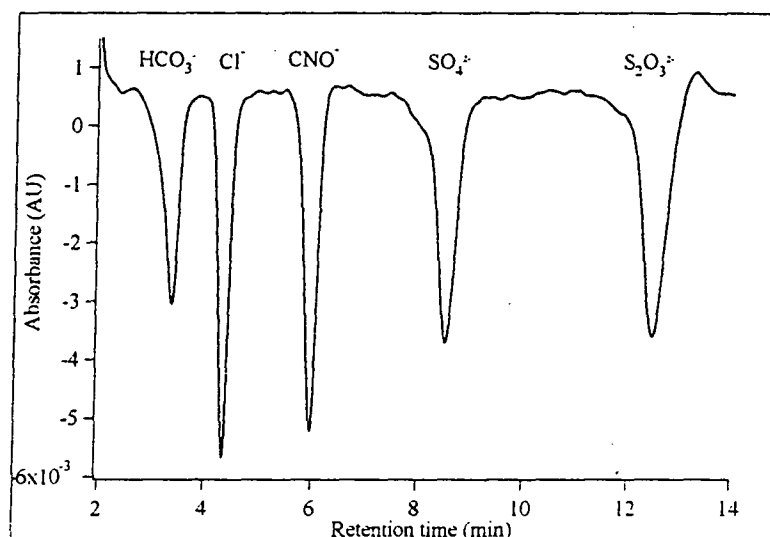

Fig. 7.6: Chromatogram of a pyrite leach sample after the on-line removal of the metallo-cyanide complexes.

7.3.6 Comparison of IC and Kjeldahl methods for cyanate analysis

Some samples obtained from the cyanidation of high grade cupriferous gold ores containing high concentrations (78-95 mM) of the Cu(I)-cyanide complexes were analysed for cyanate using a standard method [6]. This method involves the Kjeldahl digestion of the sample, followed by ammonia analysis. A comparison of the results obtained by the IC and Kjeldahl methods is shown in Table 7.3, which indicates that a large discrepancy exists between the two methods, with the IC method reporting a

considerably lower cyanate concentration. This interference was further investigated at the LRC using Cu(I)-cyanide standards (prepared by mixing CuCN and cyanide) containing Cu concentrations between 16 and 470 mM and a CN:Cu mole ratio of 3, as shown in Table 7.4. The results of this study showed that significant levels of cyanate were recorded by the Kjeldahl method in the presence of Cu(I)-cyanide complexes, despite the fact that no cyanate was detected in these Cu(I)-cyanide standards using the IC method. The source of error in the Kjeldahl method is not known but may be due to the production of cyanate during the acid hydrolysis step of the Kjeldahl analysis during which copper(II) is formed and then reacts in a manner similar to that depicted in eqns 7.1 and 7.2. The same effects of Cu(I)-cyanide complexes on the Kjeldahl analysis were observed at CN:Cu mole ratios of 4 and 5, which reflect the range of typical values found during the cyanidation of cupriferous ores. These results show the unreliability of the Kjeldahl method for the determination of cyanate in the presence of significant levels of Cu(I)-cyanide complexes and suggest that the IC method offers significant advantages for the analysis of such samples.

Sample	[OCN⁻] (mM)	
	Kjeldahl method	IC method
#1	5.00	2.69
#2	5.59	3.83
#3	8.09	5.66
#4	12.6	7.00
#5	10.0	6.12

Table 7.3: Comparison of cyanate analyses using the Kjeldahl and IC methods. The samples contained large concentrations (78 - 95 mM) of Cu(I)-cyanide complexes.

[CN] (M)	[Cu] (M)	CN:Cu mole ratio	[CNO⁻] (mM)
0.192	0.000	-	0.14
0.047	0.016	3.0	1.33
0.165	0.055	3.0	7.81
0.236	0.079	3.0	16.54
0.473	0.157	3.0	22.94
0.707	0.236	3.0	30.53
1.414	0.472	3.0	26.13

Table 7.4: Cyanate analysis using the Kjeldahl hydrolysis method of standards of various Cu(I)-cyanide complexes. Note that the formation of cyanate becomes significant at higher Cu concentrations, irrespective of the CN:Cu mole ratio. These results were provided by Dr. Hesham Kamar of the LRC.

7.3.7 Summary of problems encountered with the cyanate analysis

This section summarises the problems noted with the methods developed for cyanate analysis in this Chapter. Some possible solutions to these problems are also briefly discussed. The first problem was due to degradation (oxidation) of the anthranilic acid eluent, as was mentioned in section 7.3.2. It was likely that the degradation products were at least partly responsible for the gradual loss of column performance. Attempts at restoring the column performance by flushing routines were not overly successful. It is quite probable that the organic products from the degradation of anthranilic acid could be removed with organic solvents. However, this could not be attempted since the Waters IC Pak A column cannot be treated with more than 10% acetonitrile. To overcome this problem, a Hamilton PRP-X100 anion exchange column was purchased. On the advice of Hamilton, an eluent containing 4 mM 4-hydroxy benzoic acid in 4% (v/v) aq. methanol was used for the cyanate analysis. Both conductivity and indirect UV detection (λ = 300 nm) were used with this eluent, as shown in Fig. 7.7. It was found that the slightly greater sensitivity was observed with the conductivity detector. However, when compared to the results

obtained with the anthranilic acid eluent, the resolution of chloride and cyanate was reduced with the above chromatographic conditions. In addition, the retention time of sulfate was increased to 24 min with the analyses performed on the Hamilton column (Fig. 7.7), thereby significantly in creasing the analysis time per sample.

The on-line sample clean-up was successfully used with the 4-hydroxy benzoic acid eluent, although the samples analysed with this eluent contained lower Cu concentrations (approximately 500-800 ppm Cu as the cyano complexes). This was approximately 15% of the Cu concentration in the samples analysed with the anthranilic acid eluent.

The cyanate analytical methods developed in this Chapter are part of an overall package for the analysis of cyanidation leachate samples. Consequently, switching between the different analytical methods described in this and the preceding Chapter required changes to the instrumental configuration. Since this is time-consuming and likely to cause problems when performed routinely, a new instrument configuration has been designed to enable automated switching between the different instrumental configurations. This instrumental configuration will be constructed in a new project designed to continue the work described in this thesis. It is intended that the cyanate analyses will only be performed at 6-hourly intervals (for example), since the concentrations of cyanide and the Cu(I)-cyanide species control the gold cyanidation process.

If more frequent cyanate analyse are required, then two alternative approaches may be required. The simplest (but possibly more expensive) approach it to use two HPLC instruments, with one instrument dedicated to cyanate analyses, while the second instrument is dedicated to cyanide speciation analyses. The second approach is to use to a coupled system similar to that described in Chapter three. This would allow the separation of cyanide and cyanate on a second separation column (either anion exchange or ion exclusion). Two possible detection systems suitable for these two analytes and compatible with a coupled system are electrochemical (amperometric) detection or a PCR based on the indophenol (or Berthelot) reaction [18].
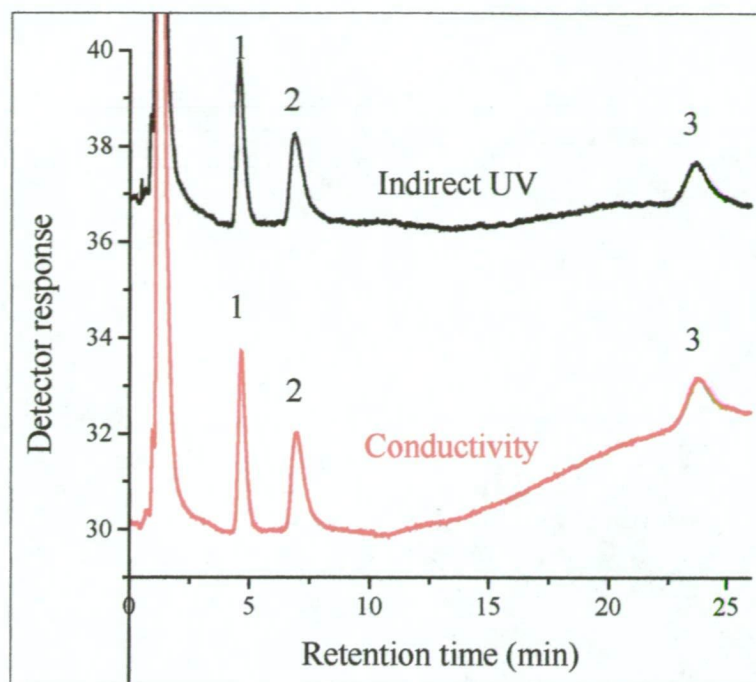

Fig. 7.7: Comparison of non-suppressed conductivity and indirect UV (300 nm) detection modes for the analysis of cyanate in a Cu(I)-cyanide leach sample. The Cu(I)-cyanide complexes were removed from the sample by the on-line method. The Cu concentration in the sample was approximately 800 ppm. Legend: **(1)** Cl^-; **(2)** CNO^-; **(3)** SO_4^{2-}. Column: 30 cm Hamilton PRP-X100. Eluent and back-flushing solution (for on-line sample clean-up): 4 mM 4-hydroxybenzoic acid in 96:4 H_2O:MeOH, pH = 8.4. Injection volume: 0.2 µL.

The indophenol reaction is widely used for the analysis of ammonia and involves chlorination of ammonia, followed by reaction with a phenol to form a highly coloured product (λ_{max}: 600-660 nm) [38, 39]. This reaction would be a suitable for the analysis of cyanide and cyanate since ammonia is the final product when these two species are treated with an excess of a chlorination reagent. While both these detection systems have potential problems associated with their routine use, the PCR detection system may have greater long-term stability. In addition, an on-line chlorination device as described in Chapter six (section 6.3.9) would improve the long-term stability of the indophenol PCR detection system.

The major disadvantages of the indophenol reaction for use as a PCR are the long reaction time (at least 2 min) and high reaction temperature (80°C) required. Koshiishi *et al.* [18] have reported the use of the indophenol reaction for the

PCR detection of cyanate. However, due to the long reaction time and the use of 1 mm I.D. reaction tubing, band broadening resulted in a peak width of approximately 4 min.

An additional advantage of a coupled system is that the metallo-cyanide complexes are removed from the cyanide and cyanate following injection onto the RPIIC separation column. Thus an on-line sample clean-up procedure is not required with a coupled system. This is a significant advantage since the guard column needs to be periodically replaced in the on-line sample clean-up method. A potential disadvantage of a coupled system compared to the on-line sample clean-up method is that other anions (such as Cl^- and SO_4^{2-}) cannot be determined. Analytical data concerning theses anions may be of assistance to metallurgists when they are trying to further understand aspects of the cyanidation process.

7.4 References

1 D. M. Muir, M. Aziz and W. Hoeker, " First International Conference on Hydrometallurgy (ICHM '88)"; Beijing, People's Republic of China, 1988; International Academic Publishers; 461.

2 M. D. Adams, *J. S. Afr. Inst. Min. Metall.*, 90 (1990) 37.

3 M. D. Adams, *J. S. Afr. Inst. Min. Metall.*, 90 (1990) 67.

4 R. Parkash and J. Zyka, *Microchemical J.*, 17 (1972) 309 .

5 F. D. Snell, *Photometric and Fluorometric Methods of Analysis (Non Metals)*; Wiley Interscience, New York, 1981.

6 A. P. H. Association and A. W. W. Association, *Standard methods for the examination of water and wastewater*, 16th ed.; APHA: Washington, D.C., 1985.

7 S. Musha and S. Ikeda, *Bunseki Kagaku*, 14 (1965) 795.

8 S. Musha and S. Ikeda, *J. Chem. Soc. Japan, pure Chem. Sect.*, 89 (1968) 767.

9 S. Yamasaki, H. Ohura and S. Hayashi, *Bunseki Kagaku*, 23 (1974) 1489.

10 E. Martin and J. McClelland, *Anal. Chem.*, 23 (1951) 1519 .

11 C. W. Wrightley, *J. Chromatogr.*, 66 (1972) 189 .

12 A. I. Finkel'shtein and G. A. Khukova, *Industrial Laboratory*, 30 (1964) 1166.

13 F. Trussel, P. A. Arabright and W. F. McKenzie, *Anal. Chem.*, 39 (1967) 1025.

14 J. Kruse and M. Mellon, *Anal. Chem.*, 25 (1953) 1188 .

15 J. Epstein, *Anal. Chem.*, 19 (1947) 272.

16 M. Guilloton and F. Karst, *Anal. Biochem., Sep*, 149 (1985) 291.

17 S. Eiger and S. D. Black, *Anal. Biochem.*, 146 (1985) 321.

18 I. Koshiishi, J. Isono and T. Imanari, *Anal. Sci.*, 2 (1986) 81.

19 P. Lundquist, B. Backman Gullers, B. Kagedal, L. Nilsson and H. Rosling, *Anal. Biochem.*, 211 (1993) 23.

20 K. Harrison, W. C. j. Beckham, T. Yates and C. D. Carr, *Int. Lab., Apr*, 16 (1986) 90.

---

21   B. R. McCord, K. A. Hargadon, K. E. Hall and S. G. Burmeister, *Anal. Chim. Acta*, 288 (1994) 43.

22   P. Silinger, *Plating and Surface Finishing*, 72 (1985) 82.

23   M. Nonomura, *Anal. Chem.*, 59 (1987) 2073.

24   W. E. Barber and P. W. Carr, *J. Chromatogr.*, 301 (1984) 25.

25   T. E. Boothe, A. M. Emran, R. D. Finn, P. J. Kothari and M. M. Vora, *J. Chromatogr.*, 333 (1985) 269.

26   D. J. Barkley, T. E. Dahms and K. N. Villeneuve, *J. Chromatogr.*, 395 (1987) 631.

27   M. C. Mehra and C. Pelletier, *Chromatographia, Sep,* 30 (1990) 337.

28   M. E. Windholz, *The Merck Index, 9th ed.,* 9 ed.; Merck & Co.: Rahway, N.J., 1976.

29   P. R. Haddad and P. E. Jackson, *Ion Chromatography. Principles and Applications*; Elsevier Science Publishers B.V.: Amsterdam, 1990.

30   F. H. Burstall, P. J. Forrest, N. F. Kember and R. A. Wells, *Ind. Eng. Chem.*, 45 (1953) 1648.

31   J. Aveston, D. A. Everest and R. A. Wells, *J. Chem. Soc.*, 1958 (1958) 231.

32   A. Gupta, E. F. Johnson and R. H. Schlossel, *Industrial and Engineering Chemistry Research*, 26 (1987) 588.

33   G. Vautour, M. C. Mehra and V. N. Mallet, *Mikrochim. Acta*, 1 (1990) 113.

34   M. S. K. Niazi and J. Mollin, *Bull. Chem. Soc. Jpn.*, 60 (1987) 2605.

35   R. D. Rocklin and E. L. Johnson, *Anal. Chem.*, 55 (1983) 4.

36   R. M. Smith and A. E. Martell, *Critical Stability Constants. Volume 4: Inorganic Ligands*; Plenum Press: London, 1976.

37   F. A. Cotton, G. Wilkinson and P. L. Gaus, *Basic Inorganic Chemistry*, 2 ed.; John Wiley & Sons, Inc.: New York, 1987.

38   P. L. Searle, *Analyst*, 109 (1984) 549.

39   A. P. H. Association, A. W. W. Association and W. E. Federation, *Standard methods for the examaination of water and wastewater*, 18th ed.; American Public Health Association (APHA): Washington, DC, 1992.

CHAPTER EIGHT

Conclusions

A post-column reaction (PCR) detection system incorporating a selective cyanide reaction was successfully coupled to a reversed-phase ion interaction chromatographic (RPIIC) system for separation of the metallo-cyanide complexes. This enabled all the cyanide species in gold cyanidation leachates to be determined with a single analysis. It was found that a tandem system in which the effluent from the RPIIC system was allowed to flow directly into the PCR detection system was the simplest and most useful coupling method for a range of samples. This PCR detection system also provided an alternative detection system for thiocyanate and the Cu(I) and Ag(I)-cyanide complexes.

A field trial of this coupled RPIIC-PCR system at an operational gold mine system revealed several major problems with respect to routine operation and interference from high concentrations of Cu(I)-cyanide complexes.

The interference from the Cu(I)-cyanide complexes was due to the partial dissociation of these complexes on the HPLC column. It was observed that the addition of cyanide to the eluent resulted in significant improvements to the cyanide and Cu(I)-cyanide peak shapes. Furthermore, retention of the Cu(I)-cyanide complex was increased with the addition of cyanide to the eluent. This chromatographic evidence suggested that nature of the eluted Cu(I)-cyanide complex was altered by the addition of cyanide to the eluent.

UV spectroscopic investigations showed that the addition of cyanide to the eluent resulted in changes to the eluted complex. Further development of the PCR detection system enabled the cyanide distributed between the cyanide and Cu(I)-cyanide peaks to be determined quantitatively. This cyanide balance enabled changes in the CN:Cu mole ratio in the Cu(I)-cyanide peak to be quantified. Using this approach, it was possible to show that the composition of the Cu(I)-cyanide peak was not homogenous in an eluent without added cyanide, while the addition of 100 μM cyanide to the eluent resulted in a homogenous Cu(I)-cyanide peak.

A second series of field trials was then undertaken. Following further improvements to the RPIIC-PCR system, Carbon-in-Leach (CIL) and Dump Leach (DL) samples were analysed. An important development was the use of a short (5 cm) analytical column to enable analysis of all species within 10 minutes. The IC results were compared to those obtained by standard methods (AAS for Cu and Au, $AgNO_3$ titration and acid distillation for cyanide). Good agreement was found for the Cu analyses, while was there up to an 8% difference between the Au analyses. Significant differences were observed for some DL samples when the RPIIC-PCR and titrimetric results were compared. However, recovery studies performed on the cyanide analyses obtained by RPIIC-PCR indicated almost complete recovery. The reason for the difference in results was unknown.

The RPIIC-PCR system was then used to monitor a new leaching operation undergoing trials at the gold mine. This leaching operation required the determination of the CN:Cu mole ratio (R), metallo-cyanide complexes, thiocyanate and cyanate. It was found that R could be determined readily using the CN:Cu(I) peak area ratio obtained from the PCR detector chromatogram. Due to the very high concentrations of Cu(I)-cyanide complexes in this leaching operation, a 1-2 μL injection volume was required to minimise sample preparation time and a 15 cm analytical column was required to resolve the Cu(I) and Fe(II)-cyanide complexes.

While the robustness of the PCR detection system was improved, 12 hourly calibrations were still required. However, the use of the CN:Cu(I) peak area ratio virtually eliminated the need for re-calibration, as the drift of the PCR detection system was cancelled out in the peak area ratio. It was found that the peak area ratio was dependent on the cyanide concentration in the eluent. This suggested further work to incorporate a gradient HPLC pump for continuous preparation of the isocratic eluent and/or use of a pH stable reversed phase column. A more detailed discussion of these issues is presented in Chapter Six (Sections 6.3.9).

While the other metallo-cyanide complexes and thiocyanate were determined from the RPIIC system, an alternative separation system was required for the analysis for cyanate. It was found that cyanate and the weakly retained anions (such as chloride)

could be separated on an anion exchange column with an eluent containing a benzoic acid derivative. This eluent also allowed the use of indirect UV detection.

Since the metallo-cyanide complexes were very strongly retained on an anion exchange column, two procedures were developed for removal of these complexes from the sample using anion-exchange resins. The first procedure utilised solid phase extraction (SPE) cartridges packed with an anion-exchange resin, while the second procedure utilised an anion-exchange guard column that was back-flushed after each injection. The SPE procedure was not developed fully, as it required considerable sample preparation time. The procedure employing the guard column was fully automated by use of a six-port column-switching valve and allowed a sample to be analysed every 12 min.

It was suggested that further work should examine the possibility of combining the two separation systems to allow automated analysis of all cyano species. It was also suggested that two alternative detection systems might allow selective detection of both cyanide and cyanate, these being a PCR detection system based on the indophenol reaction or amperometric detection. A more detailed discussion of these issues is presented in Chapter Seven (Section 7.3.7).

Utilising all the information provided by the RPIIC-PCR and cyanate IC methods enabled a cyanide mass balance to be determined to within 5%, which provided considerable confidence in these methods.

It is anticipated that the analytical methodology developed in this thesis will be incorporated into an on-line monitoring system for the cyanidation treatment of cupriferous and pyritic gold ores.